

DISS. ETH NO: 29974

KINETIC FIELD THEORY
A NEW FORMALISM FOR
MICROSCOPIC PERTURBATION THEORY

A thesis submitted to attain the degree of
DOCTOR OF SCIENCES
(Dr. Sc. ETH Zurich)

presented by

STEFAN ZENTARRA

M. Sc. Physics, Heidelberg University
M. Sc. Mathematics, Heidelberg University

born on 02.01.1993

accepted on the recommendation of

PROF. DR. LAVINIA HEISENBERG

PROF. DR. ALEXANDRE REFREGIER

PROF. DR. MATTHIAS BARTELMANN

PROF. DR. JAIYUL YOO

2024

KINETIC FIELD THEORY
A NEW FORMALISM FOR
MICROSCOPIC PERTURBATION THEORY

Doctoral Thesis by **STEFAN ZENTARRA**
supervised by **PROF. DR. LAVINIA HEISENBERG**

Stefan Zentarra

Kinetic Field Theory: a new formalism for Microscopic Perturbation Theory

February 2024

ABSTRACT

This thesis provides a general construction of the Kinetic Field Theory (KFT) framework and its microscopic perturbation theory for any classical physical system which can be described by a Hamiltonian. The generating functional of KFT is constructed based on a definition of phase space in terms of the cotangent bundle of configuration space and utilizing methods borrowed from the path integral formulation of classical mechanics. From it, observables of the system and their expectation values are derived. In order to facilitate calculations, an expansion in the interactions is performed leading to a microscopic perturbation theory. Improvements over previous approaches to this perturbative treatment include novel expressions for contributions to observables as well as a transparent diagrammatic formalism, both in a significantly generalized setting. The results are applied to two problems from the field of cosmology: cosmic structure formation and clustering of cosmic neutrinos.

ZUSAMMENFASSUNG (GERMAN ABSTRACT)

Diese Dissertation beschreibt die Konstruktion von Kinetischer Feldtheorie und seiner mikroskopischen Störungstheorie für beliebige klassische physikalische Systeme, die durch eine Hamilton-Funktion beschrieben werden können. Basierend auf einer Definition des Phasenraums als Tangentialbündel des Konfigurationsraums und unter Verwendung von Methoden, die aus der Pfadintegralformulierung der klassischen Mechanik entlehnt sind, wird das erzeugende Funktional von Kinetischer Feldtheorie konstruiert. Aus diesem Funktional werden Beobachtungsgrößen des Systems und ihre Erwartungswerte abgeleitet. Um Berechnungen zu ermöglichen wird eine Entwicklung in den Wechselwirkungen durchgeführt, die zu einer mikroskopischen Störungstheorie führt. Verbesserungen gegenüber früheren Ansätzen dieser perturbativen Behandlung sind unter anderem neue Ausdrücke für Beiträge zu Beobachtungsgrößen sowie ein transparenter diagrammatischer Formalismus, beides in einem erheblich verallgemeinerten Kontext. Die Ergebnisse werden auf zwei Probleme aus dem Bereich der Kosmologie angewendet, der Bildung kosmischer Strukturen und der Überdichte kosmischer Neutrinos.

CONTENTS

1	Introduction	1
2	Kinetic Field Theory	9
2.1	Phase Space	10
2.1.1	Configuration Space	10
2.1.2	Tangent Bundle and Velocity	13
2.1.3	Cotangent Bundle and Momentum	15
2.1.4	Hamilton's Equations	20
2.1.5	Example: Harmonic Oscillator (I)	23
2.2	Generating Functional	25
2.2.1	Classical Observables	25
2.2.2	Example: Harmonic Oscillator (II)	32
2.2.3	Classical Path Integrals	33
2.3	Free Evolution and Interactions	38
2.3.1	Green's Functions	39
2.3.2	Splitting Freedom	43
2.3.3	Example: Harmonic Oscillator (III)	46
2.3.4	Splitting of Generating Functional	48
2.4	Initial Values	56
2.4.1	Smoothed Macroscopic Description	56
2.4.2	Example: Harmonic Oscillator (IV)	58
2.4.3	Expectation Values	59
2.4.4	Example: Harmonic Oscillator (V)	61
2.4.5	Density Correlation Functions	62
3	Microscopic Perturbation Theory	67
3.1	Perturbative Treatment	68
3.1.1	Expansion in Interactions	69
3.1.2	Approximations for Observables	75
3.1.3	Example: Harmonic Oscillator (VI)	79
3.2	Feynman Rules	81
3.2.1	Defining Diagrams	82
3.2.2	Physical Interpretation	86
3.2.3	Diagram Properties	88
3.2.4	Example: Harmonic Oscillator (VII)	91
3.3	Self-Gravitating Systems	93
3.3.1	N-Body Phase Space	94
3.3.2	N-Body Green's Function	95
3.3.3	Fourier Space Description	97
3.3.4	N-Body Feynman Rules	99

4	Applications to Cosmology	105
4.1	Standard Model of Cosmology	106
4.1.1	FLRW Metric	107
4.1.2	Cosmic Neutrino Background	109
4.1.3	Cosmic Microwave Background	111
4.2	Large-Scale Structure	115
4.2.1	Correlated Initial Conditions	115
4.2.2	Series Expansion of Correlations	118
4.2.3	Correlated Feynman Rules	121
4.2.4	Density-Fluctuation Power Spectrum	128
4.3	Neutrino Clustering	131
4.3.1	N-1-body Approximation	131
4.3.2	Density Expectation Value	134
4.3.3	Local Neutrino Density	139
5	Conclusion	142
	List of Publications	148
	Bibliography	149
	Acknowledgments	154
	Declaration	155

ACRONYMS

BAO	Baryonic Acoustic Oscillations
BBN	Big Bang Nucleosynthesis
CDM	Cold Dark Matter
CMB	Cosmic Microwave Background
C ν B	Cosmic Neutrino Background
DE	Dark Energy
DM	Dark Matter
FLRW metric	Friedmann-Lemaître-Robertson-Walker metric
KFT	Kinetic Field Theory
Λ	Cosmological Constant
Λ CDM-model	Cosmological Standard Model
RKFT	Resummed Kinetic Field Theory
QFT	Quantum Field Theory

INTRODUCTION

In the beginning, the big bang created the universe. What happened within the first billionth part of a second of its lifetime is currently far from understood. It is a monumental achievement of cosmology, physics and science in general that we have a quite detailed understanding of the evolution of the universe since then—a time span between 10^{-9} and 10^{17} seconds after the big bang.

Granted, there is a lot which we do not know yet. Dark Energy (DE) seems to be described well by a Cosmological Constant (Λ), but its magnitude is far smaller than naively expected.[11] It is possible that DE is dynamic and better described by a scalar, vector or tensor field. Alternatively, it could be that Einstein's theory of general relativity does not quite describe gravity correctly and instead a modification is necessary. Such modified theories of gravity can give rise to the observed accelerated expansion of the universe at late times.[12]

Conveniently, modified theories of gravity and additional fields might also be an explanation of the second elusive dark component of our universe, Dark Matter (DM).[13] Well described as a particle which does not interact electromagnetically with other standard model particles[14], DM manifests its presence through its gravitational attraction. We can indirectly observe halos of invisible mass around galaxies through observations of gravitational lensing and other observables. Moreover, baryonic matter is more clustered than would be expected from its own gravitational attraction alone.[15]

While DE and DM account for at least 95% of our lack of knowledge (by present time energy density [16]), the about 5% of the universe we call ordinary matter are not fully understood either. Depending on the context, stars or even galaxies can be regarded as point particles in cosmology. In such cases, three of the four fundamental forces of nature can mostly be ignored and only gravitational interactions need to be considered.

When considering processes on smaller scales, at higher energies or in the early universe, such a simplification is not possible. Then, knowledge from particle physics, astrophysics and many other areas need to be combined in order to understand the universe as a whole. Examples are black holes and their formation, the genesis of baryons and their subsequent nuclear reactions, formation of stars and reionization. Any uncertainties or gaps in knowledge regarding any of these areas induces uncertainty about the universe as a whole.

Yet, it is a fortuitous fact that often in physics understanding of a system does not necessitate full knowledge of its constituents. It is rarely appreciated how conceptually counterintuitive this is. Our experience is that we can describe the orbits of the planets without knowing anything about them except for their mass. We can describe fluids and gases without knowing positions and momenta of their atoms. We can describe the energy levels of electrons bound in atoms without knowing about quarks and gluons. Somehow, more often than not, it is possible to integrate out microscopic information and describe a system with a few macroscopic observables.

In the same way, we have arrived at a description of the universe as a whole despite vast gaps in our knowledge about its constituents. Many open questions persist about DE, DM, black holes, galaxies, stars, neutrinos and yet we are able to predict the age of the universe with an uncertainty of less than two percent.[16]

We know that minutes after the big bang, hydrogen atoms combined to helium and are able to predict—and observationally confirm—the fractions of ^2H , ^3He and ^4He in the universe.[17] We are able to run simulations which produce stars, galaxies and even larger structures matching observations.[14, 18]

Much of our collective knowledge of the universe as a whole is encapsulated in the Cosmological Standard Model (ΛCDM -model). This model asserts that the universe contains Cold Dark Matter (CDM)¹ in addition to the usual baryonic matter of the standard model of particle physics and that this form of matter does not interact with ordinary matter except through gravity. Moreover, DE in the form of Λ causes a late-time acceleration of the expansion of the universe.

Dependent on seven free parameters, the ΛCDM -model provides a framework to study not only the background evolution of the spacetime manifold, but also the matter perturbations within it. One standard technique to do so is to perform a hydrodynamic approximation: DE, DM and baryonic matter are regarded as fluids and described by their respective density and velocity fields. When modeled by Λ , this approximation is actually exact for DE. For baryonic matter the approximation is very well satisfied for some components (e.g. intergalactic gas) up to very small scales, but for other components it is only valid on large scales or early times. For CDM the hydrodynamic approximation likewise breaks down at small scales or late times.[19]

The fact that neither dark nor baryonic matter can be fully described by fluids limits our understanding of the formation of structures in the universe. Contrary to the background evolution which can be described with very simple equations originally derived by Friedmann, the evolution of (matter) perturbations can currently be described analytically only at large scales or early times. As soon as streams of matter—in the form of dark matter, halos, galaxies, stars, etc.—cross, it is no longer possible to describe the “fluid” in terms of a density and velocity field. Specifically, one can no longer assign a unique bulk velocity to a point in space, but rather individual streams would need to be assigned individual velocities.

On even smaller scales, the assumption of streams itself breaks down and each point-particle carries its own velocity vector. Throughout this thesis and the field of cosmology the term “point-particle” may refer to elementary particles (including particle-DM), but also stars, galaxies, halos or even larger gravitationally bound objects. Conceptually, therefore, a description making use of these microscopic properties captures the actual physics much better. In principle, the macroscopic fields can still be derived from the microscopic data, e.g., by suitable averaging.

In practice, of course, using a microscopic description tends to be significantly more involved. No longer does the microscopic complexity get averaged over, reducing the degrees of freedom by tens of orders of magnitude. Instead of keeping track of a few macroscopic fields subject to a small number of simple field equations, an extremely high number of coupled point-particles need to be evolved according to a correspondingly large number of kinetic equations.

¹ DM being cold, as opposed to being hot, refers to them being non-relativistic for the majority of cosmic history.

To deal with these large numbers of point-particles, numerical simulations can be used. Simulating millions, billions or even trillions of interacting particles has become an indispensable tool in cosmology to model how matter forms structures on various scales. In many cases, the setup of N gravitationally interacting point-particles has been augmented to include other forces or effects like baryonic pressure or supernova explosions.[18] Numerical simulations have been used to study the formation of stars, galaxies and even the entirety of the universe.[14, 18, 20]

In this thesis, we investigate and further develop an analytic approach to studying the formation of structure in the universe: Kinetic Field Theory (KFT). This recently developed framework attempts to mimic the conceptual approach of numerical simulations in an analytic fashion. Specifically, instead of performing a hydrodynamic approximation, KFT considers gravitationally interacting point-particles. Just like numerical simulations in cosmology, Newtonian gravitational interactions on an expanding background are used—a well-justified approximation.[21]

Of course there is a reason why such systems are usually not studied analytically. Even a system of three gravitationally interacting point particles does not permit an analytical solution in the sense that there is no elementary function describing the particle trajectories.[22] Numerical methods can provide accurate approximations to these trajectories by solving the equations of motion of the system. Accuracy and particle number are only limited by computation requirements. Simulations used in cosmology are extremely sophisticated and rely on approximations of the gravitational interaction like tree and particle-mesh methods to minimize computational cost.

It may seem as if analytical methods are significantly disadvantaged in dealing with this problem. Hydrodynamic approximations only work on large scales or early times. Analytical approximations to the trajectories of particles like a Born approximation are significantly outclassed by numerical approximations. And even more generally it appears tedious to trace a large number of point-particles subject to individual initial conditions and forces.

Nonetheless, the prospect of an analytical approach to this problem is tempting. Analytically there is no limit in resolution—exactly described forces at arbitrarily small distances, infinitesimally small time-steps, infinite extent of the system and even an infinite number of particles are feasible in principle. All these aspects are limiting factors in numerical simulations and need to be dealt with by smoothing of the interacting potential or by refinement of the grid-size, time-step optimizations, boundary conditions and extrapolation, respectively.[14]

In order to realize these ambitious goals and to combat the aforementioned challenges, KFT relies on three key ideas:

1. *Determine analytic expressions for observables without explicitly solving the system.*
2. *Split free evolution from interactions while keeping the description exact.*
3. *Determine observables given a stochastic initial state.*

The first key idea addresses the problem that trajectories of particles are a particularly difficult observable. They contain effectively all information available in the system and any other observable of the system can be derived from them. In many applications this amount of information is not needed. As an example, the main observable in many simulations of cosmic structure formation is the matter-fluctuation power spectrum $P_\delta(k)$, a single function. It is arguably excessive to compute the trajectory of N particles for a total of $3N$ functions, especially if this number N is very large.

While for numerical methods such an approach may be feasible and potentially even optimal, an analytical method needs to aim for a more direct way of determining observables. In KFT this is achieved by relying on a generating functional as a central mathematical object. While it contains all the information of the system, it is never explicitly computed. Still, analytical expressions for observables can be obtained from it via suitable functional derivatives.

The second key idea of KFT is inspired by perturbation theory. In many areas of physics it is easy to analytically solve a system in absence of interactions. The resulting free evolution of the system serves as a background or reference evolution. Interactions cause deviations from it which are much more difficult or impossible to analytically solve. By performing such a splitting in free evolution and interactions we obtain a partial analytical solution.

In the KFT framework, the choice what we regard as free evolution and interactions has significant freedom. Conceptually, an optimal split should minimize the interactions while keeping the free evolution simple enough to be solved analytically. Importantly, the split should not necessitate a perturbative treatment of the interactions, making perturbation theory one of multiple possible approaches for their treatment.

The third idea stated above is both of conceptual and practical nature. In many applications the precise initial conditions are unknown or irrelevant. For example, in cosmic structure formation initial positions and momenta of the point-particles are usually obtained via the sampling of a smooth density field. Numerical approaches usually solve the system subject to the initial conditions of one single sampling and rely on the ergodic hypothesis to identify sample and spatial averages. In KFT the initial conditions are taken to be intrinsically stochastic, i.e., given by a probability distribution.

Working with stochastic initial conditions can lead to significant simplifications. Averaging an observable over the probability distribution of initial values yields an expectation value which is often of much simpler form than the observable itself. The reason for this is that certain sources of difficulty affecting the observable may be irrelevant upon averaging, especially if the initial conditions are subject to a high degree of symmetry.

KFT has been proposed in 2016 by [23] with substantial foundational work having been performed in [24]. It is based on a path integral formulation of classical mechanics suggested in [25] and further developed in [26–29]. The early development of KFT relied significantly on the works [30, 31]. For further references relevant to the initial proposal of KFT, we refer to [23, 24].

Since its inception, KFT has seen significant further development. It has been applied predominantly to cosmic structure formation, but the framework is very general and allows for applications in other areas of physics, too. We refer to the review [32] for the details and references.

There is one notable direction of work in KFT which is not directly related to this thesis, but very well demonstrates the advantages of an analytic approach to cosmic structure formation and therefore is worth highlighting here. In [33] it was shown that the asymptotic behavior of the cosmic density-fluctuation power spectrum is $P_\delta(k) \propto k^{-3}$ for $k \rightarrow \infty$. This behavior is independent of the choice of cosmological model and type of DM. Such a result is fundamentally out of reach for numerical approaches to cosmic structure formation.

The main focus of this thesis is the general and mathematically rigorous construction of the KFT framework as well as the perturbative treatment of interactions. The work presented here can arguably be seen as a reassessment of the original KFT proposal in [23]. Relying on the further development and improved understanding of KFT over the past years, the framework is presented here in a very general form applicable to any classical physical system subject to Hamiltonian equations of motion and a probability distribution of initial values.

Our construction of KFT in chapter 2 is carried out in the language of differential geometry to allow for applications, where the configuration space is a manifold. However, by choosing a chart which contains the entirety of the system's evolution, we are able work exclusively in coordinates. We provide a rigorous definition of phase space, states of system, the Hamiltonian and evolution maps in section 2.1.

In section 2.2 we define the generating functional as the central mathematical object of KFT. Implementing the first key idea stated above, we show how observables can be derived from it. A significant part of this section is dedicated to manipulating the expression of the generating functional to not explicitly depend on the evolution of the system.

The second key idea is addressed in section 2.3. We define conditions for an admissible split of the equations of motion into a free and interaction part. To ensure that the free evolution can be solved analytically, we demand the existence of a Green's function. Implementing the splitting on the level of the generating functional, we arrive at one of the central equations of KFT at the end of this section: The generating functional expressed as the exponential of an interaction operator acting on a simple exponential of the free evolution.

Section 2.4 explores the third key idea of KFT. We briefly describe the method of smoothing discrete observables which is used, e.g., to extract smooth density fields from numerical simulations. This is contrasted to the averaging method employed in KFT which yields expectation values of observables from a probability distribution of initial values.

The entirety of chapter 2 is based on [23]. Similarly to the construction presented in [1], it generalizes and simplifies the treatment and aims to make it simultaneously more rigorous and accessible. Unlike [1], the construction of KFT is not tailored to the application to interacting N-body systems.

Chapter 3 presents microscopic perturbation theory in KFT. The underlying idea is the expansion of the generating functional in the interactions. In practice, this is achieved via a series expansion of the exponential of the interaction operator in the aforementioned central equation. Truncation of this series yields approximations to observables.

While the perturbative treatment of interactions is in slight dissonance with the second key idea above, it allows to obtain expressions for observables which can be evaluated more easily. We remark that other approaches for evaluating interactions in KFT are feasible, too. A prominent one is the mean field approximation which performs an averaging of the interaction operator.[34]

Section 3.1 performs the series expansion of interactions. We present a novel formalism here, which takes inspiration from Quantum Mechanics to express the action of operators in terms of commutators. In the process we are able to completely avoid the auxiliary source field \mathbf{K} which is present in most of the KFT literature. In fact, even the omnipresent source field \mathbf{J} is eventually eliminated from the formalism and we are able to express perturbative corrections to observables solely in terms of the free evolution and functional derivatives with respect to it.

The description of perturbative corrections in terms of operators is replaced by a diagrammatic treatment in section 3.2. The diagrams facilitate both the construction of expressions for observables and the interpretation of the perturbative treatment of interactions in KFT. We carefully discuss the properties of diagrams, comment on their construction and perform a comparison of the perturbative treatment in KFT to the iterative Born approximation.

In section 3.3 we specialize the formalism to self-gravitating systems. Also referred to as interacting N-body systems, these are systems of N classical point-particles which interact via Newtonian gravitational potential. This is the context in which KFT is constructed and applied in most of the literature. We show that the special properties of these systems allow for some substantial simplifications compared to the general formalism.

As a major part of this thesis, chapter 3 expands upon the perturbative treatment in [23]. It also generalizes the formalism presented in [1] beyond interacting N-body systems. While many constructions, expressions and conclusions are original, the chapter relies on the ideas present in both these works. The diagrammatic treatment in terms of Feynman diagrams was actually introduced in [7], but it is possible to find an equivalence to the diagrams in [24]. The diagrams and Feynman rules in this thesis are a generalization.

Throughout chapters 2 and 3 we use the one-dimensional harmonic oscillator as a recurring example. While mostly intended to demonstrate the application of the formalism, it provides an example in which the perturbative expansion of KFT is convergent and can be completely resummed.

In chapter 4 we highlight two applications of the formalism developed in this thesis. Both of these are in the area of cosmology, hence we provide a brief introduction to relevant equations and concepts in section 4.1. In particular, we show how the dynamics of point-particles on an expanding background can be described. We also introduce the Cosmic Microwave Background (CMB)

and Cosmic Neutrino Background ($C\nu B$) which are directly relevant to our applications.

As described above, KFT has been developed specifically for the application to cosmic structure formation. In section 4.2 we consider this problem from the perspective of microscopic perturbation theory. In particular, we adapt our Feynman rules to obtain expressions for expectation values of density correlation functions provided correlated initial conditions. It is shown that the linear growth of the cosmic matter fluctuation power spectrum can be reproduced by a first order expansion in the initial particle correlations, as reported in [1].

The second application presented in this thesis is the clustering of the $C\nu B$. In section 4.3 we show that neutrinos which decoupled in the early universe are more abundant in dark matter halos compared to their mean number density in the universe. This result is based on [2] and agrees with earlier studies relying on numerical simulations.

As a final remark in this introductory chapter, we mention that while conducting this thesis, a mostly independent investigation of microscopic perturbation theory in KFT has been performed in [35]. Naturally, there is a certain overlap in the methods and results. However, in this thesis the focus is on the mathematical constructions in a general setting, while [35] aims more at the application to cosmic structure formation.

2.1 PHASE SPACE

Kinetic Field Theory (KFT) is a framework for analytically describing classical physical systems. For technical reasons discussed in later sections, the system ought to be described in the Hamiltonian formalism of classical mechanics. In this section we lay the groundwork for such a description and introduce the notation used throughout this thesis.

We start out by defining the configuration space of the system. Unlike previous works in KFT, we explicitly allow for the configuration space to be a d -dimensional manifold. However, utilizing a special choice of chart, it is possible to find a description in terms of coordinates which coincides with the common construction of KFT in Euclidean space. The potentially non-trivial structure of configuration space is completely absorbed into the equations of motion.

In subsection 2.1.2, we introduce the tangent bundle of configuration space which allows us to define a velocity of the system. Supposing that the equations governing the evolution are of second order in the configuration, the velocity is needed to specify initial conditions for the system. Based on this observation, an element of the tangent bundle offers a more complete characterization of the configuration of the system.

Subsequently, we translate the description in the tangent bundle to the cotangent bundle. The latter is the natural habitat of Hamiltonian mechanics and we show how the Hamiltonian of the system can be obtained from the Lagrangian in such a general setting. Using a local trivialization of the cotangent bundle induced by the aforementioned chart, we obtain a definition of phase space.

Subsection 2.1.4 extracts the key definitions of the previous subsections and introduces Hamilton's equations. The description is presented completely in coordinates and the existence of the manifold structure is hidden. As such, the constructions in this subsection—and the remainder of this thesis—are directly applicable if one were to start out with a phase space $\mathbf{X} = \mathbb{R}^{2d}$.

We conclude the section by applying the definitions and constructions to the one-dimensional harmonic oscillator. This recurring example shows how the abstract formalism of the first three subsections yields familiar equations and definitions upon using the local trivialization of the cotangent bundle. The equations of motion as well as the analytic solution of the harmonic oscillator are referred to repeatedly in the subsequent sections.

This section introduces the notation and defines the mathematical objects used throughout this thesis. As such it is a general introduction to Hamiltonian mechanics on manifolds utilizing standard definitions and constructions from differential geometry which mainly relied on [36]. Additional references were [37, 38].

2.1.1 Configuration Space

Let \mathbf{M} be the space of possible configurations of a classical physical system. Generically, \mathbf{M} is a manifold of dimension d , where d is the number of (mi-

croscopic) degrees of freedom of the system. Points in this manifold specify the configuration the system is in. More precisely, a point $\mu \in \mathbf{M}$ contains all information about the instantaneous properties of the system, e.g., all the positions of the particles in an N-body system. It does not, however, specify the rate of change of this configuration and thus it is not possible to infer quantities like the total energy of the system just from knowing the point μ .

However, there is an even more significant roadblock for defining mathematical objects and quantities given a configuration $\mu \in \mathbf{M}$. Namely, general manifolds lack addition and scalar multiplication. This absence of a vector space structure prevents direct calculations of physical quantities. Hence, before we tackle the issue of describing the rate of change of classical physical configurations, we first explain how to ingrain a vector space structure into the manifold \mathbf{M} .

In fact, there is a vector space structure concealed in manifolds already from their definition. Indeed, for any point $\mu \in \mathbf{M}$ there is a neighborhood \mathbf{U} of μ which admits a diffeomorphism $\psi: \mathbf{U} \xrightarrow{\sim} \mathbb{R}^d$. Such a pair (\mathbf{U}, ψ) is called a chart and it allows to transfer calculations performed in Euclidean space onto the manifold. To a physicist, charts are also known by the name of *coordinate systems*, emphasizing that they allow to describe a point μ in an abstract space \mathbf{M} by a finite set of real numbers—its coordinates.

The freedom of choice of a chart corresponds to the freedom of choosing a coordinate system. Therefore, the transition functions between different charts are simply coordinate transformations. From a physicist's perspective, calculations in a manifold are thus facilitated significantly by working in coordinates. It allows to pretend that physics is taking place in Euclidean space despite the configurations of the system forming much more difficult abstract space. In practice, this difficulty can mostly be avoided locally, although care has to be taken when studying global properties of such systems.

It should be stressed that it is possible to perform calculations on manifolds without relying on charts this heavily. Classical field theory on manifolds describes the evolution of fields using tensor calculus in tangent spaces—which are intrinsically Euclidean. Points in the manifolds thus appear only implicitly in the field equations and it is possible to proceed largely without explicit use of charts. However, note that in this case, the manifold is *not* the configuration space of the system. The configuration space would be the set of all allowed configurations of the involved fields. Unless there exist severe constraints on the allowed field configurations, this space is of infinite dimension and applying the formalism introduced here might potentially be infeasible.

One main aim of classical physics is to describe—and ideally also to predict—the evolution of a physical system. Mathematically, such an evolution can be modeled by a smooth map $\mathbb{R} \rightarrow \mathbf{M}$ which assigns a specific configuration μ to every value of a time parameter $t \in \mathbb{R}$. In practice, the time parameter t usually takes values in a finite interval between an initial time t_i and a finite time t_f . The initial time t_i can correspond to, e.g., the time at which an experiment is started or an instance of time where the configuration of a system is known. The final time t_f can be, e.g., the time at which a measurement is conducted

or the instance of time for which a prediction is made. While we continue to denote the evolution of a classical system by map $\mathbb{R} \rightarrow \mathbf{M}$, we understand that only a finite interval $[t_i, t_f]$ is considered.

The reason for emphasizing the finite time interval is that this implies the configurations μ the classical physical system goes through in its evolution forms a compact subset of \mathbf{M} . Basic topology therefore implies that the evolution of the system can be covered by a finite set of charts. When describing the evolution of the system using coordinates, at most a finite number coordinate transformations is required. Under relatively weak assumptions this number can be reduced to zero. For example, assuming that the evolution is non-intersecting, i.e., the configuration of the system at different instances of time is always different, then by choosing a metric on the manifold in which the evolution is a geodesic and using Fermi normal coordinates along this geodesic, a coordinate system can be constructed which covers the entire evolution of the system. Other assumptions are possible, too, the simplest of which— \mathbf{M} admits a global coordinate system—is true for the majority of systems which have been studied using KFT.

To avoid the technical details and the notation involved when allowing for coordinate transformations, throughout this thesis we demand that the evolution of the classical physical system under consideration shall be contained in a single chart. As pointed out above, this is not a particularly strong assumption and it poses no loss of generality for the system studied in this thesis. In fact, it would have been adequate for the applications considered here to simply set $\mathbf{M} = \mathbb{R}^d$ from the beginning. However, for the sake of generality and in order to introduce expanding backgrounds in a natural way, we shall consider the real numbers with which we describe our physical system as coordinates in the sense of differential geometry.

Utilizing this assumption our setup is henceforth: \mathbf{M} is a manifold of dimension d and (\mathbf{U}, ψ) is a chart of \mathbf{M} . Any point $\mu \in \mathbf{U}$ specifies the configuration of the classical physical system under consideration and via ψ has coordinates $\psi(\mu)$. Any map $\mathbb{R} \rightarrow \mathbf{M}$ describing the evolution of the system within the neighborhood \mathbf{U} , i.e., mapping $[t_i, t_f]$ into \mathbf{U} , can be composed with ψ to yield a map $\varphi^{(q)}: \mathbb{R} \rightarrow \mathbb{R}^d$. Such a map $\varphi^{(q)}$ describes the configuration space evolution of the physical system with respect to the coordinate system (\mathbf{U}, ψ) .

The choice of notation $\varphi^{(q)}$ for the evolution map is anticipating the introduction of phase space—the superscript (q) indicates that this map only contains the coordinate information of the evolution, while a superscript (p) is reserved for the momentum information. Effectively, our setup allows us to mostly forget about the existence of the manifold and focus on the map $\varphi^{(q)}: \mathbb{R} \rightarrow \mathbb{R}^d$ between Euclidean spaces. This allows us to employ common mathematical tools like tensor calculus and Fourier transforms.

One might wonder how the manifold geometry influences the evolution of the system. It should make a difference for the evolution of the system whether the configuration space \mathbf{M} is curved, even if the evolution is entirely contained in the chart \mathbf{U} . Indeed, this is the case, although the dependence on the manifold geometry is somewhat indirect: The equations of motion for the

system depend on the choice of coordinates (\mathbf{U}, ψ) and thus on the geometry of the manifold \mathbf{M} . We will see in the following section how in the KFT-framework the equations of motion select the physical evolution of the system from the many possible ways how the system could change over time.

Selecting the physical evolution from the set of possible maps $\varphi^{(q)}$ is in fact a central step in our setup. Not any map $\varphi^{(q)}: \mathbb{R} \rightarrow \mathbb{R}^d$ describes an evolution of the physical system which is possible. Indeed, any classical physical system is subject to some set of differential equations governing the allowed dynamics of this system—the equations of motion. They ensure, e.g., the conservation of certain quantities like the total energy.

The equations of motion impose a strong constraint on the allowed evolutions $\varphi^{(q)}$. Given a physical evolution $\tilde{\varphi}^{(q)}$ on any time interval (t_1, t_2) , there is one and only one way of extending it to a physical evolution for all times $t \in \mathbb{R}$. For the sake of rigor it we mention that this assumes having chosen an arbitrary, but fixed chart (\mathbf{U}, ψ) as well as a specific time parameter t —although while the mathematical form of $\tilde{\varphi}^{(q)}$ changes under changes of coordinates and reparametrizations of time, it still describes the same physical evolution $\mathbb{R} \rightarrow \mathbf{M}$ of the system.

This constraint on physical evolutions is directly related to the existence and uniqueness of solutions of differential equations. The knowledge of the configuration of a classical physical system in a time interval (t_1, t_2) determines the initial conditions $\mathbf{x}^{(q)}$ for its equations of motion. The unique solution $\tilde{\varphi}^{(q)}(t; \mathbf{x})$ of these equations given those initial conditions \mathbf{x} , is precisely the physical evolution for all times. Note that while the theory of differential equations does not guarantee the existence of a solution for all times $t \in \mathbb{R}$ in general, one might hope that a well-posed physical system would be subject to sufficiently well-behaved equations of motion with such a global solution. In fact, otherwise the system would need to feature a singularity with a loss of predictability—a severe physical and even philosophical problem.[39]

For this thesis, we only consider systems which do not feature a singularity in their physical evolution within the considered time interval. Specifically, we assume that the system and its initial conditions at a time t_i are such that the solution of its equations of motion exists for all times $t \in [t_i, t_f]$. The final time t_f here is chosen such that it is larger than all values of time relevant to the physical problem considered.

2.1.2 Tangent Bundle and Velocity

Aside from the conceptual issue of predictability, the discussion above also displayed a more practical aspect. In order to uniquely determine the physical evolution $\tilde{\varphi}^{(q)}(t; \mathbf{x})$ of the system, we need to know it on a time interval (t_1, t_2) . This is, because the initial conditions \mathbf{x} do not only depend on the instantaneous configuration of the system $\mathbf{x}^{(q)}$, but also on its rate of change. In fact, in principle it is possible that the initial conditions depend even on higher order time-derivatives of the configuration. This can happen if the equations of

motion are (equivalent to) differential equations of at least third order in the coordinates of the system. In this thesis we do not consider such systems.

In fact, appearance of derivatives higher than second order in the equations of motion is highly unusual for classical physical systems.² In the language of both Lagrangian and Hamiltonian mechanics, the equations of motion are generically of at most second order in the system's configuration. In the case of Lagrangian mechanics, this corresponds to Lagrangians \mathcal{L} which contain time-derivatives of up to first order. This allows for the usual kinetic term as well as all commonly occurring interactions. The Euler-Lagrange equations are differential equations of second order in the coordinates in this case. Consequently, the initial conditions for these equations require the configuration of the system and its rate of change at a given initial instance of time.

For reasons which become apparent in section 2.2.3, KFT is usually formulated in the realm of Hamiltonian mechanics. Here, the equations of motion contain only first order time-derivatives. However, the first order time-derivative of the momentum p corresponds to a second order time-derivative of the associated coordinate. Indeed, using Hamilton's equations, a simple calculation

$$\frac{d^2q}{dt^2} = \frac{d}{dt} \frac{\partial H}{\partial p} = \frac{\partial^2 H}{\partial p^2} \frac{dp}{dt} + \frac{\partial^2 H}{\partial q \partial p} \frac{dq}{dt} + \frac{\partial^2 H}{\partial p \partial t}, \quad (1)$$

where $H = H(q, p, t)$ is the Hamiltonian function, yields a relationship between $\frac{dp}{dt}$ and $\frac{d^2q}{dt^2}$ which in practice often simplifies to a proportionality. Therefore, Hamilton's equations can be regarded as second order differential equations for the coordinates q .

This further motivates to restrict ourselves to equations of motion which are of at most second order in the system's configuration. Crucially, however, this still implies that the initial conditions for the system contain not only the instantaneous configuration, but also its rate of change. This prompts the question whether the configuration space of the system \mathbf{M} actually contains the full information about the system. In fact, we implicitly raised that question already in the very first paragraph of the previous subsection when we asserted that certain quantities like the total energy of a classical physical system cannot be determined from its configuration $\mu \in \mathbf{M}$.

We summarize that the configuration of a classical physical system $\mu \in \mathbf{M}$ does give the full information of the instantaneous properties and observables. But it does not give access to all relevant physical quantities and in particular does not uniquely determine the evolution of the configuration. However, this shortcoming can be fully remedied by having simultaneous knowledge of the rate of change of the configuration of the system. Therefore, given an evolution map of a classical physical system $\varphi^{(q)}: \mathbb{R} \rightarrow \mathbb{R}^d$ in a chart (\mathbf{U}, ψ) the pair

$$\left(\mathbf{x}^{(q)}, \mathbf{x}^{(v)} \right) := \left(\varphi^{(q)}(t), \frac{d}{dt} \varphi^{(q)}(t) \right) \quad (2)$$

gives the full information about the system at the time $t \in [t_i, t_f]$ and determines its evolution for all times in $[t_i, t_f]$. The quantity $\mathbf{x}^{(v)}$ encodes the rate of change

² In large part, this is due to the Ostrogradsky instability.[40]

of the system and thus may be referred to as the *velocity coordinate* of the system. For an N-body system, where $\mathbf{x}^{(q)}$ is the set of all particle positions, the velocity $\mathbf{x}^{(v)}$ is the set of all particle velocities.

The velocity of the system can be defined independently of the chart (\mathbf{U}, ψ) . Let $\psi^{-1} \circ \varphi^{(q)}: \mathbb{R} \rightarrow \mathbf{M}$ be the corresponding map assigning to a time t the point $\mu := \psi^{-1}(\varphi^{(q)}(t)) \in \mathbf{M}$. The *velocity* of the configuration μ then can be defined as

$$\mathbf{v} := \frac{d}{dt} \left(\psi^{-1} \circ \varphi^{(q)} \right) (t) \quad (3)$$

and thus is an element of the tangent space $T_{\mu}\mathbf{M}$ at the point μ . Clearly, it is $\mathbf{x}^{(v)} = d\psi_{\mu}(\mathbf{v})$, where $d\psi_{\mu}: T_{\mu}\mathbf{M} \xrightarrow{\sim} T_{\mathbf{x}^{(q)}}\mathbb{R}^d \cong \mathbb{R}^d$ is the differential of the map ψ .

The pair (μ, \mathbf{v}) can be regarded as an element of the tangent bundle \mathbf{TM} of the manifold \mathbf{M} . In analogy to equation (3), the evolution map $\varphi^{(q)}: \mathbb{R} \rightarrow \mathbb{R}^d$ induces a map to the tangent bundle by

$$\left(\psi^{-1} \circ \varphi^{(q)}, \frac{d}{dt} \left(\psi^{-1} \circ \varphi^{(q)} \right) \right): \mathbb{R} \rightarrow \mathbf{TM}. \quad (4)$$

This definition uses that locally in the chart (\mathbf{U}, ψ) the tangent bundle has a product structure $\mathbf{TU} \cong \mathbf{U} \times \mathbb{R}^d$, but does not rely on our previous assumptions on the properties of (\mathbf{U}, ψ) . Following our earlier discussion, this map is advantageous for describing the evolution of the system. Indeed, for any instance of time t , this map yields not only the configuration of the classical physical system, but also its rate of change. Therefore, it allows us to directly extract any instantaneous observables and quantities including, e.g., the total energy of the system. Moreover, given second order equations of motion, the value of this map at a single instance of time uniquely determines the physical evolution of the system.

2.1.3 Cotangent Bundle and Momentum

At this point it may seem natural to use the tangent bundle and these definitions to describe the classical physical system. In this case, one obtains a construction of KFT on the tangent bundle of a manifold which is suited for Lagrangian equations of motion. It may also be a good starting point for formulating KFT for particles following geodesic motion within a (possibly dynamic) manifold. However, traditionally KFT has been formulated within the framework of Hamiltonian mechanics which allows for a substantial simplification in the formalism. Specifically, a certain functional determinant is particularly simple for Hamilton's equations of motion and would otherwise have to be dealt with by introducing Grassmann fields. Therefore, we formulate and apply KFT in the language of Hamiltonian mechanics in this thesis.

The natural habitat of Hamiltonian mechanics is the cotangent bundle $\mathbf{T}^*\mathbf{M}$ of the manifold \mathbf{M} . It is very closely related to the tangent bundle \mathbf{TM} introduced above, but possesses a canonical symplectic 2-form. Together with this differential form, the cotangent bundle becomes a symplectic manifold. In fact,

any real valued function on a symplectic manifold can naturally take the role of a Hamiltonian.[36, section 21.2] Below we obtain the Hamiltonian of the system in a more conventional way via a Legendre transform of the Lagrangian of the system.

As shown below, the Lagrangian can be used to provide a vector bundle isomorphism between tangent and cotangent bundle. This allows us to obtain a mapping between velocity \mathbf{v} and momentum $\boldsymbol{\pi}$. This way, in complete analogy to the velocity above, the momentum below supplies information about the rate of change of the configuration of a classical physical system. Therefore, a map $\mathbb{R} \rightarrow \mathbf{T}^*\mathbf{M}$ uniquely determines the evolution of a system and allows the direct extraction of observables and other relevant quantities given its value at a single instance of time, too.

The cotangent bundle $\mathbf{T}^*\mathbf{M}$ of a manifold \mathbf{M} can be defined independently of the tangent bundle \mathbf{TM} as the quotient of certain function spaces on the product $\mathbf{M} \times \mathbf{M}$. However, it is neither enlightening, nor useful for our purposes to employ such an abstract definition. Instead, we shall define the cotangent bundle as the dual bundle of the tangent bundle. Moreover, for the sake of simplicity, we give most definitions in local coordinates. While this surrenders the coordinate-independent language of abstract differential geometry, the gain in clarity is amplified by our assumptions of the existence of a chart containing the entire evolution of the system. Indeed, this allows us to work in coordinates without being concerned about coordinate transformations.

By definition, given any vector bundle $\xi: \mathbf{E} \rightarrow \mathbf{M}$, the preimage of any point $\boldsymbol{\mu} \in \mathbf{M}$ under the bundle projection ξ is a finite-dimensional real vector space called the fiber $\mathbf{F} := \xi^{-1}(\boldsymbol{\mu})$ of the bundle. This definition is justified, because the preimages of different points are isomorphic and therefore the fiber is well-defined up to vector space isomorphism. Let \mathbf{F}^* be the dual vector space of \mathbf{F} defined as $\mathbf{F}^* = \text{Hom}(\mathbf{F}, \mathbb{R}) = \{f: \mathbf{F} \rightarrow \mathbb{R} \mid f \text{ linear}\}$. Then the dual bundle is the vector bundle $\xi^*: \mathbf{E}^* \rightarrow \mathbf{M}$, where $\mathbf{E}^* = \{(\boldsymbol{\mu}, f) \mid \boldsymbol{\mu} \in \mathbf{M}, f \in \mathbf{F}^*\}$ and ξ^* is the projection on the first factor.

In order to confirm that the dual bundle is indeed a vector bundle, let $(\mathbf{U}, \boldsymbol{\psi})$ be a chart of \mathbf{M} . Then the map $(\boldsymbol{\psi}, d\boldsymbol{\psi}): \mathbf{T}\mathbf{U} \xrightarrow{\sim} \mathbb{R}^d \times \mathbb{R}^d$ induces a local trivialization of the bundle $\xi: \mathbf{E} \rightarrow \mathbf{M}$, i.e., it gives rise to a fiber-preserving diffeomorphism $\mathbf{U} \times \mathbb{R}^k \xrightarrow{\sim} \xi^{-1}(\mathbf{U}) = \mathbf{T}\mathbf{U}$. Using that any vector space is isomorphic to its dual³, this diffeomorphism induces a local trivialization of the dual bundle $\xi^*: \mathbf{E}^* \rightarrow \mathbf{M}$ over \mathbf{U} , too. Applied specifically to the tangent bundle of the manifold \mathbf{M} , this implies that within any chosen chart we may think of the cotangent bundle $\mathbf{T}^*\mathbf{M}$ as a Cartesian product $\mathbf{T}^*\mathbf{U} \cong \mathbf{U} \times \mathbb{R}^d$. As such, the physical picture is indeed very similar to the one of the tangent bundle \mathbf{TM} discussed above.

The fibers \mathbf{F} of the tangent bundle are the tangent spaces $\mathbf{T}_{\boldsymbol{\mu}}\mathbf{M} = \xi^{-1}(\boldsymbol{\mu}) = \mathbf{F}$. Their elements are the velocities \mathbf{v} which can be associated to the configuration $\boldsymbol{\mu}$. In perfect analogy, the fibers of the cotangent bundle \mathbf{F}^* are called

³ Note that this isomorphism is not canonical, i.e., its construction requires choices. Hence it cannot easily be used for identifications of elements of $\mathbf{T}^*\mathbf{M}$ with those of \mathbf{TM} which ultimately necessitates the lengthy construction below. For finding a local trivialization, however, any isomorphism is sufficient.

cotangent spaces $\mathbf{T}_\mu^*\mathbf{M} = (\xi^*)^{-1}(\mu) = \mathbf{F}^*$. An element π of the cotangent space $\mathbf{T}_\mu^*\mathbf{M}$ is called *momentum* of a configuration μ . This nomenclature is not yet justified at this stage, but it is explained below how the cotangent bundle can be identified with phase space.

To bridge this gap, we need to introduce the Legendre transform which under certain conditions provides a natural vector bundle isomorphism $\mathbf{TM} \xrightarrow{\sim} \mathbf{T}^*\mathbf{M}$. It should be noted that using local trivializations $\mathbf{T}\mathbf{U} \cong \mathbf{U} \times \mathbb{R}^d \cong \mathbf{T}^*\mathbf{U}$ it is simple to obtain some (local) bijection between the tangent and the cotangent bundle. This is not surprising, given that real vector spaces of equal dimension are always isomorphic. However, even if such a bijection can be extended to the entire vector bundles, it is not a canonical isomorphism because its construction involves choices (cf. footnote 3). Therefore, such a naive procedure does not yield a meaningful relationship between velocity \mathbf{v} and momentum π .

The Legendre transform can be defined for any real-valued function on \mathbf{TM} , but for the sake of concreteness we define it directly for the Lagrangian. In our setting, the Lagrangian L of a classical physical system is a function $L: \mathbf{TM} \rightarrow \mathbb{R}$. In cases where the Lagrangian is explicitly time-dependent, one can replace $\mathbf{M} \mapsto \mathbb{R} \times \mathbf{M}$ throughout—the first factor provides the time-coordinate—and proceed analogously. Despite anticipating to encounter this case in our applications, we refrain from formulating this entire section for systems with time-dependent Lagrangians as it would unnecessarily clutter the discussion and notation. Instead, we mention the necessary changes wherever they appear.

The Legendre transform is defined fiber-wise, so let $\mu \in \mathbf{M}$ and let $L|_\mu$ be the Lagrangian restricted to the fiber $\mathbf{T}_\mu\mathbf{M} = \xi^{-1}(\mu)$. We demand that the Hessian of $L|_\mu$ is a positive definite quadratic form on all of $\mathbf{T}_\mu\mathbf{M}$. We define the *Hamiltonian* H fiber-wise via

$$H|_\mu: \mathbf{T}_\mu^*\mathbf{M} \rightarrow \mathbb{R}, \quad H|_\mu(\pi) := \pi(\mathbf{v}) - L|_\mu(\mathbf{v}), \quad (5)$$

where \mathbf{v} is the unique element of $\mathbf{T}_\mu\mathbf{M}$ such that

$$\pi = \mathbf{d}(L|_\mu)_{\mathbf{v}} \in \text{Hom}(\mathbf{T}_\mu\mathbf{M}) = \mathbf{T}_\mu^*\mathbf{M}. \quad (6)$$

Several comments are required at this point: Firstly, the Hessian $\mathbf{d}^2(L|_\mu)_{\mathbf{v}}$ can be viewed as a bilinear map $\mathbf{T}_\mu\mathbf{M} \times \mathbf{T}_\mu\mathbf{M} \rightarrow \mathbb{R}$ and thus induces a quadratic form. Indeed, it is

$$\mathbf{d}^2(L|_\mu)_{\mathbf{v}}: \mathbf{u} \mapsto \mathbf{u}^T \frac{\partial^2(L|_\mu)(\mathbf{v})}{\partial \mathbf{v} \partial \mathbf{v}} \mathbf{u} = \frac{\partial^2}{\partial^2 \lambda} L|_\mu(\mathbf{v} + \lambda \mathbf{u}) \Big|_{\lambda=0}. \quad (7)$$

Secondly, given that this quadratic form is assumed to be positive definite, the Lagrangian restricted to the fiber $\mathbf{T}_\mu\mathbf{M}$ is strictly convex and, in particular, has a unique critical point which is a global minimum. Crucially, this implies that, thirdly, the map $\mathbf{v} \mapsto \mathbf{d}(L|_\mu)_{\mathbf{v}}$ is an isomorphism between the tangent and the cotangent spaces. In particular, there is a natural relationship between velocity \mathbf{v} and momentum π of the system justifying the implicit definition of \mathbf{v} via equation (6).

As a fourth comment it should be noted that as an element of $\mathbf{T}_\mu^*\mathbf{M}$ the momentum is a map $\pi: \mathbf{T}_\mu\mathbf{M} \rightarrow \mathbb{R}$ and thus can be evaluated on elements of $\mathbf{T}_\mu\mathbf{M}$ justifying the notation $\pi(\mathbf{v})$ in equation (5). It is shown below that upon choosing dual bases of $\mathbf{T}_\mu\mathbf{M}$ and $\mathbf{T}_\mu^*\mathbf{M}$, this expression can be transformed into the expected scalar product “ $\pi \cdot \mathbf{v}$ ”. This way the definition of the Hamiltonian takes its commonly known form.

We have shown that a Lagrangian with a positive definite Hessian induces a fiber-wise isomorphism $\mathbf{TM} \xrightarrow{\sim} \mathbf{T}^*\mathbf{M}$. For many commonly encountered terms in the Lagrangian—e.g. a standard kinetic term—this assumption is satisfied. However, exceptions exist and give rise to so-called constrained Hamiltonian systems. For these, the naive Legendre transformation fails because equation (6) cannot be solved (uniquely) for the velocity \mathbf{v} .

Throughout this thesis all considered classical physical systems satisfy our assumption and thus allow for a Hamiltonian to be constructed in the described way. In fact, below we simply define systems via their Hamiltonian description instead of taking the detour over the Lagrangian formulation. However, it should be emphasized that the relationship between tangent and cotangent bundles established above is a prerequisite for our discussions.

One key motivation for our discussion about velocities and momenta was that the instantaneous configuration of a system does not determine its evolution. Complementary information about the rate of change of the configuration is required to provide proper initial conditions for the equations of motion. While it is in principle possible to formulate the equations of motion directly on the (co)tangent bundle, it is convenient to choose a chart and formulate them on Euclidean space. Recall that having a vector space structure available facilitates practical calculations.

For this purpose we want to define a momentum coordinate $\mathbf{x}^{(p)}$ in analogy to the definition in equation (2). Let $\varphi^{(q)}: \mathbb{R} \rightarrow \mathbf{M}$ be an evolution map for the system such that $\varphi^{(q)}([t_i, t_f])$ is contained in a chart (\mathbf{U}, ψ) . We assume that the Lagrangian L of the system has a positive definite Hessian on fibers such that it induces a natural isomorphism $\mathbf{d}(L|_{\bullet})_{\bullet}: \mathbf{TM} \xrightarrow{\sim} \mathbf{T}^*\mathbf{M}$. The \bullet s indicate the slots to be taken by elements on which this function is evaluated, i.e.,

$$(\mu, \mathbf{v}) \mapsto \mathbf{d}(L|_{\bullet})_{\bullet}(\mu, \mathbf{v}) := \mathbf{d}(L|_{\mu})_{\mathbf{v}} \in \mathbf{T}_\mu^*\mathbf{M}. \quad (8)$$

As above, the resulting element of the cotangent space $\mathbf{T}_\mu^*\mathbf{M}$ is the momentum π associated to the velocity \mathbf{v} .

Using local trivializations induced by the chart (\mathbf{U}, ψ) , we can create a commutative diagram of isomorphisms

$$\begin{array}{ccc} \mathbb{R}^d \times \mathbb{R}^d & \xrightarrow{f_L} & \mathbb{R}^d \times \mathbb{R}^d =: \mathbf{X} \\ (\psi, \mathbf{d}\psi) \uparrow & & \uparrow (\psi, \mathbf{d}\psi^*) \\ \mathbf{T}\mathbf{U} & \xrightarrow{\mathbf{d}(L|_{\bullet})_{\bullet}} & \mathbf{T}^*\mathbf{U} \end{array}$$

which defines an isomorphism $f_L: \mathbb{R}^d \times \mathbb{R}^d \xrightarrow{\sim} \mathbf{X}$. It should be emphasized again that it is trivial to find *some* isomorphism between these spaces, but the

map f_L has physical significance. Using these definitions, we can define the *momentum coordinate* as

$$\mathbf{x}^{(p)} := f_L^{(p)}(\mathbf{x}^{(v)}) = \left(\mathbf{d}\psi_\mu^* \circ \mathbf{d}(L|_\mu)_\bullet \circ \mathbf{d}\psi_\mu^{-1} \right) (\mathbf{x}^{(v)}) = \mathbf{d}\psi_\mu^*(\boldsymbol{\pi}) \quad (9)$$

given a velocity coordinate $\mathbf{x}^{(v)}$. The notation $f_L^{(p)}$ refers to the second component of the map f_L . Its first component $f_L^{(q)}$ is simply the identity map. Thus, f_L maps the pair $(\mathbf{x}^{(q)}, \mathbf{x}^{(v)})$ to the pair $(\mathbf{x}^{(q)}, \mathbf{x}^{(p)})$ providing a connection between velocity and momentum coordinates of the system.

In the above diagram we already introduced the abbreviation \mathbf{X} for the space of pairs of configuration and momentum coordinates $(\mathbf{x}^{(q)}, \mathbf{x}^{(p)})$. This space is the familiar *phase space* of Hamiltonian mechanics. Any element $\mathbf{x} \in \mathbf{X}$ provides the *state* of the classical physical system under consideration. Formalizing the notation used above, we refer to the first component of \mathbf{x} as the configuration part and denote it by $\mathbf{x}^{(q)}$. The second component of \mathbf{x} is the momentum part and is denoted by $\mathbf{x}^{(p)}$. More generally, if $\boldsymbol{\varphi}: \mathbb{R} \rightarrow \mathbf{X}$ is an evolution map, we denote its configuration and momentum parts by $\boldsymbol{\varphi}^{(q)}$ and $\boldsymbol{\varphi}^{(p)}$, respectively. This allows for a natural generalization of the notion of evolution maps to describe paths in phase space instead of configuration space. Further comments and details on this are supplied in the following subsection.

As a final task in this subsection, let us transfer the Hamiltonian from the cotangent bundle to phase space. This allows us to work exclusively with configuration and momentum coordinates without having to refer to the tangent and cotangent bundles, their local trivializations and, more generally, the language of differential geometry. Consider equation (5), which defines the Hamiltonian fiber-wise as a function $H: \mathbf{T}^*\mathbf{M} \rightarrow \mathbb{R}$. Within the chart $(\mathbf{U}, \boldsymbol{\psi})$ we can use the local trivialization of the cotangent bundle to define the Hamiltonian of coordinates \mathcal{H} via a commutative diagram

$$\begin{array}{ccc} \mathbf{X} & \xrightarrow{\mathcal{H}} & \mathbb{R} \\ (\boldsymbol{\psi}, \mathbf{d}\boldsymbol{\psi}^*)^{-1} \searrow & & \nearrow H \\ & \mathbf{T}^*\mathbf{U} & \end{array}$$

Written as an equation, the definition displayed in the diagram becomes

$$\mathcal{H}(\mathbf{x}) = H|_{\boldsymbol{\psi}^{-1}(\mathbf{x}^{(q)})} \left(\left(\mathbf{d}\boldsymbol{\psi}_{\boldsymbol{\psi}^{-1}(\mathbf{x}^{(q)})}^* \right)^{-1} (\mathbf{x}^{(p)}) \right). \quad (10)$$

Analogously, the Lagrangian of coordinates \mathcal{L} is the composition $L \circ (\boldsymbol{\psi}, \mathbf{d}\boldsymbol{\psi})^{-1}$. In terms of the Lagrangian, the Hamiltonian then is given by

$$\mathcal{H}(\mathbf{x}) = \mathbf{x}^{(p)} \cdot \left(\left(f_L^{(p)} \right)^{-1} (\mathbf{x}^{(p)}) \right) - \mathcal{L} \left(f_L^{-1}(\mathbf{x}) \right). \quad (11)$$

Note that the velocity coordinate $\mathbf{x}^{(v)} = \left(\left(f_L^{(p)} \right)^{-1} (\mathbf{x}^{(p)}) \right)$ and the momentum coordinate $\mathbf{x}^{(p)}$ are not elements of the same space such that their scalar product can actually only be taken upon mapping $\mathbf{x}^{(v)}$ back into \mathbf{X} via the identity map. However, for the sake of compactness we omit this identity map from such scalar products and simply write $\mathbf{x}^{(p)} \cdot \mathbf{x}^{(v)}$. This way, equation (11) takes the familiar form.

2.1.4 Hamilton's Equations

The construction of phase space was the main aim of the previous section. While it would in principle be possible to start out our construction of KFT using a naive definition of phase space as the set of configurations and momenta, there are several advantages of constructing rather than postulating phase space. Firstly, it explicitly provides a rigorous connection between the Lagrangian and Hamiltonian formulations of mechanics and between velocity and momentum of the system. Secondly, the entire construction was done on a manifold and thus is very general and in particular completely coordinate independent. And lastly, it provides a mathematical context for our constructions and ensures that they are well-defined.

Nonetheless, the remainder of this thesis is agnostic to whether we regard phase space as the local trivialization of the cotangent bundle or simply assert that $\mathbf{X} = \mathbb{R}^{2d}$, where d is the number of microscopic degrees of freedom of the system. As has been pointed out above, if the underlying manifold \mathbf{M} has a non-trivial geometric structure, then (locally) it only affects the equations of motion. Crucially, though, the key assumption that the evolution is contained in a single chart needs to be satisfied. Otherwise the above construction needs to be significantly altered.

Summarizing the construction above, we have defined the central mathematical objects needed for constructing the formalism of KFT. These are:

- phase space \mathbf{X} ,
- states $\mathbf{x} = (\mathbf{x}^{(q)}, \mathbf{x}^{(p)}) \in \mathbf{X}$,
- Hamiltonian $\mathcal{H}: \mathbf{X} \rightarrow \mathbb{R}$,
- evolution maps $\varphi: \mathbb{R} \rightarrow \mathbf{X}$.

The aim of this subsection is to introduce the equations of motion of the classical physical system under consideration as well as its physical evolution $\tilde{\varphi}$.

In the previous subsections, it was already mentioned that while any smooth map $\varphi: \mathbb{R} \rightarrow \mathbf{X}$ describes an evolution of our system, this evolution might not be physical. Indeed, for any instance of time t , such a map provides a valid configuration $\varphi^{(q)}(t)$ of the system. However, due to uniqueness of solutions to differential equations, providing initial conditions $\mathbf{x} = \varphi(t_i)$ to the equations of motion of the system determines the physical evolution completely (up to reparametrization). We have discussed that these initial conditions need to include the rate of change of the system at t_i provided our assumption that the equations of motion are of second order in the configuration of the system.

In the Lagrangian formalism for classical mechanics, the measure for the rate of change is the velocity of the system $\mathbf{x}^{(v)}$. Demanding that

$$\mathbf{x}^{(q)} = \varphi^{(q)}(t_i) \quad \text{and} \quad \mathbf{x}^{(v)} = \frac{\partial}{\partial t} \varphi^{(q)}(t_i) \quad (12)$$

uniquely determines the physical evolution $\tilde{\varphi}^{(q)}(t; (\mathbf{x}^{(q)}, \mathbf{x}^{(v)}))$ as well as its rate of change for all times $t \in [t_i, t_f]$. Of course there are infinitely many other

evolution maps $\varphi^{(q)}$ satisfying equation (12). These maps do not describe an evolution compatible with the equations and thus are unphysical.

The Hamiltonian formalism—which is the one adopted in this thesis—likewise considers evolution maps $\varphi: \mathbb{R} \rightarrow \mathbf{X}$ of the system's configuration and needs to provide initial conditions. While equation (12) would be legitimate for that purpose, these initial conditions are clearly not adapted to the language of Hamiltonian mechanics. Instead of specifying the velocity $\mathbf{x}^{(v)}$, in this case the initial conditions should specify the momentum $\mathbf{x}^{(p)}$. However, given that the momentum is connected only indirectly to the rate of change of the configuration, expressing the initial conditions in terms of only the configuration part of the evolution map $\varphi^{(q)}(t)$ is not optimal.

Instead, we should consider the *evolution map* as a pair $\varphi = (\varphi^{(q)}, \varphi^{(p)})$ which provides the state, i.e., the configuration and momentum of the system given a time t . Instead of considering the evolution purely in configuration space \mathbf{M} , we consider paths in the cotangent bundle $\mathbf{T}^*\mathbf{M}$, or, equivalently, in phase space. This way we are also taking full advantage of a key feature of Hamiltonian mechanics, namely that the equations of motion are first order differential equations in the phase space coordinates \mathbf{x} . In particular, initial conditions $\mathbf{x} = \varphi(t_i)$ do not need to include the rate of change of φ at initial time. The required rate of change of the configuration part $\varphi^{(q)}$ is supplied by the momentum part $\varphi^{(p)}$.

As a result of the generalization of our notion of evolution maps, our entire setup is now adapted to phase space. A central aim of Hamiltonian mechanics is then to select the *physical evolution map* $\tilde{\varphi}(\bullet; \mathbf{x}): \mathbb{R} \rightarrow \mathbf{X}$ given a Hamiltonian \mathcal{H} and initial conditions \mathbf{x} . If this can be accomplished, then the behavior of the classical physical system described by \mathcal{H} is solved in the sense that its state is known for all times. This, of course, also allows us to determine the value of any observable for the system at all times.

The selection of the physical evolution among the uncountable number of maps φ happens via the equations of motion. In Hamilton's formalism of classical mechanics, these are Hamilton's equations and read in our notational conventions

$$\frac{d\varphi}{dt}(t) = \mathcal{J} \frac{\delta \mathcal{H}(\varphi(t), t)}{\delta \varphi(t)} \quad \text{with} \quad \mathcal{J} = \begin{pmatrix} \mathbf{0} & \mathbb{I}_d \\ -\mathbb{I}_d & \mathbf{0} \end{pmatrix}. \quad (13)$$

The symplectic matrix \mathcal{J} is induced by the canonical symplectic form ω on the cotangent bundle $\mathbf{T}^*\mathbf{M}$ and is made up from d -dimensional unit matrices \mathbb{I}_d on the off-diagonal blocks.⁴ We can rewrite this equation for the configuration and momentum parts of φ separately and obtain the most familiar form of Hamilton's equations

$$\frac{d\varphi^{(q)}}{dt}(t) = \frac{\delta \mathcal{H}(\varphi(t), t)}{\delta \varphi^{(p)}(t)} \quad \text{and} \quad \frac{d\varphi^{(p)}}{dt}(t) = -\frac{\delta \mathcal{H}(\varphi(t), t)}{\delta \varphi^{(q)}(t)}. \quad (14)$$

Note that it is common to write the derivatives on the right-hand sides of the equations as partial derivatives. Here, we write them as functional derivatives

⁴ For details on deriving Hamilton's equations directly from the symplectic form, confer chapter 18 of [38].

to emphasize that the equations are evaluated on phase space paths φ , not phase space points \mathbf{x} .

As a further remark we should mention that we allow for an explicit time-dependence of the Hamiltonian. In the previous subsection it was discussed that this can be achieved formally by enlarging configuration space $\mathbf{M} \mapsto \mathbb{R} \times \mathbf{M}$, i.e., by treating time as an additional coordinate. However, following this suggestion literally enlarges phase space, too, and requires us to deal with the time coordinate and its canonical momentum. Moreover, one would need to distinguish between the proper time which parameterizes the evolution maps and the coordinate time which becomes the first component of the evolution map. While this can be done in principle, it adds additional complexity to our discussion and particularly to our notation.

Fortunately, this issue can be sidestepped completely under the assumption that the Lagrangian of the system does not depend on the (proper time) derivative of the time coordinate. This is generally true for non-relativistic classical systems with time-dependent Lagrangians.⁵ Given that we are not considering relativistic systems in this thesis, we can therefore deduce that the canonical momentum associated to the time coordinate vanishes. Hence, projecting the $(2d + 2)$ -dimensional enlarged phase space along this dimension does not lose any information resulting in the space $\mathbb{R} \times \mathbf{X}$, where \mathbf{X} is the non-enlarged phase space. The Hamiltonian on enlarged phase space is equivalent to the one on this space and hence can be regarded as a map $\mathcal{H}: \mathbf{X} \times \mathbb{R} \rightarrow \mathbb{R}$, where we swapped the two factors in $\mathbb{R} \times \mathbf{X}$ for purely aesthetic reasons.

Together with initial conditions $\varphi(t_i) = \mathbf{x} \in \mathbf{X}$ at time t_i , Hamilton's equations form an initial value problem. Due to classical mechanics being deterministic, its solution is unique and we call it the physical evolution of the system and denote it by $\tilde{\varphi}$. For any value of the time parameter $t \in [t_i, t_f]$, it yields the state of the system $\tilde{\varphi}(t; \mathbf{x})$. In our notation we make the dependence on the initial conditions \mathbf{x} explicit and thus can regard the physical evolution as a map $\tilde{\varphi}: \mathbb{R} \times \mathbf{X} \rightarrow \mathbf{X}$. In this form, it describes the *Hamiltonian flow*: for any state \mathbf{x} the system evolves along the paths $\tilde{\varphi}(t; \mathbf{x})$ for $t \in [t_i, t_f]$.

The Hamiltonian flow has a couple of important properties which we exploit at various steps in the following, particularly in subsection 2.4.3. Firstly, due to determinism, paths in phase space cannot intersect. Indeed, for any point in phase space, there is a unique future and past trajectory given by the Hamiltonian flow. Secondly, Liouville's theorem implies that infinitesimal phase space regions retain their volume under the Hamiltonian flow. This implies that

$$\det \left(\frac{\partial \tilde{\varphi}(t; \mathbf{x})}{\partial \mathbf{x}} \right) = 1 \tag{15}$$

for all $t \in [t_i, t_f]$. We remark that the proof of this statement only relies on the symplectic structure of Hamilton's equations and thus is valid even if the Hamiltonian is explicitly time-dependent.[37, Corollary 1.10]

⁵ Note that in non-relativistic classical mechanics there is a freedom of choosing a time parameter. In special relativity, the natural time parameter is the proper time and thus acquires physical meaning.

There is another interpretation of the equations of motion which provides a key shift in perspective enabling the formulation of KFT. Let us rewrite the equations of motion as

$$\mathbf{E}[\boldsymbol{\varphi}](t) := \frac{d\boldsymbol{\varphi}}{dt}(t) - \mathcal{J} \frac{\delta \mathcal{H}(\boldsymbol{\varphi}(t), t)}{\delta \boldsymbol{\varphi}(t)} = \mathbf{0}. \quad (16)$$

The object \mathbf{E} can be regarded as a map $\mathbf{E}: C^\infty(\mathbb{R}, \mathbf{X}) \times \mathbb{R} \rightarrow \mathbf{X}$, where $C^\infty(\mathbb{R}, \mathbf{X})$ is the space of all smooth maps from \mathbb{R} to \mathbf{X} . However, we may also consider it as a map $\mathbf{E}[\bullet]: C^\infty(\mathbb{R}, \mathbf{X}) \rightarrow C^\infty(\mathbb{R}, \mathbf{X})$. In this form it is an operator and can be written as

$$\mathbf{E}[\bullet] = \frac{d}{dt}[\bullet] - \mathcal{J} \frac{\delta \mathcal{H}(\bullet)}{\delta \boldsymbol{\varphi}}. \quad (17)$$

The definition of \mathbf{E} in equation (16) applies to any evolution map $\boldsymbol{\varphi}$. The object $\mathbf{E}[\boldsymbol{\varphi}](t)$ measures if and by how much such an evolution violates the equations of motion at time t . Any map $\boldsymbol{\varphi}: [t_i, t_f] \rightarrow \mathbf{X}$ for which $\mathbf{E}[\boldsymbol{\varphi}] = \mathbf{0}$, i.e., $\mathbf{E}[\boldsymbol{\varphi}](t) = \mathbf{0}$ for all $t \in [t_i, t_f]$, is a physical evolution with initial conditions given by $\mathbf{x} = \boldsymbol{\varphi}(t_i)$. As mentioned above, due to determinism in classical physics, upon fixing the initial conditions, there is exactly one such map.

Of course this perspective is essentially just rephrasing Hamilton's principle of stationary action. In fact, the quantity $\mathbf{E}[\boldsymbol{\varphi}](t)$ can be related to the variation of the action. However, instead of using this principle as a global criterion, we intend to use it locally. Specifically, given explicit initial conditions \mathbf{x} , KFT identifies the physical evolution $\tilde{\boldsymbol{\varphi}}$ as the unique map $\boldsymbol{\varphi}: [t_i, t_f] \rightarrow \mathbf{X}$ with $\boldsymbol{\varphi}(t_i) = \mathbf{x}$ and $\mathbf{E}[\boldsymbol{\varphi}](t) = \mathbf{0}$ for all $t \in [t_i, t_f]$. We elaborate on this idea in the following section where we introduce the KFT formalism.

2.1.5 Example: Harmonic Oscillator (I)

As a recurring example throughout the first two chapters of this thesis, we consider the harmonic oscillator as a toy model. Our intention is to show the construction of KFT for a simple classical system and to point out some properties. Furthermore we perform some basic comparisons to the exact solution and to standard approximations. In this subsection, we define the phase space, the Hamiltonian and the equations of motion of the harmonic oscillator. We then solve them to obtain the exact analytic solution of the system.

We are considering a standard one-dimensional harmonic oscillator, i.e., a system evolving in $D = 1$ dimensions with configuration space $M = \mathbb{R}^1$. The associated tangent bundle is $TM = \mathbb{R}^2$ and the velocity is simply $\mathbf{v} = \frac{d}{dt}\boldsymbol{\varphi}^{(q)}(t)$ using a trivial global chart $(U, \psi) = (\mathbb{R}, \text{id})$. Phase space and the cotangent bundle coincide and we have $\mathbf{X} = T^*M = \mathbb{R}^2$.

While the identity map $\text{id}: \mathbb{R}^2 \rightarrow \mathbb{R}^2$ is a possible isomorphism between TM and T^*M , it would just be an arbitrary choice. Instead, we consider the Lagrangian of the system

$$L((\boldsymbol{\mu}, \mathbf{v})) = \frac{1}{2}m\mathbf{v}^2 - \frac{1}{2}\kappa\boldsymbol{\mu}^2, \quad (18)$$

where $m, \kappa \in \mathbb{R}$ are some positive constants. Its Hessian is $d^2(L|_{\mu})_{\nu} = m\mathbb{I}_1$ and thus corresponds to a positive definite bilinear map. Therefore, the map

$$(L|_{\bullet})_{\bullet}: (\mu, \nu) \mapsto d(L|_{\mu})_{\nu} \quad \text{with} \quad (19)$$

$$\mathbf{d}(L|_{\mu})_{\nu}: \mathbf{u} \mapsto \left. \frac{\partial}{\partial \lambda} L|_{\mu}(v + \lambda \mathbf{u}) \right|_{\lambda=0} = m\nu \cdot \mathbf{u} \quad (20)$$

is a physically meaningful isomorphism $(L|_{\bullet})_{\bullet}: TM \rightarrow T^*M$. Using the isomorphism $(L|_{\bullet})_{\bullet}$, we find the momentum of the system to be

$$\pi = d(L|_{\mu})_{\nu} \in \text{Hom}(T_{\mu}M) \quad \text{with} \quad \pi(\mathbf{u}) = m\nu \cdot \mathbf{u}. \quad (21)$$

We can use it to define the Hamiltonian via the Legendre transform

$$H((\mu, \pi)) = \pi(\nu) - L((\mu, \nu)) = m\nu \cdot \nu - \frac{1}{2}m\nu^2 + \frac{1}{2}\kappa\mu^2 = \frac{1}{2}m\nu^2 + \frac{1}{2}\kappa\mu^2 \quad (22)$$

which coincides with the total energy of the system. However, the Hamiltonian should of course be expressed as a function of π and not of ν . Hence, we need to invert equation (21) which yields the final form of the Hamiltonian

$$H((\mu, \pi)) = \frac{\pi^2}{2m} + \frac{1}{2}\kappa\mu^2. \quad (23)$$

Exploiting the choice of a trivial chart $(U, \psi) = (\mathbb{R}, \text{id})$, we can replace (μ, π) by the associated coordinates and obtain

$$\mathcal{H}(x) = \frac{(x^{(p)})^2}{2m} + \frac{1}{2}\kappa(x^{(q)})^2 \quad (24)$$

for the Hamiltonian. Hence, Hamilton's equations take the familiar form

$$\frac{d\varphi}{dt}(t) = \mathcal{J} \frac{\delta \mathcal{H}(\varphi(t), t)}{\delta \varphi(t)} = \begin{pmatrix} \frac{\varphi^{(p)}(t)}{m} \\ -\kappa \varphi^{(q)}(t) \end{pmatrix}. \quad (25)$$

The physical evolution map $\tilde{\varphi}(\bullet; x)$ is the unique solution of these equations for initial value x at time t_i . In the case of the harmonic oscillator an analytic form for the physical evolution can be obtained. By standard methods we find

$$\tilde{\varphi}(t; x) = \begin{pmatrix} \cos(\sqrt{\frac{\kappa}{m}}(t - t_i)) x^{(q)} + \frac{1}{\sqrt{\kappa m}} \sin(\sqrt{\frac{\kappa}{m}}(t - t_i)) x^{(p)} \\ -\sqrt{\kappa m} \sin(\sqrt{\frac{\kappa}{m}}(t - t_i)) x^{(q)} + \cos(\sqrt{\frac{\kappa}{m}}(t - t_i)) x^{(p)} \end{pmatrix}. \quad (26)$$

2.2 GENERATING FUNCTIONAL

The generating functional is the central mathematical object in KFT. This section is dedicated to its definition as well as its use to derive classical observables. Moreover, we manipulate the expression for the generating functional in such a way that the explicit dependence on the physical evolution in its definition is avoided. Through this, we realize the first of the three key ideas of KFT listed in the introductory chapter: *Determine analytic expressions for observables without explicitly solving the system.*

We start out in subsection 2.2.1 with a definition of the generating functional in its simplest form. We show that the physical evolution map can be derived from it. This demonstrates that the generating functional contains the full information about the system. We proceed to define composite systems which are the basis of applications of KFT to N-body systems. Subsequently, we define several important observables like the macroscopic density and its correlation functions.

These definitions are applied to the harmonic oscillator in the following subsection. In order to provide an example for composite systems, we consider a collection of N independent harmonic oscillators and define its macroscopic density. We also explain the differences between microscopic and macroscopic densities as well as the densities of components.

In the final subsection we perform the aforementioned manipulations of the expression for the generating functional. We discuss in detail how the description of the dynamics with Hamilton's equations avoids the appearance of a complicated functional determinant. The resulting expression for the generating functional depends only on the equations of motion, the initial conditions and an auxiliary source field J.

The constructions and definitions as well as manipulations in this section are standard in the KFT literature, e.g., in [1, 23, 35] and others.

2.2.1 Classical Observables

In the previous section we have introduced several central mathematical objects relevant to the construction of KFT: phase space \mathbf{X} , states $\mathbf{x} \in \mathbf{X}$, the Hamiltonian $\mathcal{H}: \mathbf{X} \rightarrow \mathbb{R}$, evolution maps $\boldsymbol{\varphi}: \mathbb{R} \rightarrow \mathbf{X}$ and the equations of motion $\mathbf{E}[\boldsymbol{\varphi}] = \mathbf{0}$. Given an initial state \mathbf{x} at time t_i there is a unique evolution map $\tilde{\boldsymbol{\varphi}}$ for which the equations of motion are valid for all times $t \in [t_i, t_f]$. We refer to this map as the physical evolution of the system. Explicitly, it satisfies

$$\tilde{\boldsymbol{\varphi}}(t_i; \mathbf{x}) = \mathbf{x} \quad \text{and} \quad \frac{d}{dt} \tilde{\boldsymbol{\varphi}}(t; \mathbf{x}) - \mathcal{J} \frac{\delta \mathcal{H}(\tilde{\boldsymbol{\varphi}}(t; \mathbf{x}), t)}{\delta \boldsymbol{\varphi}(t)} = \mathbf{0} \quad \forall t \in [t_i, t_f]. \quad (27)$$

Equivalently, the physical evolution is the solution of the initial value problem given by the equations of motion $\mathbf{E}[\boldsymbol{\varphi}] = \mathbf{0}$ and the initial conditions \mathbf{x} .

In practice, it is quite rare that an interesting classical physical system has a physical evolution which can be found by explicitly solving the initial value problem. In fact, it is not uncommon that differential equations do not have

a solution which can be expressed in terms of elementary functions. Thus, it is often too ambitious to attempt to analytically find an expression for $\tilde{\varphi}$. Fortunately, often a lot of information about the system under consideration can be extracted even without having an explicit expression for the physical evolution. This is the first key idea of KFT: *Determine analytic expressions for observables without explicitly solving the system.*

At first glance, this idea might seem to be doomed to fail: How can we determine observables of a system at some time $t > t_i$ without knowing the state of the system $\tilde{\varphi}(t; \mathbf{x})$? However, a simple example shows that this pessimism is unfounded: Consider a system of N interacting point-particles with arbitrary initial positions and momenta. For $N > 2$ one can mathematically prove that the phase space trajectory of this system cannot be expressed in terms of elementary functions, unless one assumes very special initial conditions.[22] Yet, the center-of-mass position is an observable for this system and it can be calculated easily from the initial state and the elapsed time.

This example shows that there are observables which are significantly simpler to determine than the physical evolution. In fact, arguably the physical evolution is an observable itself and conceptually it is the most difficult of all possible observables of the system because it contains the maximal amount of information. Conservation laws and simplifications due to projection and averaging processes allow us sometimes to determine observables even though the state of the system remains unknown.

While the mentioned reasons for simplifications can be exploited purposefully, this usually requires developing a specific approach for any given system. For example, many textbook problems in classical mechanics can be solved using, e.g., energy conservation. However, in order to extract certain information about the system might require creative application of this concept or use it in conjunction with other tools and methods. KFT is a general formalism applicable to any classical physical system described by a Hamiltonian. Therefore, we cannot use, e.g., conservation laws explicitly. Nonetheless, our key idea relies strongly on their effect in simplifying the calculation of certain observables.

Having outlined our aim of determining observables without relying on the physical evolution map $\tilde{\varphi}$, let us do the exact opposite. Assume that a classical physical system is described by an Hamiltonian \mathcal{H} which induces equations of motion $\mathbf{E}[\varphi] = \mathbf{0}$. Let $\mathbf{x} \in \mathbf{X}$ be the state of the system at the initial time t_i . Assume further that $\tilde{\varphi}$ is the physical evolution, i.e., for any time $t \in [t_i, t_f]$ the state of the system is given by $\tilde{\varphi}(t; \mathbf{x})$.

Continuing contrary to our goal, let us define the *generating functional* of the system in terms of $\tilde{\varphi}$. This mathematical object is the central quantity of KFT and is defined as

$$Z[\mathbf{J}; \mathbf{x}] = \exp\left(i \int_{t_i}^{t_f} dt' \mathbf{J}(t') \cdot \tilde{\varphi}(t'; \mathbf{x})\right). \quad (28)$$

The generating functional Z functionally depends on an auxiliary source function $\mathbf{J}: \mathbb{R} \rightarrow \mathbf{X}$. This function does not have a relevant physical interpretation

and is introduced for the sole reason to allow us to extract $\tilde{\varphi}$ from Z via a simple functional derivative. Indeed, it is

$$\left. \frac{\delta}{i \delta \mathbf{J}^T(t)} Z[\mathbf{J}; \mathbf{x}] \right|_{\mathbf{J}=0} = \left. \frac{\delta}{i \delta \mathbf{J}^T(t)} \exp \left(i \int_{t_i}^{t_f} dt' \mathbf{J}(t') \cdot \tilde{\varphi}(t'; \mathbf{x}) \right) \right|_{\mathbf{J}=0} \quad (29)$$

$$= \int_{t_i}^{t_f} dt' \delta_D(t' - t) \tilde{\varphi}(t'; \mathbf{x}) \quad (30)$$

$$= \tilde{\varphi}(t; \mathbf{x}). \quad (31)$$

The notation δ_D will be used throughout this thesis for the Dirac δ -function. Note that in this calculation it ensures that $\tilde{\varphi}$ is evaluated at the instance of time at which we take the functional derivative. By construction, we get a vanishing contribution if our time parameter is outside the interval $[t_i, t_f]$.

The calculation above is our first example of how to derive—or generate—an observable from the generating functional. Given $Z[\mathbf{J}; \mathbf{x}]$ the phase space trajectory of the system can be obtained by a simple functional derivative. If the system considered is, e.g., an N -body system this allows access to all particle positions and momenta at all times $t \in [t_i, t_f]$. For the remainder of this subsection we define some other observables which can be derived from the generating functional. Following some examples, subsection 2.2.3 achieves our current aim of removing the explicit dependence of the generating functional on the physical evolution $\tilde{\varphi}$. This way our definitions here are realigned with the first key idea of KFT formulated above.

The idea of having a mathematical object from which observables can be obtained via functional derivation is taken from Quantum Field Theory (QFT). In the path integral formulation of QFT, the partition function is a generating functional for correlation functions and takes a very similar form to equation (28). Here, we apply the same concept to classical mechanics. Instead of correlation functions of quantum fields, our observables are classical. Specifically, the observables we are most interested in are the phase space trajectory, the density field as well as (classical) correlation functions of the density field.

We have already shown above how the phase space trajectory can be derived from the generating functional. In order to generate the phase space trajectory at time $t \in [t_i, t_f]$ we simply take a functional derivative of the generating functional with respect to the source field $\mathbf{J}(t)$. Written as an equation, we have

$$\left. \frac{\delta}{i \delta \mathbf{J}^T(t)} Z[\mathbf{J}; \mathbf{x}] \right|_{\mathbf{J}=0} = \tilde{\varphi}(t; \mathbf{x}). \quad (32)$$

We can also easily extract only the configuration or momentum parts of the phase space trajectory $\tilde{\varphi}^{(q)}(t; \mathbf{x})$ and $\tilde{\varphi}^{(p)}(t; \mathbf{x})$ by taking functional derivatives with respect to $\mathbf{J}^{(q)}(t)$ and $\mathbf{J}^{(p)}(t)$, respectively. Particularly the configuration space trajectory $\tilde{\varphi}^{(q)}(t; \mathbf{x})$ is of importance given that most properties of a classical system do not rely explicitly on the momentum.

The second important observable is the density field. It is different from the phase space trajectory in that it can be regarded as a macroscopic object. In order to make clear what is meant by this assertion, let us define the notions of microscopic and macroscopic in our setting. We are considering

a classical physical system with d degrees of freedom, i.e., the configuration space of our system has d dimensions. We refer to these degrees of freedom as microscopic and usually we consider systems with $d \gg 1$. An important example is interacting N -body systems in 3 dimensions for which $d = 3N$, namely every position coordinate of each particle acts as a microscopic degree of freedom.

KFT is a framework in which we can analytically keep track of large numbers of microscopic degrees of freedom. In fact, in some cases it is even possible to analytically take the limit of $d \rightarrow \infty$. However, we are rarely interested in microscopic quantities, e.g., for an interacting N -body system it is often irrelevant to precisely know the individual positions of all particles at all times. Instead, it is usually sufficient to know the collective properties of the system via macroscopic observables. These are functions which depend on the microscopic configuration in such a way that most of the complexity is projected out. Mathematically, they are maps from X to a low-dimensional space with a significant amount of symmetry or which have a very weak dependence on individual degrees of freedom.

For certain macroscopic observables it is possible to find an (approximate) evolution equation. An example for this are oscillations of crystals, so-called phonons, whose dynamics can be described without explicit reference to the configuration of the underlying system of a large number of periodically arranged atoms. In this case we may refer to macroscopic degrees of freedom and completely avoid dealing with the microscopic dynamics. One potential problem with such macroscopic descriptions is that the evolution equations are usually only approximately correct. Often, they result from smoothing over discrete particles to obtain a continuous smooth macroscopic field and then describing its perturbations around a certain background field value or evolution. Care has to be taken that these approximations are valid for the entirety of the evolution of the system.

Instead of attempting to model the evolution of macroscopic fields, KFT conventionally derives these macroscopic quantities directly from the microscopic dynamics. It should be mentioned, however, that so-called Resummed Kinetic Field Theory (RKFT) provides a formalism for working directly with macroscopic fields, though the underlying dynamical equations remain microscopic.[41, 42] In this thesis we work with the conventional approach to KFT. In particular, we describe the evolution of the microscopic degrees of freedom in phase space and treat macroscopic observables as derived quantities.

In our discussion it has become apparent that the definition of a macroscopic observable usually requires the existence of components of our system. Indeed, the macroscopic system is made up from the collection of these microscopic components—providing a separation of scales. In many examples, the microscopic components are particles, while the macroscopic system may, e.g., be a crystal or a fluid. Mathematically, we encode such a property as follows: Let X_j for $1 \leq j \leq N$ be the phase spaces of the microscopic components. We allow for the case of $N = 1$, where the entire system is treated as microscopic. Together,

these components make up the classical physical system under consideration, i.e., we demand that

$$\mathbf{X} = X_1 \times X_2 \times \dots \times X_N \quad \text{with} \quad \mathbf{x} = (x_1, x_2, \dots, x_N). \quad (33)$$

Given our definition of phase space $\mathbf{X} = (\mathbf{X}^{(q)}, \mathbf{X}^{(p)})$ the equality above is understood to be valid up to reordering. In many applications we have $X_j = X_k$ for all j, k and we can simply write $\mathbf{X} = X^N$.

At this point we can finally explain why we have been using bold faced mathematical symbols so far: From the beginning, we were anticipating that the classical physical system is allowed to result from combining a potentially large number of components. In fact, even the limit $N \rightarrow \infty$ can be taken in some cases. Throughout this thesis, bold faced mathematical symbols are related to the entire system. Quantities involving components are regular faced and indexed by subscripts. We use letters from the middle of the Roman alphabet for these subscripts, usually j, k, ℓ, m . The Einstein sum convention does not apply to these indices.

Our discussion and construction of phase space \mathbf{X} transfers completely to the component phase spaces X_j except for aspects related to the equations of motion. Due to interactions between the components, it may not be possible to find equations of motion for each component individually. But even if this is feasible, the solution of such equations for the j^{th} component would require initial conditions for all components and not only $x_j \in X_j$.

Let us return to the density field as a specific example for a macroscopic observable. We define the *microscopic density* of the j^{th} component as

$$\rho_j : X_j \rightarrow \bar{C}^\infty(X_j, \mathbb{R}) \quad \text{with} \quad \rho_j(x; x_j) := \delta_D(x - x_j). \quad (34)$$

We denoted by $\bar{C}^\infty(X_j, \mathbb{R})$ the set of distributions from X_j to \mathbb{R} . The definition is to be understood in the sense that given the state of the component $x_j \in X_j$, the density is a distribution which returns a real number $\rho_j(x; x_j)$ given (almost) any state $x \in X_j$. This distribution is a Dirac δ -function because once we fix the state of the component to be $x_j \in X_j$, the density needs to be zero for any state $x \neq x_j$.

Given an evolution map $\varphi_j(t)$ for the j^{th} component, the density $\rho_j(x; \varphi_j(t))$ effectively becomes a time dependent distribution on X_j . In this context, the physical microscopic density of the j^{th} component

$$\tilde{\rho}_j(x, t; \mathbf{x}) := \rho_j(x; \tilde{\varphi}_j(t; \mathbf{x})) \quad (35)$$

is of special importance. It is the microscopic density of the component when evaluated on the physical evolution. This is indicated by an overset tilde, which we use throughout this thesis to denote observables of a physically evolving system. Note that this notation is consistent, since the physical evolution map $\tilde{\varphi}$ itself can be regarded as such an observable.

The physical microscopic density can be easily obtained from the generating functional. Indeed, we simply replace

$$\tilde{\varphi}_j(t; \mathbf{x}) \mapsto \frac{\delta}{i \delta J^T(t)} \quad (36)$$

in its definition. The idea is that this derivative turns back into the phase space trajectory upon acting on the generating functional and setting the source field \mathbf{J} to zero. This way, the original expression is recovered. Explicitly, it is

$$\tilde{\rho}_j(\mathbf{x}, t; \mathbf{x}) = \rho_j \left(\mathbf{x}; \frac{\delta}{i \delta \mathbf{J}_j^T(t)} \right) Z[\mathbf{J}; \mathbf{x}] \Big|_{\mathbf{J}=0}, \quad (37)$$

though it is somewhat technically involved to show this explicitly here due to the Dirac δ -function in ρ_j . Instead we provide a proof of concept for the Fourier transform of the density defined below. In the equation, the quantity J_j is the component of the source field \mathbf{J} corresponding to $\tilde{\varphi}_j$, i.e., the component which gets coupled to $\tilde{\varphi}_j$ via the scalar product $\mathbf{J} \cdot \tilde{\varphi}$ in equation (28).

For various reasons we will often encounter the Fourier transform of the density in our applications. We use the convention

$$f(\mathbf{k}) = \int_{-\infty}^{\infty} d\mathbf{x} f(\mathbf{x}) e^{-i\mathbf{k} \cdot \mathbf{x}} \quad \text{and} \quad f(\mathbf{x}) = \int_{-\infty}^{\infty} \frac{d\mathbf{k}}{(2\pi)^d} f(\mathbf{k}) e^{i\mathbf{x} \cdot \mathbf{k}} \quad (38)$$

for the Fourier transform of a function $f: \mathbf{X} \rightarrow \mathbb{R}$. Specifically, the minus sign appears in the Fourier transform and the numerical prefactor in the inverse Fourier transform. Note that we distinguish between the function f and its Fourier transform only via their argument. In Fourier space, the physical microscopic density takes the form

$$\tilde{\rho}_j(\mathbf{k}, t; \mathbf{x}) := \exp(-i\mathbf{k} \cdot \tilde{\varphi}_j(t; \mathbf{x})). \quad (39)$$

Again, through the replacement (36) we can extract $\tilde{\rho}_j(\mathbf{k}, t; \mathbf{x})$ directly from the generating functional. As promised above, in this case we can explicitly prove this assertion without resorting to an abundance of technical subtleties. The key idea is to expand the exponential function into a power series—which actually is the way to properly define what is meant by an (exponential) function evaluated on an expression involving a derivative. It is

$$\begin{aligned} & \exp \left(-i\mathbf{k} \cdot \frac{\delta}{i \delta \mathbf{J}_j^T(t)} \right) Z[\mathbf{J}; \mathbf{x}] \Big|_{\mathbf{J}=0} \\ &= \left(\sum_{m=0}^{\infty} \frac{(-i)^m}{m!} \left(\mathbf{k} \cdot \frac{\delta}{i \delta \mathbf{J}_j^T(t)} \right)^m \right) \exp \left(i \int_{t_i}^{t_f} dt' \mathbf{J}(t') \cdot \tilde{\varphi}(t'; \mathbf{x}) \right) \Big|_{\mathbf{J}=0} \end{aligned} \quad (40)$$

$$= \left(\sum_{m=0}^{\infty} \frac{(-i)^m}{m!} (\mathbf{k} \cdot \tilde{\varphi}_j(t; \mathbf{x}))^m \right) \exp \left(i \int_{t_i}^{t_f} dt' \mathbf{J}(t') \cdot \tilde{\varphi}(t'; \mathbf{x}) \right) \Big|_{\mathbf{J}=0} \quad (41)$$

$$= \tilde{\rho}_j(\mathbf{k}, t; \mathbf{x}). \quad (42)$$

We remark that inserting derivatives into a function has similarities to the more common occurrence of inserting a matrix into a function. The formal definition of this procedure is via a power series expansion, too. Conversely, difficulty caused due to non-commutativity of matrices is also a recurring issue for this kind of operations with derivatives.

Let us now define the macroscopic density function. For this purpose, we assume that all component phase spaces are equal, i.e., it is $\mathbf{X} = X^N$. We define the *macroscopic density* as

$$\rho: \mathbf{X} \rightarrow \bar{C}^\infty(X, \mathbb{R}) \quad \text{with} \quad \rho(\mathbf{x}; \mathbf{x}) := \sum_{j=1}^N \rho_j(\mathbf{x}; \mathbf{x}_j) . \quad (43)$$

For the special case $N = 1$ we obtain the system's phase space density. For $N > 1$ we effectively project onto the component phase space X and sum over the contributions of the various components. As an example, the macroscopic density for an N -body system is the sum over the contributions to the density from all particles. The macroscopic density is thus a sum over Dirac δ -functions.

Just as for the microscopic density, we are usually most interested in the physical macroscopic density, i.e., the density evaluated along the physical evolution of the system. It is simply given by

$$\tilde{\rho}(\mathbf{x}, t; \mathbf{x}) := \sum_{j=1}^N \tilde{\rho}_j(\mathbf{x}, t; \mathbf{x}) . \quad (44)$$

Due to linearity of the Fourier transform, this relationship holds analogously in Fourier space. In both cases, the component densities $\tilde{\rho}_j$ can be obtained from the generating functional and thus the physical macroscopic density can be extracted from the generating functional via functional derivation with respect to the source field \mathbf{J} , too. The same holds true for the following observables.

In many physical systems, the interactions depend on the configuration of a system, but not its momentum. In fact, quite often the interactions have the form of a convolution of an interaction potential with the configuration space density. Above, the density functions we defined were phase space densities, i.e., they were distributions on the component phase space X . We define the *spatial macroscopic density* as

$$\tilde{\rho}^{(q)}(\mathbf{x}^{(q)}, t; \mathbf{x}) := \sum_{j=1}^N \tilde{\rho}_j^{(q)}(\mathbf{x}^{(q)}, t; \mathbf{x}) := \sum_{j=1}^N \delta_D(\mathbf{x}^{(q)} - \tilde{\varphi}_j^{(q)}(t; \mathbf{x})) . \quad (45)$$

This is a slight abuse of our notation of superscribed $\bullet^{(q)}$ which in this particular case does not pick out elements of a vector, but rather terms from a product. The spatial density is one of the most important observables for the applications considered in this thesis.

Equally important to the spatial macroscopic density are its r -point correlation functions⁶. These are closely related to the density power spectrum which is an important observable in cosmological applications. Notably, the density correlation functions encode properties of the density field which are obscured when analyzing the density in a statistical setting. While this statement becomes clear once we define expectation values of observables in section 2.4.3, we remark already at this point that expectation values of density correlation

⁶ We refrain from using the more common term n -point correlation function because the letter n acts as a central expansion index in the perturbative approach to KFT.

functions supply vastly more information in a statistically homogeneous setting than the expectation value of the density itself.

We define the density correlation functions only in Fourier space and only for the macroscopic density functions. The r -point density correlation function is given by

$$G_{\underbrace{\tilde{\rho} \dots \tilde{\rho}}_{r \text{ times}}}(k_1, k_2, \dots, k_r, t; \mathbf{x}) := \prod_{s=1}^r \tilde{\rho}(k_s, t; \mathbf{x}). \quad (46)$$

Analogously, the r -point correlation function for the spatial density $G_{\tilde{\rho} \dots \tilde{\rho}}^{(q)}$ is defined as the product over r Fourier space spatial densities. Note that these products become convolutions upon performing an inverse Fourier transform. Fortunately, we only need the density correlation functions in Fourier space as our primary use of them is to extract the density power spectrum—which likewise is a Fourier space object.

We close this subsection by defining general observables. Let \mathcal{O} be any function or distribution of $\mathbf{x} \in \mathbf{X}$ and potentially some other parameters χ such that $\mathcal{O}(\chi; \mathbf{x})$ is a quantity of interest. The associated physical observable, i.e., the function \mathcal{O} evaluated along the physical phase space trajectory is then

$$\tilde{\mathcal{O}}(\chi, t; \mathbf{x}) = \mathcal{O}(\chi; \tilde{\varphi}(t; \mathbf{x})) = \mathcal{O}\left(\chi; \frac{\delta}{i \delta \mathbf{J}^T(t)}\right) Z[\mathbf{J}; \mathbf{x}] \Big|_{\mathbf{J}=0}. \quad (47)$$

Note that the replacement (36) in the last step requires that \mathcal{O} is an analytic function of \mathbf{x} . Otherwise inserting a functional derivative into the function \mathcal{O} might not be well-defined.

2.2.2 Example: Harmonic Oscillator (II)

Let us briefly return to the harmonic oscillator as an example. Given its simplicity, it admits an analytic solution $\tilde{\varphi}$ which can be found in equation (26). Thus, its generating functional

$$Z[\mathbf{J}; \mathbf{x}] = \exp\left(\int dt' \mathbf{J}(t') \cdot \tilde{\varphi}(t'; \mathbf{x})\right) \quad (48)$$

is an analytic function in \mathbf{J} . There is little point in writing it down explicitly here, but we emphasize that given the existence of such an analytic expression the equations of the previous subsection are no longer purely formal for the harmonic oscillator.

The focus of this subsection is instead to provide an example for the definition of the microscopic and macroscopic density fields defined above. We have already prepared for this: By using normal faced symbols in subsection 2.1.5, we reserved bold faced symbols for a composite system made up from N independent harmonic oscillators. The mathematical objects and equations in subsection 2.1.5 can then be regarded as describing any one of them.

The full system has phase space $\mathbf{X} = \mathbf{X}^N$, i.e., its state is simply given as an N -tuple of states in \mathbf{X} . The physical evolution of the composite system is

$$\tilde{\varphi}(t; \mathbf{x}) = \left(\left(\tilde{\varphi}_1^{(q)}(t; \mathbf{x}), \dots, \tilde{\varphi}_N^{(q)}(t; \mathbf{x}) \right), \left(\tilde{\varphi}_1^{(p)}(t; \mathbf{x}), \dots, \tilde{\varphi}_N^{(p)}(t; \mathbf{x}) \right) \right). \quad (49)$$

Note that in general the physical evolution of, e.g., the first component $\tilde{\varphi}_1$ depends on the initial state of the full composite system \mathbf{x} . Here, we assumed the harmonic oscillators to be independent, hence $\tilde{\varphi}_1$ actually only depends on the initial state of the first component \mathbf{x}_1 .

The independence between the components is also reflected by the form of the Hamiltonian which is simply a sum over the component Hamiltonians

$$\mathcal{H}(\mathbf{x}) = \sum_{j=1}^N \mathcal{H}_j(\mathbf{x}_j) = \sum_{j=1}^N \left(\frac{(\mathbf{x}_j^{(p)})^2}{2m} + \frac{1}{2} \kappa (\mathbf{x}_j^{(q)})^2 \right). \quad (50)$$

Deriving Hamilton's equations consequently yields N independent copies of equation (25) from which analytic expressions for the component physical evolutions $\tilde{\varphi}_j$ for all j can be derived. The generating functional of the combined system simply is

$$Z[\mathbf{J}; \mathbf{x}] = \exp \left(\int dt' \mathbf{J}(t') \cdot \tilde{\boldsymbol{\varphi}}(t'; \mathbf{x}) \right). \quad (51)$$

The physical microscopic density of the j^{th} component is given by

$$\tilde{\rho}_j(\mathbf{x}, t; \mathbf{x}) = \delta_D(\mathbf{x} - \tilde{\boldsymbol{\varphi}}_j(t; \mathbf{x})) = \delta_D \left(\mathbf{x} - \frac{\delta}{i \delta \mathbf{J}_j^T(t)} \right) Z[\mathbf{J}; \mathbf{x}]. \quad (52)$$

One can write down an analogue expression for the combined system. This yields the microscopic density of the system of N harmonic oscillators which is non-zero at time t if and only if the argument $\mathbf{x} \in \mathcal{X}$ matches the state of the entire system $\tilde{\boldsymbol{\varphi}}(t; \mathbf{x})$. It can be regarded as the product of the component microscopic densities. However, more important in applications, particularly if the components are indistinguishable, is the macroscopic density of the system. It is given as the sum over the component densities $\tilde{\rho}_j$ for all j . As an equation, we obtain

$$\tilde{\rho}(\mathbf{x}, t; \mathbf{x}) = \sum_{j=1}^N \delta_D \left(\mathbf{x} - \frac{\delta}{i \delta \mathbf{J}_j^T(t)} \right) Z[\mathbf{J}; \mathbf{x}]. \quad (53)$$

Given initial conditions \mathbf{x} and fixing a time t , it is a distribution on \mathcal{X} , i.e., on component phase space. The Dirac δ -functions give a contribution for argument \mathbf{x} if any of the harmonic oscillators is in state \mathbf{x} as opposed to $\tilde{\rho}_j$ which gives a contribution for this argument only if the j^{th} harmonic oscillator is in this state. The spatial version $\tilde{\rho}^{(q)}$ as well as expressions in Fourier space can be obtained easily using the definitions above.

2.2.3 Classical Path Integrals

Above we introduced an important idea of KFT: *Determine analytic expressions for observables without explicitly solving the system.* We showed that the generating functional $Z[\mathbf{J}; \mathbf{x}]$ can be used to analytically derive expressions for observables $\tilde{\mathcal{O}}$ from a single mathematical object. However, our definition of $Z[\mathbf{J}; \mathbf{x}]$

in equation (28) explicitly involves the physical evolution map $\tilde{\varphi}$. This is contrary to our idea, because this means that in order to construct the generating functional we first need to explicitly solve the system to find an expression for $\tilde{\varphi}$.

In this subsection we manipulate our expression for the generating functional in order to avoid explicit dependence on the solution of the equations of motion. At least conceptually, this allows us to analytically find an expression for the generating functional without first having to explicitly solve the system. Such an expression could then be used to accomplish our aim of determining observables without solving the equations of motion. In practice, finding an analytic form for the generating functional is usually of similar difficulty as finding an analytic form for the physical evolution. However, this is not true for the expressions for many observables derived from the generating functional, particularly in the case of statistical initial conditions. Thus, even if the generating functional remains an abstract mathematical object, it provides the basis of a formalism to explicitly determine observables.

Recall that the generating functional is defined as

$$Z[\mathbf{J}; \mathbf{x}] = \exp\left(i \int_{t_i}^{t_f} dt' \mathbf{J}(t') \cdot \tilde{\varphi}(t'; \mathbf{x})\right). \quad (54)$$

It depends explicitly on the physical evolution map $\tilde{\varphi}(t'; \mathbf{x})$ and through it also on the initial conditions $\mathbf{x} \in \mathbf{X}$. We can write the generating functional equivalently in the form

$$Z[\mathbf{J}; \mathbf{x}] = \int \mathcal{D}\varphi \delta_{\mathcal{D}}[\varphi - \tilde{\varphi}(\bullet; \mathbf{x})] \exp\left(i \int_{t_i}^{t_f} dt' \mathbf{J}(t') \cdot \varphi(t')\right). \quad (55)$$

As usual, the \bullet is a placeholder for the parameter of the function, in this case the time t . It is required, given that the Dirac δ -functional is to be evaluated on a function, not a number. Effectively, it encodes the condition $\varphi = \tilde{\varphi}(\bullet; \mathbf{x})$ which is equivalent to $\varphi(t) = \tilde{\varphi}(t; \mathbf{x})$ for all $t \in \mathbb{R}$. The Dirac δ -functional thus is a generalized version of the Dirac δ -function. Its defining properties are

$$\delta_{\mathcal{D}}[f] = 0 \quad \forall f \neq 0 \quad \text{and} \quad \int \mathcal{D}f G[f] \delta_{\mathcal{D}}[f] = G[0] \quad \forall \text{ functional } G \quad (56)$$

in perfect analogy to the defining properties of the Dirac δ -function.

The Dirac δ -functional's key property of canceling path integrals yields the equivalence of the two expressions for the generating functional above. Clearly, the expression in equation (55) reduces to our original definition of $Z[\mathbf{J}; \mathbf{x}]$ when the path integral over φ is canceled by the Dirac δ -functional and thereby replaces the evolution map φ by the physical evolution map $\tilde{\varphi}(\bullet; \mathbf{x})$.

Of course we did not make our expression more difficult without an ulterior motive. Equation (55) allows us to interpret the generating functional as a mathematical object with the potential of receiving contributions from all possible evolutions of the system, but then the Dirac δ -functional selects the classical solution of the equations of motion as the unique path whose contribution is taken into account. This is of course very reminiscent of the path integral

approach to quantum mechanics, with the key difference that in the quantum realm the contributions of all paths are relevant. The sharp Dirac δ -distribution of classical mechanics is replaced by a smooth function $\exp\left(\frac{i}{\hbar}S[\varphi]\right)$, where S is the action.[36, chapter 20]

Apart from the similarities to the path integral formulation of quantum mechanics, equation (55) provides an expression for the generating functional which reminds of Hamilton's principle of stationary action. This principle implies that the phase space trajectory chosen by the Dirac δ -functional is the one which extremizes the action. More specifically, recalling our discussion at the end of subsection 2.1.4, this trajectory is the one along which the equations of motion are satisfied. Therefore, the conditions

$$\varphi - \tilde{\varphi}(\bullet; \mathbf{x}) = 0 \quad \text{and} \quad \mathbf{E}[\varphi] = 0 \quad (57)$$

are equivalent once we demand separately that $\varphi(t_i) = \mathbf{x}$.

While the left-hand condition equation (57) is the one appearing in the Dirac δ -functional in equation (55), the right-hand condition has the significant advantage of not explicitly involving the physical evolution map $\tilde{\varphi}$. Hence, we would like to replace the former condition by the latter and thereby get rid of the explicit dependence of the generating functional on the solution of the equations of motion. This would accomplish the first key idea of KFT we have been working towards throughout this section. In order to achieve this, we need to overcome two technical problems. Firstly, we need to separately encode the condition $\varphi(t_i) = \mathbf{x}$. And secondly, we need to rigorously replace the conditions in the Dirac δ -functional.

The first issue is quite minor. The path integral over all evolution maps φ in general places no constraints on the boundary values $\varphi(t_i)$ and $\varphi(t_f)$. However, such conditions frequently arise in practice, hence there exists the notion of definite path integrals, i.e., path integrals subject to boundary conditions. Thus, the condition $\varphi(t_i) = \mathbf{x}$ can be accounted for via the replacement

$$\int \mathcal{D}\varphi \mapsto \int_{\mathbf{x}} \mathcal{D}\varphi := \int_{\varphi(t_i)=\mathbf{x}} \mathcal{D}\varphi, \quad (58)$$

where the notation $\int_{\mathbf{x}}$ is an abbreviation used throughout this thesis. The resulting path integral is restricted to all phase space trajectories satisfying the initial conditions which is exactly what we require.

The second problem is mathematically more involved. While it is true that

$$\delta_{\mathbf{D}}[\varphi - \tilde{\varphi}(\bullet; \mathbf{x})] = 0 \quad \Leftrightarrow \quad \delta_{\mathbf{D}}[\mathbf{E}[\varphi]] = 0, \quad (59)$$

the normalization condition in equation (56) needs to be checked, too, if we intend to replace the left-hand Dirac δ -function by the right-hand one. Recall that the multidimensional Dirac δ -function satisfies

$$\delta_{\mathbf{D}}(f(\mathbf{x})) = \sum_{\text{roots } \tilde{\mathbf{x}}} \left(\det \left(\frac{\partial f}{\partial \mathbf{x}}(\tilde{\mathbf{x}}) \right) \right)^{-1} \delta_{\mathbf{D}}(\mathbf{x} - \tilde{\mathbf{x}}) \quad (60)$$

under the assumption that the roots $\tilde{\mathbf{x}}$ of the function $f: \mathbb{R}^d \rightarrow \mathbb{R}^d$ are isolated. This equation can be generalized to the Dirac δ -functional by replacing the

function f by a functional and the Jacobian matrix $\frac{\partial f}{\partial \mathbf{x}}$ by its functional analogue. In our case, it is

$$\delta_{\mathbb{D}}[\mathbf{E}[\boldsymbol{\varphi}]] = \left(\det \left(\frac{\delta \mathbf{E}}{\delta \boldsymbol{\varphi}} [\tilde{\boldsymbol{\varphi}}(\bullet; \mathbf{x})] \right) \right)^{-1} \delta_{\mathbb{D}}[\boldsymbol{\varphi} - \tilde{\boldsymbol{\varphi}}(\bullet; \mathbf{x})], \quad (61)$$

using that the equations of motion are uniquely solved by the physical evolution. Note that we assume here that the initial conditions are fixed via the replacement (58).

Equation (61) requires us to compute the functional determinant of the functional Jacobi matrix of the equations of motion $\mathbf{E}[\boldsymbol{\varphi}]$. Using that the equations of motion are Hamilton's equations (16), it is

$$\frac{\delta \mathbf{E}}{\delta \boldsymbol{\varphi}} [\tilde{\boldsymbol{\varphi}}(\bullet; \mathbf{x})](t) = \frac{\delta}{\delta \boldsymbol{\varphi}(t)} \left(\frac{d}{dt'} \boldsymbol{\varphi}(t') - \mathcal{J} \frac{\delta \mathcal{H}(\boldsymbol{\varphi}(t'))}{\delta \boldsymbol{\varphi}(t')} \right) \Big|_{\boldsymbol{\varphi}(t) = \tilde{\boldsymbol{\varphi}}(t; \mathbf{x})} \quad (62)$$

$$= \frac{d}{dt'} \delta_{\mathbb{D}}(t' - t) \mathbb{I}_{2d} - \underbrace{\mathcal{J} \frac{\delta^2 \mathcal{H}(\tilde{\boldsymbol{\varphi}}(t; \mathbf{x}))}{\delta \boldsymbol{\varphi}(t) \delta \boldsymbol{\varphi}(t)}}_{=: M(t)}. \quad (63)$$

The quadratic derivative of the Hamiltonian \mathcal{H} in the last line is the functional Hessian and thus is a symmetric matrix. It can be shown via elementary linear algebra that the product of a symplectic with a symmetric matrix has vanishing trace, hence the second term in the last line is a traceless matrix $M(t)$.

Following the treatment in [43], we can write the functional determinant as

$$\det \left(\frac{\delta \mathbf{E}}{\delta \boldsymbol{\varphi}} [\tilde{\boldsymbol{\varphi}}(\bullet; \mathbf{x})] \right) = \underbrace{\det \left(\frac{d}{dt} \right)}_{=: C} \det \left(\mathbb{I}_{2d} - \left(\frac{d}{dt} \right)^{-1} M \right). \quad (64)$$

The first term C can be evaluated by using tools from functional analysis. However, as it turns out, we do not need to actually evaluate it. The important term is the second factor, which can be rewritten as

$$\det \left(\mathbb{I}_{2d} - \left(\frac{d}{dt} \right)^{-1} M \right) = \exp \left(\text{tr} \left(\ln \left(\mathbb{I}_{2d} - \left(\frac{d}{dt} \right)^{-1} M \right) \right) \right) \quad (65)$$

$$= \exp \left(-\theta(0) \int dt \text{tr}(M(t)) \right). \quad (66)$$

The second equality uses that the Heaviside function θ is a Green's function for the derivative operator $\frac{d}{dt}$. Applying the functional trace to a series expansion of the logarithm, all higher order terms vanish due to properties of the Heaviside function.

In [35, section 3.2], it is argued that in classical mechanics we ought to set $\theta(0) = 0$, such that the determinant in equation (65) is unity. We adopt this convention and discuss the topic in more detail in section 2.3.1, where we demand that in KFT Green's functions need to be causal. In order for the Heaviside function θ to qualify as a Green's function, we thus need $\theta(t) = 0$ for $t \leq 0$. Nonetheless, using the symplectic structure of Hamilton's equations, we have seen above that $\text{tr}(M(t)) = 0$ such that the determinant is unity even if one were to adopt the more common choice $\theta(0) = \frac{1}{2}$.

Making use of the identity

$$\delta_D[\mathbf{E}[\boldsymbol{\varphi}]] = C \delta_D[\boldsymbol{\varphi} - \tilde{\boldsymbol{\varphi}}(\bullet; \boldsymbol{\chi})] \quad (67)$$

established by the detailed discussion above, we can rewrite the generating functional as

$$Z[\mathbf{J}; \boldsymbol{\chi}] = \int \mathcal{D}\boldsymbol{\varphi} \delta_D[\boldsymbol{\varphi} - \tilde{\boldsymbol{\varphi}}(\bullet; \boldsymbol{\chi})] \exp\left(i \int_{t_i}^{t_f} dt' \mathbf{J}(t') \cdot \boldsymbol{\varphi}(t')\right) \quad (68)$$

$$= C^{-1} \int_{\boldsymbol{\chi}} \mathcal{D}\boldsymbol{\varphi} \delta_D[\mathbf{E}[\boldsymbol{\varphi}]] \exp\left(i \int_{t_i}^{t_f} dt' \mathbf{J}(t') \cdot \boldsymbol{\varphi}(t')\right). \quad (69)$$

This achieves a main goal set out above: The generating functional is no longer explicitly dependent on the solution of the equations of motion. Using a functional Fourier transform of the Dirac δ -functional, we obtain a fully analytic expression for the generating functional

$$Z[\mathbf{J}; \boldsymbol{\chi}] = C^{-1} \int_{\boldsymbol{\chi}} \mathcal{D}\boldsymbol{\varphi} \int \mathcal{D}\boldsymbol{\chi} \exp\left(i \int_{t_i}^{t_f} dt' (\boldsymbol{\chi}(t') \cdot \mathbf{E}[\boldsymbol{\varphi]}(t') + \mathbf{J}(t') \cdot \boldsymbol{\varphi}(t'))\right). \quad (70)$$

2.3 FREE EVOLUTION AND INTERACTIONS

In a slight shift of style, let us introduce this section by referencing a subtle and instructive question: *Newton's second law implies that for vanishing force there is no acceleration—why then is Newton's first law needed?* One could even elaborate and deduce the equation for uniform motion of a point-particle from the vanishing of the second derivative of its position. Why does this not show that Newton's first law is implied by his second law?

The answer is connected to two important concepts in physics: Firstly, a deviation is only ever well-defined provided a reference. Interactions are always to be considered relative to free evolution. This is the basis for any perturbative treatment of a physical system. Secondly, one might wonder what happens if one were to abandon Newton's first law. Clearly, the second law would need to be adjusted depending on the chosen reference motion. This freedom of choice can be regarded as an example of gauge freedom.

Whenever we refer to free evolution in a physical system, we presume that this implies simplicity. Interactions make a system complicated, while free evolution usually can be solved exactly. In order to formalize this idea, we introduce Green's functions in the first subsection below. We require their existence for the free system to ensure it can be solved. Based on this, we perform a split in the equations of motion of the system in a free and an interaction part.

In subsection 2.3.2 we investigate the freedom in choosing the free motion. We refer to a choice of split in the equations of motion as splitting gauge and introduce a few natural gauge choices. The most important of these is Newtonian gauge which reproduces Newton's first law of motion. We briefly discuss an approach to formalize the gauge freedom and gauge transformations.

The Harmonic Oscillator serves yet again as an example. We consider the splitting of its equations of motion in the various gauge choices introduced in subsection 2.3.2. Regardless of gauge choice, the physical evolution can be obtained by taking the sum of free evolution and the interactions as evaluated along the physical evolution. We confirm this explicitly for the Harmonic Oscillator.

The final and by far longest subsection of this section investigates the effect of splitting the equations of motion on the generating functional. After a series of manipulations we obtain one of the central equations of KFT which takes the form

$$Z[\mathbf{J}; \mathbf{x}] = \exp\left(i \int_{t_i}^{t_f} dt' \frac{\delta}{i \delta \mathbf{K}(t')} \cdot \mathbf{E}_I \left[\frac{\delta}{i \delta \mathbf{J}^T} \right] (t')\right) \exp\left(i \int_{t_i}^{t_f} dt' \int_{t_i}^{t'} dt'' \mathbf{J}^T(t') \mathbf{G}(t', t'') (\delta_D(t'' - t_i) \mathbf{x} - \mathbf{K}(t''))\right) \Big|_{\mathbf{K}=0} \quad (71)$$

and thus achieves a split of the generating functional. The argument of the first exponential is the so-called interaction operator, while the second exponential contains the free evolution.

Subsequently we perform simplifications of this expression. In particular, we are able to remove the auxiliary field \mathbf{K} from the formalism. We remark

that all manipulations performed in this section are exact. This accomplishes the second key idea of KFT: *Split free evolution from interactions while keeping the description exact.*

The splitting of the equations of motion is central to KFT, especially in the perturbative treatment of interactions. Thus it is present in the works of [23, 24] and most of the later literature in the field. To the best of my knowledge, the removal of the field \mathbf{K} was first presented in [1], though a slight inaccuracy is corrected here. The splitting freedom is discussed in [1], but more details are presented here. Unfortunately, I cannot recall who first mentioned the brilliant question regarding Newton's laws to me.

2.3.1 Green's Functions

The easiest classical physical systems are those for which we can solve the initial value problem consisting of the equations of motions $\mathbf{E}[\boldsymbol{\varphi}] = \mathbf{0}$ and the initial conditions $\boldsymbol{\varphi}(t_i) = \mathbf{x}$. We usually say that we analytically solved such an initial value problem if we can find an explicit expression for the physical evolution map $\tilde{\boldsymbol{\varphi}}(t; \mathbf{x})$. However, there is a somewhat stronger notion of having solved the system which the discussion in this section relies on: a Green's function or propagator.

Given an equation of motion $\mathbf{E}[\boldsymbol{\varphi}] = \mathbf{0}$ we say that $\tilde{\mathbf{G}}$ is a *Green's function* if

$$\mathbf{E}[\tilde{\mathbf{G}}(\bullet, t')](t) = \delta_D(t - t') \mathbb{I}_{2d} \quad (72)$$

for all $t, t' \in [t_i, t_f]$. Mathematically, the Green's function can be regarded as a map $\tilde{\mathbf{G}}: \mathbb{R} \times \mathbb{R} \rightarrow \mathcal{M}_{2d \times 2d}(\mathbb{R})$, i.e., yields real square matrices given two real parameters. Using that $\mathbf{X} = \mathbb{R}^{2d}$ by definition, we can consider the Green's function as a map

$$\tilde{\mathbf{G}}(t, t'): \mathbf{X} \rightarrow \mathbf{X} \quad \text{with} \quad \mathbf{x} \mapsto \tilde{\mathbf{G}}(t, t') \mathbf{x} \quad (73)$$

given arbitrary, but fixed parameters $t, t' \in [t_i, t_f]$. The action of $\tilde{\mathbf{G}}$ on \mathbf{x} is by standard matrix multiplication.

In order to make equation (72) well-defined, we need to specify how \mathbf{E} acts on objects in $\mathcal{M}_{2d \times 2d}(\mathbb{R})$. In case \mathbf{E} is a linear (differential) operator, i.e., the action of \mathbf{E} is by right-multiplication, $\mathbf{E}[\boldsymbol{\varphi}] = \mathbf{E}\boldsymbol{\varphi}$, the generalization is trivially $\mathbf{E}[\tilde{\mathbf{G}}] = \mathbf{E}\tilde{\mathbf{G}}$. Otherwise, we demand that \mathbf{E} acts column-wise which coincides with the mentioned right-multiplication in the linear case.

In this thesis we consider classical physical systems. In particular, the equations of motion describe deterministic and causal physical evolution. Therefore, we restrict ourselves to *causal Green's functions* which incorporate these properties. In order to qualify as causal, we demand that a Green's function $\tilde{\mathbf{G}}$ satisfies

$$\tilde{\mathbf{G}}(t, t') = \mathbf{0} \quad \text{for} \quad t, t' \in [t_i, t_f] \quad \text{with} \quad t \leq t'. \quad (74)$$

This condition ensures causality in the sense that the map $\tilde{\mathbf{G}}(t, t'): \mathbf{X} \rightarrow \mathbf{X}$ gives a non-zero contribution only if time-ordering $t > t'$ is obeyed. We see below more specifically that otherwise causality can be violated.

Finding a (causal) Green's function is a stronger notion of solving a differential equation than determining the solution $\tilde{\varphi}$, because the latter can be obtained from the former. Indeed, provided that the initial value problem has a unique solution, it is

$$\tilde{\varphi}(t; \mathbf{x}) = \tilde{\mathbf{G}}(t, t_i) \mathbf{x}. \quad (75)$$

Inserting this expression for the physical evolution map into the equations of motion one obtains $\mathbf{E}[\tilde{\varphi}(\bullet; \mathbf{x})](t) = \delta_{\mathbb{D}}(t - t_i) \mathbf{x}$. Clearly, this implies that the equations of motion are satisfied for $t > t_i$, but they appear to be violated at initial time t_i . However, this is only a technicality: Generically Green's functions give the fundamental solution to a differential equation, so in order to apply the formalism to initial value problems, we treat the initial value \mathbf{x} as a source at initial time t_i . While this means that we cannot use equation (75) for $t \leq t_i$, it provides a simple and correct expression for $t > t_i$.

We emphasize that it is rare for a general differential equation to allow for a Green's function. In fact, commonly they are only defined for linear differential equations, where they usually exist⁷ and are a standard tool. Our reason for introducing Green's functions here is their very useful property of providing a solution not only to a given differential equation, but also to inhomogeneous modifications of it. Specifically, assuming that $\tilde{\mathbf{G}}$ is a Green's function for a differential equation $\mathbf{E}[\varphi] = \mathbf{0}$, then

$$\tilde{\varphi}_{\mathbf{K}}(t; \mathbf{x}) = \tilde{\mathbf{G}}(t, t_i) \mathbf{x} - \int_{t_i}^t dt' \tilde{\mathbf{G}}(t, t') \mathbf{K}(t') \quad (76)$$

is the solution of the inhomogeneous equation $\mathbf{E}[\varphi] + \mathbf{K} = \mathbf{0}$ with initial value \mathbf{x} . Note that if the Green's function would not satisfy equation (74), the upper integral boundary would need to be t_f instead of t and $\tilde{\varphi}_{\mathbf{K}}$ would receive acausal contributions. Indeed, $\tilde{\varphi}_{\mathbf{K}}$ at time t would then depend on the behavior of $\mathbf{K}(t')$ for $t' > t$. We further remark that setting $\mathbf{K}(t) = -\delta_{\mathbb{D}}(t - t_i) \mathbf{x}$ one obtains precisely the source term for the initial conditions \mathbf{x} we implicitly used above to apply the Green's function formalism to initial value problems.

The key benefit of the just described property is that if finding a Green's function for the equation $\mathbf{E}[\varphi] = \mathbf{0}$ is difficult or impossible, then we may try to find a Green's function for the equation $\mathbf{E}[\varphi] + \mathbf{K} = \mathbf{0}$ instead. Then $\tilde{\varphi}_{\mathbf{K}}$ as defined in equation (76) for the Green's function of the latter equation is a solution for the original equation. To reiterate in words, in order to solve an equation of motion we may modify it by addition of a function of time.

The additional flexibility of adding a function of time to the equations of motion is of course somewhat useful, but the main difficulty in finding solutions and Green's functions for non-trivial equations of motion is a non-linear dependence on the evolution map φ . Clearly, this issue cannot be remedied via adding a function of time to the equations of motion. While this is true in the

⁷ We are deliberately vague here in order to avoid a lengthy and irrelevant discussion. However, it should be mentioned that the question of the existence of Green's functions for a linear differential operator is different from the question of its existence for an initial (or boundary) value problem.

literal sense, within the formalism of KFT it is in fact possible to use a function of time to split off terms which depend on the evolution map φ . However, this splitting happens in the generating functional, not directly in the solution.

On a conceptual level, KFT thus provides a framework in which non-linear differential equations can be solved with Green's functions. Firstly, the equations of motion need to be split into a (usually linear) part which admits a Green's function and another term which may depend not only on the time parameter, but also on the evolution map. We usually refer to the former as the free part of the equations of motion \mathbf{E}_0 and the latter as the interaction part \mathbf{E}_I . Secondly, this splitting of the equations of motion provides a splitting in the generating functional which can, thirdly, be exploited in the calculation of observables. The remainder of this section is dedicated to a detailed description of this procedure.

Separating a free—or background—evolution from interactions is a key concept in many areas of physics and is strongly related with perturbation theory. Granted, such a separation does not necessarily need to be treated perturbatively. In principle, it is possible to describe the deflection of a particle from a straight path exactly even if the deflection is large. However, assuming that this deflection from free motion is small often allows for a significant simplification, terms which depend quadratically on the deflection can be neglected. Of course, this comes at the price that the solution obtained is only ever an approximation of the exact solution. This approximation can become arbitrarily inaccurate if the perturbation becomes large—a common feature in non-linear systems where often the error increases quickly with time. Unless the perturbation series can be resummed to recover the exact solution, care has to be taken with the validity of a perturbative treatment.

While we intend to treat interactions perturbatively in this thesis, in this chapter we merely perform a splitting in the equations of motion and investigate its effects on the generating functional and observables. No approximation is performed and thus the resulting expressions provide an exact physical description of the classical system we consider. This is the second key idea of KFT: *Split free evolution from interactions while keeping the description exact.*

Following the description above, let us assume that the equations of motion split into a free part \mathbf{E}_0 and an interaction part \mathbf{E}_I , i.e., the equations of motion read

$$\mathbf{E}[\varphi] = \mathbf{E}_0[\varphi] + \mathbf{E}_I[\varphi] = 0. \quad (77)$$

We demand that the free equation $\mathbf{E}_0[\varphi] = 0$ admits a causal Green's function \mathbf{G} . The only demand on \mathbf{E}_I is to be analytic, i.e., admitting a convergent series expansion in φ , hence there are infinitely many ways of performing such a split. We investigate this splitting freedom in more detail in the following subsection. For now, it is sufficient to assume that there is at least one such splitting.

There is one additional assumption on the free equation $\mathbf{E}_0[\boldsymbol{\varphi}] = \mathbf{0}$. In order for some manipulations performed below to be mathematically rigorous, we need to demand that

$$\det\left(\frac{d\mathbf{E}_0}{d\boldsymbol{\varphi}}[\bar{\boldsymbol{\varphi}}(\bullet; \mathbf{x})]\right) = \det\left(\frac{d\mathbf{E}}{d\boldsymbol{\varphi}}[\bar{\boldsymbol{\varphi}}(\bullet; \mathbf{x})]\right) \quad (78)$$

Here, $\bar{\boldsymbol{\varphi}}(\bullet, t)$ is the solution of the initial value problem given by $\mathbf{E}_0[\boldsymbol{\varphi}] = \mathbf{0}$ with $\boldsymbol{\varphi}(t_i) = \mathbf{x}$. We refer to it as the *free physical evolution map* $\bar{\boldsymbol{\varphi}}: \mathbb{R} \times \mathbf{X} \rightarrow \mathbf{X}^8$. Recalling equation (64), this is equivalent to the demand that the functional determinant above equals $C = \det\left(\frac{d}{dt}\right)$.

It follows immediately from the discussion in section 2.1.4 that the condition (78) is satisfied if $\mathbf{E}_0[\boldsymbol{\varphi}] = \mathbf{0}$ are Hamilton's equations. Hence, the easiest way of conforming to this technical demand is to consider a split in the Hamiltonian which induces the separation of the equations of motion in the form of equation (77). Let

$$\mathcal{H} = \mathcal{H}_0 + \mathcal{H}_I \quad (79)$$

be such a splitting and suppose that $\mathbf{E}_0[\boldsymbol{\varphi}] = \mathbf{0}$ are Hamilton's equations for \mathcal{H}_0 . Specifically, this means that

$$\mathbf{E}_0[\boldsymbol{\varphi}](t) = \frac{d}{dt}\boldsymbol{\varphi}(t) - \mathcal{J} \frac{\delta\mathcal{H}_0(\boldsymbol{\varphi}(t), t)}{\delta\boldsymbol{\varphi}(t)} \quad \text{and} \quad (80)$$

$$\mathbf{E}_I[\boldsymbol{\varphi}](t) = -\mathcal{J} \frac{\delta\mathcal{H}_I(\boldsymbol{\varphi}(t), t)}{\delta\boldsymbol{\varphi}(t)} \quad (81)$$

for all $t \in [t_i, t_f]$. We still have to explicitly require that the free equation admits a Green's function and that the interaction part is analytic in $\boldsymbol{\varphi}$, but the condition on the functional determinant in equation (78) is automatically satisfied.

Our guiding idea is to use the Green's function of the free equation to express the solution of the full equations of motion. Ideally, we would like to obtain an equation similar to (76). In analogy, we have the relationship

$$\bar{\boldsymbol{\varphi}}(t; \mathbf{x}) = \mathbf{G}(t, t_i) \mathbf{x} - \int_{t_i}^t dt' \mathbf{G}(t, t') \mathbf{E}_I[\bar{\boldsymbol{\varphi}}(\bullet; \mathbf{x})](t'). \quad (82)$$

This expression does solve the equations of motion $\mathbf{E}_0[\boldsymbol{\varphi}](t) + \mathbf{E}_I[\boldsymbol{\varphi}](t) = \mathbf{0}$ for $t > t_i$ as can be confirmed easily. However, due to the self-referential nature of this expression, its practical use is somewhat limited. Nonetheless, it provides a natural approximation scheme for $\bar{\boldsymbol{\varphi}}$.

The first term in equation (82) is the free physical evolution map $\bar{\boldsymbol{\varphi}}$ defined above. In fact, we may consider the relationship

$$\bar{\boldsymbol{\varphi}}(t; \mathbf{x}) = \mathbf{G}(t, t_i) \mathbf{x} \quad (83)$$

⁸ The notation with an overset bar $\bar{\boldsymbol{\varphi}}$ in contrast to the overset tilde $\tilde{\boldsymbol{\varphi}}$ for the (full) physical evolution map is inspired by the fact that for many systems the free evolution map does indeed describe a straight path in phase space while the path described by the physical evolution has a more complicated shape.

as its definition. If interactions are very small, the free evolution can be an approximation for the physical evolution, albeit not a very sophisticated one. However, as a slightly improved approximation, we can replace the argument of \mathbf{E}_I in equation (82) by the free evolution. This yields the well-known *Born approximation*

$$\boldsymbol{\varphi}_{\text{Born}}(\mathbf{t}; \boldsymbol{\chi}) = \bar{\boldsymbol{\varphi}}(\mathbf{t}; \boldsymbol{\chi}) - \int_{t_i}^{\mathbf{t}} dt' \mathbf{G}(\mathbf{t}, t') \mathbf{E}_I[\bar{\boldsymbol{\varphi}}(\bullet; \boldsymbol{\chi})](t'). \quad (84)$$

While in equation (82) the deviation from the free evolution is given by the interactions evaluated along the true physical evolution, the Born approximation evaluates them along the free physical evolution. This way, the expression is no longer self-referential and thus can be evaluated in a straightforward manner.

If interactions are sufficiently small, the Born approximation describes a phase space trajectory which is close to the physical evolution. This is exploited, e.g., in classical scattering problems with high impact parameter and similar physical systems. In such cases, it usually performs best for a single scattering. For a particle which is scattered multiple times, the second and subsequent scatterings are highly affected by the error incurred by the approximate treatment in the first scattering. This is especially true if the time interval between scatterings is large, as then a small difference in scattering angle severely affects the impact parameter for the subsequent scattering.

One can attempt to remedy this, by performing a so-called iterative Born approximation. Its second iteration evaluates the interactions along $\boldsymbol{\varphi}_{\text{Born}}$ which itself is considered as the first iteration. In turn, evaluating the interactions along the resulting second iteration yields the third iteration and so forth. We compare the Born approximation to the perturbative treatment of interactions in KFT in subsection 3.2.2.

2.3.2 *Splitting Freedom*

In this subsection, we investigate the freedom of performing a split of the equations of motion into a free and an interaction part in more detail. The focus is in particular on the question how we can find admissible splits of the equations of motion. Ideally, one would be able to completely parameterize the splitting freedom and leave the split arbitrary for as long as possible. In a final expression one could then choose the “optimal splitting” which, e.g., minimizes approximation errors.

Before diving into the mathematics of parameterizing the splitting freedom, let us return to the discussion of Newton’s laws in the introduction of this section. There, the question about free motion is answered by Newton’s first law. His second law tells us the acceleration relative to this free motion. However, if we are describing physics in an accelerated reference frame, inertial motion corresponds to an accelerated trajectory in that frame. Newton’s first law does not hold in the accelerated frame. As a consequence, Newton’s second law needs modification in the form of fictitious forces.

The splitting of the equations of motion into a free and an interaction part in KFT is somewhat analogous. The difference is that we might deliberately regard

a more complicated evolution as free, in hopes that the deviation relative to it remains small. In many areas of physics, such a choice is referred to as *gauge freedom*. The term does have a more precise definition in some areas compared to others. Here, we use it quite liberally without, e.g., demanding that the freedom of choice can be parametrized by a gauge group.

In an ideal case, we would regard the physical evolution $\tilde{\varphi}$ as free motion such that there are no deviations from it due to interactions at all. We refer to this choice as *solution gauge*. Unfortunately, this gauge choice is only rarely admissible due to the condition of the existence of a Green's function for the free equation of motion $\mathbf{E}_0 = 0$. For the remainder of this section we focus on admissible gauge choices.

A gauge choice which is always possible for systems described by a Hamiltonian \mathcal{H} is *stationary gauge*. This is the choice of splitting Hamilton's equations as

$$\mathbf{E}_0[\boldsymbol{\varphi}](t) = \frac{d}{dt} \boldsymbol{\varphi}(t) \quad \text{and} \quad \mathbf{E}_I[\boldsymbol{\varphi}](t) = -\mathcal{J} \frac{\delta \mathcal{H}(\boldsymbol{\varphi}(t), t)}{\delta \boldsymbol{\varphi}(t)}, \quad (85)$$

i.e., the Hamiltonian is split as $\mathcal{H}_0 = 0$ and $\mathcal{H}_I = \mathcal{H}$. In stationary gauge, free evolution is given by $\tilde{\varphi}(t; \mathbf{x}) = \mathbf{x}$ for all $t \in [t_i, t_f]$. We regard a constant trajectory in phase space as free evolution. The corresponding Green's function is $\mathbf{G}(t, t') = \theta(t - t') \mathbb{I}_{2d}$. This is a poor gauge choice in most situations, because even the standard kinetic term is considered as an interaction.

The most natural gauge choice for systems described by a Hamiltonian \mathcal{H} which contains a standard kinetic term $\mathcal{K} = \frac{1}{2m} \boldsymbol{\varphi}^{(p)} \cdot \boldsymbol{\varphi}^{(p)}$ is *Newtonian gauge*. The kinetic term is regarded as the free Hamiltonian $\mathcal{H}_0 = \mathcal{K}$ and the remainder of the Hamiltonian acts as interactions. This choice is admissible, because the free equation of motion

$$\mathbf{E}_0[\boldsymbol{\varphi}](t) = \frac{d}{dt} \boldsymbol{\varphi}(t) - \mathcal{J} \frac{\delta \mathcal{K}(\boldsymbol{\varphi}(t), t)}{\delta \boldsymbol{\varphi}(t)} = \frac{d}{dt} \boldsymbol{\varphi}(t) - \begin{pmatrix} \frac{1}{m} \boldsymbol{\varphi}^{(p)} \\ 0 \end{pmatrix} \quad (86)$$

admits the Green's function

$$\mathbf{G}(t, t') := \begin{pmatrix} \theta(t - t') \mathbb{I}_d & \frac{1}{m}(t - t') \theta(t - t') \mathbb{I}_d \\ 0 & \theta(t - t') \mathbb{I}_d \end{pmatrix}. \quad (87)$$

Newtonian gauge can be regarded as an implementation of Newton's first law.

Given the physical importance of Newtonian gauge and our preferred use of it throughout this thesis, let us confirm that \mathbf{G} is indeed a Green's function in the sense of equation (72). Using that the equations above can be written as a linear differential equation of the form

$$\left(\frac{d}{dt} - \begin{pmatrix} 0 & \frac{1}{m} \mathbb{I}_d \\ 0 & 0 \end{pmatrix} \right) \boldsymbol{\varphi}(t) = 0, \quad (88)$$

the linear differential operator in the round brackets can be applied to the Green's function. This yields

$$\begin{aligned} & \left(\frac{d}{dt} - \begin{pmatrix} 0 & \frac{1}{m} \mathbb{I}_d \\ 0 & 0 \end{pmatrix} \right) \mathbf{G}(t, t') \\ &= \begin{pmatrix} \delta_D(t-t') \mathbb{I}_d & \frac{1}{m} (\theta(t-t') + (t-t') \delta_D(t-t')) \mathbb{I}_d \\ 0 & \delta_D(t-t') \mathbb{I}_d \end{pmatrix} \\ & \quad - \begin{pmatrix} 0 & \frac{1}{m} \theta(t-t') \mathbb{I}_d \\ 0 & 0 \end{pmatrix} \end{aligned} \quad (89)$$

$$= \delta_D(t-t') \mathbb{I}_{2d}, \quad (90)$$

where we used $(t-t') \delta_D(t-t') = 0$ in the last equality.

In a cosmological setting, the optimal choice of gauge might be *Zel'dovich gauge*. As described in detail in appendix B of [35], this choice of free motion already incorporates the part of the large-scale gravitational force into free motion. It has been suggested in [34] that the interactions in Zel'dovich gauge can be described by a purely $\varphi^{(q)}$ -dependent Yukawa potential. In this context, the "improved Zel'dovich trajectories" proposed in [44] might also be of interest. Given that Zel'dovich gauge is specifically adapted to N-body systems, we provide a few remarks on it in section 3.3.

Having introduced a few possible gauge choices, we return to a more conceptual viewpoint. Our aim is to study how the gauge freedom can be parametrized. The obvious answer of a gauge transformation

$$\mathbf{E}_0 \mapsto \mathbf{E}_0 + \mathbf{E}_g \quad \text{and} \quad \mathbf{E}_I \mapsto \mathbf{E}_I - \mathbf{E}_g \quad (91)$$

is not satisfactory, because even if \mathbf{E}_0 and \mathbf{E}_g admit Green's functions, respectively, it is not clear how to construct a Green's function for their sum.

A more promising approach is based on the fact that it is easy to construct a Green's function for a product of differential operators. Indeed, let \mathbf{G} and \mathbf{G}_g be Green's functions for linear operators $\mathbf{E}_0[\varphi] = \mathbf{E}_0 \varphi$ and $\mathbf{E}_g[\varphi] = \mathbf{E}_g \varphi$, then

$$\mathbf{G}_*(t, t') := \int_{-\infty}^{\infty} dt'' \mathbf{G}_g(t, t'') \mathbf{G}(t'', t') \quad (92)$$

is a Green's function for the linear differential operator $\mathbf{E}_*[\varphi] = \mathbf{E}_0 \mathbf{E}_g \varphi$. Using this, we have the gauge freedom

$$\mathbf{E}_0 \mapsto \mathbf{E}_0 \mathbf{E}_g \quad \text{and} \quad \mathbf{E}_I \mapsto \mathbf{E}_I + (\mathbb{I}_{2d} - \mathbf{E}_0) \mathbf{E}_g \quad (93)$$

for any linear differential operator \mathbf{E}_g which admits a Green's function.

In principle, any possible transformation $\mathbf{E}_0 \mapsto \mathbf{E}_?$ can be realized by setting

$$\mathbf{E}_g[\varphi](t) := \int_{-\infty}^{\infty} dt' \mathbf{G}(t, t') \mathbf{E}_?[\varphi](t') \quad (94)$$

in the gauge transformation (93). However, without providing a Green's function for \mathbf{E}_g we cannot claim that our naive prescription above incorporates the

entire gauge freedom. It would be an interesting subject of further research to formalize the ideas presented here and study the splitting freedom in more detail. Provided such a formalism, one might then be able to study the effect of gauge choices on the expressions obtained from the perturbative treatment presented in the following chapter with the aim of minimizing the truncation error by optimal choice of gauge.

2.3.3 Example: Harmonic Oscillator (III)

The harmonic oscillator is an idealized example for the splitting of the equations of motion because it admits a Green's function for its equations of motion $E[\varphi] = 0$. We consider here a single one-dimensional harmonic oscillator as introduced in subsection 2.1.5. Indeed, a Green's function for the equations of motion (25) is given by

$$\tilde{G}(t, t') = \begin{pmatrix} \cos(\sqrt{\frac{\kappa}{m}}(t - t')) & \frac{1}{\sqrt{\kappa m}} \sin(\sqrt{\frac{\kappa}{m}}(t - t')) \\ -\sqrt{\kappa m} \sin(\sqrt{\frac{\kappa}{m}}(t - t')) & \cos(\sqrt{\frac{\kappa}{m}}(t - t')) \end{pmatrix} \quad (95)$$

for $t' < t$ and $t, t' \in (t_i, t_f]$. One can easily confirm that the analytic solution in equation (26) is recovered via $\tilde{\varphi}(t; x) = \tilde{G}(t, t_i) x$. This corresponds to the solution gauge choice of the splitting. There are no interactions relative to $\tilde{\varphi}$.

Newtonian gauge corresponds to the splitting

$$E_0[\varphi](t) = \frac{d\varphi}{dt}(t) - \begin{pmatrix} \frac{1}{m} \varphi^{(p)}(t) \\ 0 \end{pmatrix} \quad \text{and} \quad E_I[\varphi](t) = \begin{pmatrix} 0 \\ \kappa \varphi^{(q)}(t) \end{pmatrix} \quad (96)$$

of the equations of motion induced by setting $\mathcal{H}_0 = \mathcal{K} = \frac{1}{2m} \varphi^{(p)}(t) \cdot \varphi^{(p)}(t)$ and $\mathcal{H}_I = \frac{\kappa}{2} \varphi^{(q)}(t) \cdot \varphi^{(q)}(t)$. The Green's function for E_0 is the one given in equation (87). Free evolution is now

$$\tilde{\varphi}(t; x) = G(t, t_i) x = \begin{pmatrix} x^{(q)} + \frac{1}{m} x^{(p)}(t - t_i) \\ x^{(p)} \end{pmatrix} \quad (97)$$

just as Newton's first law would suggest.

According to equation (82) the physical evolution of the harmonic oscillator satisfies

$$\tilde{\varphi}(t; x) = G(t, t_i) x - \int_{t_i}^t dt' G(t, t') E_I[\tilde{\varphi}(\bullet; x)](t'). \quad (98)$$

The right-hand side of the equation can be simplified by inserting our expressions for G and E_I . We obtain

$$\begin{aligned} \tilde{\varphi}(t; \mathbf{x}) &= \begin{pmatrix} \mathbf{x}^{(q)} + \frac{1}{m} \mathbf{x}^{(p)}(t - t_i) \\ \mathbf{x}^{(p)} \end{pmatrix} \\ &\quad - \int_{t_i}^t dt' \begin{pmatrix} \theta(t-t') \mathbb{I}_d & \frac{1}{m}(t-t') \theta(t-t') \mathbb{I}_d \\ 0 & \theta(t-t') \mathbb{I}_d \end{pmatrix} \begin{pmatrix} 0 \\ \kappa \tilde{\varphi}^{(q)}(t'; \mathbf{x}) \end{pmatrix} \quad (99) \end{aligned}$$

$$= \begin{pmatrix} \mathbf{x}^{(q)} + \frac{1}{m} \mathbf{x}^{(p)}(t - t_i) \\ \mathbf{x}^{(p)} \end{pmatrix} - \int_{t_i}^t dt' \begin{pmatrix} \frac{1}{m}(t-t') \kappa \tilde{\varphi}^{(q)}(t'; \mathbf{x}) \\ \kappa \tilde{\varphi}^{(q)}(t'; \mathbf{x}) \end{pmatrix} \quad (100)$$

$$= \begin{pmatrix} \mathbf{x}^{(q)} + \frac{1}{m} \mathbf{x}^{(p)}(t - t_i) - \int_{t_i}^t dt' \frac{1}{m}(t-t') \kappa \tilde{\varphi}^{(q)}(t'; \mathbf{x}) \\ \mathbf{x}^{(p)} - \int_{t_i}^t dt' \kappa \tilde{\varphi}^{(q)}(t'; \mathbf{x}) \end{pmatrix}. \quad (101)$$

Using the expression for $\tilde{\varphi}$ in equation (26) we can evaluate the integrals. It is

$$\int_{t_i}^t dt' \kappa \tilde{\varphi}^{(q)}(t'; \mathbf{x}) = -\tilde{\varphi}^{(p)}(t; \mathbf{x}) + \tilde{\varphi}^{(p)}(t_i; \mathbf{x}) \quad \text{and} \quad (102)$$

$$\int_{t_i}^t dt' \frac{\kappa}{m}(t-t') \tilde{\varphi}^{(q)}(t'; \mathbf{x}) = \left[-\frac{(t-t')}{m} \tilde{\varphi}^{(p)}(t'; \mathbf{x}) \right]_{t_i}^t - \int_{t_i}^t dt' \frac{1}{m} \tilde{\varphi}^{(p)}(t'; \mathbf{x}) \quad (103)$$

$$= \frac{t-t_i}{m} \tilde{\varphi}^{(p)}(t_i; \mathbf{x}) - \tilde{\varphi}^{(q)}(t; \mathbf{x}) + \tilde{\varphi}^{(q)}(t_i; \mathbf{x}) \quad (104)$$

as one can either obtain by performing the integrals explicitly or by using Hamilton's equations (25). Inserting the expressions for the integrals into the equation above we obtain the tautology $\tilde{\varphi} = \tilde{\varphi}$.

The physical meaning of this result is that the interactions evaluated along the physical evolution provide a deviation from the free evolution $\tilde{\varphi}$ to exactly match the physical evolution $\tilde{\varphi}$ itself. Here, we confirmed this explicitly for the harmonic oscillator in Newtonian gauge, but the result holds true for any gauge choice. In fact, equation (82) is trivially fulfilled in solution gauge due to $E_I = 0$.

In stationary gauge free motion is constant in phase space, $\tilde{\varphi}(t; \mathbf{x}) = \mathbf{x}$. The interaction part of the equations of motion are induced the entirety of the Hamiltonian \mathcal{H} and are thus given by

$$E_I[\varphi](t) = -\mathcal{J} \frac{\delta \mathcal{H}(\varphi(t), t)}{\delta \varphi(t)} = \begin{pmatrix} -\frac{1}{m} \varphi^{(p)}(t) \\ \kappa \varphi^{(q)}(t) \end{pmatrix}. \quad (105)$$

The deviation from free evolution according to equation (82) turns out to be

$$\int_{t_i}^t dt' G(t, t') E_I[\tilde{\varphi}(\bullet; \mathbf{x})](t') = \begin{pmatrix} -\tilde{\varphi}^{(q)}(t; \mathbf{x}) + \tilde{\varphi}^{(q)}(t_i; \mathbf{x}) \\ -\tilde{\varphi}^{(p)}(t; \mathbf{x}) + \tilde{\varphi}^{(p)}(t_i; \mathbf{x}) \end{pmatrix} \quad (106)$$

and thus exactly recovers $\tilde{\varphi}$ from $\tilde{\varphi}$. This follows to a calculation analogous to the one in Newtonian gauge. Observe that the deviation in position is bounded here, while it is unbounded in Newtonian gauge. Including the kinetic term into \mathcal{H}_I instead of \mathcal{H}_0 makes free motion a better approximation at large times t , though it worsens the approximation for small times $t \approx t_i$.

2.3.4 Splitting of Generating Functional

The aim of this subsection is to obtain an expression for the generating functional in terms of the Green's function. Our starting point is equation (70) which provides the expression

$$Z[\mathbf{J}; \mathbf{x}] = C^{-1} \int_{\mathbf{x}} \mathcal{D}\boldsymbol{\varphi} \int \mathcal{D}\boldsymbol{\chi} \exp\left(i \int_{t_i}^{t_f} dt' (\boldsymbol{\chi} \cdot \mathbf{E}[\boldsymbol{\varphi}] + \mathbf{J} \cdot \boldsymbol{\varphi})\right) \quad (107)$$

for the generating functional. Here and in some of the following expressions we do not explicitly write down the time-dependencies for compactness. Using the splitting in equation (77) we can rewrite this as

$$\begin{aligned} Z[\mathbf{J}; \mathbf{x}] &= C^{-1} \int_{\mathbf{x}} \mathcal{D}\boldsymbol{\varphi} \int \mathcal{D}\boldsymbol{\chi} \exp\left(i \int_{t_i}^{t_f} dt' (\boldsymbol{\chi} \cdot \mathbf{E}_0[\boldsymbol{\varphi}] + \boldsymbol{\chi} \cdot \mathbf{E}_I[\boldsymbol{\varphi}] + \mathbf{J} \cdot \boldsymbol{\varphi})\right) \quad (108) \\ &= C^{-1} \int_{\mathbf{x}} \mathcal{D}\boldsymbol{\varphi} \int \mathcal{D}\boldsymbol{\chi} \exp\left(i \int_{t_i}^{t_f} dt' \boldsymbol{\chi} \cdot \mathbf{E}_I[\boldsymbol{\varphi}]\right) \\ &\quad \exp\left(i \int_{t_i}^{t_f} dt' (\boldsymbol{\chi} \cdot \mathbf{E}_0[\boldsymbol{\varphi}] + \mathbf{J} \cdot \boldsymbol{\varphi})\right). \quad (109) \end{aligned}$$

To achieve a proper splitting of interactions and free evolution we want to position the exponential factor containing \mathbf{E}_I in front of the path integrals. This would allow us to perform them and to express the resulting expression in terms of the free physical solution. Indeed, it is

$$Z_0[\mathbf{J}; \mathbf{x}] := C^{-1} \int_{\mathbf{x}} \mathcal{D}\boldsymbol{\varphi} \int \mathcal{D}\boldsymbol{\chi} \exp\left(i \int_{t_i}^{t_f} dt' (\boldsymbol{\chi} \cdot \mathbf{E}_0[\boldsymbol{\varphi}] + \mathbf{J} \cdot \boldsymbol{\varphi})\right) \quad (110)$$

$$= C^{-1} \int_{\mathbf{x}} \mathcal{D}\boldsymbol{\varphi} \delta_D[\mathbf{E}_0(\boldsymbol{\varphi})] \exp\left(i \int_{t_i}^{t_f} dt' \mathbf{J} \cdot \boldsymbol{\varphi}\right) \quad (111)$$

$$= \int \mathcal{D}\boldsymbol{\varphi} \delta_D[\boldsymbol{\varphi} - \bar{\boldsymbol{\varphi}}(\bullet; \mathbf{x})] \exp\left(i \int_{t_i}^{t_f} dt' \mathbf{J} \cdot \boldsymbol{\varphi}\right) \quad (112)$$

$$= \exp\left(i \int_{t_i}^{t_f} dt' \mathbf{J}(t') \cdot \bar{\boldsymbol{\varphi}}(t'; \mathbf{x})\right). \quad (113)$$

We have followed the exact same manipulations we performed on the generating functional in section 2.2.3. We refer to the Z_0 as the *free generating functional*.

It is worthwhile to point out the condition in equation (78) is sufficient to perform the manipulations above. It is not necessary to demand that these determinants have a specific value $C = \det\left(\frac{d\mathbf{E}}{d\boldsymbol{\varphi}}\right)$. Indeed, by defining

$$C' := \det\left(\frac{d\mathbf{E}}{d\boldsymbol{\varphi}}[\bar{\boldsymbol{\varphi}}(\bullet; \mathbf{x})]\right) \quad (114)$$

and replacing $C \mapsto C'$ in all equations above, the final form for Z_0 would have been the same. The fact that in Hamiltonian mechanics $C' = C$ does merely allow to easily choose splittings of the equations of motion while satisfying equation (78).

Given our conditions on the splitting of the equations of motion, the free solution is obtainable analytically and hence the free generating functional

is given as a simple function of known quantities. Therefore, expressions for observables generated from Z_0 can be evaluated completely. For example, the phase space trajectory, obtained as an observable from the free generating functional by taking the functional derivative with respect to \mathbf{J} , is simply the free physical evolution. Similarly, the density obtained from Z_0 is a sum of Dirac δ -functions depending on $\bar{\varphi}$ instead of φ .

If we can manipulate our expression for the generating functional in equation (109) such that the exponential containing \mathbf{E}_I is positioned in front of the path integrals, the remaining expression is just the free generating functional. For the path integral over φ this can be achieved by replacing

$$\mathbf{E}_I[\varphi] \mapsto \mathbf{E}_I \left[\frac{\delta}{i \delta \mathbf{J}^T} \right]. \quad (115)$$

This is analogous to the replacement used in the definition of observables in section 2.2.1.

The explicit dependence on χ can be removed by the same idea. This requires us to introduce an additional source field \mathbf{K} for χ . Doing so, we obtain the expression

$$\begin{aligned} Z[\mathbf{J}; \chi] = C^{-1} \int_{\mathbf{x}} \mathcal{D}\varphi \int \mathcal{D}\chi \exp \left(i \int_{t_i}^{t_f} dt' \frac{\delta}{i \delta \mathbf{K}} \cdot \mathbf{E}_I \left[\frac{\delta}{i \delta \mathbf{J}^T} \right] \right) \\ \exp \left(i \int_{t_i}^{t_f} dt' (\chi \cdot \mathbf{E}_0[\varphi] + \chi \cdot \mathbf{K} + \mathbf{J} \cdot \varphi) \right) \Big|_{\mathbf{K}=0} \end{aligned} \quad (116)$$

for the generating functional. Note that we recover the expression in equation (109) upon performing the functional derivatives in the first line. Having replaced the explicit dependence on φ and χ by the corresponding functional derivatives, it is now possible to exchange the order of the integrals and the exponential factor in the first line of the equation above.

The resulting expression has the form of a functional derivative operator acting on a functional of \mathbf{J} and \mathbf{K} . Afterwards, the function \mathbf{K} is set to zero, while the function \mathbf{J} remains to be acted upon by observables. The functional of \mathbf{J} and \mathbf{K} almost has the form of the free generating functional defined in equation (110), but features additionally the function \mathbf{K} which is coupled to χ . Generalizing the free generating functional Z_0 , we define

$$Z_{\mathbf{K}}[\mathbf{J}; \chi] := C^{-1} \int_{\mathbf{x}} \mathcal{D}\varphi \int \mathcal{D}\chi \exp \left(i \int_{t_i}^{t_f} dt' (\chi \cdot (\mathbf{E}_0[\varphi] + \mathbf{K}) + \mathbf{J} \cdot \varphi) \right) \quad (117)$$

$$= C^{-1} \int_{\mathbf{x}} \mathcal{D}\varphi \delta_{\mathbf{D}}[\mathbf{E}_0(\varphi) + \mathbf{K}] \exp \left(i \int_{t_i}^{t_f} dt' \mathbf{J} \cdot \varphi \right) \quad (118)$$

$$= \int \mathcal{D}\varphi \delta_{\mathbf{D}}[\varphi - \bar{\varphi}_{\mathbf{K}}(\bullet; \chi)] \exp \left(i \int_{t_i}^{t_f} dt' \mathbf{J} \cdot \varphi \right) \quad (119)$$

$$= \exp \left(i \int_{t_i}^{t_f} dt' \mathbf{J}(t') \cdot \bar{\varphi}_{\mathbf{K}}(t'; \chi) \right). \quad (120)$$

From the first to the second line we evaluated the path integral over χ obtaining a Dirac δ -functional. In the third line we replaced the condition in this Dirac

δ -function from the inhomogeneous free equation of motion $\mathbf{E}_0 + \mathbf{K} = 0$ by its solution

$$\bar{\varphi}_{\mathbf{K}}(t; \mathbf{x}) = \mathbf{G}(t, t_i) \mathbf{x} - \int_{t_i}^t dt' \mathbf{G}(t, t') \mathbf{K}(t'). \quad (121)$$

Note that the upper integral boundary in this expression follows from the fact that \mathbf{G} is causal, analogously to equation (76). This replacement of arguments of the Dirac δ -functional comes with a functional determinant which is equal to the one in equation (78) and thus cancels the factor C .

Using the definition of $Z_{\mathbf{K}}[\mathbf{J}; \mathbf{x}]$, we obtain the expression

$$Z[\mathbf{J}; \mathbf{x}] = \exp\left(i \int_{t_i}^{t_f} dt' \frac{\delta}{i \delta \mathbf{K}} \cdot \mathbf{E}_{\mathbf{I}} \left[\frac{\delta}{i \delta \mathbf{J}^T} \right]\right) Z_{\mathbf{K}}[\mathbf{J}; \mathbf{x}] \Big|_{\mathbf{K}=0} \quad (122)$$

for the generating functional. We have thus achieved our aim of splitting the generating functional into parts encoding the interactions and free evolution, respectively. We refer to the argument of the exponential

$$\hat{S}_{\mathbf{I}} := \int_{t_i}^{t_f} dt' \frac{\delta}{i \delta \mathbf{K}(t')} \cdot \mathbf{E}_{\mathbf{I}} \left[\frac{\delta}{i \delta \mathbf{J}^T} \right] (t') \quad (123)$$

as the *interaction operator*. By acting with its exponential on $Z_{\mathbf{K}}[\mathbf{J}; \mathbf{x}]$, it adjusts the system's evolution from being a solution to the free equation $\mathbf{E}_0 = 0$ to solving the full equations of motion $\mathbf{E} = \mathbf{E}_0 + \mathbf{E}_{\mathbf{I}} = 0$.

As a final step in this subsection, we evaluate the functional derivatives with respect to \mathbf{K} in equation (122). For this purpose, we first observe that

$$\frac{\delta}{i \delta \mathbf{K}(t)} Z_{\mathbf{K}}[\mathbf{J}; \mathbf{x}] = - \int_t^{t_f} dt' \mathbf{J}^T(t') \mathbf{G}(t', t) Z_{\mathbf{K}}[\mathbf{J}; \mathbf{x}], \quad (124)$$

where the term $\mathbf{J}^T \mathbf{G}$ is to be understood as a matrix product. The form of the integral boundaries $t \leq t' \leq t_f$ follow from the causality structure induced by equation (121). Unfortunately, it is not quite straightforward to replace the functional derivative in the interaction operator $\hat{S}_{\mathbf{I}}$ with the expression on the right-hand side of this relationship. The problem is that this expression depends on the function \mathbf{J} with respect to which the interaction operator contains a functional derivative. Therefore, care has to be taken with the order in which the derivatives are taken.

Let us consider explicitly the action with the interaction operator on $Z_{\mathbf{K}}[\mathbf{J}; \mathbf{x}]$ to investigate this issue in detail. It is

$$\hat{S}_{\mathbf{I}} Z_{\mathbf{K}}[\mathbf{J}; \mathbf{x}] = \int_{t_i}^{t_f} dt' \frac{\delta}{i \delta \mathbf{K}(t')} \cdot \mathbf{E}_{\mathbf{I}} \left[\frac{\delta}{i \delta \mathbf{J}^T} \right] (t') Z_{\mathbf{K}}[\mathbf{J}; \mathbf{x}] \quad (125)$$

$$= - \int_{t_i}^{t_f} dt' \mathbf{E}_{\mathbf{I}}^T \left[\frac{\delta}{i \delta \mathbf{J}^T(t')} \right] \int_{t'}^{t_f} dt'' \mathbf{G}^T(t'', t') \mathbf{J}(t'') Z_{\mathbf{K}}[\mathbf{J}; \mathbf{x}] \quad (126)$$

$$= - \int_{t_i}^{t_f} dt' \text{tr} \left(\mathbf{G}^T(t', t') \frac{1}{i} \nabla^T \mathbf{E}_{\mathbf{I}} \left[\frac{\delta}{i \delta \mathbf{J}^T} \right] (t') \right) Z_{\mathbf{K}}[\mathbf{J}; \mathbf{x}] \\ - \int_{t_i}^{t_f} dt' \int_{t'}^{t_f} dt'' \mathbf{J}^T(t'') \mathbf{G}(t'', t') \mathbf{E}_{\mathbf{I}} \left[\frac{\delta}{i \delta \mathbf{J}^T} \right] (t') Z_{\mathbf{K}}[\mathbf{J}; \mathbf{x}]. \quad (127)$$

The last equality requires some further explanation and investigation. Firstly, the derivatives inside \mathbf{E}_I are to be understood in terms of a power series of \mathbf{E}_I . Schematically, for functions $\epsilon, \zeta: \mathbb{R} \rightarrow \mathbb{R}$, the last equality thus has the form

$$\epsilon(\partial_{\mathbf{k}}) \mathbf{k} \zeta(\mathbf{k}) = \sum_{n=0}^{\infty} \frac{\epsilon^{(n)}(0)}{n!} \partial_{\mathbf{k}}^n \mathbf{k} \zeta(\mathbf{k}) \quad (128)$$

$$= \mathbf{k} \zeta(\mathbf{k}) + \sum_{n=1}^{\infty} \frac{\epsilon^{(n)}(0)}{n!} (n \partial_{\mathbf{k}}^{n-1} \zeta(\mathbf{k}) + \mathbf{k} \partial_{\mathbf{k}}^n \zeta(\mathbf{k})) \quad (129)$$

$$= \epsilon'(\partial_{\mathbf{k}}) \zeta(\mathbf{k}) + \mathbf{k} \epsilon(\partial_{\mathbf{k}}) \zeta(\mathbf{k}). \quad (130)$$

In the second equality there are n choices for which derivative acts on the single factor of \mathbf{k} as well as the option of none of the derivatives acting on it. Upon relabeling $n \mapsto n+1$ the first term in the second line is then simply the series expansion of the first derivative of the function ϵ . Secondly, in the actual calculation we have to keep track of the tensorial contractions of the various quantities. Promoting the functions ϵ and ζ to maps $\epsilon: \mathbb{R}^d \rightarrow \mathbb{R}^d$ and $\zeta: \mathbb{R}^d \rightarrow \mathbb{R}$, respectively, and performing the same calculation yields

$$(\epsilon(\partial_{\mathbf{k}}) \cdot \mathbf{k}) \zeta(\mathbf{k}) = (\nabla^T \epsilon)(\partial_{\mathbf{k}}) \zeta(\mathbf{k}) + \mathbf{k} \cdot \epsilon(\partial_{\mathbf{k}}) \zeta(\mathbf{k}). \quad (131)$$

Note that the first term is the Jacobian matrix of ϵ , not its divergence. This is already of very similar form to the calculation of $\hat{S}_I Z_{\mathbf{K}}$ above, except for the Green's function as well as the time dependencies and integrals. The contraction with the Green's function has the role of the scalar product in our toy calculation. For the left-hand side and the second term on the right-hand side of the equation above, this replacement is straightforward. The only slightly more difficult term is the divergence of ϵ in the first term on the right-hand side of the equation. Its analogue is the full contraction of the Jacobian with the Green's function which is achieved via the trace in equation (127).

In the first line of equation (127) there is a factor $\mathbf{G}^T(t', t')$. Recalling that the Green's function \mathbf{G} is assumed to be causal and thus satisfies the condition in equation (74), this factor and with it the entire term vanishes. Consequently, we are left with the result

$$\hat{S}_I Z_{\mathbf{K}}[\mathbf{J}; \mathbf{x}] = - \int_{t_i}^{t_f} dt' \int_{t'}^{t_f} dt'' \mathbf{J}^T(t'') \mathbf{G}(t'', t') \mathbf{E}_I \left[\frac{\delta}{i \delta \mathbf{J}^T} \right] (t') Z_{\mathbf{K}}[\mathbf{J}; \mathbf{x}]. \quad (132)$$

Upon expanding the exponential in equation (122) into a power series, we obtain terms containing multiple copies of the interaction operator. We have seen above how an individual operator \hat{S}_I acts on the functional $Z_{\mathbf{K}}$. However, the action of multiple such operators is of course significantly more complicated. It is instructive to explicitly consider the case of two copies of the interaction operator acting on the functional $Z_{\mathbf{K}}$. This might be thought of as the second order term in a series expansion of the exponential in equation (122).

Using the result in equation (132), we have

$$\begin{aligned}
\hat{S}_I^2 Z_K[\mathbf{J}; \mathbf{x}] &= - \int_{t_i}^{t_f} dt'_2 \mathbf{E}_I \left[\frac{\delta}{i \delta \mathbf{J}^T} \right] (t'_2) \cdot \frac{\delta}{i \delta \mathbf{K}(t'_2)} \\
&\quad \left[\int_{t_i}^{t_f} dt'_1 \int_{t'_1}^{t_f} dt''_1 \mathbf{J}^T(t''_1) \mathbf{G}(t''_1, t'_1) \mathbf{E}_I \left[\frac{\delta}{i \delta \mathbf{J}^T} \right] (t'_1) Z_K[\mathbf{J}; \mathbf{x}] \right] \quad (133) \\
&= \int_{t_i}^{t_f} dt'_2 \mathbf{E}_I^T \left[\frac{\delta}{i \delta \mathbf{J}^T} \right] (t'_2) \left(\int_{t_i}^{t_f} dt'_1 \int_{t'_1}^{t_f} dt''_1 \mathbf{J}^T(t''_1) \mathbf{G}(t''_1, t'_1) \right. \\
&\quad \left. \mathbf{E}_I \left[\frac{\delta}{i \delta \mathbf{J}^T} \right] (t'_1) \right) \int_{t'_2}^{t_f} dt''_2 \mathbf{G}^T(t''_2, t'_2) \mathbf{J}(t''_2) Z_K[\mathbf{J}; \mathbf{x}]. \quad (134)
\end{aligned}$$

Note that in the last expression the factor \mathbf{E}_I^T in the first line is contracted with the factor $\mathbf{G}^T \mathbf{J}$ in the second line across the term in the round brackets. While the functional derivative with respect to \mathbf{K} could be moved to the right to act on Z_K , the term resulting from it cannot immediately be moved back past the term in the round brackets due to the functional derivative with respect to $\mathbf{J}(t'_1)$.

Once more, causality of the Green's function yields a significant simplification. For this purpose, we adjust the integration boundaries such that all four integrals are over the full range $[t_i, t_f]$. This is possible because the additional contributions are zero due to the two Green's functions, respectively, in the same way as in equation (132). This yields

$$\begin{aligned}
\hat{S}_I^2 Z_K[\mathbf{J}; \mathbf{x}] &= \int_{t_i}^{t_f} dt'_1 \int_{t_i}^{t_f} dt''_1 \int_{t_i}^{t_f} dt'_2 \int_{t_i}^{t_f} dt''_2 \mathbf{E}_I^T \left[\frac{\delta}{i \delta \mathbf{J}^T} \right] (t'_2) \left(\mathbf{J}^T(t''_1) \mathbf{G}(t''_1, t'_1) \right. \\
&\quad \left. \mathbf{E}_I \left[\frac{\delta}{i \delta \mathbf{J}^T} \right] (t'_1) \right) \mathbf{G}^T(t''_2, t'_2) \mathbf{J}(t''_2) Z_K[\mathbf{J}; \mathbf{x}], \quad (135)
\end{aligned}$$

though we keep in mind that contributions are non-zero only if $t'_1 < t''_1$ and $t'_2 < t''_2$. We now split the integral over t'_2 into two contributions: For $t'_2 \leq t'_1$ the applying functional derivative with respect to $\mathbf{J}(t'_2)$ to $\mathbf{J}^T(t''_1)$ yields zero due to the resulting factor $\mathbf{G}(t'_2, t'_1)$. Therefore, in this case the term in the round brackets can be moved to the left \mathbf{E}_I in the first line. Conversely, if $t'_2 \geq t'_1$, applying the functional derivative with respect to $\mathbf{J}(t'_1)$ to $\mathbf{J}(t'_2)$ in the second line yields zero due to the resulting factor $\mathbf{G}^T(t'_1, t'_2)$. In that case, this functional derivative can thus only act directly on Z_K and we can move the factor $\mathbf{G}^T \mathbf{J}$ in the second line to the left of the term in the round brackets.

We have shown that the expression for $\hat{S}_I^2 Z_K$ can be written as the sum of the two contributions

$$\begin{aligned}
&\int_{t_i}^{t_f} dt'_1 \int_{t_i}^{t_f} dt''_1 \int_{t_i}^{t'_1} dt'_2 \int_{t_i}^{t_f} dt''_2 \left(\mathbf{J}^T(t''_1) \mathbf{G}(t''_1, t'_1) \mathbf{E}_I \left[\frac{\delta}{i \delta \mathbf{J}^T} \right] (t'_1) \right) \\
&\quad \mathbf{E}_I^T \left[\frac{\delta}{i \delta \mathbf{J}^T} \right] (t'_2) \mathbf{G}^T(t''_2, t'_2) \mathbf{J}(t''_2) Z_K[\mathbf{J}; \mathbf{x}] \quad \text{and} \quad (136)
\end{aligned}$$

$$\begin{aligned}
&\int_{t_i}^{t_f} dt'_1 \int_{t_i}^{t_f} dt''_1 \int_{t'_1}^{t_f} dt'_2 \int_{t_i}^{t_f} dt''_2 \mathbf{E}_I^T \left[\frac{\delta}{i \delta \mathbf{J}^T} \right] (t'_2) \mathbf{G}^T(t''_2, t'_2) \mathbf{J}(t''_2) \\
&\quad \left(\mathbf{J}^T(t''_1) \mathbf{G}(t''_1, t'_1) \mathbf{E}_I \left[\frac{\delta}{i \delta \mathbf{J}^T} \right] (t'_1) \right) Z_K[\mathbf{J}; \mathbf{x}]. \quad (137)
\end{aligned}$$

In the second contribution, the condition $t'_2 \geq t'_1$ is encoded via the integral boundaries of t'_2 . Equivalently, it can be encoded via the integration boundaries of t'_1 by replacing the upper limit by t'_2 . This change of course also necessitates exchanging the ordering of the integrals making the second contribution an exact copy of the first up to relabeling $1 \leftrightarrow 2$. We conclude

$$\begin{aligned} \hat{S}_I^2 Z_K[J; \mathbf{x}] &= 2 \int_{t_i}^{t_f} dt'_2 \int_{t'_2}^{t_f} dt''_2 J^T(t''_2) \mathbf{G}(t''_2, t'_2) \mathbf{E}_I \left[\frac{\delta}{i \delta J^T} \right] (t'_2) \\ &\quad \int_{t_i}^{t'_2} dt'_1 \int_{t'_1}^{t_f} dt''_1 J^T(t''_1) \mathbf{G}(t''_1, t'_1) \mathbf{E}_I \left[\frac{\delta}{i \delta J^T} \right] (t'_1) Z_K[J; \mathbf{x}], \end{aligned} \quad (138)$$

where we adjusted the integral boundaries for t''_1 and t''_2 in accordance with causality of the Green's function.

For the sake of compactness, we introduce the quantity

$$\hat{L}_I(t) := - \int_t^{t_f} dt'' J^T(t'') \mathbf{G}(t'', t) \mathbf{E}_I \left[\frac{\delta}{i \delta J^T} \right] (t). \quad (139)$$

It allows us to write the results obtained above compactly as

$$\hat{S}_I Z_K[J; \mathbf{x}] = \int_{t_i}^{t_f} dt'_1 \hat{L}_I(t'_1) Z_K[J; \mathbf{x}], \quad (140)$$

$$\hat{S}_I^2 Z_K[J; \mathbf{x}] = 2 \int_{t_i}^{t_f} dt'_2 \int_{t_i}^{t'_2} dt'_1 \hat{L}_I(t'_2) \hat{L}_I(t'_1) Z_K[J; \mathbf{x}]. \quad (141)$$

This pattern continues to hold for higher powers of the interaction operator \hat{S}_I . The general case can be proven by induction. For this we assume the identity

$$\hat{S}_I^n Z_K[J; \mathbf{x}] = n! \int_{t_i}^{t_f} dt'_n \int_{t_i}^{t'_n} dt'_{n-1} \cdots \int_{t_i}^{t'_2} dt'_1 \hat{L}_I(t'_n) \cdots \hat{L}_I(t'_1) Z_K[J; \mathbf{x}] \quad (142)$$

to hold for $n \in \mathbb{N}$. Abbreviate $N := n + 1$. Adding another factor \hat{S}_I on the left-hand side results in the expression

$$\begin{aligned} \hat{S}_I^N Z_K[J; \mathbf{x}] &= n! \int_{t_i}^{t_f} dt'_N \mathbf{E}_I^T \left[\frac{\delta}{i \delta J^T} \right] (t'_N) \left(\int_{t_i}^{t'_N} dt'_n \int_{t_i}^{t'_n} dt'_{n-1} \cdots \int_{t_i}^{t'_2} dt'_1 \right. \\ &\quad \left. \hat{L}_I(t'_n) \cdots \hat{L}_I(t'_1) \right) \int_{t'_N}^{t_f} dt''_N \mathbf{G}^T(t''_N, t'_N) J(t''_N) Z_K[J; \mathbf{x}]. \end{aligned} \quad (143)$$

The integral over t'_N can be split into $N = n + 1$ contributions relative to the variables (t'_1, \dots, t'_n) . For any such contribution the factor \mathbf{E}_I^T can be moved to the right past factors of $\hat{L}_I(t'_j)$ with $t'_j \geq t'_N$. Indeed, the functional derivative with respect to $J(t'_N)$ acting on the factor $J(t'_j)$ would yield a vanishing Green's function $\mathbf{G}(t'_N, t'_j)$. Conversely, the factor $\mathbf{G}^T J$ can be moved to the left past fac-

tors of $\hat{L}_I(t'_j)$ with $t'_j \leq t'_N$ for analogous reasons. We obtain thus contributions of the form

$$n! \int_{t'_{j-1}}^{t'_j} dt'_N \int_{t_i}^{t_f} dt'_n \int_{t_i}^{t'_n} dt'_{n-1} \cdots \int_{t_i}^{t'_2} dt'_1 \hat{L}_I(t'_n) \cdots \hat{L}_I(t'_{j-1}) \\ \mathbf{E}_I^T \left[\frac{\delta}{i \delta \mathbf{J}^T} \right] (t'_N) \int_{t'_N}^{t_f} dt''_N \mathbf{G}^T(t''_N, t'_N) \mathbf{J}(t''_N) \hat{L}_I(t'_{j-1}) \cdots \hat{L}_I(t'_1) Z_{\mathbf{K}}[\mathbf{J}; \mathbf{x}] \quad (144)$$

$$= n! \int_{t_i}^{t_f} dt'_n \cdots \int_{t_i}^{t'_{j+1}} dt'_j \int_{t'_{j-1}}^{t'_j} dt'_N \int_{t_i}^{t'_j} dt'_{j-1} \cdots \int_{t_i}^{t'_2} dt'_1 \\ \hat{L}_I(t'_n) \cdots \hat{L}_I(t'_{j-1}) \hat{L}_I(t'_N) \hat{L}_I(t'_{j-1}) \cdots \hat{L}_I(t'_1) Z_{\mathbf{K}}[\mathbf{J}; \mathbf{x}] \quad (145)$$

for all $j \in \mathbb{N}$ with $1 \leq j \leq n$. The condition $t'_N \geq t'_{j-1}$ can be encoded via the upper integration boundary of t'_{j-1} instead of the lower integration boundary of t'_N . Relabeling integration variables then yields the expression on the right-hand side of equation (142) for $n \mapsto N$ except for the prefactor. However, since we have a total of N such contributions, the prefactor of their sum is $N n! = N!$. This concludes the proof of equation (142) by induction over n .

Recall from equation (122) that the generating functional can be written in the compact form

$$Z[\mathbf{J}; \mathbf{x}] = \exp(i \hat{S}_I) Z_{\mathbf{K}}[\mathbf{J}; \mathbf{x}] \Big|_{\mathbf{K}=0}. \quad (146)$$

Using a series expansion of the exponential in combination with the expression we obtained in equation (142) we can rewrite this formula as

$$Z[\mathbf{J}; \mathbf{x}] = \sum_{n=0}^{\infty} \frac{i^n}{n!} \hat{S}_I^n Z_{\mathbf{K}}[\mathbf{J}; \mathbf{x}] \Big|_{\mathbf{K}=0} \quad (147)$$

$$= \sum_{n=0}^{\infty} i^n \int_{t_i}^{t_f} dt'_n \cdots \int_{t_i}^{t'_2} dt'_1 \hat{L}_I(t'_n) \cdots \hat{L}_I(t'_1) Z_{\mathbf{K}}[\mathbf{J}; \mathbf{x}] \Big|_{\mathbf{K}=0} \quad (148)$$

$$= \mathcal{T} \exp \left(i \int_{t_i}^{t_f} dt' \hat{L}_I(t') \right) Z_0[\mathbf{J}; \mathbf{x}]. \quad (149)$$

In the last line we introduced the time-ordered exponential $\mathcal{T} \exp$ which is defined by the series expansion in the line above. Note the absence of the factor $n!$ which would usually appear in the series expansion of an exponential function.

We remark that in [1] it was claimed that

$$Z[\mathbf{J}; \mathbf{x}] = \exp \left(i \int_{t_i}^{t_f} dt' \hat{L}_I(t') \right) Z_0[\mathbf{J}; \mathbf{x}]. \quad (150)$$

This is based on an incorrect procedure of recombining time-ordered integrals outlined in footnote 3 of that article. Instead, the expression is only correct if one demands that functional derivatives act towards both the left and right in a series expansion of the exponential. Equivalently, as described at the introductory paragraph of section IV of [1], all functional derivatives should be thought of positioned to the left of all factors of \mathbf{J} —which, fortunately, is the interpretation on which the results of the article are based. In either case,

causality of the Green's function then yields the time-ordered expression above. In this thesis, we refrain from using this equation to avoid possible confusion.

The final result of this (sub-)section is the expression

$$Z[\mathbf{J}; \mathbf{x}] = \mathcal{T} \exp \left(i \int_{t_i}^{t_f} dt' \hat{\mathbf{L}}_I(t') \right) Z_0[\mathbf{J}; \mathbf{x}] \quad \text{with} \quad (151)$$

$$\hat{\mathbf{L}}_I(t') = - \int_{t'}^{t_f} dt'' \mathbf{J}^T(t'') \mathbf{G}(t'', t') \mathbf{E}_I \left[\frac{\delta}{i \delta \mathbf{J}^T} \right] (t') \quad \text{and} \quad (152)$$

$$Z_0[\mathbf{J}; \mathbf{x}] = \exp \left(i \int_{t_i}^{t_f} dt' \mathbf{J}^T(t') \mathbf{G}(t', t_i) \mathbf{x} \right). \quad (153)$$

We emphasize that this is a fully general result and does not rely on any approximations. The only assumptions made are that the equations of motion $\mathbf{E}[\boldsymbol{\varphi}] = \mathbf{0}$ can be split into a free and an interaction parts, $\mathbf{E}[\boldsymbol{\varphi}] = \mathbf{E}_0[\boldsymbol{\varphi}] + \mathbf{E}_I[\boldsymbol{\varphi}]$, and the free part $\mathbf{E}_0[\boldsymbol{\varphi}]$ admits a Green's function \mathbf{G} . Moreover, we require that the functional determinants

$$\det \left(\frac{d\mathbf{E}}{d\boldsymbol{\varphi}} [\tilde{\boldsymbol{\varphi}}(\bullet; \mathbf{x})] \right) \quad \text{and} \quad \det \left(\frac{d\mathbf{E}_0}{d\boldsymbol{\varphi}} [\tilde{\boldsymbol{\varphi}}(\bullet; \mathbf{x})] \right) \quad (154)$$

are equal.

While most of the discussion above was quite general and is valid for any equations of motion as long as they satisfy the conditions mentioned, we are considering Hamilton's equations in this thesis. Assuming that the split in the equations of motion is induced by a split of the Hamiltonian in the form of equation (79), the technical conditions on the functional determinants are automatically fulfilled.

2.4 INITIAL VALUES

The last of the three key ideas of KFT presented in the introductory chapter is to *determine observables given a stochastic initial state*. In the previous sections, our initial conditions $\mathbf{x} \in \mathbf{X}$ were exactly specified. Consequently, all quantities considered—the generating functional, the physical evolution and other observables—had an explicit dependence on \mathbf{x} . As such, our system and the derived observables were discretized.

In this section, we briefly discuss a standard method of obtaining smooth observables from a discretized system. Forming the convolution of an observable with a smoothing kernel yields a smooth function even if the observable is a distribution. We apply this specifically to the macroscopic density of general composite systems as well as for a system of N independent harmonic oscillators.

In subsection 2.4.3 we introduce probability distributions of initial values. These provide a stochastic initial state in accordance with the key idea referenced above. Using once more that our classical physical system is described by the Hamiltonian formalism of mechanics, we express expectation values of observables at time $t \geq t_i$ as averages over initial conditions.

As in previous sections, the newly introduced concepts are applied to the harmonic oscillator. We pick a probability distribution of initial values with a Gaussian distribution of position and vanishing momentum. The expectation value of the physical evolution is shown to coincide with the peak of the distribution of initial positions. We then consider the phase space density and obtain its expectation value which yields the probability distributions of the state of the system at all times.

Subsection 2.4.5 considers expectation values of r -point correlation functions of the macroscopic density. In this context, we discuss in detail two limits which can be taken by sending the component number N to infinity. This leads to a discussion of shot noise terms and a prescription of how they can be avoided. Finally, we define the density fluctuation power spectrum which is an important observable in applications to cosmology.

Most of the constructions, discussions and results of this section are based on [1] which in turn heavily relies on [23, 24].

2.4.1 Smoothed Macroscopic Description

Up until now we have considered a classical physical system with phase space \mathbf{X} which given an initial state $\mathbf{x} \in \mathbf{X}$ at t_i follows a physical evolution $\tilde{\varphi}(t; \mathbf{x})$ for $t > t_i$. This physical evolution map is the unique solution of the equations of motion $\mathbf{E}[\varphi] = \mathbf{0}$ given the initial value $\varphi(t_i) = \mathbf{x}$. We have shown how to create a functional $Z[\mathbf{J}; \mathbf{x}]$ for such a system which generates expressions for observables \mathcal{O} via suitable functional derivatives.

As an example for such an observable we have defined the macroscopic density, given by

$$\tilde{\rho}(\mathbf{x}, t; \mathbf{x}) = \sum_{j=1}^N \delta_D(\mathbf{x} - \tilde{\varphi}_j(t; \mathbf{x})) , \quad (155)$$

where we assumed that the system is made up from N equal components such that $\mathbf{X} = X^N$. The key example for such a system is an N -body system consisting of N interacting point-particles. In the limit of $N \gg 1$ we usually think of the macroscopic density of such a system as a smooth field, rather than as a sum of Dirac δ -functions. While this is an approximation, it is a vast conceptual simplification. Indeed, it often allows us to work with relatively simple macroscopic field equations to describe the evolution of a system with a huge number of microscopic degrees of freedom.

It should be emphasized that describing the evolution of such systems via macroscopic field equations necessarily is approximate. Fundamentally, in a system of point-particles the microscopic density is discretized. At any instance of time, the system occupies one single state in phase space \mathbf{X} . Projected on the component phase space X this yields a distribution, not a smooth field. Macroscopic field equations are in general unable to take such distributions as an input or produce them as an output.

Instead, most macroscopic descriptions introduce some kind of smoothing process by which a state $\mathbf{x} \in \mathbf{X}$ yields a continuous field. A naive implementation of such a smoothing is to convolve the macroscopic density with a so-called smoothing kernel $K: X \rightarrow \mathbb{R}$. The smoothed density field then is given by

$$\tilde{\rho}_K(\mathbf{x}, t; \mathbf{x}) := \int d\mathbf{y} \tilde{\rho}(\mathbf{x} - \mathbf{y}, t; \mathbf{x}) K(\mathbf{y}) = \sum_{j=1}^N K(\mathbf{x} - \tilde{\varphi}_j(t; \mathbf{x})) . \quad (156)$$

We can see that for the macroscopic density specifically the contribution of each component is now not given by a Dirac δ -function, but by the smoothing kernel. Consequently, if K is a smooth field, the density $\tilde{\rho}_K$ becomes a smooth field, too. In the case of an N -body system, we can think of the smoothing procedure as replacing each point particle by a density peak of the shape K .

To preserve normalization, the smoothing kernel needs to satisfy the condition

$$\int d\mathbf{x} K(\mathbf{x}) = 1 , \quad (157)$$

where the main contribution to this integral should come from a neighborhood around the origin. The probably most commonly encountered type of kernel is a normalized Gaussian peak centered around the origin. The width of this peak determines the smoothing scale and should be larger than the distance between neighboring particles. This ensures that the gradient of the smoothed density $\tilde{\rho}_K$ is dominated by the particle positions rather than by the rate of change of the kernel associated to the nearest particle.

While our discussion of smoothing takes the macroscopic density as a key example, it can of course also be performed for other observables. In the context

of interacting N-body systems, the most commonly smoothed quantities are the spatial and velocity densities as well as, in a certain sense, the gravitational force. This gives rise to a hydrodynamic description, where the system of point-particles is considered as a fluid with spatially varying density. Fluid elements move according to the velocity field and source the gravitational potential.

2.4.2 Example: Harmonic Oscillator (IV)

In this subsection, we apply the smoothing procedure outlined above to the macroscopic density of a collection of N independent one-dimensional harmonic oscillators. For the definitions we rely on subsection 2.2.2. Our discussion is quite brief, because in the framework of KFT smoothing is usually replaced by working with expectation values as explained in the following subsection.

Let us consider a Gaussian smoothing kernel in one dimension

$$K(q) = \frac{1}{\sqrt{2\pi\sigma^2}} \exp\left(-\frac{q^2}{2\sigma^2}\right). \quad (158)$$

This kernel can be used to transform the spatial macroscopic density of our collection of oscillators

$$\tilde{\rho}^{(q)}(q; \mathbf{x}) = \sum_{j=1}^N \delta_D(q - \tilde{\varphi}_j(t; \mathbf{x})) \quad (159)$$

into a smooth function. The analytic form of $\tilde{\rho}^{(q)}$ is given in equation (26), though we remark that in more complicated examples it would have to be obtained from the generating functional or an approximation thereof.

Following the prescription in equation (156), the smoothed spatial macroscopic density field is given by

$$\tilde{\rho}_K^{(q)}(q, t; \mathbf{x}) = \int dq' \tilde{\rho}^{(q)}(q - q', t; \mathbf{x}) K(q') = \sum_{j=1}^N K(q - \tilde{\varphi}_j^{(q)}(t; \mathbf{x})) \quad (160)$$

$$= \sum_{j=1}^N \frac{1}{\sqrt{2\pi\sigma^2}} \exp\left(-\frac{(q - \tilde{\varphi}_j^{(q)}(t; \mathbf{x}))^2}{2\sigma^2}\right). \quad (161)$$

Note that the smoothed version of the macroscopic phase space density can be obtained by omitting the superscripts $\bullet^{(q)}$ and employing a two-dimensional Gaussian. While the smoothed density $\tilde{\rho}_K^{(q)}$ is a smooth function as desired, it still is explicitly dependent on the initial conditions \mathbf{x} . However, for large particle numbers N and if the variance σ^2 is sufficiently larger than mean nearest neighbor distance of the particles

$$\frac{1}{N} \sum_{j=1}^N \min_{\ell \neq j} \left\| \mathbf{x}_j^{(q)} - \mathbf{x}_\ell^{(q)} \right\|, \quad (162)$$

the dependence on individual particle positions $\mathbf{x}_j^{(q)}$ is small.

2.4.3 Expectation Values

Above we have described how we can convolve a discretized observable with a smoothing kernel to obtain a smoothed version of that observable. Within the formalism of KFT, such a procedure of smoothing would happen as a final step in the calculation. Indeed, the convolution is formed with the observable evaluated at the final state of the system which thus needs to be known. However, there are alternative smoothing procedures which—conceptually—take place earlier in the calculation.

So far, we assumed that the classical physical system under consideration occupies one single state \mathbf{x} in phase space at initial time t_i . Given this initial value, the evolution is deterministic and yields a unique state $\tilde{\varphi}(t; \mathbf{x})$ at a later time $t > t_i$. The smoothing procedure described above corresponds to replacing this final state by a probability distribution of final states, though this replacement is hidden and not unique.

In contrast, there are two ways of obtaining a well-defined probability distribution of final states. The first of these is to work with stochastic evolution equations, i.e., equations of motion containing inherent noise. In certain physical systems such a description might be adequate due to a high degree of complexity or an environmental coupling. The second way of obtaining a stochastic final state is to start out with a stochastic initial state, i.e., the initial value \mathbf{x} is replaced by a distribution of initial values.

In KFT, we work with the latter of these options. In fact, it is the third and final key idea of KFT we encounter in this chapter: *Determine observables given a stochastic initial state*. Its importance is not primarily due to allowing us to obtain smoothed versions of observables. It is due to the significant simplification stochastic initial conditions provide. Especially in the presence of symmetries, the averaging of an observable over a probability distribution of initial values often yields a simpler expression. Therefore we not only allow for, but actually demand that the system is prepared with initial conditions subject to a probability distribution.

Conceptually, the mentioned simplification results from the fact that the final state of the system does not need to be found explicitly, but only stochastically. When subject to a probability distribution with sufficient symmetry, much of the complexity in the microscopic description cancels out. This is in spirit similar to a hydrodynamic approximation, but with the advantage that the microscopic evolution equations are still fully satisfied.

In order to formally implement the outlined ideas, we need to define probability distributions on phase space. These are maps

$$P: \mathbf{X} \rightarrow \mathbb{R} \quad \text{with} \quad \int d\mathbf{x} P(\mathbf{x}) = 1, \quad (163)$$

where we in particular demand that the integral is well-defined in an appropriate sense. Physically, such a probability distribution usually encodes incomplete knowledge of the state of a system and may be the result of sampling a density field. In accordance with our discussion above, we focus on the case where the initial state of the system is subject to such a probability distribution.

Given a probability distribution of initial states and deterministic equations of motion, we naturally obtain a probability distribution for all times $t > t_i$. Indeed, for any possible initial value \mathbf{x} , the physical evolution map $\tilde{\varphi}$ yields a state $\mathbf{y} = \tilde{\varphi}(t; \mathbf{x})$ at a time $t > t_i$. The probability of finding the system in state \mathbf{y} at time t is then precisely $P(\mathbf{x})$. Note that this works because of phase space trajectories cannot cross in classical mechanics and thus it is not possible that different initial states yield the same final state.

Written as an equation, the probability distributions at initial and later time, $P(\mathbf{x})$ and $P_t(\mathbf{y})$, are related via

$$P(\mathbf{x}) = P_t(\mathbf{y}) \quad \text{with} \quad \mathbf{y} = \tilde{\varphi}(t; \mathbf{x}). \quad (164)$$

This equation relies on the fact that the Jacobi determinant associated to the change of variables $\mathbf{y} \mapsto \mathbf{x}$ satisfies

$$\det\left(\frac{d\mathbf{y}}{d\mathbf{x}}\right) = \det\left(\frac{d\tilde{\varphi}(t; \mathbf{x})}{d\mathbf{x}}\right) = 1 \quad (165)$$

by equation (15). Otherwise $P_t(\mathbf{y})$ would not be normalized and thus could not be regarded as a probability distribution in \mathbf{y} .

This relationship in equation (164) is crucial for the calculation of expectation values for observables. Recall that we defined a classical observable \mathcal{O} as a map depending on the state of the system \mathbf{y} at time $t \geq t_i$ (and potentially additional parameters χ). Given the probability distribution $P_t(\mathbf{y})$ at this time, the expectation value of \mathcal{O} is

$$\langle \mathcal{O} \rangle(\chi, t) := \int d\mathbf{y} P_t(\mathbf{y}) \mathcal{O}(\chi; \mathbf{y}). \quad (166)$$

Note that the integration is over the state \mathbf{y} of the system at time t .

The definition of the expectation value provided above is of little use in practice, because the probability distribution P_t is difficult to determine. However, using equation (164) as well as the fact that the physical observable is given by

$$\tilde{\mathcal{O}}(\chi, t; \mathbf{x}) = \mathcal{O}(\chi; \tilde{\varphi}(t; \mathbf{x})), \quad (167)$$

we can obtain the expectation value of the physical observable via an integral over the initial state,

$$\langle \tilde{\mathcal{O}} \rangle(\chi, t) = \int d\mathbf{x} P(\mathbf{x}) \tilde{\mathcal{O}}(\chi, t; \mathbf{x}). \quad (168)$$

This expression follows from the definition of the expectation value above via the identification $\mathbf{y} = \tilde{\varphi}(t; \mathbf{x})$. Equation (168) provides an expression for the expectation value of an observable without direct dependence on the phase space trajectory of the system. This combines the first and third key ideas of KFT we mentioned.

It is possible to perform the averaging on the generating functional instead of for observables. This exploits the commutativity of the integration over \mathbf{x} with functional derivatives with respect to \mathbf{J} . Specifically, the averaged generating functional can be defined as

$$\langle Z \rangle[\mathbf{J}] = \int d\mathbf{x} P(\mathbf{x}) Z[\mathbf{J}; \mathbf{x}]. \quad (169)$$

In much of the KFT literature this approach is followed and $\langle Z \rangle$ is taken as the central object of the theory.[23, 32] In this thesis, we work in the spirit of [1] which places more emphasis on systems with explicit initial conditions in the construction of KFT. The averaged generating functional can be used to directly extract expectation values

$$\langle \tilde{\mathcal{O}} \rangle(\chi, t) = \mathcal{O} \left(\chi; \frac{\delta}{i \delta J^T(t)} \right) \langle Z \rangle[J] \Big|_{J=0}, \quad (170)$$

though it should be mentioned that performing the averaging in equation (169) explicitly is infeasible in most situations such that in practice the averaging over \mathbf{x} is usually performed as a final step in calculations anyway.

2.4.4 Example: Harmonic Oscillator (V)

In this subsection, we determine expectation values for the harmonic oscillator. In order to do so, we first have to choose a probability distribution of initial values $P(\mathbf{x})$. In applications, such a probability distribution is usually given due to imperfect knowledge of the initial state of the system. This can be caused by experimental or observational uncertainties or because the initial state is obtained via sampling of a macroscopic field. We refer to our applications in chapter 4 for specific examples.

The first choice of a probability distribution of initial values we consider is a perfectly sharp distribution $P(\mathbf{x}) = \delta_D(\mathbf{x} - \mathbf{x}_0)$. It corresponds to the case of perfect knowledge of the initial state of the system and accordingly, the expectation value for any observable is $\langle \tilde{\mathcal{O}} \rangle(t) = \tilde{\mathcal{O}}(t; \mathbf{x}_0)$ for all times $t \in [t_i, t_f]$. While this distribution may seem artificial, in some application it may happen that part of the initial conditions are exactly known and others have uncertainty. For our example we pick precisely such a distribution and set

$$P(\mathbf{x}) = \delta_D(\mathbf{x}^{(p)}) \frac{1}{\sqrt{2\pi\sigma^2}} \exp\left(-\frac{(\mathbf{x}^{(q)})^2}{2\sigma^2}\right). \quad (171)$$

The initial momentum is fixed to $\mathbf{x}^{(p)} = 0$, while the initial position is distributed according to a symmetric Gaussian distribution. In fact, this Gaussian is exactly the smoothing kernel $K(q)$ we defined in subsection 2.4.2.

Let us pick the physical evolution map of the one-dimensional oscillator as our first observable, i.e., $\tilde{\mathcal{O}}(t; \mathbf{x}) = \tilde{\varphi}(t; \mathbf{x})$. Being a very simple system, the harmonic oscillator admits an analytic expression for its physical evolution as given in equation (26). Given any explicit initial condition $\mathbf{x} = (\mathbf{x}^{(q)}, \mathbf{x}^{(p)}) \in \mathcal{X}$, this formula yields the phase space position of the harmonic oscillator at time $t \in [t_i, t_f]$. Its expectation value is

$$\begin{aligned} \langle \tilde{\varphi} \rangle(t) &= \int d\mathbf{x} P(\mathbf{x}) \tilde{\varphi}(t; \mathbf{x}) \quad (172) \\ &= \int d\mathbf{x}^{(q)} \frac{1}{\sqrt{2\pi\sigma^2}} \exp\left(-\frac{(\mathbf{x}^{(q)})^2}{2\sigma^2}\right) \begin{pmatrix} \cos(\sqrt{\frac{\kappa}{m}}(t - t_i)) \mathbf{x}^{(q)} \\ -\sqrt{\kappa m} \sin(\sqrt{\frac{\kappa}{m}}(t - t_i)) \mathbf{x}^{(q)} \end{pmatrix} \quad (173) \end{aligned}$$

The integrals are clearly zero, thus $\langle \tilde{\varphi} \rangle(t) = 0$ for all times t .

For a more non-trivial result, consider the microscopic phase space density

$$\tilde{\rho}(t; \mathbf{x}) = \tilde{\rho}(\mathbf{y}, t; \mathbf{x}) = \delta_D(\mathbf{y} - \tilde{\varphi}(t; \mathbf{x})) . \quad (174)$$

In order to determine its expectation value, we ought to solve the integral

$$\langle \tilde{\rho} \rangle(\mathbf{y}, t) = \int d\mathbf{x} P(\mathbf{x}) \delta_D(\mathbf{y} - \tilde{\varphi}(t; \mathbf{x})) . \quad (175)$$

For initial time $t = t_i$ this is simple, because we can use $\tilde{\varphi}(t_i; \mathbf{x}) = \mathbf{x}$ and obtain $\langle \tilde{\rho} \rangle(\mathbf{y}, t_i) = P(\mathbf{y})$. This exposes that probability distribution of initial values simply corresponds to the phase space density of the system at initial time.

For times $t > t_i$ solving the integral seems more difficult. However, using that equation (26) provides a solution for $t < t_i$, too, it is

$$\delta_D(\mathbf{y} - \tilde{\varphi}(t; \mathbf{x})) = \frac{1}{\det\left(\frac{d\tilde{\varphi}(t; \mathbf{x})}{d\mathbf{x}}\right)} \delta_D(\mathbf{x} - \tilde{\varphi}(2t_i - t; \mathbf{y})) . \quad (176)$$

The determinant is unity by Liouville's theorem (or by direct calculation) and we thus obtain the result

$$\langle \tilde{\rho} \rangle(\mathbf{y}, t) = P(\tilde{\varphi}(2t_i - t; \mathbf{y})) \quad (177)$$

$$= \delta_D\left(\tilde{\varphi}^{(p)}(2t_i - t; \mathbf{y})\right) \frac{1}{\sqrt{2\pi\sigma^2}} \exp\left(-\frac{(\tilde{\varphi}^{(q)}(2t_i - t; \mathbf{y}))^2}{2\sigma^2}\right) . \quad (178)$$

Introducing scaled polar coordinates in phase space given by

$$r = \sqrt{\kappa m (y^{(q)})^2 + (y^{(p)})^2} \quad \text{and} \quad \theta = \arctan\left(\frac{\sqrt{\kappa m} y^{(q)}}{y^{(p)}}\right) \quad (179)$$

One can show that our result can be rewritten as

$$\langle \tilde{\rho} \rangle(\mathbf{y}, t) = \delta_D\left(\theta - \sqrt{\frac{\kappa}{m}}(t + t_i)\right) \frac{1}{r\sqrt{2\pi\kappa m\sigma^2}} \exp\left(-\frac{r^2}{2\kappa m\sigma^2}\right) . \quad (180)$$

Given the interpretation of the expectation value of the microscopic phase space density as a probability distribution, $\langle \tilde{\rho} \rangle(\mathbf{x}, t)$ could be used to set initial conditions for a harmonic oscillator for any value of t . Unless $\theta = 0$, the resulting probability distribution of initial values does not factorize into a product of distributions for $x^{(q)}$ and $x^{(p)}$, respectively. Instead, we are faced with *correlations* between position and momenta. If we were to take a sample from such a distribution, the likelihood function for the momentum would be dependent on the position and vice versa. Such correlations may also exist between the different components of a composite system.

2.4.5 Density Correlation Functions

For the applications of the KFT framework considered in this thesis, the relevant observables are Fourier space density r -point correlation functions. These were defined in section 2.2.1 as

$$G_{\underbrace{\tilde{\rho} \dots \tilde{\rho}}_{r \text{ times}}}(k_1, \dots, k_r, t; \mathbf{x}) = \prod_{s=1}^r \sum_{j_s=1}^N \exp\left(-ik_s \cdot \frac{\delta}{i\delta_{j_s}^T(t)}\right) Z[\mathbf{J}; \mathbf{x}] \Big|_{\mathbf{J}=0} , \quad (181)$$

where the Fourier space macroscopic density $\tilde{\rho}(\mathbf{k}, t; \mathbf{x})$ is recovered for $r = 1$. Recall that in constructing these objects we assumed that the phase space of the system factorizes $\mathbf{X} = \mathbf{X}^N$, i.e., the system is made up from N components with identical component phase space X . In particular, the Fourier transform we use here is of dimension $\frac{2d}{N}$. Abbreviating this fraction via the definition $D := \frac{d}{N}$, it is $k_s \in \mathbb{R}^{2D} \cong X$ for all s . Note that D is the dimension of $X^{(q)}$. In case of an N -body system, it is the number of spatial dimensions in which the particles move.

In our applications the macroscopic phase space density is usually of less interest than the macroscopic spatial density $\tilde{\rho}^{(q)}(\mathbf{k}, t; \mathbf{x})$ and its correlation functions. The wave-vector \mathbf{k} appearing as its argument is an element of \mathbb{R}^D , because the 2D-dimensional Fourier transform is replaced by a D -dimensional one. Its correlation functions are given by

$$G_{\underbrace{\tilde{\rho} \dots \tilde{\rho}}_{r \text{ times}}}^{(q)}(k_1, \dots, k_r, t; \mathbf{x}) = \prod_{s=1}^r \sum_{j_s=1}^N \exp\left(-ik_s \cdot \frac{\delta}{i \delta \left(J_{j_s}^{(q)}\right)^T(t)}\right) Z[\mathbf{J}; \mathbf{x}] \Big|_{\mathbf{J}=0} \quad (182)$$

with $G_{\tilde{\rho}}^{(q)} = \tilde{\rho}^{(q)}$. Given the similarity of the expressions for $G_{\tilde{\rho} \dots \tilde{\rho}}$ and $G_{\tilde{\rho} \dots \tilde{\rho}}^{(q)}$, we consider only the latter in this subsection. The translation into the phase space version requires only the removal of all superscripts $\bullet^{(q)}$, understanding that the dimension of the wave-vectors doubles.

In the spirit of the third key idea of KFT discussed above, we intend to consider expectation values of the correlation functions. Given a probability distribution of initial values P , we have

$$\left\langle G_{\tilde{\rho} \dots \tilde{\rho}}^{(q)} \right\rangle(k_1, k_2, \dots, k_r, t) = \int d\mathbf{x} P(\mathbf{x}) G_{\tilde{\rho} \dots \tilde{\rho}}^{(q)}(k_1, k_2, \dots, k_r, t; \mathbf{x}) \quad (183)$$

in accordance with the definitions above. This expression can be used in a setting where the number of components N is finite.

One of the nice features of the KFT framework is that one can often formally take the limit $N \rightarrow \infty$ in calculations. This continuum or *hydrodynamic limit* allows us to consider systems which have infinite volume V or sidestep issues related to finite resolution. Specifically, there are two limits:

- The limit of infinite component number $N \rightarrow \infty$ and volume $V \rightarrow \infty$ under constant mean density $\bar{\rho} = \frac{N}{V}$. This limit allows the description of an infinitely extended distribution of point masses.
- The limit of infinite component number $N \rightarrow \infty$ and vanishing component mass $m \rightarrow 0$ under constant total mass $M = Nm$. This limit yields a continuous mass distribution.

Both limits can also be taken simultaneously to obtain the description of an infinitely extended continuous mass distribution. An investigation of the mathematical well-definedness of these limits is beyond the scope of this thesis.

In applications, the first of these limits can often be taken as a final step in a calculation. The second limit is sometimes useful when obtaining initial

conditions from a continuous mass distribution. In many cases, the component mass can be absorbed into physical constants or a reparametrization of time. It is then possible to avoid explicit dependence of results on the component mass such that the second of the limits rarely needs to be taken explicitly. We comment more on these limiting procedures in our applications.

Here, the relevant piece of information is that our density correlation functions may describe a system with an infinite number of components. In this case, there is an issue with so-called *shot noise* terms. Essentially, we attempt to describe a continuous system with a particle-based approach and acquire certain relics of the discretization. To exemplify this, consider the two-point density correlation function at initial time $t = t_i$ for an uncorrelated homogeneous system, i.e., $P(\mathbf{x}) = V^{-N} P^{(p)}(\mathbf{x}^{(p)})$. Here, $P^{(p)}$ is any normalized momentum distribution. According to our definitions above, it is

$$\begin{aligned} & \langle G_{\bar{\rho}\bar{\rho}}^{(q)} \rangle(k_1, k_2, t_i) \\ &= \int d\mathbf{x} P(\mathbf{x}) \sum_{j_1, j_2=1}^N \exp \left(-ik_1 \cdot \frac{\delta}{i \delta \left(J_{j_1}^{(q)} \right)^T(t_i)} - ik_2 \cdot \frac{\delta}{i \delta \left(J_{j_2}^{(q)} \right)^T(t_i)} \right) Z[J; \mathbf{x}] \Bigg|_{J=0} \end{aligned} \quad (184)$$

$$= \frac{1}{V^N} \sum_{j_1, j_2=1}^N \int d\mathbf{x}^{(q)} \exp \left(-ik_1 \cdot x_{j_1}^{(q)} - ik_2 \cdot x_{j_2}^{(q)} \right). \quad (185)$$

We have used that $\bar{\varphi}(t_i; \mathbf{x}) = \mathbf{x}$ and have already evaluated the integrations over $\mathbf{x}^{(p)}$. The integrations over $x_\ell^{(q)}$ for $\ell \neq j_1, j_2$ can be evaluated, too, and cancel a number of copies of V . Depending on whether $j_1 = j_2$ either one or two of these factors remain and are paired with a factor N each coming from the sum over component indices. Using $N(N-1) \approx N^2$ in the limit $N \rightarrow \infty$ and introducing the mean density $\bar{\rho}^{(q)} = \frac{N}{V}$, we obtain

$$\langle G_{\bar{\rho}\bar{\rho}}^{(q)} \rangle(k_1, k_2, t_i) = (2\pi)^D \delta_D(k_1 + k_2) \bar{\rho}^{(q)} + (2\pi)^{2D} \delta_D(k_1) \delta_D(k_2) (\bar{\rho}^{(q)})^2. \quad (186)$$

The second term is the expected result

$$\langle G_{\bar{\rho}\bar{\rho}}^{(q)} \rangle(k_1, k_2, t_i) = \langle \bar{\rho}^{(q)} \rangle(k_1, t_i) \langle \bar{\rho}^{(q)} \rangle(k_2, t_i) \quad (187)$$

$$= (2\pi)^{2D} \delta_D(k_1) \delta_D(k_2) (\bar{\rho}^{(q)})^2, \quad (188)$$

where we emphasize that the first equality is valid only if the state is uncorrelated, i.e., knowledge of the state of component j does not provide any information on the state of any other components. The first term in equation (186) should thus not be present. Its appearance stems from the case $j_1 = j_2$, i.e., it is an auto-correlation of a discrete component. Evidently, this is a relic of the discretization and characteristic of shot noise. In the continuum limit $N \rightarrow \infty$, specifically the second of the two limits discussed above, such terms are irrelevant.

Generalizing the example, any terms arising from sums over identical components are shot noise terms. In order to remove these ultimately irrelevant terms for systems subject to a continuum limit $N \rightarrow \infty$, only a slight modification

of our definitions is needed: In our definition of $G_{\tilde{\rho}\dots\tilde{\rho}}^{(q)}$ in equation (182) we remove the terms with identical indices from the sum

$$G_{\underbrace{\tilde{\rho}\dots\tilde{\rho}}_{r \text{ times}}}(k_1, \dots, k_r, t; \mathbf{x}) = \prod_{s=1}^r \sum_{\substack{j_s=1 \\ j_s \neq j_t \forall t}}^N \exp\left(-ik_s \cdot \frac{\delta}{i \delta(J_{j_s}^{(q)})^T(t)}\right) Z[\mathbf{J}; \mathbf{x}] \Big|_{\mathbf{J}=0} \quad (189)$$

$$= \sum_{\substack{\{j_1, \dots, j_r\} \\ j_s \neq j_t \forall s, t}}^N \exp\left(-ik_s \cdot \frac{\delta}{i \delta(J_{j_s}^{(q)})^T(t)}\right) Z[\mathbf{J}; \mathbf{x}] \Big|_{\mathbf{J}=0} \quad (190)$$

and similarly for the equations in section 2.2.1. For further details on shot noise in this context, we refer to [1, 23, 24].

As a final task in this section, we consider density correlation functions in a statistically homogeneous and isotropic setting. However, in contrast to the calculation above, we allow for correlation between the components. Nonetheless, the form of $\langle G_{\tilde{\rho}\tilde{\rho}}^{(q)} \rangle$ remains quite constrained. Indeed, homogeneity and isotropy imply that the expectation value of the macroscopic density field is invariant under translations and rotations in $X^{(q)}$. This implies that its position space two-point correlation function—which is the inverse Fourier transform of $\langle G_{\tilde{\rho}\tilde{\rho}}^{(q)} \rangle$ —can only depend on the norm of the distance between any two points.

As the Fourier transform of a function in a single one-dimensional variable, the (Fourier space) density two-point correlation function $\langle G_{\tilde{\rho}\tilde{\rho}}^{(q)} \rangle$ likewise can be written in terms of a single wave-number. In very similar fashion to the calculation above, we obtain the well-known result

$$\langle G_{\tilde{\rho}\tilde{\rho}}^{(q)} \rangle(k_1, k_2, t) = (2\pi)^D \delta_D(k_1 + k_2) P_{\tilde{\rho}}^{(q)}(k_1, t). \quad (191)$$

Here, the function $P_{\tilde{\rho}}^{(q)}$ is the density power spectrum. Given that it is not apparent from our notation, we point out that $P_{\tilde{\rho}}^{(q)}(k_1, t) = P_{\tilde{\rho}}^{(q)}(\|k_1\|, t)$, i.e., the power spectrum is a function of the norm of k_1 only. Note that provided equations of motion which are invariant under translations and rotations, statistical homogeneity and isotropy are conserved during evolution. Therefore, if the probability distribution of initial values $P(\mathbf{x})$ satisfies these properties, then equation (191) is valid for all $t \in [t_i, t_f]$.

Compared to equation (186), the absence of a term proportional to the product $\delta_D(k_1) \delta_D(k_2)$ in equation (191) might be surprising at first glance. This apparent inconsistency is explained by the fact that due to the non-vanishing expectation value of the density

$$\langle \tilde{\rho}^{(q)} \rangle(\mathbf{k}, t) = (2\pi)^D \delta_D(\mathbf{k}) \bar{\rho}^{(q)} \quad (192)$$

its power spectrum acquires a term proportional to $\bar{\rho}^{(q)} \delta_D(k_1)$. For this and other reasons it is common in the field of cosmic structure formation to consider the power spectrum of the *spatial density contrast*

$$\delta^{(q)}(\mathbf{q}; \mathbf{x}) := \frac{\rho^{(q)}(\mathbf{q}; \mathbf{x}) - \bar{\rho}^{(q)}}{\bar{\rho}^{(q)}} \quad (193)$$

instead. The spatial macroscopic density ρ appearing here has been defined in equation (43) and $\bar{\rho}^{(q)}$ is its expectation value provided a statistically homogeneous and isotropic probability distribution of initial values.

Evaluating the density contrast along the physical evolution $\tilde{\varphi}$ and performing a Fourier transform yields

$$\tilde{\delta}^{(q)}(\mathbf{k}, t; \mathbf{x}) := \frac{\tilde{\rho}^{(q)}(\mathbf{k}, t; \mathbf{x})}{\bar{\rho}^{(q)}} - (2\pi)^D \delta_D(\mathbf{k}). \quad (194)$$

and thus its (Fourier space) two-point correlation function is related to $G_{\tilde{\rho}\tilde{\rho}}^{(q)}$ via the equation

$$\begin{aligned} & \tilde{\delta}^{(q)}(\mathbf{k}_1, t; \mathbf{x}) \tilde{\delta}^{(q)}(\mathbf{k}_2, t; \mathbf{x}) \\ &= (\bar{\rho}^{(q)})^{-2} G_{\tilde{\rho}\tilde{\rho}}^{(q)}(\mathbf{k}_1, \mathbf{k}_2, t; \mathbf{x}) + (2\pi)^{2D} \delta_D(\mathbf{k}_1) \delta_D(\mathbf{k}_2) \\ & \quad - \frac{\tilde{\rho}^{(q)}(\mathbf{k}_1, t; \mathbf{x})}{\bar{\rho}^{(q)}} (2\pi)^D \delta_D(\mathbf{k}_2) - \frac{\tilde{\rho}^{(q)}(\mathbf{k}_2, t; \mathbf{x})}{\bar{\rho}^{(q)}} (2\pi)^D \delta_D(\mathbf{k}_1). \end{aligned} \quad (195)$$

Taking the expectation value over a homogeneous and isotropic probability distribution of initial values of this equation, we obtain

$$\begin{aligned} \langle G_{\tilde{\rho}\tilde{\rho}}^{(q)}(\mathbf{k}_1, \mathbf{k}_2, t) \rangle &= (2\pi)^{2D} \delta_D(\mathbf{k}_1) \delta_D(\mathbf{k}_2) (\bar{\rho}^{(q)})^2 \\ & \quad + (2\pi)^D \delta_D(\mathbf{k}_1 + \mathbf{k}_2) P_{\tilde{\delta}}^{(q)}(\mathbf{k}_1, t), \end{aligned} \quad (196)$$

where we defined the *density fluctuation power spectrum* as

$$\langle \tilde{\delta}^{(q)}(\mathbf{k}_1, t; \mathbf{x}) \tilde{\delta}^{(q)}(\mathbf{k}_2, t; \mathbf{x}) \rangle = (2\pi)^D \delta_D(\mathbf{k}_1 + \mathbf{k}_2) P_{\tilde{\delta}}^{(q)}(\mathbf{k}_1, t). \quad (197)$$

This is well-defined because invariance under translations and rotations of its expectation value is inherited from the spatial macroscopic density to the density contrast.

Equation (196) is an important result of this subsection. It shows that the density fluctuation power spectrum can be obtained from the two-point correlation function of the spatial macroscopic density as the prefactor of the term $(2\pi)^D \delta_D(\mathbf{k}_1 + \mathbf{k}_2)$. The function $P_{\tilde{\delta}}^{(q)}$ is a very important observable in cosmological applications. Its computation for an interacting N-body system is the main goal of section 4.2.

3.1 PERTURBATIVE TREATMENT

In the previous chapter we introduced the formalism of Kinetic Field Theory (KFT). We have defined the generating functional as the central mathematical object and have shown that it can be written as

$$Z[\mathbf{J}; \mathbf{x}] = \mathcal{T} \exp \left(-i \int_{t_i}^{t_f} dt' \int_{t'}^{t_f} dt'' \mathbf{J}^T(t'') \mathbf{G}(t'', t') \mathbf{E}_I \left[\frac{\delta}{i \delta \mathbf{J}^T} \right] (t') \right) \exp \left(i \int_{t_i}^{t_f} dt' \mathbf{J}^T(t') \mathbf{G}(t', t_i) \mathbf{x} \right) \quad (198)$$

by performing a split of the equations of motion into a free and an interaction part. From the generating functional we can derive observables. Provided a probability distribution of initial values, these observables acquire expectation values.

It is possible to proceed in different ways to further evaluate the expression for the generating functional above. One of them is the so-called mean field approximation for which we refer to [34] and the references within. In this thesis we follow the perturbative approach proposed in the original proposal of KFT [23]. It is based on a series expansion of the first exponential in the above equation.

Below we perform such a series expansion and study in detail the low order contributions. We utilize a formalism involving operators and commutators inspired by Quantum Mechanics. It soon becomes clear that the main difficulty in the series expansion is of combinatorial nature. Every functional derivative with respect to \mathbf{J} has plenty of options which factors of \mathbf{J} to act on which needs to be accounted for by appropriate product rules.

In subsection 3.1.2 we translate the series expansion of the generating functional into a series expansion for observables. By replacing the source field \mathbf{J} by functional derivatives with respect to the free evolution $\bar{\varphi}$ and functional derivatives with respect to \mathbf{J} by the free evolution itself, we are able to derive the formula

$$\tilde{\mathcal{O}}_n(\chi; t; \mathbf{x}) = i^n \int_{t_i}^{t_f} dt'_n \cdots \int_{t_i}^{t'_2} dt'_1 \hat{\Gamma}_I(t'_1) \cdots \hat{\Gamma}_I(t'_n) \mathcal{O}(\chi; \bar{\varphi}(t; \mathbf{x})) \quad (199)$$

for the n^{th} order contribution to the observable $\tilde{\mathcal{O}}$. Importantly, the operators $\hat{\Gamma}_I$ are defined solely in terms of the free evolution and functional derivatives with respect to it. No reference to the field \mathbf{J} or the generating functional remain.

We apply the perturbative expression for observables to the physical evolution $\bar{\varphi}$ of the harmonic oscillator in subsection 3.1.3. Working in Newtonian Gauge we determine the contributions $\tilde{\varphi}_n$ up to second order $n \leq 2$. The resulting expressions are Taylor approximations of the analytical solution given in equation (26), though their order is different for the position and momentum parts.

Except for the idea of performing a series expansion in the interactions, the entirety of this section is original work. To the best of my knowledge, equation (252) referenced above is the simplest mathematical expression for the n^{th} order contribution to a general observable in the KFT literature.

3.1.1 Expansion in Interactions

The main result of the previous chapter is the expression

$$Z[\mathbf{J}; \mathbf{x}] = \mathcal{T} \exp \left(i \int_{t_i}^{t_f} dt' \hat{L}_I(t') \right) Z_0[\mathbf{J}; \mathbf{x}] \quad \text{with} \quad (200)$$

$$\hat{L}_I(t') = - \int_{t'}^{t_f} dt'' \mathbf{J}^T(t'') \mathbf{G}(t'', t') \mathbf{E}_I \left[\frac{\delta}{i \delta \mathbf{J}^T} \right] (t') \quad \text{and} \quad (201)$$

$$Z_0[\mathbf{J}; \mathbf{x}] = \exp \left(i \int_{t_i}^{t_f} dt' \mathbf{J}(t') \cdot \bar{\boldsymbol{\varphi}}(t'; \mathbf{x}) \right). \quad (202)$$

for the generating functional given in equation (151). It separates free motion given by the free physical evolution $\bar{\boldsymbol{\varphi}}(t; \mathbf{x}) = \mathbf{G}(t, t_i) \mathbf{x}$ from the interactions encoded in \mathbf{E}_I . Observables and their expectation values can be obtained from the generating functional via functional derivatives with respect to the field \mathbf{J} . For this procedure to be facilitated in practice, one would prefer the functional derivatives in $Z[\mathbf{J}; \mathbf{x}]$ to be evaluated explicitly. Ideally, we would have a closed form for the generating functional as a functional of \mathbf{J} .

As explained in the introduction to this section, it is in general not feasible to achieve this. On a technical level, a central problem is that the operators $\hat{L}_I(t)$ at different times t do not commute for non-trivial interactions \mathbf{E}_I . As a result, in a series expansion of the time-ordered exponential the higher order terms acquire substantial combinatorial complexity which impedes a resummation of the resulting expression. This suggests a perturbative treatment of interactions based on a truncation of such an expansion.

Without resigning yet to the inevitable need for an approximate treatment, let us attempt to explicitly evaluate the functional derivatives with respect to \mathbf{J} in our expression for the generating functional. As a preparatory step, consider the action of a single operator \hat{L}_I on the free generating functional. Recalling our assumption that \mathbf{E}_I is a convergent analytic power series in its argument and abbreviating $\bar{\mathbf{E}}_I(t'; \mathbf{x}) := \mathbf{E}_I[\bar{\boldsymbol{\varphi}}(\bullet; \mathbf{x})](t')$, it is

$$\mathbf{E}_I \left[\frac{\delta}{i \delta \mathbf{J}^T} \right] (t') Z_0[\mathbf{J}; \mathbf{x}] = \bar{\mathbf{E}}_I(t'; \mathbf{x}) Z_0[\mathbf{J}; \mathbf{x}] \quad \text{and hence} \quad (203)$$

$$\hat{L}_I(t') Z_0[\mathbf{J}; \mathbf{x}] = - \int_{t'}^{t_f} dt'' \mathbf{J}^T(t'') \mathbf{G}(t'', t') \bar{\mathbf{E}}_I(t'; \mathbf{x}) Z_0[\mathbf{J}; \mathbf{x}]. \quad (204)$$

As we can see, the functional derivatives merely get replaced by the free physical evolution. This is completely analogous to the action of classical observables on the generating functional discussed in subsection 2.2.1. For compactness of notation in the following, let us abbreviate

$$\bar{L}_I(t'; \mathbf{x}) := - \int_{t'}^{t_f} dt'' \mathbf{J}^T(t'') \mathbf{G}(t'', t') \bar{\mathbf{E}}_I(t'; \mathbf{x}) \quad (205)$$

such that $\hat{L}_I(t') Z_0[\mathbf{J}; \mathbf{x}] = \bar{L}_I(t'; \mathbf{x}) Z_0[\mathbf{J}; \mathbf{x}]$. In analogy to the path integral formulation of Quantum Field Theory (QFT), we may think of \bar{L}_I as the vacuum expectation value of the operator \hat{L}_I , though we refrain from using this terminology to avoid confusion with expectation values of classical observables defined in subsection 2.4.3.

While it was almost trivial to determine the action of a single operator \hat{L}_I on the free generating functional, the aforementioned combinatorial complexity at higher orders becomes apparent already when considering the action of two such operators. Indeed, it is

$$\hat{L}_I(t'_2) \hat{L}_I(t'_1) Z_0[\mathbf{J}; \mathbf{x}] = \bar{L}_I(t'_2; \mathbf{x}) \bar{L}_I(t'_1; \mathbf{x}) Z_0[\mathbf{J}; \mathbf{x}] + [\hat{L}_I(t'_2), \hat{L}_I(t'_1)] Z_0[\mathbf{J}; \mathbf{x}] \quad (206)$$

for $t'_1 \leq t'_2$. In this expression we use the standard commutator given by

$$[\hat{L}_I(t'_2), \hat{L}_I(t'_1)] = \hat{L}_I(t'_2) \hat{L}_I(t'_1) - \hat{L}_I(t'_1) \hat{L}_I(t'_2). \quad (207)$$

Equation (206) follows from causality of the Green's function which implies

$$\hat{L}_I(t'_1) \hat{L}_I(t'_2) Z_0[\mathbf{J}; \mathbf{x}] = \bar{L}_I(t'_2; \mathbf{x}) \bar{L}_I(t'_1; \mathbf{x}) Z_0[\mathbf{J}; \mathbf{x}]. \quad (208)$$

Indeed, acting with $\hat{L}_I(t'_1)$ on the factor $\mathbf{J}^T(t'_2)$ inside $\hat{L}_I(t'_2)$ yields a vanishing factor $\mathbf{G}(t'_1, t'_2)$ due to $t'_1 \leq t'_2$. Hence, the only non-zero contribution comes from both these operators acting directly on Z_0 .

There are two interesting avenues of investigation suggested by equation (206). Firstly, the action of the commutator on the free generating functional should be determined. Secondly, the generalization to higher numbers of operators needs to be obtained. Independently of these, we remark that the non-zero commutator in this equation is indeed the source of complexity as claimed above.

As a first task, let us obtain an explicit expression for the commutator acting on the free generating functional. For this purpose, we need to calculate the action of the interaction part of the equations of motion \mathbf{E}_I on \bar{L}_I . The result is

$$\begin{aligned} & \mathbf{E}_I \left[\frac{\delta}{i \delta \mathbf{J}^T} \right] (t'_2) \bar{L}_I(t'_1; \mathbf{x}) Z_0[\mathbf{J}; \mathbf{x}] \\ &= - \mathbf{E}_I \left[\frac{\delta}{i \delta \mathbf{J}^T} \right] (t'_2) \int_{t'_1}^{t_f} dt''_1 \mathbf{J}^T(t''_1) \mathbf{G}(t''_1, t'_1) \bar{\mathbf{E}}_I(t'_1; \mathbf{x}) Z_0[\mathbf{J}; \mathbf{x}] \end{aligned} \quad (209)$$

$$\begin{aligned} &= (\bar{\mathbf{E}}_I^T(t'_1; \mathbf{x}) \mathbf{G}^T(t'_2, t'_1) i \nabla^T) \mathbf{E}_I \left[\frac{\delta}{i \delta \mathbf{J}^T} \right] (t'_2) Z_0[\mathbf{J}; \mathbf{x}] \\ &\quad - \int_{t'_1}^{t_f} dt''_1 \mathbf{J}^T(t''_1) \mathbf{G}(t''_1, t'_1) \bar{\mathbf{E}}_I(t'_1; \mathbf{x}) \mathbf{E}_I \left[\frac{\delta}{i \delta \mathbf{J}^T} \right] (t'_2) Z_0[\mathbf{J}; \mathbf{x}] \end{aligned} \quad (210)$$

$$= \bar{\mathbf{E}}_I^T(t'_1; \mathbf{x}) \mathbf{G}^T(t'_2, t'_1) i \nabla^T \bar{\mathbf{E}}_I(t'_2; \mathbf{x}) Z_0[\mathbf{J}; \mathbf{x}] + \bar{L}_I(t'_1; \mathbf{x}) \bar{\mathbf{E}}_I(t'_2; \mathbf{x}) Z_0[\mathbf{J}; \mathbf{x}], \quad (211)$$

in analogy to the calculation performed in equation (127). In particular, the appearance of the Jacobian of \mathbf{E}_I is explained in equation (128).

If we replace the factor \mathbf{E}_I by $\hat{L}_I(t'_2)$ in the calculation above, the second term in equation (211) coincides with the one in equation (208). Consequently, it cancels with the second term of equation (207) when calculating the commutator. As a result, we obtain

$$\begin{aligned} [\hat{L}_I(t'_2), \hat{L}_I(t'_1)] Z_0[\mathbf{J}; \mathbf{x}] &= - \int_{t'_2}^{t_f} dt''_2 \mathbf{J}^T(t''_2) \mathbf{G}(t''_2, t'_2) \\ &\quad (\bar{\mathbf{E}}_I^T(t'_1; \mathbf{x}) \mathbf{G}^T(t'_2, t'_1) i \nabla^T) \bar{\mathbf{E}}_I(t'_2; \mathbf{x}) Z_0[\mathbf{J}; \mathbf{x}]. \end{aligned} \quad (212)$$

While it is possible to fully evaluate the functional derivatives with respect to \mathbf{J} , the resulting expression is somewhat complicated in structure. Note that the term in the round brackets and thus also the entire term is a scalar quantity as it should be.

The obtained form of the commutator $[\hat{\mathbb{L}}_I(t'_2), \hat{\mathbb{L}}_I(t'_1)] Z_0[\mathbf{J}; \mathbf{x}]$ is similar to the form of $\bar{\mathbb{L}}_I(t'_2)$ in that it is linear in $\mathbf{J}(t'_2)$ which is contracted via a Green's function with the term involving \mathbf{E}_I . However, the this term is no longer just \mathbf{E}_I itself, but a certain derivative operator applied to it. Given that this derivative cannot act on either \mathbf{J} or \mathbf{G} , we can write more compactly

$$[\hat{\mathbb{L}}_I(t'_2), \hat{\mathbb{L}}_I(t'_1)] Z_0[\mathbf{J}; \mathbf{x}] = \bar{\mathbf{E}}_I^T(t'_1; \mathbf{x}) \mathbf{G}^T(t'_2, t'_1) i \nabla^T \bar{\mathbb{L}}_I(t'_2; \mathbf{x}) Z_0[\mathbf{J}; \mathbf{x}]. \quad (213)$$

It is worthwhile to comment on the derivative operator ∇ here. We have used it somewhat symbolically so far, understanding that it is supposed to provide us with the Jacobian matrix of \mathbf{E}_I when it is regarded as a function of its argument. However, given that \mathbf{E}_I is a functional, ∇ is technically a functional derivative

$$\nabla^T \bar{\mathbf{E}}_I(t'_2; \mathbf{x}) = \frac{\delta}{\delta \bar{\boldsymbol{\varphi}}^T(t'_2; \mathbf{x})} \mathbf{E}_I[\bar{\boldsymbol{\varphi}}(\bullet; \mathbf{x})](t'_2). \quad (214)$$

Evaluating the functional at the same time parameter as the functional derivative is unusual, hence it is natural to reintroduce the integration over t''_1 . This transforms equation (213) into

$$[\hat{\mathbb{L}}_I(t'_2), \hat{\mathbb{L}}_I(t'_1)] Z_0[\mathbf{J}; \mathbf{x}] = - \int_{t'_1}^{t'_f} dt''_1 \bar{\mathbf{E}}_I^T(t'_1; \mathbf{x}) \mathbf{G}^T(t''_1, t'_1) \left(\frac{\delta}{i \delta \bar{\boldsymbol{\varphi}}^T(t''_1; \mathbf{x})} \bar{\mathbb{L}}_I(t'_2; \mathbf{x}) \right) Z_0[\mathbf{J}; \mathbf{x}]. \quad (215)$$

Conveniently, the action of the functional derivative with respect to the free physical evolution $\bar{\boldsymbol{\varphi}}$ on the free generating functional yields a factor of $i\mathbf{J}$. Specifically, it is

$$- \int_{t'_1}^{t'_f} dt''_1 \bar{\mathbf{E}}_I^T(t'_1; \mathbf{x}) \mathbf{G}^T(t''_1, t'_1) \frac{\delta}{i \delta \bar{\boldsymbol{\varphi}}^T(t''_1; \mathbf{x})} Z_0[\mathbf{J}; \mathbf{x}] = \bar{\mathbb{L}}_I(t'_1; \mathbf{x}) Z_0[\mathbf{J}; \mathbf{x}]. \quad (216)$$

This allows us to combine the two terms on the right-hand side of equation (206) and we obtain

$$\hat{\mathbb{L}}_I(t'_2) \hat{\mathbb{L}}_I(t'_1) Z_0[\mathbf{J}; \mathbf{x}] = - \int_{t'_1}^{t'_f} dt''_1 \bar{\mathbf{E}}_I^T(t'_1; \mathbf{x}) \mathbf{G}^T(t''_1, t'_1) \frac{\delta}{i \delta \bar{\boldsymbol{\varphi}}^T(t''_1; \mathbf{x})} \bar{\mathbb{L}}_I(t'_2; \mathbf{x}) Z_0[\mathbf{J}; \mathbf{x}]. \quad (217)$$

The functional derivative acts on all terms to its right here such that the two terms are recovered via a product rule. Given that the factor $\bar{\mathbb{L}}_I(t'_2; \mathbf{x})$ is adjacent to Z_0 , we can replace its factor \mathbf{J} by a functional derivative, too. Doing so yields the important identity

$$\hat{\mathbb{L}}_I(t'_2) \hat{\mathbb{L}}_I(t'_1) Z_0[\mathbf{J}; \mathbf{x}] = \hat{\Gamma}_I(t'_1) \hat{\Gamma}_I(t'_2) Z_0[\mathbf{J}; \mathbf{x}] \quad \text{with} \quad (218)$$

$$\hat{\Gamma}_I(t') := - \int_{t'}^{t'_f} dt'' \bar{\mathbf{E}}_I^T(t'; \mathbf{x}) \mathbf{G}^T(t'', t') \frac{\delta}{i \delta \bar{\boldsymbol{\varphi}}^T(t''; \mathbf{x})}. \quad (219)$$

Note that while on the left-hand side of equation (218) the functional derivatives are the argument of \mathbf{E}_I , they appear as an independent factor on the right-hand side. Effectively, we have replaced

$$\left(\mathbf{J}(t), \frac{\delta}{i \delta \mathbf{J}^T(t)} \right) \mapsto \left(\frac{\delta}{i \delta \bar{\boldsymbol{\varphi}}^T(t; \mathbf{x})}, \bar{\boldsymbol{\varphi}}(t; \mathbf{x}) \right) \quad (220)$$

in going from $\hat{\mathbf{L}}_I$ to $\hat{\Gamma}_I$. This works because of their dual nature in Z_0 .

As our second task, consider the case of three operators $\hat{\mathbf{L}}_I$ acting on the free generating functional Z_0 . Suppose that $t'_1 \leq t'_2 \leq t'_3$. Using the definition of the commutator, we have simply

$$\begin{aligned} & \hat{\mathbf{L}}_I(t'_3) \hat{\mathbf{L}}_I(t'_2) \hat{\mathbf{L}}_I(t'_1) Z_0[\mathbf{J}; \mathbf{x}] \\ &= \hat{\mathbf{L}}_I(t'_3) \hat{\mathbf{L}}_I(t'_1) \hat{\mathbf{L}}_I(t'_2) Z_0[\mathbf{J}; \mathbf{x}] + \hat{\mathbf{L}}_I(t'_3) [\hat{\mathbf{L}}_I(t'_2), \hat{\mathbf{L}}_I(t'_1)] Z_0[\mathbf{J}; \mathbf{x}] \end{aligned} \quad (221)$$

$$\begin{aligned} &= \hat{\mathbf{L}}_I(t'_1) \hat{\mathbf{L}}_I(t'_2) \hat{\mathbf{L}}_I(t'_3) Z_0[\mathbf{J}; \mathbf{x}] + [\hat{\mathbf{L}}_I(t'_3), \hat{\mathbf{L}}_I(t'_1) \hat{\mathbf{L}}_I(t'_2)] Z_0[\mathbf{J}; \mathbf{x}] \\ &+ [\hat{\mathbf{L}}_I(t'_2), \hat{\mathbf{L}}_I(t'_1)] \hat{\mathbf{L}}_I(t'_3) Z_0[\mathbf{J}; \mathbf{x}] + [\hat{\mathbf{L}}_I(t'_3), [\hat{\mathbf{L}}_I(t'_2), \hat{\mathbf{L}}_I(t'_1)]] Z_0[\mathbf{J}; \mathbf{x}]. \end{aligned} \quad (222)$$

Alternatively, the same result is obtained by applying the product rule. Let us consider the four terms individually. The first one is clearly the easiest, because the reversed time-ordering allows to act with all three operators directly on Z_0 . This yields

$$\hat{\mathbf{L}}_I(t'_1) \hat{\mathbf{L}}_I(t'_2) \hat{\mathbf{L}}_I(t'_3) Z_0[\mathbf{J}; \mathbf{x}] = \bar{\mathbf{L}}_I(t'_3; \mathbf{x}) \bar{\mathbf{L}}_I(t'_2; \mathbf{x}) \bar{\mathbf{L}}_I(t'_1; \mathbf{x}) Z_0[\mathbf{J}; \mathbf{x}], \quad (223)$$

where on the right-hand side the ordering can be exchanged.

The remaining terms in equation (222) are the ones which enable the simplicity of the first one. Indeed, the commutators are the price to pay for ordering the operators such that their functional derivatives do not interfere with each other. Considering this calculation in terms of product rules, it is the term in which all functional derivatives act directly on Z_0 . From this point of view, the terms involving commutators are the ones for which derivatives act on the factors of \mathbf{J} contained in the $\hat{\mathbf{L}}_I$.

Let us consider the second term of equation (222) next. It can be simplified using a commutator identity or, equivalently, a product rule, to yield

$$\begin{aligned} [\hat{\mathbf{L}}_I(t'_3), \hat{\mathbf{L}}_I(t'_1) \hat{\mathbf{L}}_I(t'_2)] Z_0[\mathbf{J}; \mathbf{x}] &= \hat{\mathbf{L}}_I(t'_1) [\hat{\mathbf{L}}_I(t'_3), \hat{\mathbf{L}}_I(t'_2)] Z_0[\mathbf{J}; \mathbf{x}] \\ &+ [\hat{\mathbf{L}}_I(t'_3), \hat{\mathbf{L}}_I(t'_1)] \hat{\mathbf{L}}_I(t'_2) Z_0[\mathbf{J}; \mathbf{x}]. \end{aligned} \quad (224)$$

Using causality of the Green's function and our calculation of the Green's function above, the first of the resulting terms yields

$$\bar{\mathbf{L}}_I(t'_1; \mathbf{x}) \bar{\mathbf{E}}_I^T(t'_2; \mathbf{x}) \mathbf{G}^T(t'_3, t'_2) i \nabla^T \bar{\mathbf{L}}_I(t'_3; \mathbf{x}) Z_0[\mathbf{J}; \mathbf{x}]. \quad (225)$$

The other term is more complicated, because the functional derivative in $\hat{\mathbf{L}}_I(t'_3)$ can act on the factor $\mathbf{J}^T(t'_2)$ in $\hat{\mathbf{L}}_I(t'_2)$. This necessitates yet another use of the product rule and we obtain two contributions

$$\begin{aligned} & \bar{\mathbf{E}}_I^T(t'_2; \mathbf{x}) \mathbf{G}^T(t'_3, t'_2) (\bar{\mathbf{E}}_I^T(t'_1; \mathbf{x}) \mathbf{G}^T(t'_3, t'_1) i \nabla^T) i \nabla^T \bar{\mathbf{L}}_I(t'_3; \mathbf{x}) Z_0[\mathbf{J}; \mathbf{x}] \\ &+ \bar{\mathbf{L}}_I(t'_2; \mathbf{x}) \bar{\mathbf{E}}_I^T(t'_1; \mathbf{x}) \mathbf{G}^T(t'_3, t'_1) i \nabla^T \bar{\mathbf{L}}_I(t'_3; \mathbf{x}) Z_0[\mathbf{J}; \mathbf{x}] \end{aligned} \quad (226)$$

for the second term. Note that a second derivative of the interaction part of the equations of motion \mathbf{E}_I appears in the first of the two contributions.

The third term of equation (222) is simpler again, because the largest time coordinate t'_3 appears on the right. Therefore, we get

$$\begin{aligned} & [\hat{L}_I(t'_2), \hat{L}_I(t'_1)] \hat{L}_I(t'_3) Z_0[\mathbf{J}; \mathbf{x}] \\ &= \bar{L}_I(t'_3; \mathbf{x}) \bar{\mathbf{E}}_I^\top(t'_1; \mathbf{x}) \mathbf{G}^\top(t'_2, t'_1) i \nabla^\top \bar{L}_I(t'_2; \mathbf{x}) Z_0[\mathbf{J}; \mathbf{x}], \end{aligned} \quad (227)$$

where we moved $\bar{L}_I(t'_3; \mathbf{x})$ to the left to make clear that the derivative acts exclusively on $\bar{L}_I(t'_2; \mathbf{x})$.

Finally, the fourth term more complicated as it contains two nested commutators. However, we can use that the inner commutator can be rewritten as the right-hand side of equation (213). This leaves only a single factor of \mathbf{J} to be acted upon by $\hat{L}_I(t'_3)$. The resulting expression is

$$\begin{aligned} & [\hat{L}_I(t'_3), [\hat{L}_I(t'_2), \hat{L}_I(t'_1)]] Z_0[\mathbf{J}; \mathbf{x}] \\ &= \bar{\mathbf{E}}_I^\top(t'_1; \mathbf{x}) \mathbf{G}^\top(t'_2, t'_1) i \nabla^\top \bar{\mathbf{E}}_I^\top(t'_2; \mathbf{x}) \mathbf{G}^\top(t'_3, t'_2) i \nabla^\top \bar{L}_I(t'_3; \mathbf{x}) Z_0[\mathbf{J}; \mathbf{x}], \end{aligned} \quad (228)$$

where each of the derivatives ∇^\top acts only on the object to their immediate right.

Combining the results above, we have

$$\begin{aligned} & \hat{L}_I(t'_3) \hat{L}_I(t'_2) \hat{L}_I(t'_1) Z_0[\mathbf{J}; \mathbf{x}] \\ &= \bar{L}_I(t'_3; \mathbf{x}) \bar{L}_I(t'_2; \mathbf{x}) \bar{L}_I(t'_1; \mathbf{x}) Z_0[\mathbf{J}; \mathbf{x}] \\ & \quad + \bar{L}_I(t'_1; \mathbf{x}) \bar{\mathbf{E}}_I^\top(t'_2; \mathbf{x}) \mathbf{G}^\top(t'_3, t'_2) i \nabla^\top \bar{L}_I(t'_3; \mathbf{x}) Z_0[\mathbf{J}; \mathbf{x}] \\ & \quad + \bar{L}_I(t'_2; \mathbf{x}) \bar{\mathbf{E}}_I^\top(t'_1; \mathbf{x}) \mathbf{G}^\top(t'_3, t'_1) i \nabla^\top \bar{L}_I(t'_3; \mathbf{x}) Z_0[\mathbf{J}; \mathbf{x}] \\ & \quad + \bar{L}_I(t'_3; \mathbf{x}) \bar{\mathbf{E}}_I^\top(t'_1; \mathbf{x}) \mathbf{G}^\top(t'_2, t'_1) i \nabla^\top \bar{L}_I(t'_2; \mathbf{x}) Z_0[\mathbf{J}; \mathbf{x}] \\ & \quad + \bar{\mathbf{E}}_I^\top(t'_2; \mathbf{x}) \mathbf{G}^\top(t'_3, t'_2) (\bar{\mathbf{E}}_I^\top(t'_1; \mathbf{x}) \mathbf{G}^\top(t'_3, t'_1) i \nabla^\top) i \nabla^\top \bar{L}_I(t'_3; \mathbf{x}) Z_0[\mathbf{J}; \mathbf{x}] \\ & \quad + \bar{\mathbf{E}}_I^\top(t'_1; \mathbf{x}) \mathbf{G}^\top(t'_2, t'_1) i \nabla^\top \bar{\mathbf{E}}_I^\top(t'_2; \mathbf{x}) \mathbf{G}^\top(t'_3, t'_2) i \nabla^\top \bar{L}_I(t'_3; \mathbf{x}) Z_0[\mathbf{J}; \mathbf{x}] \end{aligned} \quad (229)$$

under the assumption $t'_1 \leq t'_2 \leq t'_3$. Again, in the spirit of the replacement (220), we can combine these terms and obtain

$$\hat{L}_I(t'_3) \hat{L}_I(t'_2) \hat{L}_I(t'_1) Z_0[\mathbf{J}; \mathbf{x}] = \hat{\Gamma}_I(t'_1) \hat{\Gamma}_I(t'_2) \hat{\Gamma}_I(t'_3) Z_0[\mathbf{J}; \mathbf{x}]. \quad (230)$$

By studying the action of small numbers of operators \hat{L}_I on the free generating functional, we have gained a few important insights:

- The main complexity appearing in a series expansion is due to the non-vanishing commutator $[\hat{L}_I(t'_2), \hat{L}_I(t'_1)]$. At higher orders the number of these terms increases rapidly. There does not appear to be a way to perform a resummation of these terms without reintroducing functional derivatives.
- For any order $n \in \mathbb{N}$, the terms not involving commutators are of the form $\bar{L}_I(t'_n) \cdots \bar{L}_I(t'_2) \bar{L}_I(t'_1) Z_0[\mathbf{J}; \mathbf{x}]$ and thus can be resummed yielding

$$\mathcal{T} \exp \left(i \int_{t_i}^{t_f} dt' \bar{L}_I(t') \right) Z_0[\mathbf{J}; \mathbf{x}] = \exp \left(i \int_{t_i}^{t_f} dt' \bar{L}_I(t') \right) Z_0[\mathbf{J}; \mathbf{x}]. \quad (231)$$

However, in absence of a resummation of the terms involving commutators, such a partial resummation might be difficult to justify.

- It is possible to replace \mathbf{J} and functional derivative with respect to it by functional derivatives to $\bar{\varphi}$ and by $\bar{\varphi}$, respectively. In fact, the replacement (220) can be applied directly on the interaction operator \hat{S}_I , and we obtain the equality

$$Z[\mathbf{J}; \mathbf{x}] = \mathcal{T} \exp \left(i \int_{t_i}^{t_f} dt' \hat{\Gamma}_I(t') \right) Z_0[\mathbf{J}; \mathbf{x}] \quad \text{with} \quad (232)$$

$$\hat{\Gamma}_I(t') = - \int_{t'}^{t_f} dt'' \bar{\mathbf{E}}_I^T(t'; \mathbf{x}) \mathbf{G}^T(t'', t') \frac{\delta}{i \delta \bar{\varphi}^T(t''; \mathbf{x})}. \quad (233)$$

We denoted the reverse time-ordered exponential by $\mathcal{T} \exp$. It appears because the direction in which the derivatives act is effectively reversed be the replacement.

We remark that the exponential given in equation (232) is better suited to an expansion of the exponential. The main advantage is that the commutator satisfies

$$[\hat{\Gamma}_I(t'_1), \hat{\Gamma}_I(t'_2)] \zeta[\bar{\varphi}(\bullet; \mathbf{x})] = (\hat{\Gamma}_I(t'_1) \hat{\Gamma}_I(t'_2)) \zeta[\bar{\varphi}(\bullet; \mathbf{x})] \quad (234)$$

for any functional ζ . The round bracket on the right-hand side indicates that the derivative inside $\hat{\Gamma}_I(t'_1)$ only acts on $\hat{\Gamma}_I(t'_2)$ instead of on all terms to its right. The fact that the commutator can be expressed in terms of contractions of $\hat{\Gamma}_I$ itself provides a more straightforward way to obtain the results in equation (229).

To demonstrate the advantage using $\hat{\Gamma}_I$, let us repeat the calculations for the second and third order terms in the series expansion. It is

$$\begin{aligned} & \hat{\Gamma}_I(t'_1) \hat{\Gamma}_I(t'_2) Z_0[\mathbf{J}; \mathbf{x}] \\ &= \bar{\mathbf{L}}_I(t'_1; \mathbf{x}) \bar{\mathbf{L}}_I(t'_2; \mathbf{x}) Z_0[\mathbf{J}; \mathbf{x}] + [\hat{\Gamma}_I(t'_1), \bar{\mathbf{L}}_I(t'_2; \mathbf{x})] Z_0[\mathbf{J}; \mathbf{x}], \end{aligned} \quad (235)$$

where neither term on the right-hand side retains derivatives acting on Z_0 . In particular, the only appearances of \mathbf{J} outside Z_0 is in the factors of $\bar{\mathbf{L}}_I$. The third order term is

$$\begin{aligned} & \hat{\Gamma}_I(t'_1) \hat{\Gamma}_I(t'_2) \hat{\Gamma}_I(t'_3) Z_0[\mathbf{J}; \mathbf{x}] \\ &= \hat{\Gamma}_I(t'_1) \bar{\mathbf{L}}_I(t'_2; \mathbf{x}) \bar{\mathbf{L}}_I(t'_3; \mathbf{x}) Z_0[\mathbf{J}; \mathbf{x}] + \hat{\Gamma}_I(t'_1) [\hat{\Gamma}_I(t'_2), \bar{\mathbf{L}}_I(t'_3; \mathbf{x})] Z_0[\mathbf{J}; \mathbf{x}] \quad (236) \\ &= \bar{\mathbf{L}}_I(t'_1; \mathbf{x}) \bar{\mathbf{L}}_I(t'_2; \mathbf{x}) \bar{\mathbf{L}}_I(t'_3; \mathbf{x}) Z_0[\mathbf{J}; \mathbf{x}] + \bar{\mathbf{L}}_I(t'_1; \mathbf{x}) [\hat{\Gamma}_I(t'_2), \bar{\mathbf{L}}_I(t'_3; \mathbf{x})] Z_0[\mathbf{J}; \mathbf{x}] \\ & \quad + \bar{\mathbf{L}}_I(t'_2; \mathbf{x}) [\hat{\Gamma}_I(t'_1), \bar{\mathbf{L}}_I(t'_3; \mathbf{x})] Z_0[\mathbf{J}; \mathbf{x}] + \bar{\mathbf{L}}_I(t'_3; \mathbf{x}) [\hat{\Gamma}_I(t'_1), \bar{\mathbf{L}}_I(t'_2; \mathbf{x})] Z_0[\mathbf{J}; \mathbf{x}] \\ & \quad + [\hat{\Gamma}_I(t'_1), [\hat{\Gamma}_I(t'_2), \bar{\mathbf{L}}_I(t'_3; \mathbf{x})]] Z_0[\mathbf{J}; \mathbf{x}], \end{aligned} \quad (237)$$

where the last term can be rewritten using the Jacobi identity

$$\begin{aligned} [\hat{\Gamma}_I(t'_1), [\hat{\Gamma}_I(t'_2), \bar{\mathbf{L}}_I(t'_3; \mathbf{x})]] &= [\hat{\Gamma}_I(t'_2), [\hat{\Gamma}_I(t'_1), \bar{\mathbf{L}}_I(t'_3; \mathbf{x})]] \\ & \quad + [[\hat{\Gamma}_I(t'_1), \hat{\Gamma}_I(t'_2)], \bar{\mathbf{L}}_I(t'_3; \mathbf{x})]. \end{aligned} \quad (238)$$

This recovers the result in equation (229). To facilitate a comparison we put the terms in the same order here. Note that none of the six terms include any derivatives acting on the free generating functional which justifies omitting Z_0 in the last equation.

We conclude this subsection by explicitly writing down a series expansion of the generating functional in the interaction part of the equations of motion E_I . We can do so based on either \hat{L}_I or \hat{r}_I , obtaining

$$Z[\mathbf{J}; \mathbf{x}] = \sum_{n=0}^{\infty} i^n \int_{t_i}^{t_f} dt'_n \cdots \int_{t_i}^{t'_2} dt'_1 \hat{L}_I(t'_n) \cdots \hat{L}_I(t'_1) Z_0[\mathbf{J}; \mathbf{x}] \quad (239)$$

$$= \sum_{n=0}^{\infty} i^n \int_{t_i}^{t_f} dt'_n \cdots \int_{t_i}^{t'_2} dt'_1 \hat{r}_I(t'_1) \cdots \hat{r}_I(t'_n) Z_0[\mathbf{J}; \mathbf{x}], \quad (240)$$

respectively. Instead of reversing the order of the factors \hat{r}_I , the reverse time-ordered exponential can also be implemented by changing the integral boundaries. Here, we chose this convention such that the ordering $t'_j \leq t'_\ell$ for $j < \ell$ is valid in both cases.

3.1.2 Approximations for Observables

In the previous subsection we have investigated a series expansion of the generating functional Z in the interaction part of the equations of motion E_I . While the generating functional is the central mathematical object of KFT, in applications we are primarily interested in observables. Therefore, this subsection is dedicated to investigate how a series expansion of the generating functional yields suitable approximations for observables. Below we obtain exact series expansions for observables, but the need to work with explicit equations necessitates to truncate them. This introduces a truncation error which under certain conditions can be small enough to provide approximations to the physical observables.

Recall that we defined the physical observable associated to a function \mathcal{O} depending on the state of the system \mathbf{x} as well as some parameters χ as

$$\tilde{\mathcal{O}}(\chi, t; \mathbf{x}) = \mathcal{O}(\chi; \tilde{\varphi}(t; \mathbf{x})) = \mathcal{O}\left(\chi; \frac{\delta}{i \delta \mathbf{J}^T(t)}\right) Z[\mathbf{J}; \mathbf{x}] \Big|_{\mathbf{J}=0}. \quad (241)$$

Examples for an observable are the phase space trajectory or the density field. The fact that the right-hand expression acts on the generation functional only by functional derivatives with respect to \mathbf{J} means that the factors of \mathbf{J} in the series expansions in the previous subsection are of prime importance. Moreover, the function \mathbf{J} being set to zero after the derivatives have been evaluated has a few important implications. We study these in detail below.

Consider a generic observable acting on the series expansion of the generating functional in terms of \hat{L}_I . It is

$$\tilde{\mathcal{O}}(\chi, t; \mathbf{x}) = \sum_{n=0}^{\infty} i^n \int_{t_i}^{t_f} dt'_n \cdots \int_{t_i}^{t'_2} dt'_1 \mathcal{O}\left(\chi; \frac{\delta}{i \delta \mathbf{J}^T(t)}\right) \hat{L}_I(t'_n) \cdots \hat{L}_I(t'_1) Z_0[\mathbf{J}; \mathbf{x}] \Big|_{\mathbf{J}=0}. \quad (242)$$

Focusing on the second line of this equation, the first key observation is that the operator $\hat{L}_I(t'_n)$ always contains a factor $\mathbf{J}^T(t'_n)$ prior to the action of the

functional derivatives in \mathcal{O} . Due to product rules, the result of evaluating the derivatives in \mathcal{O} is a sum of terms of which in some the factor $\mathbf{J}^T(t_n'')$ is not acted upon. However, these terms vanish upon setting the $\mathbf{J} = \mathbf{0}$ in the end. The product rule involving $\mathbf{J}^T(t_n'')$ thus trivializes in the sense that for a non-vanishing result \mathcal{O} must act on $\mathbf{J}^T(t_n'')$.

The statement above can be generalized. For the same reason of obtaining a vanishing term upon setting $\mathbf{J} = \mathbf{0}$, the functional derivatives in \mathcal{O} must act on every factor \mathbf{J} present in front of Z_0 . As an example of this assertion, consider the second order term of the series expansion. We have found above that

$$Z_2[\mathbf{J}; \mathbf{x}] = i^2 \int_{t_i}^{t_f} dt_2' \int_{t_i}^{t_2'} dt_1' \hat{\mathbf{L}}_I(t_2') \hat{\mathbf{L}}_I(t_1') Z_0[\mathbf{J}; \mathbf{x}] \quad (243)$$

$$= \int_{t_i}^{t_f} dt_2' \int_{t_i}^{t_2'} dt_1' i^2 (\bar{\mathbf{L}}_I(t_2'; \mathbf{x}) \bar{\mathbf{L}}_I(t_1'; \mathbf{x}) + [\hat{\mathbf{L}}_I(t_2'), \hat{\mathbf{L}}_I(t_1')]) Z_0[\mathbf{J}; \mathbf{x}] \quad (244)$$

$$\begin{aligned} &= \int_{t_i}^{t_f} dt_2' \int_{t_i}^{t_2'} dt_1' \int_{t_1'}^{t_f} dt'' i \mathbf{J}^T(t'') \mathbf{G}(t'', t') \bar{\mathbf{E}}_I(t'; \mathbf{x}) \\ &\quad \int_{t_2'}^{t_f} dt'' i \mathbf{J}^T(t'') \mathbf{G}(t'', t') \bar{\mathbf{E}}_I(t'; \mathbf{x}) Z_0[\mathbf{J}; \mathbf{x}] \\ &\quad + \int_{t_i}^{t_f} dt_2' \int_{t_i}^{t_2'} dt_1' \int_{t_2'}^{t_f} dt_2'' i \mathbf{J}^T(t_2'') \mathbf{G}(t_2'', t_2') \\ &\quad (\bar{\mathbf{E}}_I^T(t_1'; \mathbf{x}) \mathbf{G}^T(t_2', t_1') \nabla^T) \bar{\mathbf{E}}_I(t_2'; \mathbf{x}) Z_0[\mathbf{J}; \mathbf{x}]. \end{aligned} \quad (245)$$

We have denoted the second order contribution of the series expansion to the generating functional by Z_2 . Note that this is not the second order approximation, i.e., the result of a truncation of the series after the second order term. For that one would need to add $Z_0 + Z_1 + Z_2$. We use this convention for the remainder of the thesis.

For the second order contribution to the observable, we have to act with \mathcal{O} on Z_2 . For the sake of being specific, let the observable in this example be the phase space trajectory $\mathcal{O}(\mathbf{y}) = \mathbf{y}$ for $\mathbf{y} \in \mathbf{X}$, i.e., $\tilde{\mathcal{O}} = \tilde{\varphi}$. The second order contribution to the phase space evolution map is then given by

$$\tilde{\varphi}_2(t; \mathbf{x}) = \frac{\delta}{i \delta \mathbf{J}^T(t)} Z_2[\mathbf{J}; \mathbf{x}] \Big|_{\mathbf{J}=\mathbf{0}} \quad (246)$$

$$= 0 + \int_{t_i}^t dt_2' \int_{t_i}^{t_2'} dt_1' \mathbf{G}(t, t_2') (\bar{\mathbf{E}}_I^T(t_1'; \mathbf{x}) \mathbf{G}^T(t_2', t_1') \nabla^T) \bar{\mathbf{E}}_I(t_2'; \mathbf{x}). \quad (247)$$

We used that $Z_0[\mathbf{0}; \mathbf{x}] = 1$. The first term in Z_2 contains two factors of \mathbf{J} of which only one can be removed by the functional derivative in \mathcal{O} and thus the term vanishes upon setting $\mathbf{J} = \mathbf{0}$. To prevent this in the second term, the functional derivative necessarily acts on the factor $\mathbf{J}^T(t_2'')$ yielding $\delta_D(t - t_2'')$. Aside from replacing t_2'' by t in the expression, this Dirac δ -function conspires with the lower integration boundary $t_2' \leq t_2''$ for the t_2'' integration to yield an upper integration boundary $t_2' \leq t$ for the t_2' integration. Once more, causality is obeyed as there are no contributions from times later than the one at which the observable is evaluated t .

The last statement about causality is generally true, given that we argued above that there always is a factor J evaluated at the latest time variable t_n'' in the contribution to the generating functional Z_n of any order $n \geq 1$. At zeroth order or if the observable contains higher powers of the functional derivative with respect to J , it can act on the free generating functional Z_0 . Causality is obeyed in this case, too, since the derivatives simply yield copies of $\bar{\varphi}(t; \mathbf{x})$.

For a general observable \mathcal{O} we define its n^{th} order contribution as

$$\tilde{\mathcal{O}}_n(\chi, t; \mathbf{x}) := \mathcal{O}\left(\chi; \frac{\delta}{i \delta J^\Gamma(t)}\right) Z_n[J; \mathbf{x}] \Big|_{J=0} \quad \text{with} \quad (248)$$

$$Z_n[J; \mathbf{x}] := i^n \int_{t_i}^{t_f} dt'_n \cdots \int_{t_i}^{t'_2} dt'_1 \hat{L}_I(t'_n) \cdots \hat{L}_I(t'_1) Z_0[J; \mathbf{x}]. \quad (249)$$

Here, the n^{th} order contribution to the generating functional Z_n appearing in the first equality is defined via the second. It is the n^{th} order term in the series expansion of the generating functional in terms of \hat{L}_I which is consistent with Z_2 introduced above and even with Z_0 . As mentioned above, an approximation to the observable \mathcal{O} can be obtained by a truncation of the series expansion. A truncation to n^{th} order results in the approximation

$$\tilde{\mathcal{O}}(\chi, t; \mathbf{x}) \approx \tilde{\mathcal{O}}_0(\chi, t; \mathbf{x}) + \dots + \tilde{\mathcal{O}}_n(\chi, t; \mathbf{x}), \quad (250)$$

where the first term on the right-hand side $\tilde{\mathcal{O}}_0(\chi, t; \mathbf{x}) = \mathcal{O}(\chi; \bar{\varphi}(t))$ is the observable evaluated along the free evolution.

Using the series expansion of the generating functional in terms of \hat{L}_I , we can obtain slightly more compact expressions for the contribution to an observable at given order n . Applying the replacement (220) to the observable itself, too, one can show that

$$\tilde{\mathcal{O}}(\chi, t; \mathbf{x}) = \sum_{n=0}^{\infty} i^n \int_{t_i}^{t_f} dt'_n \cdots \int_{t_i}^{t'_2} dt'_1 \hat{L}_I(t'_1) \cdots \hat{L}_I(t'_n) \mathcal{O}(\chi; \bar{\varphi}(t; \mathbf{x})). \quad (251)$$

Here the causality condition $t'_n \leq t$ emerges through the action of the derivative with respect to $\bar{\varphi}(t''_n; \mathbf{x})$ in $\hat{L}_I(t'_n)$ on $\mathcal{O}(\chi; \bar{\varphi}(t; \mathbf{x}))$. Given that this is a central equation, it demands a detailed explanation.

The key ideas for deriving equation (251) is the replacement (220) as well as the observation that in equation (229) no derivatives remain acting on the free generating functional. The latter statement is true for any order and is somewhat of a tautology—after evaluating all functional derivatives, none remain. Crucially, for any factor \hat{L}_I there are two possibilities: Either it acts via a functional derivative with respect to $\bar{\varphi}$ on some E_I or it contains a factor J . Suppose now that the observable acts on such an expression. The functional derivative within it needs to act on all these factors of J because otherwise the term vanishes upon setting $J = 0$. Effectively, this replaces the factors of J by derivatives acting on the observable. Eventually, the observable reaches Z_0 and the remaining functional derivatives are replaced by the free trajectory $\bar{\varphi}$. The derivatives in factors \hat{L}_I acting on it can now be written as functional derivatives with respect to $\bar{\varphi}$ and we can set $J = 0$ reducing Z_0 to a factor of unity. However, recall that the expression we consider emerged as one term in a

series of product rules of derivatives acting on the free generating functional. In each such term, the derivatives acting on other factors $\hat{\Gamma}_1$ remained unchanged, while the derivatives acting formerly on Z_0 and yielded factors of J now act on $\mathcal{O}(\chi; \bar{\varphi}(t; \mathbf{x}))$. Hence, the terms emerging from the product rules can be recombined yielding equation (251).

The big advantage of equation (251) is its independence of the free generating functional Z_0 and, simultaneously, of the auxiliary function J . For any observable, it provides a series expansion of contributions which modify it from being evaluated along the free evolution to being evaluated along the physical evolution. Once more it is emphasized that we are considering any classical physical system allowing for a split of its equations of motion into a free and an interaction part, E_0 and E_I , respectively. Aside from a couple of technical conditions on certain functional determinants, the main demands are that E_0 admits a Green's function \mathbf{G} and E_I is analytic in its argument.

Supposing the convergence of the series expansion in (251), one might expect its truncations to provide approximations for observables. While in a slightly different form, we recover the n^{th} order contribution to the observable \mathcal{O} introduced in equation (248). Specifically, it is

$$\tilde{\mathcal{O}}_n(\chi, t; \mathbf{x}) = i^n \int_{t_i}^{t_f} dt'_n \cdots \int_{t_i}^{t'_2} dt'_1 \hat{\Gamma}_1(t'_1) \cdots \hat{\Gamma}_1(t'_n) \mathcal{O}(\chi; \bar{\varphi}(t; \mathbf{x})). \quad (252)$$

Again, adding the contributions up to n^{th} order yields an approximation for the physical observable $\tilde{\mathcal{O}}(\chi, t; \mathbf{x})$.

We conclude this subsection by transferring these results for approximations of physical observables to their expectation values. Based on their definition in equation (168), the n^{th} order contribution to the expectation value is simply the expectation value of the n^{th} order contribution to the physical observable. In the form of an equation, this amounts to

$$\langle \mathcal{O} \rangle_n(\chi, t) := \langle \mathcal{O}_n \rangle(\chi, t) = \int d\mathbf{x} P(\mathbf{x}) \tilde{\mathcal{O}}_n(\chi, t; \mathbf{x}), \quad (253)$$

where P is a probability distribution of initial values.

It is noteworthy that the dependence of $\tilde{\mathcal{O}}_n$ is exclusively via the free solution $\bar{\varphi}(t; \mathbf{x}) = \mathbf{G}(t, t_i) \mathbf{x}$. This seems to suggest to perform the averaging not over the initial value \mathbf{x} , but over $\mathbf{y} := \bar{\varphi}(t; \mathbf{x})$. Constructing a probability distribution of \mathbf{y} from $P(\mathbf{x})$ would be facilitated by the Hamiltonian nature of the free equations of motion which ensure that the Jacobi determinant of the transformation of integration variable is unity. Unfortunately, this approach fails in this naive implementation due to the appearance of factors $\bar{\varphi}(t'; \mathbf{x})$ with different time arguments t' in $\tilde{\mathcal{O}}_n$.

3.1.3 Example: Harmonic Oscillator (VI)

We return to our recurring example, the harmonic oscillator. In Newtonian gauge, its equation of motion splits into

$$E_0[\varphi](t) = \frac{d\varphi}{dt}(t) - \begin{pmatrix} \frac{1}{m} \varphi^{(p)}(t) \\ 0 \end{pmatrix} \quad \text{and} \quad E_I[\varphi](t) = \begin{pmatrix} 0 \\ \kappa \varphi^{(q)}(t) \end{pmatrix} \quad (254)$$

The Green's function for the free part of the equations of motion is

$$G(t, t') = \begin{pmatrix} \theta(t-t') & \frac{1}{m}(t-t')\theta(t-t') \\ 0 & \theta(t-t') \end{pmatrix}, \quad (255)$$

corresponding to equation (87). Given these ingredients, we can determine the perturbative approximations of the phase space trajectory $\tilde{\varphi}$ as given by microscopic perturbation theory in the KFT framework. Here, we consider the approximations to the phase space trajectory up to second order.

The zeroth order contribution to the phase space trajectory is simply given by the free evolution of the system. Specifically, we have

$$\tilde{\varphi}_0(t; \mathbf{x}) = \tilde{\varphi}(t; \mathbf{x}) = G(t, t_i) \mathbf{x} = \begin{pmatrix} x^{(q)} + \frac{1}{m}(t-t_i)x^{(p)} \\ x^{(p)} \end{pmatrix} \quad (256)$$

for $t \in [t_i, t_f]$, i.e., free motion given the initial conditions \mathbf{x} . Comparing to the analytic expression of the trajectory given in equation (26), we observe that this corresponds to a first order Taylor approximation of $\tilde{\varphi}^{(q)}$ in the position and a zeroth order Taylor approximation of $\tilde{\varphi}^{(p)}$ in the momentum.

According to equation (252), the first order correction to is given by

$$\tilde{\varphi}_1(t; \mathbf{x}) = \int_{t_i}^{t_f} dt'_1 i\hat{\Gamma}_1(t'_1) \tilde{\varphi}(t; \mathbf{x}) \quad \text{with} \quad (257)$$

$$i\hat{\Gamma}_1(t'_1) = - \int_{t'_1}^{t_f} dt''_1 \begin{pmatrix} 0 & \kappa \tilde{\varphi}^{(q)}(t''_1; \mathbf{x}) \end{pmatrix} \begin{pmatrix} 1 & 0 \\ \frac{1}{m}(t''_1 - t'_1) & 1 \end{pmatrix} \frac{\delta}{\delta \tilde{\varphi}^T(t''_1; \mathbf{x})}. \quad (258)$$

The second line follows from equation (219). Note that in the transpose of the Green's function we have omitted the Heaviside θ -functions as they are automatically satisfied due to the integration boundaries for t'' . Evaluating the functional derivative yields

$$\int_{t'_1}^{t_f} dt''_1 \begin{pmatrix} 1 & 0 \\ \frac{1}{m}(t''_1 - t'_1) & 1 \end{pmatrix} \frac{\delta}{\delta \tilde{\varphi}^T(t''_1; \mathbf{x})} \tilde{\varphi}(t; \mathbf{x}) = \begin{pmatrix} 1 & 0 \\ \frac{1}{m}(t-t'_1) & 1 \end{pmatrix} \theta(t-t'_1) \quad (259)$$

and thus

$$\tilde{\varphi}_1(t; \mathbf{x}) = - \int_{t_i}^t dt'_1 \begin{pmatrix} \frac{\kappa}{m}(t-t'_1) \tilde{\varphi}^{(q)}(t'_1; \mathbf{x}) \\ \kappa \tilde{\varphi}^{(q)}(t'_1; \mathbf{x}) \end{pmatrix} \quad (260)$$

$$= - \int_{t_i}^t dt'_1 \begin{pmatrix} \frac{\kappa}{m}(t-t'_1)x^{(q)} + \frac{\kappa}{m^2}(t-t'_1)(t'_1-t_i)x^{(p)} \\ \kappa x^{(q)} + \frac{\kappa}{m}(t'_1-t_i)x^{(p)} \end{pmatrix} \quad (261)$$

$$= \begin{pmatrix} -\frac{\kappa}{2m}(t-t_i)^2 x^{(q)} - \frac{\kappa}{3!m^2}(t-t_i)^3 x^{(p)} \\ -\kappa(t-t_i)x^{(q)} - \frac{\kappa}{2m}(t-t_i)^2 x^{(p)} \end{pmatrix}. \quad (262)$$

The sum $\tilde{\varphi}_0^{(q)} + \tilde{\varphi}_1^{(q)}$ is a third order Taylor approximation of $\tilde{\varphi}^{(q)}$, while the sum $\tilde{\varphi}_0^{(p)} + \tilde{\varphi}_1^{(p)}$ is a second order Taylor approximation of $\tilde{\varphi}^{(p)}$. A pattern seems to emerge—a natural expectation for the result in second order KFT perturbation theory would be to obtain a fifth order Taylor approximation in position and a fourth order Taylor approximation in momentum.

The second order term $\tilde{\varphi}_2$ contains only one contribution. Indeed, while it may seem that there are two possible ways for $\hat{\Gamma}_I(t'_2)$ to act in the equation

$$\tilde{\varphi}_2(t; \mathbf{x}) = \int_{t_i}^{t_f} dt'_2 \int_{t_i}^{t'_2} dt'_1 i\hat{\Gamma}_I(t'_1) i\hat{\Gamma}_I(t'_2) \tilde{\varphi}(t; \mathbf{x}), \quad (263)$$

the factor $\tilde{\varphi}(t; \mathbf{x})$ vanishes after it has been acted upon by $\hat{\Gamma}_I(t'_1)$. This is a special property of the physical evolution map. Let us determine the action of $\hat{\Gamma}_I$ on E_I . We find

$$\begin{aligned} & \int_{t_i}^{t'_2} dt'_1 i\hat{\Gamma}_I(t'_1) E_I^\dagger[\tilde{\varphi}(t'_2; \mathbf{x})] \\ &= - \int_{t_i}^{t'_2} dt'_1 \int_{t'_1}^{t_f} dt''_1 \left(0 \quad \kappa \tilde{\varphi}^{(q)}(t'_1; \mathbf{x}) \right) \begin{pmatrix} 1 & 0 \\ \frac{1}{m}(t''_1 - t'_1) & 1 \end{pmatrix} \\ & \quad \frac{\delta}{\delta \tilde{\varphi}^\dagger(t''_1; \mathbf{x})} \left(0 \quad \kappa \tilde{\varphi}^{(q)}(t'_2; \mathbf{x}) \right) \end{aligned} \quad (264)$$

$$= - \int_{t_i}^{t'_2} dt'_1 \left(0 \quad \kappa \tilde{\varphi}^{(q)}(t'_1; \mathbf{x}) \right) \begin{pmatrix} 0 & \kappa \\ 0 & \frac{\kappa}{m}(t'_2 - t'_1) \end{pmatrix} \quad (265)$$

$$= - \int_{t_i}^{t'_2} dt'_1 \left(0 \quad \frac{\kappa^2}{m}(t'_2 - t'_1) \tilde{\varphi}^{(q)}(t'_1; \mathbf{x}) \right). \quad (266)$$

Using this result as well as equation (259), it is

$$\tilde{\varphi}_2(t; \mathbf{x}) = \int_{t_i}^t dt'_2 \int_{t_i}^{t'_2} dt'_1 \left(0 \quad \frac{\kappa^2}{m}(t'_2 - t'_1) \tilde{\varphi}^{(q)}(t'_1; \mathbf{x}) \right) \begin{pmatrix} 1 & 0 \\ \frac{1}{m}(t - t'_2) & 1 \end{pmatrix} \quad (267)$$

$$= \int_{t_i}^t dt'_2 \int_{t_i}^{t'_2} dt'_1 \begin{pmatrix} \frac{\kappa^2}{m^2}(t - t'_2)(t'_2 - t'_1) \tilde{\varphi}^{(q)}(t'_1; \mathbf{x}) \\ \frac{\kappa^2}{m}(t'_2 - t'_1) \tilde{\varphi}^{(q)}(t'_1; \mathbf{x}) \end{pmatrix} \quad (268)$$

$$= \begin{pmatrix} \frac{\kappa^2}{4! m^2} (t - t_i)^4 \chi^{(q)} + \frac{\kappa^2}{5! m^3} (t - t_i)^5 \chi^{(p)} \\ \frac{\kappa^2}{3! m} (t - t_i)^3 \chi^{(q)} + \frac{\kappa^2}{4! m^2} (t - t_i)^4 \chi^{(p)} \end{pmatrix}. \quad (269)$$

In the last line we inserted the expression for $\tilde{\varphi}^{(q)}(t'_1; \mathbf{x})$ and performed the resulting elementary integrals. The result matches our expectation, by adding $\tilde{\varphi}_2$ to the lower order terms, we obtain a fifth and fourth order Taylor approximation of the physical evolution $\tilde{\varphi}$ in position and momentum, respectively.

3.2 FEYNMAN RULES

In the previous section we have introduced a perturbative treatment of interactions in KFT based on a series expansion of the generating functional. This induced series expansions for observables. We obtained approximations to observables and their expectation values via truncation of this series. The contributions at any order n are complicated due to the combinatorics of product rules.

The construction of KFT via a path integral formalism already takes inspiration from QFT. While the interaction operator in KFT is of unusual form from the perspective of QFT, it nonetheless is worthwhile to take additional inspiration from QFT for the evaluation of perturbative expressions. Indeed, the combinatorial difficulty present in the contributions to observables $\tilde{\mathcal{O}}_n$ can be dealt with in similar fashion as combinatorial difficulty is treated in QFT—via a diagrammatic approach.

In subsection 3.2.1 we investigate this idea by defining vertices in terms of the mathematical objects appearing in the expression for $\tilde{\mathcal{O}}_n$. The action of functional derivatives can then be symbolized by edges between vertices. The various terms appearing from product rules correspond vaguely to all possible ways of connecting vertices to edges.

We carefully study the construction of diagrams and constraints on their form. Importantly, we find that all diagrams are trees, i.e., have a relatively simple graph-theoretical form. The diagrammatic treatment facilitates an interpretation of the perturbative contributions which we present in subsection 3.2.2. We also perform a comparison to the iterative Born approximation and find that microscopic perturbation theory in KFT adds interactions significantly slower. Specifically, at any iteration $n \geq 2$, the iterative Born approximation contains terms which appear at arbitrarily high order in KFT.

Subsection 3.2.3 further investigates the properties of Feynman diagrams in KFT. We then outline an alternative notion of equivalence of diagrams. By removing the time-ordering induced by the time-ordered exponential in equation (151), some diagrams can be combined. More importantly, though, is that it allows for a recursive computation of contributions to observables $\tilde{\mathcal{O}}_n$. The price to pay is the appearance of symmetry factors.

In the last subsection we consider the harmonic oscillator for a final time in this thesis. We show how the contributions to its physical evolution $\tilde{\varphi}$ computed in subsection 3.1.3 can be expressed in terms of diagrams. Due to the simple forms of the observable and the interactions of the harmonic oscillator, only one diagram has a non-vanishing contribution at any order. Using the aforementioned recursive formula, we obtain the contributions $\tilde{\varphi}_n$ for all $n \geq 0$ and are able to show that their sum exactly reproduces the Taylor series of the exact solution $\tilde{\varphi}$.

The diagrammatic treatment of perturbations in this section is a generalization of the treatment in [1] which in turn was inspired by the diagrams in [7]. A very limited comparison to the Born approximation was performed in [7]. The recursive formula for the n^{th} order observable is a novel result.

3.2.1 Defining Diagrams

The results of the previous section form the basis for a perturbative treatment of interactions in KFT. We have derived series expansions for the generating functional, for observables and their expectation values. Truncating these expansions yields approximations for these quantities. However, such a strategy is only viable if the contribution at any order n is significantly easier to determine than the original expression.

The main complexity of the expressions in equations (151) and (232) for the generating functional is the presence of functional derivatives in the argument of the (reverse) time-ordered exponential function. This inhibits a direct evaluation of the expressions. Fundamentally, the fact that, respectively, copies of $\hat{L}_I(t)$ and $\hat{\Gamma}_I(t)$ with different time-arguments do not commute, prevents any naive attempts of non-approximate treatment.

While there is no certainty that a truncation of a series expansion for the generating functional and derived quantities is unavoidable, it definitely is a daunting task. We remark that Resummed Kinetic Field Theory (RKFT) achieves a resummation of the interactions in a statistical setting, but still requires so-called macroscopic perturbation theory to determine expectation values of observables.[41, 42] We note that in certain simple examples a complete resummation is feasible. An example is the harmonic oscillator, cf. subsection 3.2.4.

The usefulness of a truncation of the series expansions is not only motivated by the difficulty of an exact treatment. It is primarily suggested due to the simplicity of the expressions for the contributions at individual orders n . As we have seen in the previous section, it is possible to fully evaluate the functional derivatives using product rules or commutators when evaluating the action of n operators $\hat{L}_I(t)$ or $\hat{\Gamma}_I(t)$ on the free generating functional. The main remaining difficulty is the combinatorics of which operator acts on which of the terms to its right.

The aim of this section is to establish a diagrammatic treatment of expressions appearing at n^{th} order in series expansions in the interactions \mathbf{E}_I . This is heavily inspired by Feynman's diagrammatic scheme of visualizing and facilitating calculations of probability amplitudes in QFT. Hence, we refer to our diagrams likewise as *Feynman diagrams* and the dictionary to translate them into mathematical equations provides *Feynman rules*.

The key equation for defining the Feynman diagrams and rules is equation (252) which can be written in the form

$$\tilde{\mathcal{O}}_n(\chi, t; \mathbf{x}) = \int_{t_i}^{t_f} dt'_1 i \hat{\Gamma}_I(t'_1) \cdots \int_{t'_{n-1}}^{t_f} dt'_n i \hat{\Gamma}_I(t'_n) \mathcal{O}(\chi; \bar{\varphi}(t; \mathbf{x})) \quad \text{with} \quad (270)$$

$$i \hat{\Gamma}_I(t') = - \int_{t'}^{t_f} dt'' \bar{\mathbf{E}}_I^T(t'; \mathbf{x}) \mathbf{G}^T(t'', t') \frac{\delta}{\delta \bar{\varphi}^T(t''; \mathbf{x})}. \quad (271)$$

Having redistributed the imaginary units, it is clear that for a real-valued observable \mathcal{O} the contributions at any order n are real-valued. Recall that we defined $\bar{\mathbf{E}}_I(t'; \mathbf{x}) = \mathbf{E}_I[\bar{\varphi}(\bullet; \mathbf{x})](t')$, i.e., $\hat{\Gamma}_I$ contains the interaction part of the equations of motion evaluated along the free evolution of the system.

$$\begin{aligned}
\tilde{\mathcal{O}}_n(\chi, t; \mathbf{x}) = & \int_{t_i}^{t_f} dt'_1 i \hat{\Gamma}_1(t'_1) \begin{array}{c} \diagdown \\ \int_{t'_1}^{t_f} dt'_2 i \hat{\Gamma}_1(t'_2) \cdots \int_{t_{n-1}}^{t_f} dt'_n i \hat{\Gamma}_1(t'_n) \mathcal{O}(\chi; \bar{\varphi}(t; \mathbf{x})) \end{array} \\
& \vdots \\
& + \int_{t_i}^{t_f} dt'_1 i \hat{\Gamma}_1(t'_1) \begin{array}{c} \diagdown \\ \int_{t'_1}^{t_f} dt'_2 i \hat{\Gamma}_1(t'_2) \cdots \int_{t_{n-1}}^{t_f} dt'_n i \hat{\Gamma}_1(t'_n) \mathcal{O}(\chi; \bar{\varphi}(t; \mathbf{x})) \end{array} \\
& + \int_{t_i}^{t_f} dt'_1 i \hat{\Gamma}_1(t'_1) \begin{array}{c} \diagdown \\ \int_{t'_1}^{t_f} dt'_2 i \hat{\Gamma}_1(t'_2) \cdots \int_{t_{n-1}}^{t_f} dt'_n i \hat{\Gamma}_1(t'_n) \mathcal{O}(\chi; \bar{\varphi}(t; \mathbf{x})) \end{array}
\end{aligned}$$

Figure 1: Schematic expression for the n^{th} order contribution to the observable \mathcal{O} . The edges indicate on which term the functional derivative in $\hat{\Gamma}_1(t'_1)$ acts. In total this is a sum over n terms, the action of $\hat{\Gamma}_1(t'_1)$ on $\hat{\Gamma}_1(t'_j)$ for $3 \leq j \leq n-1$ is not shown.

In the expression above, any factor $\hat{\Gamma}_1$ can act on any of the terms to its right. Using a product rule, this yields a total of $n!$ terms which sum to $\tilde{\mathcal{O}}_n$. These correspond to the 1, 2 and 6 terms we found in our explicit calculations of Z_1 , Z_2 and Z_3 in the previous section, respectively. Evidently, for higher orders n the number of terms increases quite quickly. The terms themselves also become more complex. While it is possible to keep the corresponding expressions relatively compact using commutators like in equations (235) and (237), their construction is not entirely trivial and the nested commutators are difficult to decipher.

However, the underlying logic for the construction of the terms adding up to $\tilde{\mathcal{O}}_n$ is quite simple. They are all n ways in which the factor $\hat{\Gamma}_1(t'_1)$ can act on the remainder of the expression—either by acting on any of the $n-1$ factors of $\hat{\Gamma}_1$ or by acting directly on $\mathcal{O}(\chi; \bar{\varphi}(t; \mathbf{x}))$. This is schematically visualized in figure 1. Of course, the remaining expression can be replaced by such a schematic, too. Iteratively, this yields a tree with root $\mathcal{O}(\chi; \bar{\varphi}(t; \mathbf{x}))$.

We use terminology of elementary graph theory here: *Vertices* are connected by *edges* forming *graphs*. In this context, we often refer to graphs synonymously as *diagrams*. A path in a graph is a sequence of distinct vertices connected by edges. A graph is called *tree* if any two vertices are connected by exactly one path. Equivalently, a tree is a connected acyclic graph, i.e., there exists a path between any two vertices and there do not exist any non-trivial paths from any

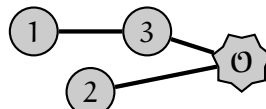
vertex to itself. Any vertex in a tree can serve as its *root*. Once designated, the root provides a tree with a natural start- or endpoint.

There is hardly any compactness gained by using mathematical expressions as vertices in our diagrams. To remedy this, let us introduce the symbolic abbreviations

$$\textcircled{j} := \int_{t'_{j-1}}^{t_f} dt'_j i \hat{\Gamma}_I(t'_j) \quad \text{for } j \in \mathbb{N} \text{ and} \tag{272}$$

$$\textcircled{\mathcal{O}} := \mathcal{O}(\chi; \bar{\varphi}(t; \mathbf{x})) \tag{273}$$

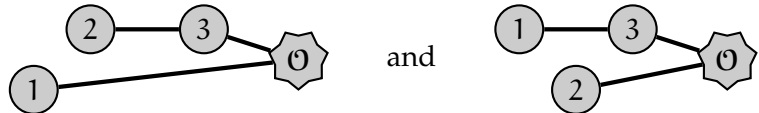
for the vertices. We call the upper vertex type *interaction vertex* and the lower one *observable vertex*. We set $t'_0 = t_i$ to make these expressions well-defined. Using this notation, we can form diagrams from vertices and edges. As in figure 1, the edges symbolize on which term the derivative in $\hat{\Gamma}_I$ acts. As an example, it is



$$= i^3 \int_{t_i}^{t_f} dt'_1 \int_{t_1}^{t_f} dt'_2 \int_{t_2}^{t_f} dt'_3 \hat{\Gamma}_I(t'_2) [\hat{\Gamma}_I(t'_1), \hat{\Gamma}_I(t'_3)] \mathcal{O}(\chi; \bar{\varphi}(t; \mathbf{x})). \tag{274}$$

This is one of the diagrams contributing to $\check{\mathcal{O}}_3(\chi, t; \mathbf{x})$. The diagram makes clear how the expression on the right-hand side is to be interpreted— $\hat{\Gamma}_I(t'_1)$ acts on $\hat{\Gamma}_I(t'_3)$ while $\hat{\Gamma}_I(t'_2)$ and $\hat{\Gamma}_I(t'_3)$ act on $\mathcal{O}(\chi; \bar{\varphi}(t; \mathbf{x}))$. Two edges end at the root, thus there are two functional derivatives acting on \mathcal{O} . The third functional derivative acts on the factor E_I inside $\hat{\Gamma}_I(t'_3)$.

In the diagram above we horizontally ordered the vertices in accordance to their time-parameter. It reflects the time-ordering and provides a simple notion of equivalence of diagrams. For example, the two diagrams



$$\tag{275}$$

are topologically equivalent graphs, but encode different mathematical expressions. Specifically, they correspond to the second and third term in equation (229). Note that due to the time-ordering it is not possible to identify them via a relabeling.

The issue of equivalence of diagrams is important, because ultimately we intend to provide an algorithm for the computation of $\check{\mathcal{O}}_n$ for any $n \geq 0$ in terms of diagrams. A natural attempt is to assert that $\check{\mathcal{O}}_n$ is given by the sum of all trees formed from an observable vertex as root and n interaction vertices. But this word “all” is well-defined only if a suitable definition of equivalence of diagrams is agreed upon. As we have just observed, topological equivalence of graphs is not a suitable definition of equivalence, but we need to also take the labels into account.

While not all possible ways of labeling vertices are permitted due to time-ordering, it is not necessary to explicitly demand that. Indeed, a graph like



$$\tag{276}$$

is automatically zero due the appearance of a vanishing factor $\mathbf{G}(t'_1, t'_2)$. However, it would be quite inefficient to allow for a large number of vanishing diagrams in our sum. Therefore, we want to restrict the labelings we consider to abide to time-ordering. Unfortunately, this is slightly more complicated than merely demanding that the labels should increase from the left to the right, because this can be circumvented by the above exemplary tree via



This loophole can be prevented by an intrinsic definition. Instead of being required to increase from left to right, the labels of the interaction vertices should increase towards the root, i.e., the observable vertex.

The diagram in equation (277) is somewhat problematic for another reason. While we have used undirected edges in our graphs, the action of the operators \hat{L}_I is fundamentally a directed operation. We have implicitly introduced the convention that if two vertices are connected by an edge, the left vertex acts on the right one. This convention does not work if there are two vertices connected to the right of an interaction vertex. Again, an intrinsic definition resolves this: Interaction vertices act towards the root.

While the intrinsic definitions of the action of operators and time-ordering of labels are mathematically rigorous, additional clarity can be achieved by the convention of vertex labels increasing from left to right. Given that we already demand the increase of vertex labels towards the root, this convention implies that vertices which are more distant from the root intrinsically are positioned more distantly, too. We say that a tree is *ordered* if its root is the right-most vertex and any two vertices connected by an edge are positioned such that the path from the right-hand vertex to the root is shorter. Note that vertices in a different branch may be positioned more to the left even if they have a smaller intrinsic distance from the root, e.g., like for the first diagram in equation (275). An ordered tree is *time-ordered* if, in addition, the labels of its interaction vertices increase from the left to the right (and thus also towards the root).

Using this terminology, we can provide a well-defined algorithm for obtaining $\tilde{\mathcal{O}}_n$ for any $n \geq 0$: It is given by the sum over all time-ordered trees formed from an observable vertex as root and n interaction vertices. Trees are identified by label-preserving topological equivalence, i.e., if two labeled trees can be transformed into each other merely by moving the vertices and attached edges, they appear only once in the sum. In practice, all diagrams of order $n \geq 1$ can be obtained from the ones of order $n - 1$ by increasing the labels of all interaction vertices by one and then attaching an interaction vertex labeled by 1 from the left to any vertex. Each diagram of order $n - 1$ gives rise to n diagrams of order n for a total of $n!$ diagrams.

The diagrams are transcribed into mathematical expressions via the Feynman rules given in equations (272) and (273). Given that exactly one edge leaves each interaction vertex, part of the expression for the interaction vertex could be assigned to the edge instead. In the specialized Feynman rules for N-body systems constructed in subsection 3.3.4 we make use of this option.

3.2.2 Physical Interpretation

The diagrams defined in the previous subsection do not only facilitate the calculations of perturbative contributions to observables in KFT. They also provide an easier physical interpretation of the series expansion in the interactions. In this subsection we interpret the physical processes encoded by the various diagrams. This also provides an interpretation of the many complicated terms involving operators and commutators in the previous section.

Starting out, the zeroth order diagram

$$\tilde{\mathcal{O}}_0(\chi, t; \mathbf{x}) = \text{⬠} \tag{278}$$

corresponds to the observable evaluated along the free evolution of the system. Higher order contributions provide corrections to it, improving the approximation to the physical observable $\tilde{\mathcal{O}}$ —provided convergence of the sum over $\tilde{\mathcal{O}}_n$.

The first order correction

$$\tilde{\mathcal{O}}_1(\chi, t; \mathbf{x}) = \text{①} \text{---} \text{⬠} \tag{279}$$

is a perturbation of the freely evolving system due to interactions. Specifically, it yields a deviation from free evolution due to interactions as evaluated along a freely evolving system. In case $\mathcal{O} = \varphi$, i.e., if the observable is the phase space trajectory, this yields exactly the Born approximation. In particular, the full effect of this kind of interactions is taken into account. However, for other observables this is not necessarily the case as becomes clear from the second order contribution.

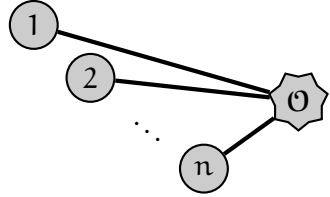
Indeed, while the first diagram of the second order contribution

$$\tilde{\mathcal{O}}_2(\chi, t; \mathbf{x}) = \text{①} \text{---} \text{②} \text{---} \text{⬠} + \text{①} \text{---} \text{⬠} \text{---} \text{②} \tag{280}$$

seems to have a transparent interpretation, the second diagram is more difficult to understand. Namely, the first diagram corrects the first order contribution to (partially) take into account that the interactions need to be evaluated along the actual physical evolution $\tilde{\varphi}$. A natural way to achieve this is by evaluating the interactions along the first order evolution map $\tilde{\varphi}_0 + \tilde{\varphi}_1$.

However, the perturbation scheme of KFT is more subtle than this. The second diagram contributing to $\tilde{\mathcal{O}}_2$ clearly shows that a singular interaction vertex does not completely capture the effect of evaluating interactions along the free evolution. It encodes a mathematical expression in which the interaction terms are evaluated along the free evolution, with two functional derivatives acting on the observable. For the phase space trajectory it is $\mathcal{O} = \varphi$ and thus this second derivative vanishes. This diagram is zero in that case.

We conclude that the diagrams of the form



$$\begin{aligned}
 &= \mathcal{O}\left(\chi; \frac{\delta}{i\delta\mathbf{J}^T(t)}\right) \int_{t_i}^{t_f} dt'_1 i\bar{L}_I(t'_1; \chi) \cdots \\
 &\quad \cdots \int_{t'_{n-1}}^{t_f} dt'_n i\bar{L}_I(t'_n; \chi) Z_0[\mathbf{J}; \chi] \quad (281)
 \end{aligned}$$

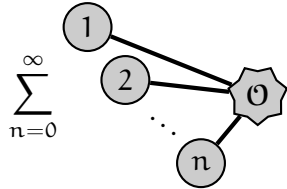
which are part of the contribution $\tilde{\mathcal{O}}_n$ encode the interactions as evaluated along the free evolution. However, for a general observable, the sum over all of them is required. We can show this explicitly by resummation of the expressions above. Indeed, it is

$$\begin{aligned}
 &\sum_{n=0}^{\infty} \int_{t_i}^{t_f} dt'_1 i\bar{L}_I(t'_1; \chi) \cdots \int_{t'_{n-1}}^{t_f} dt'_n i\bar{L}_I(t'_n; \chi) Z_0[\mathbf{J}; \chi] \\
 &= \exp\left(i \int_{t_i}^{t_f} dt' \bar{L}_I(t'; \chi)\right) \exp\left(i \int_{t_i}^{t_f} dt' \mathbf{J}(t') \cdot \bar{\boldsymbol{\varphi}}(t'; \chi)\right) \quad (282)
 \end{aligned}$$

$$= \exp\left(i \int_{t_i}^{t_f} dt' \mathbf{J}(t') \cdot \left(\bar{\boldsymbol{\varphi}}(t'; \chi) - \int_{t_i}^{t'} dt'' \mathbf{G}(t', t'') \bar{\mathbf{E}}_I(t''; \chi)\right)\right), \quad (283)$$

where in the last equality we relabeled $t' \leftrightarrow t''$ in the definition of \bar{L}_I . The term in the brackets in the last line is the Born approximation as derived in equation (84).

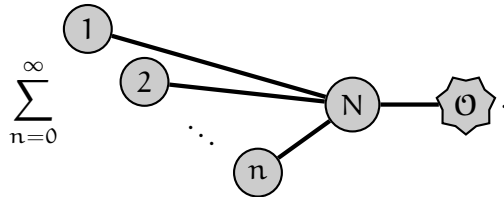
In the previous paragraph we have established the relationship



$$\sum_{n=0}^{\infty} \mathcal{O}\left(\chi; \frac{\delta}{i\delta\mathbf{J}^T(t)}\right) \exp\left(i \int_{t_i}^{t_f} dt' \mathbf{J}(t') \cdot \boldsymbol{\varphi}_{\text{Born}}(t'; \chi)\right) \quad (284)$$

which shows that the interactions evaluated along the free evolution are contributing at different orders in our perturbative series. It also shows that a partial resummation of the expansion in interactions is possible. However, there is no obvious justification for such a partial resummation in the KFT framework. Instead, contributions to observables should be computed order by order in powers of the interaction operator \hat{S}_I .

Returning to the first diagram contributing to $\tilde{\mathcal{O}}_2$ the same logic shows that in order to evaluate the interactions along the first order trajectory $\bar{\boldsymbol{\varphi}}_0 + \bar{\boldsymbol{\varphi}}_1$ we would have to perform a resummation



$$\sum_{n=0}^{\infty} \mathcal{O}\left(\chi; \frac{\delta}{i\delta\mathbf{J}^T(t)}\right) \exp\left(i \int_{t_i}^{t_f} dt' \mathbf{J}(t') \cdot \bar{\boldsymbol{\varphi}}_0(t'; \chi)\right) \quad (285)$$

Importantly, this resummation ensures only that the term \mathbf{E}_I in $\hat{\Gamma}_I(t'_N)$ is evaluated along the first order evolution. It is only one of infinitely many

terms of this type contributing to the observable \mathcal{O} , except for the special case $\mathcal{O} = \varphi$. In that particular case we actually obtain the second iteration in the iterative Born approximation. For a general observable another resummation is necessary.

We can see that the (iterative) Born approximation can be seen as a partial resummation of the perturbative series expansion of interactions in KFT. The Born approximation corresponds to the sum of all diagrams which have vertices of distance of at most one from the root. The second iteration of the Born approximation sums up all diagrams with vertices of distance of at most two from the root. In contrast, in the KFT framework these diagrams can appear at arbitrarily high orders because the number of interaction vertices and not distances from the root determine the order.

3.2.3 *Diagram Properties*

In the present form, the Feynman diagrams and rules we defined above do not resemble their ancestors from QFT much. This should not be too much of a concern, given that we consider a fully general classical physical system here. Feynman diagrams in QFT are specific to a chosen theory and depend on the particle content and their interactions. Upon choosing a specific classical theory, it is possible to refine our Feynman rules and obtain a formalism which is somewhat closer to the QFT case. In section 3.3 we consider systems of N classical point particles interacting via a pairwise interaction potential which may be regarded as an example.

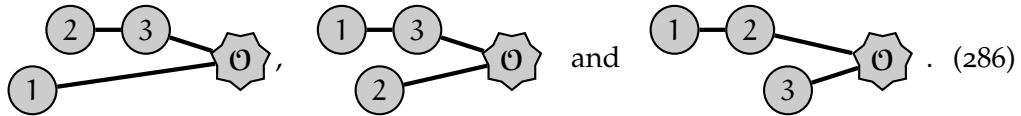
However, even in the general setting one can discuss some interesting properties of the diagrammatic treatment of interactions in KFT. The first main observation is that each interaction vertex in a time-ordered diagram has exactly one outgoing edge. As a consequence of that, the diagrams are trees. Interestingly, the acyclicity does not rely on the time-ordering and thus does not seem to be caused by the causal nature of classical physics. Instead, the form of the operator $\hat{\Gamma}_1$ featuring a single functional derivative is responsible for this property.

Interestingly, even if the form of the operator $\hat{\Gamma}_1$ was different—say, e.g., featuring two functional derivatives—acyclicity would be retained. In that case it would indeed be causality which would prevent backward directed edges. In this sense acyclicity is consistent with causality, but not implied by it. As such, the structure of the diagrams should be seen as a consequence of the KFT framework rather than as a physically meaningful property.

In QFT one tedious property of Feynman diagrams is often that they come with symmetry factors. These combinatorial factors arise due to identification of equivalent diagrams. In the formalism presented here, such symmetry factors are absent. It was already observed in section IV.C of [1] that upon ordering of the time-parameters, no symmetry factors need to be introduced. Here, the time-ordering is already incorporated into the (reversed) time-ordered exponential in equation (232) and we arrive at the same conclusion.

Generally, the existence of symmetry factors is tightly connected to the notion of equivalence of diagrams. Our deliberate definition which, e.g., distinguished between the two diagrams in equation (275), was engineered to serve the purpose of avoiding symmetry factors. However, in practical calculations it may be preferential to adapt the definition of equivalence slightly. This comes at the cost of reintroducing symmetry factors, but may be advantageous in terms of computational complexity or efficiency.

Here, we demonstrate one such modification which allows for a simplified evaluation of diagrams in certain applications. The change is motivated by the three almost equivalent diagrams which are part of the third order contribution $\tilde{\mathcal{O}}_3$. These are the diagrams



Let us relabel the vertices in the second and third diagrams such that the lower vertex is assigned the label 1 and the left and right upper vertices are 2 and 3, respectively. This makes the mathematical expressions associated to these diagrams identical up to time-ordering. The condition $t'_1 \leq t'_2 \leq t'_3$ is encoded in the integration boundaries and changes due to the relabeling. For the second diagram it becomes $t'_2 \leq t'_1 \leq t'_3$ and for the third it is $t'_2 \leq t'_3 \leq t'_1$.

We have the condition $t'_2 \leq t'_3$ commonly to all three diagrams, but the range of the parameter t'_1 is different. These ranges do not overlap (except on the measure zero set $\{t'_2, t'_3\}$) and any value $t'_1 \in [t_i, t_f]$ can be found on one of the three ranges. Therefore, the sum of these three diagrams is equal to any one of them with the condition on the time parameter of the lower vertex removed. Schematically, it is

$$\int_{t_i}^{t_f} dt'_2 \int_{t'_2}^{t_f} dt'_3 \int_{t_i}^{t'_2} dt'_1 \dots + \int_{t_i}^{t_f} dt'_2 \int_{t'_2}^{t_f} dt'_3 \int_{t'_2}^{t'_3} dt'_1 \dots + \int_{t_i}^{t_f} dt'_2 \int_{t'_2}^{t_f} dt'_3 \int_{t'_3}^{t_f} dt'_1 \dots = \int_{t_i}^{t_f} dt'_2 \int_{t'_2}^{t_f} dt'_3 \int_{t_i}^{t_f} dt'_1 \dots \tag{287}$$

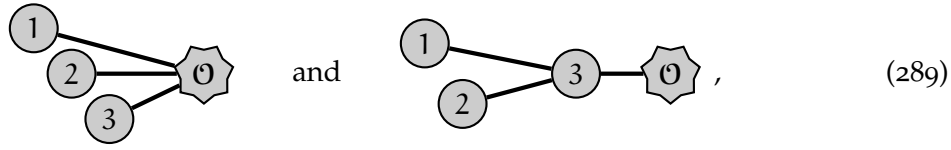
after the relabeling. Note that we transferred some ordering conditions from the integrals over t'_2 and t'_3 to the integration boundaries of t'_1 . The dots indicate the mathematical expression common to all three diagrams.

We can formalize the idea underlying the combination of these three diagrams into one. If we demand that time-ordering is not enforced universally, each of the three diagrams above would give rise to the right-hand side of equation (287). The condition $t'_2 \leq t'_3$ would still be implied by causality of the Green's function $\mathbf{G}(t'_3, t'_2)$. However, this term would then appear thrice instead of once. This could either be compensated by a symmetry factor $\frac{1}{3}$ or by identifying topologically equivalent diagrams regardless of labels. Note that this change of notion of equivalence does not affect the demand that all trees considered must be time-ordered.

The change suggested in the previous paragraph does not modify the diagram



and its associated expression. The time-ordering encoded by the causal Green's functions ensures that the expression obtains the same integral boundaries and there are no topologically equivalent graphs with three interaction vertices which could be overcounted. However, the other two diagrams in third order,



cause complications. While for these the change in our notion of equivalence does have no effect, their associated mathematical expressions are affected by the removal of universal time-ordering. Indeed, for the left-hand diagram the integral boundaries for all three time parameters t'_1 , t'_2 and t'_3 are now $[t_i, t_f]$. For the right-hand diagram the condition $t'_1 \leq t'_2$ is removed.

Due to the relabeling symmetry of these two diagrams, $(1, 2, 3) \mapsto (2, 3, 1)$ and $(1, 2) \mapsto (2, 1)$, respectively, the resulting expressions are simply multiples of the expressions under the assumption of time-ordering. The left-hand diagram is assigned a value six times, the right-hand a value two times its original one. This can be compensated by corresponding symmetry factors to ensure that the sum over all six diagrams remains unchanged.

In summary, removing the universal condition for time-ordering and replacing the notion of equivalence to allow for relabeling reduces the number of diagrams in third order from six to four. This comes at the cost of introducing symmetry factors for some diagrams. While we do not adopt these changes for our theoretical treatment here, we extensively use it in our calculations.

The main computational advantage of the modification of our Feynman rules described in this subsection is that it allows iterative calculations of observables. Consider equation (252) which states that the n^{th} order contribution to the observable $\tilde{\mathcal{O}}$ is given by

$$\tilde{\mathcal{O}}_n(\chi, t; \mathbf{x}) = i^n \int_{t_i}^{t_f} dt'_n \cdots \int_{t_i}^{t'_2} dt'_1 \hat{\Gamma}_I(t'_1) \cdots \hat{\Gamma}_I(t'_n) \mathcal{O}(\chi; \bar{\boldsymbol{\varphi}}(t; \mathbf{x})). \quad (290)$$

This almost allows for a recursive equation to calculate $\tilde{\mathcal{O}}_n$ from $\tilde{\mathcal{O}}_{n-1}$, but the time-ordering prevents it. Replacing the time-ordering by symmetry factors in the way outlined above yields

$$\tilde{\mathcal{O}}_n(\chi, t; \mathbf{x}) \propto i \int_{t_i}^{t_f} dt' \hat{\Gamma}_I(t') \tilde{\mathcal{O}}_{n-1}(\chi, t; \mathbf{x}), \quad (291)$$

where the proportionality sign is a slight oversimplification. In practice, different terms resulting from the right-hand side expressions may have different symmetry factors. Nonetheless, provided an algorithm can be developed to obtain the symmetry factors, this equation significantly reduces the computational requirements for high order contributions.⁹

⁹ While the expression in equation (252) has a computational complexity which is exponential in the order n due to the nested time-integrals, the recursive relation in equation (291) allows to calculate the contributions to $\tilde{\mathcal{O}}$ in a computation time linear in the order n . In this naive estimate, we ignored the number of terms appearing through product rules which scales exponentially with order n in the most general case.

3.2.4 Example: Harmonic Oscillator (VII)

We return to the one-dimensional harmonic oscillator for a final time in this thesis. Our aim in this subsection is to translate the results of subsection 3.1.3 into Feynman diagrams and to generalize them. Exploiting certain special properties of the harmonic oscillator, we are able to perform a complete resummation of the interactions and recover the exact analytic solution derived in subsection 2.1.5 from perturbative KFT.

Written as diagrams, the zeroth and first order contributions to the harmonic oscillator are simply

$$\tilde{\varphi}_0(t; \mathbf{x}) = \text{[diagram: star with } \varphi \text{]} \quad \text{and} \quad \tilde{\varphi}_1(t; \mathbf{x}) = \text{[diagram: circle 1 connected to star with } \varphi \text{]}. \quad (292)$$

In second order there are two possible diagrams

$$\tilde{\varphi}_2(t; \mathbf{x}) = \text{[diagram: circle 1 connected to circle 2 connected to star with } \varphi \text{]} + \text{[diagram: circle 1 and circle 2 both connected to star with } \varphi \text{]}. \quad (293)$$

However, the second diagram vanishes because it is not possible to act more than once with $\hat{\Gamma}_I$ on $\tilde{\varphi}$. Evaluating the three diagrams for the respective orders reproduces the expressions obtained in subsection 3.1.3.

In third order, we immediately omit diagrams for which more than one edge ends at the observable vertex. Only two diagrams

$$\tilde{\varphi}_3(t; \mathbf{x}) = \text{[diagram: circle 1 connected to circle 2 connected to circle 3 connected to star with } \varphi \text{]} + \text{[diagram: circle 1 and circle 2 both connected to circle 3 connected to star with } \varphi \text{]}. \quad (294)$$

remain. However, the interaction part of the equations of motion $E_I[\varphi]$ for the harmonic oscillator is linear in φ . Just like for the observable vertex it thus is not possible for more than one edge ending at an interaction vertex. Consequently, the value of the second diagram of $\tilde{\varphi}_3$ is zero.

Given the severe restrictions on where edges can end, there is actually only one possible diagram for any order n , namely

$$\tilde{\varphi}_n(t; \mathbf{x}) = \text{[diagram: circle 1 connected to circle 2 connected to } \dots \text{ connected to circle } n \text{ connected to star with } \varphi \text{]}. \quad (295)$$

Moreover, the value of this diagram can be determined via the recursive relation

$$\tilde{\varphi}_n(t; \mathbf{x}) = \int_{t_i}^{t_f} dt' i\hat{\Gamma}_I(t') \tilde{\varphi}_{n-1}(t; \mathbf{x}) \quad (296)$$

which is a special case of equation (291). This works in this particular case, because all operators $\hat{\Gamma}_I$ act on the object immediately to their right and the causality of the Green's function then ensures time-ordering. Alternatively, one can also show that the symmetry factors of these types of diagrams are always unity.

In any case, the recursive relation can be used to prove the formula

$$\tilde{\varphi}_n(t; \mathbf{x}) = \left(\frac{(-1)^n \kappa^n}{(2n)! m^n} (t - t_i)^{2n} \chi^{(q)} + \frac{(-1)^n \kappa^n}{(2n+1)! m^{n+1}} (t - t_i)^{2n+1} \chi^{(p)} \right) \quad (297)$$

via induction. Note that for $n = 1, 2$ the expressions derived in subsection 3.1.3 are recovered. It is easy to confirm that the sum of the contributions at all orders n yields the analytic solution given in equation (26). Specifically,

$$\tilde{\varphi}(t; x) = \sum_{n=0}^{\infty} \tilde{\varphi}_n(t; x) \quad (298)$$

is actually the Taylor series of $\tilde{\varphi}(t; x)$ around initial time t_i . This achieves a complete resummation of the perturbative series of the one-dimensional harmonic oscillator.

3.3 SELF-GRAVITATING SYSTEMS

The introductory chapter of this thesis clearly states that the motivation for the development of KFT was cosmic structure formation. Up until this point, the construction of KFT and its microscopic perturbation theory has been kept completely general in this thesis. The formalism presented above is applicable to any classical physical system described by Hamilton's equations of motion and subject to a probability distribution of initial values.

In order to make a connection between our perturbative treatment and the KFT literature and in preparation for the applications considered in the following chapter, we specialize to interacting N-body systems in this section. Specifically, we assume a system of N indistinguishable point-particles interacting via a position-dependent pairwise interaction potential. Moreover, we work exclusively in Newtonian gauge.

In the first subsection below we show how N-body systems are a special case of composite systems with identical components introduced in subsection 2.2.1. We comment on the consequences of having indistinguishable particles both with respect to the form of the Hamiltonian as well as the probability distribution of initial values.

In subsection 3.3.2 we specify the Hamiltonian to adhere to the aforementioned properties. Working in Newtonian Gauge, we perform a split of the Hamiltonian and obtain a split of the equations of motion. Using the special forms of the Green's function and the interaction part of the equations of motion we deduce a simplified expression for the operator $\hat{\Gamma}_1$.

In order to completely evaluate the functional derivatives with respect to $\bar{\varphi}$ from the Feynman rules, we introduce a Fourier space description in subsection 3.3.3. Specifically, we express the interaction part of the equations of motion in terms of the Fourier transform of the two-particle interaction potential. This way derivatives can be replaced by multiplication with wave vectors.

This property is immediately exploited in a specialization of our Feynman rules in subsection 3.3.4. Instead of assigning mathematical expressions exclusively to vertices, we are able to assign part of the expressions to the edges. This allows to reference both vertices which are connected by an edge in the expression. Ultimately, through various means we obtain a set of specialized Feynman rules to construct expressions for density correlation functions of an N-body system.

The specialization to N-body systems recovers the diagrammatic description in [1]. However, an adjustment is made to split the difference of Kronecker δ -symbols assigned to edges in [1]. Considering the two contributions independently has been suggested independently by Shayan Hemmatyar in the work leading up to [1] as well as by [35]. The notation used here mimics the one in [35] for ease of comparison and to avoid the parallel existence of significantly different symbolic notations.

3.3.1 *N-Body Phase Space*

As mentioned repeatedly throughout the preceding sections, our main applications for the KFT framework and its microscopic perturbation theory are N-body systems. In fact, the specialized construction of the framework for such systems in [1] would have been sufficient for the applications in the following chapter. There are of course good reasons for providing a generalized treatment here as discussed, e.g., in the introductory chapter. Nonetheless, in order to facilitate the application of KFT to cosmology, this section bridges the gap between the general formalism introduced above and the specific applications below.

Of course the equations and Feynman rules of the general treatment remain valid when considering a specific system. However, the specific system might allow for significant simplifications. In the case of an N-body system the main simplification is due to the factorization of phase space $\mathbf{X} = \mathbf{X}^N$. Importantly, the component phase space $X = \mathbb{R}^{2D}$ is the same for all particles. The integer D is the dimension of the space in which the N-body system evolves. In applications, it is usually $D = 3$ given that our universe has three spatial dimensions, but for toy models we occasionally permit $D = 1$.

We have discussed this kind of factorization already in subsections 2.2.1 and 2.4.5. There we explained how to construct macroscopic density fields and their correlation functions. Recall that they can be thought as resulting from a projection $\mathbf{X} \rightarrow X$ and are thus given as the sum over the microscopic densities of the components. The latter are Dirac δ -functions such that the macroscopic density field is the sum over Dirac δ -functions. In Fourier space, we obtain the expression

$$\tilde{\rho}(\mathbf{k}, t; \mathbf{x}) = \sum_{j=1}^N \exp\left(-i\mathbf{k} \cdot \frac{\delta}{i\delta\mathbf{J}_j^T(t)}\right) Z[\mathbf{J}; \mathbf{x}] \Big|_{\mathbf{J}=0}. \quad (299)$$

The construction of a macroscopic density field as an additional observable is only one aspect of the benefits of specifying to an N-body system. The factorization of phase space also has an effect on expectation values, evolution of the system and the Feynman rules. In all these cases the underlying reason is that the properties of each individual particle are the same as of any other particle. This makes the particles indistinguishable and therefore any observable must be invariant when changing the state of the system \mathbf{x} by an exchange of particles $x_j \leftrightarrow x_k$. Observables abiding to this principle are typically given as sums over identical contributions from all particles. An example for this is the macroscopic density field $\tilde{\rho}(\mathbf{k}, t; \mathbf{x})$.

In order for this invariance under particle exchange to be realized, both the equations of motion and the initial conditions should respect this property, too. Let us consider an N-body system with explicitly given initial conditions \mathbf{x} . The state \mathbf{x} can of course not satisfy any kind of exchange symmetry on its own unless all particles start out with the exact same initial position and momentum.

Instead, the idea of invariance under particle exchange is implemented by the requirement that

$$\begin{aligned} & \tilde{\varphi}(t; (x_1, \dots, \underbrace{x_k}_{j^{\text{th}}}, \dots, \underbrace{x_j}_{k^{\text{th}}}, \dots, x_N)) \\ &= (\tilde{\varphi}_1(t; \mathbf{x}), \dots, \underbrace{\tilde{\varphi}_k(t; \mathbf{x})}_{j^{\text{th}}}, \dots, \underbrace{\tilde{\varphi}_j(t; \mathbf{x})}_{k^{\text{th}}}, \dots, \tilde{\varphi}_N(t; \mathbf{x})), \end{aligned} \quad (300)$$

i.e., the only effect of an exchange of particles in the initial conditions is an exchange of particles after evolution of the system. In particular, the evolution of all other particles is unaffected.

The condition in equation (300) implies that the equations of motion need to be agnostic to particle indices. Usually, this property is realized by a Hamiltonian which is a sum over single-particle contributions $\mathcal{K}_j = \mathcal{K}[\varphi_j]$ plus a symmetric potential term $\mathcal{V}_{jk} = \mathcal{V}[\varphi_j, \varphi_k]$. As an equation, it is

$$\mathcal{H} = \sum_{j=1}^N \mathcal{K}_j + \frac{1}{2} \sum_{\substack{j,k=1 \\ j \neq k}}^N \mathcal{V}_{jk} \quad (301)$$

with $\mathcal{V}_{jk} = \mathcal{V}_{kj}$. In this form, the Hamiltonian is invariant under the exchange of particles.

Finally, we consider the exchange symmetry given a probability distribution of initial values $P(\mathbf{x})$. Let us define the probability distribution obtained through the exchange of the j^{th} and k^{th} particles as

$$P_{j \leftrightarrow k}(\mathbf{x}) := P((x_1, \dots, \underbrace{x_k}_{j^{\text{th}}}, \dots, \underbrace{x_j}_{k^{\text{th}}}, \dots, x_N)). \quad (302)$$

If the condition in equation (300) is satisfied and the observable $\mathcal{O}(\chi; \mathbf{x})$ is invariant under exchange of particles, then

$$\langle \tilde{\mathcal{O}} \rangle(\chi; t) = \int d\mathbf{x} \frac{1}{2} (P(\mathbf{x}) + P_{j \leftrightarrow k}(\mathbf{x})) \mathcal{O}(\chi; \mathbf{x}). \quad (303)$$

This implies that expectation values of admissible observables are unchanged by the replacement

$$P(\mathbf{x}) \mapsto \frac{1}{N!} \sum_{\sigma \in S_N} P(x_{\sigma(1)}, x_{\sigma(2)}, \dots, x_{\sigma(N)}), \quad (304)$$

where S_N is the group of all permutations of N elements. Therefore we may assume without loss of generality that the probability distribution of initial values is invariant under the exchange of particles.

3.3.2 *N-Body Green's Function*

The Hamiltonian \mathcal{H} defined above has the desired property of invariance under exchange of particles. But the form of equation (301) implies significant simplifications beyond this property. Indeed, there are no terms depending on

three or more particles such that the interactions take a particularly easy form. Moreover, the single-particle contributions \mathcal{K}_j are all of the same form $\mathcal{K}[\varphi_j]$ enabling simplifications when describing free motion. However, both these aspects depend on the choice of splitting gauge.

Here, we consider the case where the single-particle contributions \mathcal{K}_j are the kinetic terms of the particles, while the potential term \mathcal{V}_{jk} is induced by a two-particle interaction potential v . It is

$$\mathcal{K}_j = \frac{1}{2m(t)} \varphi_j^{(p)}(t) \cdot \varphi_j^{(p)}(t) \quad \text{and} \quad (305)$$

$$\mathcal{V}_{jk} = m(t) v(\varphi_j^{(q)}(t) - \varphi_k^{(q)}(t), t) \quad (306)$$

where m is the (*effective*) mass of the particles. Anticipating for application to expanding spacetimes in chapter 4 the effective mass may explicitly depend on time. We allow also for a time-dependence of the two-particle interaction potential v . The relationship $\mathcal{V}_{jk} = \mathcal{V}_{kj}$ implies that $v(-q, t) = v(q, t)$, i.e., the potential v is symmetric.

The form of the Hamiltonian strongly suggests a particular choice of splitting gauge. Recall that we discussed the freedom in splitting the equations of motion into a free and an interaction part in subsection 2.3.2. This separation of free motion and interactions can be induced by a splitting of the Hamiltonian into a free part \mathcal{H}_0 and an interaction part \mathcal{H}_I . Here, we focus on the choice of Newtonian gauge

$$\mathcal{H}_0 = \sum_{j=1}^N \mathcal{K}_j \quad \text{and} \quad \mathcal{H}_I = \frac{1}{2} \sum_{\substack{j,k=1 \\ j \neq k}}^N \mathcal{V}_{jk}. \quad (307)$$

In this gauge choice, the free part of the equations of motion reads

$$\mathbf{E}_0[\boldsymbol{\varphi}](t) = \frac{d}{dt} \boldsymbol{\varphi}(t) - \mathcal{J} \frac{\delta \mathcal{H}_0(\boldsymbol{\varphi}(t), t)}{\delta \boldsymbol{\varphi}(t)} \quad (308)$$

$$= \begin{pmatrix} \frac{d}{dt} \boldsymbol{\varphi}^{(q)}(t) - \frac{1}{m(t)} \boldsymbol{\varphi}^{(p)}(t) \\ \frac{d}{dt} \boldsymbol{\varphi}^{(p)}(t) \end{pmatrix}. \quad (309)$$

The particles are completely decoupled and each particle j evolves freely according to the equations

$$\frac{d}{dt} \varphi_j^{(q)}(t) = \frac{1}{m(t)} \varphi_j^{(p)}(t) \quad \text{and} \quad \frac{d}{dt} \varphi_j^{(p)}(t) = 0. \quad (310)$$

Given this simple structure, it is easy to construct a Green's function for the single-particle free equations of motion. Let

$$\mathbf{G}(t, t') := \begin{pmatrix} \theta(t-t') \mathbb{I}_D & g(t, t') \theta(t-t') \mathbb{I}_D \\ 0 & \theta(t-t') \mathbb{I}_D \end{pmatrix} \quad (311)$$

with

$$g(t, t') := \int_{t'}^t dt'' \frac{1}{m(t'')}. \quad (312)$$

On a static Euclidean spacetime, the effective mass is the particle rest mass $m \in \mathbb{R}$ and we recover the form of equation (87). A simple calculation analogous to the one performed there shows that G satisfies equation (72).

The single-particle Green's functions can be combined into a Green's function for the entire N -body system. The block-diagonal matrix

$$\mathbf{G}(t, t') = \text{diag}(G(t, t'), G(t, t'), \dots, G(t, t')) = \mathbb{I}_N \otimes G(t, t') \quad (313)$$

serves as a Green's function for the free equation $\mathbf{E}_0[\boldsymbol{\varphi}] = \mathbf{0}$. In this sense the factorization of phase space induces a diagonalization of the Green's function in Newtonian gauge.

The j^{th} component of the interaction part of the equations of motion takes the form

$$(\mathbf{E}_I)_j[\boldsymbol{\varphi}](t) = - \begin{pmatrix} 0 & \mathbb{I}_D \\ -\mathbb{I}_D & 0 \end{pmatrix} \frac{\delta \mathcal{H}_I(\boldsymbol{\varphi}(t), t)}{\delta \varphi_j(t)} \quad (314)$$

$$= \sum_{\substack{k=1 \\ k \neq j}}^N \begin{pmatrix} 0 \\ m(t) \nabla_{\mathbf{v}}(\varphi_j^{(q)}(t) - \varphi_k^{(q)}(t), t) \end{pmatrix} \quad (315)$$

for the case considered here. The potential terms \mathcal{V}_{jk} only depend on $\varphi^{(q)}$ and due to the symplectic matrix \mathcal{J} this implies that \mathbf{E}_I only receives contributions to $\mathbf{E}_I^{(p)}$. Again, this conclusion is only valid in Newtonian gauge. Splitting the Hamiltonian in a different way might yield a dependence of \mathcal{H}_I on $\varphi^{(p)}$.

Due to the structure of Hamilton's equations, the vanishing of $\mathbf{E}_I^{(q)}$ always occurs if the interactions only depend on particle positions. In such cases, the operator $\hat{\Gamma}_I$ can be simplified provided that only position-dependent observables are considered. The single-particle contribution to $\hat{\Gamma}_I$ is

$$i(\hat{\Gamma}_I)_j(t') = \int_{t'}^{t_f} dt'' (\bar{\mathbf{E}}_I)_j^T(t'; \mathbf{x}) G^T(t'', t') \frac{\delta}{\delta \bar{\varphi}_j^T(t''; \mathbf{x})} \quad (316)$$

in general. Recall that $(\bar{\mathbf{E}}_I)_j = (\mathbf{E}_I)_j[\bar{\boldsymbol{\varphi}}]$. If neither $\bar{\mathbf{E}}_I$ nor the considered observables depend on $\bar{\varphi}^{(p)}$, then the functional derivative in this expression can be simplified to a functional derivative with respect to $\bar{\varphi}_j^{(q)}$. However, as we have just seen, it is $(\mathbf{E}_I)_j^{(q)} = 0$ in that case, too. Therefore, contracting the functional derivative and the interaction part of the equations of motion with the Green's function picks out only the qp -component and we obtain

$$i(\hat{\Gamma}_I)_j(t') = \int_{t'}^{t_f} dt'' g(t'', t') (\bar{\mathbf{E}}_I)_j^{(p)}(t''; \mathbf{x}) \cdot \frac{\delta}{\delta (\bar{\varphi}_j^{(q)})^T(t''; \mathbf{x})}. \quad (317)$$

3.3.3 Fourier Space Description

The diagrammatic scheme developed in the previous section is supposed to facilitate obtaining the expressions for contributions to the generating functional, to observables and their expectation values. However, in the present form, our Feynman rules still involve functional derivatives. These are hidden in the

operator $\hat{\Gamma}_I$ inside the interaction vertex. Granted, all product rules are already sorted out, but it would be preferable if the derivatives were already evaluated.

More importantly, the resulting expressions have a complicated dependence on the free evolution map $\bar{\varphi}(\bullet; \mathbf{x})$. Not only does it appear in the aforementioned functional derivatives, but also inside the interaction part of the equations of motion. This poses a difficulty when considering expectation values which require integration over the initial values \mathbf{x} .

Both problems can be remedied simultaneously by performing a suitable Fourier transform. This way the derivatives become multiplications by a wave vector and the free evolution map appears in Fourier phase factors which are very suitable for integrations over \mathbf{x} . The latter is especially true if the observable under consideration is a density r -point correlation function which likewise has the form of a Fourier phase factor.

However, the price to pay for the benefits outlined above is the appearance of an integral over a wave vector for every interaction vertex. In some applications this is not a worthwhile trade at all, but in others it is a necessity. In fact, our two main applications are examples for either case. This should be kept in mind while performing a series of seemingly counterproductive modifications for the remainder of this subsection.

Let us start out from the inverse Fourier transform of the interaction part of the equations of motion E_I . For an N -body system with interactions given by a position-dependent two-particle interaction potential, it is

$$\begin{aligned} (E_I)_j^{(p)}[\boldsymbol{\varphi}](t) &= \sum_{\substack{\ell=1 \\ \ell \neq j}}^N m(t) \nabla v\left(\varphi_j^{(q)}(t) - \varphi_\ell^{(q)}(t), t\right) & (318) \\ &= \sum_{\substack{\ell=1 \\ \ell \neq j}}^N \int \frac{d\mathbf{k}'}{(2\pi)^D} i m(t) k' v(\mathbf{k}', t) \exp\left(i\mathbf{k}' \cdot \left(\varphi_j^{(q)}(t) - \varphi_\ell^{(q)}(t)\right)\right). & (319) \end{aligned}$$

Recall that our convention is to distinguish between a function and its Fourier transform only via the arguments. The object v in the second line is the Fourier transform of the two-particle interaction potential and is given by

$$v(\mathbf{k}', t) = \int d\mathbf{q} v(\mathbf{q}, t) \exp(-i\mathbf{q} \cdot \mathbf{k}'). \quad (320)$$

Using this form of the interaction part of the equations of motion, the action of operators $\hat{\Gamma}_I$ on each other becomes quite simple. Indeed, the action of a functional derivative with respect to $\varphi_\ell^{(q)}$ on $(E_I)_j^{(p)}$ yields simply

$$\begin{aligned} \frac{\delta}{\delta(\varphi_{j'}^{(q)}(t'))^T} (E_I)_j^{(p)}[\boldsymbol{\varphi}](t) &= \sum_{\substack{\ell=1 \\ \ell \neq j}}^N \int \frac{d\mathbf{k}'}{(2\pi)^D} m(t) k' (k')^T v(\mathbf{k}', t) (\delta_{j'\ell} - \delta_{j'j}) \\ &\quad \delta_D(t - t') \exp\left(i\mathbf{k}' \cdot \left(\varphi_j^{(q)}(t) - \varphi_\ell^{(q)}(t)\right)\right). & (321) \end{aligned}$$

Here, Kronecker δ -symbols appear which are unity for equal indices and zero otherwise. The difference $\delta_{j'\ell} - \delta_{j'j}$ vanishes if $\ell = j$ such that we can omit the

condition $\ell \neq j$ from the sum. The object $k'(k')^T$ is a $D \times D$ -dimensional matrix which encodes the Fourier transform of the Hessian matrix of the potential v .

The form of the expression in equation (321) shows that using a Fourier transform, the functional derivatives in $\hat{\Gamma}_I$ can essentially be replaced by multiplication with wave vectors. However, this requires that the integrations over these wave vectors are applied to the entire expression instead of inside a factor E_I . Moreover, this statement only applies to the action on other factors $\hat{\Gamma}_I$, but not for the action on a general observable.

We mentioned above that for density correlation functions the formalism in Fourier space is particularly useful. It is now evident in which sense this statement is true: The Fourier space density correlation functions are of the form

$$\left(\underbrace{G_{\tilde{\rho} \dots \tilde{\rho}}}_{r \text{ times}} \right)_0(k_1, \dots, k_r, t; \mathbf{x}) = \prod_{s=1}^r \sum_{j_s=1}^N \exp(-ik_s \cdot \tilde{\varphi}_{j_s}(t; \mathbf{x})) \quad (322)$$

when evaluated along the free evolution $\tilde{\varphi}$. For details of the derivation, confer subsections 2.2.1 and 2.4.5. Being expressed as exponential functions, the replacement of functional derivatives by wave vectors works in the same way as for factors E_I above. This allows us to obtain an expression for $\hat{\Gamma}_I$ in terms of the wave vector associated to the object acted upon.

The change proposed makes the combinatorial complexity even more important as now even the form of $\hat{\Gamma}_I$ depends on which object it acts on. Moreover, the particle indices are an additional source of difficulty, especially due to the difference of Kronecker δ -symbols appearing in equation (321). Nonetheless, the resulting expressions are significantly simplified as they feature neither functional derivatives, nor d -dimensional objects. To take full advantage of this, we adapt our Feynman rules to the N -body case in the following subsection.

3.3.4 *N-Body Feynman Rules*

We introduced Feynman rules as a tool to keep track of the various ways the operators $\hat{\Gamma}_I$ can act in expressions of the form

$$\tilde{\mathcal{O}}_n(\chi, t; \mathbf{x}) = \int_{t_i}^{t_f} dt'_1 i \hat{\Gamma}_I(t'_1) \dots \int_{t'_{n-1}}^{t_f} dt'_n i \hat{\Gamma}_I(t'_n) \mathcal{O}(\chi; \tilde{\varphi}(t; \mathbf{x})) . \quad (323)$$

These expressions yield the n^{th} order contribution to the observable \mathcal{O} in microscopic KFT perturbation theory and arise from a series expansion in the interactions of the system.

As a first step in adapting these Feynman rules to N -body systems, let us consider the effect of using the expression in equation (317) for $\hat{\Gamma}_I$. The main difference to the general case is that we have separate contributions for all particles j and have specified the interaction part of the equations of motion to be given as in equation (314). In particular, this means that we are restricting ourselves to classical N -body systems with pairwise position-dependent interactions in Newtonian gauge.

In order to investigate the effects of the changes in the case of N-body systems, let us consider an example diagram. Recall that using the Feynman rules defined above, one of the terms adding to the third order contribution of an observable \mathcal{O} is given by

$$\begin{aligned}
 \begin{array}{c} \textcircled{1} \text{---} \textcircled{3} \\ \textcircled{2} \text{---} \end{array} \text{---} \text{⬠} \mathcal{O} &= i^3 \int_{t_i}^{t_f} dt'_1 \int_{t_1}^{t_f} dt'_2 \int_{t_2}^{t_f} dt'_3 \\
 &\hat{\Gamma}_I(t'_2) [\hat{\Gamma}_I(t'_1), \hat{\Gamma}_I(t'_3)] \mathcal{O}(\chi; \bar{\varphi}(t; \mathbf{x})). \quad (324)
 \end{aligned}$$

This term arises from the general form of the third order contribution

$$\tilde{\mathcal{O}}_3(\chi, t; \mathbf{x}) = i^3 \int_{t_i}^{t_f} dt'_1 \int_{t_1}^{t_f} dt'_2 \int_{t_2}^{t_f} dt'_3 \hat{\Gamma}_I(t'_1) \hat{\Gamma}_I(t'_2) \hat{\Gamma}_I(t'_3) \mathcal{O}(\chi; \bar{\varphi}(t; \mathbf{x})) \quad (325)$$

by acting with $\hat{\Gamma}_I(t'_1)$ on $\hat{\Gamma}_I(t'_3)$ and with $\hat{\Gamma}_I(t'_2)$ and $\hat{\Gamma}_I(t'_3)$ on $\mathcal{O}(\chi; \bar{\varphi}(t; \mathbf{x}))$.

Combining equations (317) and (318), we can write $\hat{\Gamma}_I$ as

$$\begin{aligned}
 i \hat{\Gamma}_I(t') &= \sum_{\substack{j, \ell=1 \\ \ell \neq j}}^N \int_{t'}^{t_f} dt'' m(t') g(t'', t') \\
 &\nabla_{\mathbf{v}} \left(\bar{\varphi}_j^{(q)}(t'; \mathbf{x}) - \bar{\varphi}_\ell^{(q)}(t'; \mathbf{x}), t' \right) \cdot \frac{\delta}{\delta(\bar{\varphi}_j^{(q)})^T(t''; \mathbf{x})}. \quad (326)
 \end{aligned}$$

As a direct consequence of only allowing for two-particle potential terms in the Hamiltonian, cf. equation (301), this term only involves two particle indices j and ℓ . Acting with the functional derivative on another factor $\hat{\Gamma}_I$ yields Kronecker δ -symbols which cancels one of the summations. More precisely, we obtain a difference of two such Kronecker δ -symbols in analogy to equation (321).

Keeping the difference of Kronecker δ -symbols as part of our Feynman rules is undesirable, because it hides qualitatively different contributions in the same diagram. Instead, we want to distinguish whether the functional derivative in a factor $\hat{\Gamma}_I$ acts on $\bar{\varphi}_\ell^{(q)}$ or $\bar{\varphi}_j^{(q)}$ in another factor $\hat{\Gamma}_I$. To enable this, we replace the interaction vertex by

$$\textcircled{1} \mapsto \begin{array}{c} \textcircled{1} \\ \bullet \end{array}, \quad (327)$$

where the large circle corresponds to the index j , while the small black circle corresponds to the index ℓ . We refer to the large circle as the interaction vertex and the small black circle as the associated *density node*. Their combination is sometimes also referred to as interaction vertex. The diagram in our example above thus splits into two contributions

$$\begin{array}{c} \textcircled{1} \text{---} \textcircled{3} \\ \textcircled{2} \text{---} \end{array} \text{---} \text{⬠} \mathcal{O} = \begin{array}{c} \textcircled{1} \text{---} \textcircled{3} \\ \bullet \end{array} \text{---} \begin{array}{c} \textcircled{3} \\ \bullet \end{array} \text{---} \text{⬠} \mathcal{O} + \begin{array}{c} \textcircled{1} \text{---} \textcircled{3} \\ \bullet \end{array} \text{---} \begin{array}{c} \textcircled{1} \\ \bullet \end{array} \text{---} \text{⬠} \mathcal{O}, \quad (328)$$

where the first diagram corresponds to the Kronecker symbol $\delta_{j_1 j_3}$ and the second one to $\delta_{j_1 \ell_3}$. Given that the functional derivative in $\hat{\Gamma}_1$ comes with index j , each edge still starts from a large circle.

As a second step in adapting the Feynman rules constructed in subsection 3.2.1, we specialize the observable to be a density correlation function. As mentioned above, this is particularly useful when we consider the expressions in Fourier space. But it also enables a significant simplification in our diagrams by replacing the observable vertex.

The r -point correlation function of the Fourier space macroscopic density, as given in equation (322), is the product over r factors of

$$\blacksquare_{s,t} := \sum_{\ell_s=1}^N \exp\left(-ik_s \cdot \bar{\varphi}_{\ell_s}^{(q)}(t; \mathbf{x})\right). \tag{329}$$

This is a *density vertex* and can be connected to from the left with edges coming from interaction vertices via the small black circle. Observing that this small black circle corresponds to the same factor as for the interaction vertex, we also refer to it as density node.¹⁰

Using the definition of the density vertex above, the observable vertex factorizes into r density vertices,

$$\Theta = \begin{matrix} \bullet \blacksquare_{1,t} \\ \vdots \\ \bullet \blacksquare_{r,t} \end{matrix}. \tag{330}$$

This suggests the definition of multiplying connected components of diagrams which we adopt in the following. Connected components play an important role for density correlation functions because their diagrams are forests, i.e., collections of trees. Indeed, any interaction vertex only has one outgoing edge, hence it is impossible for density vertices to end up connected in diagrams of any order. In terms of equations, the functional derivative in $\hat{\Gamma}_1$ can only act on one of the exponential factors in the product.

Depending on the number r , our example diagram above splits into many contributions. Even for $r = 2$, we have

$$\begin{matrix} \text{Diagram 1} \\ \text{Diagram 2} \end{matrix} = \begin{matrix} \text{Diagram 3} \\ \text{Diagram 4} \\ \text{Diagram 5} \\ \text{Diagram 6} \end{matrix} \tag{331}$$

for the first contribution in equation (328) alone. However, it is of course preferable to have this combinatorial complexity revealed by the diagrams

¹⁰ This is of course no coincidence. The interaction term of an N -body system can be written as a convolution of the density with the interaction potential. This is very apparent in the formalism of [23].

rather than hidden in the observable vertex. Note that the diagrams on the right-hand side can be constructed from the simple instruction of connecting all edges ending at the observable index in all possible ways to the density vertices.

The third step is to use the expressions for $\hat{\Gamma}_I$ in Fourier space to define more specialized Feynman rules. Recall, that according to the Feynman rules constructed in subsection 3.2.1, we ought to assign mathematical expressions to the vertices. However, as remarked there, we have some freedom in assigning (part of) the expression to the edge leaving an interaction vertex instead.

The advantage of assigning expressions to edges is that we can refer to the labels of both its endpoints. This is particularly useful to fully evaluate the functional derivatives in factors $\hat{\Gamma}_I$. In fact, even the Kronecker δ -symbols and the Dirac δ -function in equation (321) can be canceled against some of the sums and integrals, respectively.

In accordance with the definition of the density vertex, we define the density node as

$$\bullet \boxed{s, t} := \exp\left(-ik_s \cdot \bar{\varphi}_{\ell_s}^{(q)}(t; \mathbf{x})\right) \quad \text{and} \quad (332)$$

$$\bullet \bigcirc a := \exp\left(-ik'_a \cdot \bar{\varphi}_{\ell'_a}^{(q)}(t'_a; \mathbf{x})\right), \quad (333)$$

respectively. The transparent backgrounds indicate that the expressions associated to

$$\circ \boxed{s, t} := 1 \quad \text{and} \quad (334)$$

$$\circ \bigcirc a := v(k'_a, t'_a), \quad (335)$$

respectively, are not included. Conversely, the transparent small circle \circ indicates that the factor coming from the density node is not included. Combined, we obtain

$$\bullet \boxed{s, t} = \exp\left(-ik_s \cdot \bar{\varphi}_{\ell_s}^{(q)}(t; \mathbf{x})\right) \quad \text{and} \quad (336)$$

$$\bullet \bigcirc a = v(k'_a, t'_a) \exp\left(-ik'_a \cdot \bar{\varphi}_{\ell'_a}^{(q)}(t'_a; \mathbf{x})\right). \quad (337)$$

It remains to state the Feynman rules for the edges. Comparing to equations (321) and (326), these need to include the propagator, scalar products of wave vectors as well as a Fourier phase factor. We define

$$\bigcirc a \text{---} \circ \boxed{s, t} := -m(t'_a) g(t, t'_a) k'_a \cdot k_s \exp\left(ik'_a \cdot \bar{\varphi}_{\ell'_b}^{(q)}(t'_a; \mathbf{x})\right) \quad \text{and} \quad (338)$$

$$\bigcirc a \text{---} \bigcirc b := -m(t'_a) g(t'_b, t'_a) k'_a \cdot k'_b \exp\left(ik'_a \cdot \bar{\varphi}_{\ell'_b}^{(q)}(t'_a; \mathbf{x})\right). \quad (339)$$

Again, the transparent vertices are only there to indicate the relevant indices. The remaining case of an edge ending at a large circle of an interaction vertex is slightly more difficult. Here, the Kronecker symbol $\delta_{j'_a j'_b}$ identifies the index j'_a with the index j'_b which is itself identified with indices due to the outgoing edge of the vertex labeled b. This process might happen repeatedly until eventually

an outgoing edge hits a small circle \bullet and the index j'_a is identified with its index ℓ_\bullet . Following this description, we define

$$\begin{array}{c} \text{a} \\ \circ \end{array} \text{---} \begin{array}{c} \text{b} \\ \circ \end{array} := m(t'_a) g(t'_b, t'_a) k'_a \cdot k'_b \exp\left(ik'_a \cdot \bar{\varphi}_{\ell_\bullet}^{(q)}(t'_a; \mathbf{x})\right). \quad (340)$$

Note that only the exponential phase factor is subject to this complication, while the propagator and the scalar product of wave vectors are defined with respect to the vertices which the edge connects to.

This defines the components of our diagrams, but there is one more rule which applies to the entire diagrams. It concerns the integrations over time-parameters and wave vectors which we have omitted in our Feynman rules. The reason for this is that they need to be applied to the entire expression of a diagram. Therefore, we finalize our N-body Feynman rules by stating that upon having taken the product over all terms coming from vertices and edges Π , the mathematical expression associated to the diagram is

$$\sum_{\ell_1=1}^N \dots \sum_{\ell_r=1}^N \sum_{\ell'_1=1}^N \dots \sum_{\ell'_n=1}^N \int_{t_i}^{t_f} dt'_1 \dots \int_{t'_{n-1}}^{t_f} dt'_n \int \frac{dk'_1}{(2\pi)^3} \dots \int \frac{dk'_n}{(2\pi)^3} \Pi \quad (341)$$

for a diagram with n interaction and r density vertices. Note that the integrals over t'_a and the sums over j'_a have been canceled by Dirac δ -functions and Kronecker δ -symbols, respectively.

To demonstrate how these Feynman rules are to be used, let us consider the first diagram in equation (331) which has the form

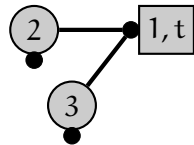


$$(342)$$

and thus is the product over two contributions coming from the two trees. The contribution from the second tree is simply

$$\begin{array}{c} \bullet \\ \square \end{array} 2, t = \exp\left(-ik_2 \cdot \bar{\varphi}_{\ell_2}^{(q)}(t; \mathbf{x})\right). \quad (343)$$

The first tree is more complicated. Using the Feynman rules above, we have

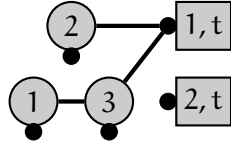


$$\begin{aligned} &= m(t'_2)g(t, t'_2) k'_2 \cdot k_1 \exp\left(ik'_2 \cdot \left(\bar{\varphi}_{\ell_1}^{(q)}(t'_2; \mathbf{x}) - \bar{\varphi}_{\ell'_2}^{(q)}(t'_2; \mathbf{x})\right)\right) \\ &\quad m(t'_3)g(t, t'_3) k'_3 \cdot k_1 \exp\left(ik'_3 \cdot \left(\bar{\varphi}_{\ell_1}^{(q)}(t'_3; \mathbf{x}) - \bar{\varphi}_{\ell'_3}^{(q)}(t'_3; \mathbf{x})\right)\right) \\ &\quad v(k'_2, t'_2) v(k'_3, t'_3) \exp\left(ik_1 \cdot \bar{\varphi}_{\ell_1}^{(q)}(t; \mathbf{x})\right). \end{aligned} \quad (344)$$

The first two lines are the contributions from the two edges combined with the corresponding exponential factor coming from the interaction vertices, respectively. In the last line we have the remaining contributions from the vertices together with the factor coming from the density vertex. The third interaction vertex together with the edge between vertices 1 and 2 supplies a factor

$$m(t'_1) g(t'_3, t'_1) k'_1 \cdot k'_3 v(k'_1, t'_1) \exp\left(ik'_1 \cdot \left(\bar{\varphi}_{\ell_1}^{(q)}(t'_1; \mathbf{x}) - \bar{\varphi}_{\ell'_1}^{(q)}(t'_1; \mathbf{x})\right)\right) \quad (345)$$

because ℓ_1 is the index associated to the small circle which is hit first when following the edge between the interaction vertices 1 and 3 to the right. Taking the product of the three expressions above and performing the integrations and sums according to the prescription in equation (341), we obtain



$$\begin{aligned}
 &= \sum_{\ell_1, \ell_2=1}^N \sum_{\ell'_1, \ell'_2, \ell'_3=1}^N \int_{t_i}^{t_f} dt'_1 \int_{t'_1}^{t_f} dt'_2 \int_{t'_2}^{t_f} dt'_3 \\
 &\int \frac{dk'_1}{(2\pi)^3} \int \frac{dk'_2}{(2\pi)^3} \int \frac{dk'_3}{(2\pi)^3} v(k'_1, t'_1) v(k'_2, t'_2) v(k'_3, t'_3) \\
 &m(t'_1) g(t'_3, t'_1) k'_1 \cdot k'_3 \exp\left(ik'_1 \cdot \left(\bar{\varphi}_{\ell'_1}^{(q)}(t'_1; \mathbf{x}) - \bar{\varphi}_{\ell'_1}^{(q)}(t'_1; \mathbf{x})\right)\right) \\
 &m(t'_2) g(t, t'_2) k'_2 \cdot k_1 \exp\left(ik'_2 \cdot \left(\bar{\varphi}_{\ell'_2}^{(q)}(t'_2; \mathbf{x}) - \bar{\varphi}_{\ell'_2}^{(q)}(t'_2; \mathbf{x})\right)\right) \\
 &m(t'_3) g(t, t'_3) k'_3 \cdot k_1 \exp\left(ik'_3 \cdot \left(\bar{\varphi}_{\ell'_3}^{(q)}(t'_3; \mathbf{x}) - \bar{\varphi}_{\ell'_3}^{(q)}(t'_3; \mathbf{x})\right)\right) \\
 &\exp\left(-ik_1 \cdot \bar{\varphi}_{\ell_1}^{(q)}(t; \mathbf{x}) - ik_2 \cdot \bar{\varphi}_{\ell_2}^{(q)}(t; \mathbf{x})\right). \tag{346}
 \end{aligned}$$

Evidently, the dependence of this expression on the initial values \mathbf{x} is of special form. Indeed, by the definition of our Feynman rules any diagram contributing to the r -point density correlation function depends on the initial conditions \mathbf{x} only via products of factors of the form

$$\exp\left(-ik \cdot \bar{\varphi}_j^{(q)}(a; \mathbf{x})\right) = \exp\left(-ik \cdot \mathbf{x}_j^{(q)}\right) \exp\left(-ig(t, t_i) k \cdot \mathbf{x}_j^{(p)}\right) \tag{347}$$

for certain wave-vectors k , time variables t and particle indices j . Note that the time variables and wave-vectors can be integration variables. All particle indices are being summed over.

For each diagram we can collect these terms by their particle index. Abbreviated the sum over all terms multiplying $\mathbf{x}_j^{(q)}$ by $f_j^{(q)}$ and the sum over all terms multiplying $\mathbf{x}_j^{(p)}$ by $f_j^{(p)}$, each diagram's dependence on the initial values \mathbf{x} thus is of the form

$$\prod_{j=1}^N \exp\left(if_j^{(q)} \cdot \mathbf{x}_j^{(q)}\right) \exp\left(if_j^{(p)} \cdot \mathbf{x}_j^{(p)}\right) =: \exp(if \cdot \mathbf{x}). \tag{348}$$

Here, $f_j^{(q)}$ is a sum over some set of wave-vectors with prefactors ± 1 , while $f_j^{(p)}$ is a sum over the same wave-vectors with prefactors $\pm g(t, t_i)$ for some time variable t .

For the n^{th} order contribution to the r -point density correlation function only $r + n$ of the factors $f_j^{(q)}$ are non-zero, and correspond to the density nodes in the diagram. In fact, one can basically read off $f_j^{(q)}$ (and $f_j^{(p)}$) from the diagrams: For the density node corresponding to index j , add to the negative of the wave-vector (times the factor g) corresponding to its vertex all wave-vectors (times the factor g) associated to all interaction vertices connecting to it, including those which connect "through" another interaction vertex.

4.1 STANDARD MODEL OF COSMOLOGY

Given the complexity of the universe and its history, it is surprising yet fortunate that there is a simple model which describes it to high accuracy. The Cosmological Standard Model (Λ CDM-model) depends only on 7 free parameters while describing the history of the universe as a whole, down to scales of roughly the size of galaxies.¹¹ Of course, the Λ CDM-model relies on a lot of implicit assumptions as pointed out in Table II of the excellent review [45]. As an example, in the Λ CDM-model a flat universe is assumed effectively setting a curvature parameter to zero which otherwise would enlarge the parameter space. Let us list the parameters of the Λ CDM-model:

- CMB temperature $T_{\text{CMB}} = 2.72548 \pm 0.00057$ K:
Temperature associated to the black body spectrum of the Cosmic Microwave Background (CMB) when averaged over the entire sky. It is related to the radiation density parameter $\Omega_{\text{R},0}$. The best measurement of this quantity is still due to the FIRAS instrument on the WMAP satellite.[46]
- angular parameter $100\theta_* = 1.04101 \pm 0.00029$:
Size of the sound horizon at recombination. Determines the scale of the baryonic acoustic oscillations and thus measured at high accuracy from the locations of the acoustic peaks in the CMB anisotropy spectra.
- power spectrum slope $n_s = 0.9665 \pm 0.0038$:
Slope of the power spectrum of primordial density fluctuations. In the probably popular scenario, these inhomogeneities in the early universe density field are directly related to quantum fluctuations of a scalar field driving an exponential spacetime expansion in the very early universe.
- power spectrum amplitude $\ln(10^{10} A_s) = 3.047 \pm 0.014$:
Amplitude of the power spectrum of aforementioned primordial density fluctuations.
- physical baryon density $h^2 \Omega_{\text{BM},0} = 0.02242 \pm 0.00014$:
Amount of baryonic (= ordinary) matter in the universe, mostly in the form of intergalactic gas.[47] Only about 5% of the current energy content of the universe is baryonic matter.
- physical CDM density $h^2 \Omega_{\text{DM},0} = 0.11933 \pm 0.00091$:
Cold Dark Matter (CDM) density in the universe, corresponding to a current energy fraction of about a quarter. The remaining approximately 70% of the energy content is Dark Energy (DE). In the Λ CDM-model it is described by a Cosmological Constant (Λ).
- reionization optical depth $\tau = 0.0561 \pm 0.0071$:
Associated to the formation of the first stars which reionized baryonic gas in the universe.

¹¹ Due to the precision of the measurement of T_{CMB} , this parameter is sometimes taken as a constant when estimating other parameters from data.

We work with the values given in [16] based on observations of the CMB with the *Planck* satellite and measurements of the Baryonic Acoustic Oscillations (BAO).¹² Combinations with other data sets would improve the precision of some parameters. However, persistent tensions predominantly in, but not limited to, the cosmic expansion rate complicate such combinations.

As for any model, there are many choices of parameterizing the Λ CDM-model. The parameters given above are particularly suited to observations of the CMB anisotropy power spectrum such as the one in [16]. Other frequently encountered parameters like the present day expansion rate H_0 or the cluster number density σ_8 can be derived from them.

In this section, we collect the necessary ingredients for the two applications of Kinetic Field Theory (KFT) in the field of cosmology presented in this chapter. Firstly, we introduce the dynamics of point particles on an expanding background in subsection 4.1.1. Important properties of cosmic neutrinos relevant for section 4.3 are summarized in subsection 4.1.2.

In the final subsection, we provide some background on the CMB. In part, this is to give slightly more context to one of the most important sources of observational data for the Λ CDM-model. However, our main motivation is related to the initial conditions for our application to cosmic structure formation in section 4.2. These are set at the time of CMB release and their statistics are directly related to the CMB anisotropy power spectra.

Subsection 4.1.1 is based on Appendix A of [1] which was originally written by Shayan Hemmatyar. Subsection 4.1.2 takes inspiration from the introduction of [2] written by Isabel M. Oldengott. Further details on the Λ CDM-model can be found in any recent book on cosmology.

4.1.1 FLRW Metric

The Λ CDM-model is based on Einstein's theory of general relativity. The spatially homogeneous and isotropic solution to its field equations is known as the Friedmann-Lemaître-Robertson-Walker metric (FLRW metric). Imposing spatial flatness, it depends on a single function of cosmic time: the scale factor $a(t)$. This quantity encodes the expansion of spatial hypersurfaces over time. We adopt the convention $a(t_{\text{today}}) = 1$.

The scale factor is directly related to the redshifting of photons which were emitted at a time t and are observed today

$$z(t) = \frac{1}{a(t)} - 1. \quad (349)$$

Since nearly all of our observations in cosmology are based on such photons, this is a very important quantity especially when considering observational data. In calculations, the monotonically decreasing dependence on cosmic time t leads to some unnatural minus signs as we see below.

The evolution of scale factor and redshift with cosmic time is determined by Friedmann's equations. They follow from Einstein's field equations under the

¹² Specifically, we take the values and uncertainties from the last column of Table 2 of [16].

aforementioned assumptions of spatial homogeneity and isotropy which not only yield the simple FLRW metric, but also force the energy-momentum tensor into the form of a perfect fluid. In the Λ CDM-model this perfect fluid is made up from DE, Dark Matter (DM), baryonic matter and radiation. In this case, the first Friedmann equation can be written as

$$\frac{H(t)^2}{H_0^2} = \Omega_{\Lambda,0} + (\Omega_{DM,0} + \Omega_{BM,0}) a(t)^{-3} + \Omega_{R,0} a(t)^{-4}. \quad (350)$$

The left-hand side of this equation features the *Hubble function* which specifies the expansion rate, while the right-hand side is a sum over the energy content of the universe. The quantities appearing are

$$H(t) = \frac{1}{a(t)} \frac{da}{dt}(t), \quad H_0 = H(t_{\text{today}}) \quad \text{and} \quad \Omega_{\bullet,0} = \frac{8\pi G \rho_{\bullet}}{3H_0^2}, \quad (351)$$

for $\bullet = \Lambda, DM, BM, R$ for DE (in form of Λ), DM, baryonic matter and radiation (including relativistic matter), respectively.

Inserting the parameters of the Λ CDM-model, equation (350) allows us to determine the Hubble function. From it we obtain the scale factor as a function of cosmic time which can be inserted into the FLRW metric. This fully specifies the spacetime manifold M which we consider as fixed for both applications provided in this chapter.

In both these applications, we consider the evolution of a set of N point-particles on this background manifold subject to gravitational interactions. In the context of General Relativity, this would require a dynamical metric. However, it is a common approximation in the field of cosmic structure formation to describe the interactions of such systems via Newtonian gravity on the expanding background manifold M . [21]

Adopting this approximation, the configuration space of our N -particle systems is $\mathbf{M} = M^N$, the N -fold product manifold of identical components M . We choose a global chart (\mathbf{U}, ψ) given by *comoving coordinates*. These are defined for each factor M of \mathbf{M} via $U = M$ and $\psi: M \rightarrow \mathbb{R}^{1,3}$ with

$$\left(t, x_1^{(q)}, x_2^{(q)}, x_3^{(q)} \right) = \psi(\mu) := \left(\mu_0, \frac{\mu_1}{a(t)}, \frac{\mu_2}{a(t)}, \frac{\mu_3}{a(t)} \right) \quad (352)$$

for $\mu \in M$. Following the definitions and constructions of section 2.1, we obtain a rigorously defined phase space $\mathbf{X} \cong \mathbf{T}^*\mathbf{M}$ for our system. Note that as described there, the time coordinate plays a special role and its simultaneous use as a time parameter allows a description in $6N$ -dimensions.

Using this description, the Hamiltonian of a system of N point-particles with rest masses m_0 subject to a gravitational potential is

$$\mathcal{H}(\boldsymbol{\varphi}(t), t) = \frac{1}{2m_0 a(t)^2} \boldsymbol{\varphi}^{(p)}(t) \cdot \boldsymbol{\varphi}^{(p)}(t) + \sum_{j=1}^N m_0 V\left(\varphi_j^{(q)}(t), t; \boldsymbol{\varphi}(t)\right). \quad (353)$$

Note that we allow for dependence of the potential on the state of the system $\boldsymbol{\varphi}(t)$ as it may be sourced by the point-particles themselves. The potential satisfies the comoving Poisson equation

$$\nabla^2 V(q, t; \boldsymbol{\varphi}(t)) = 4\pi G a(t)^2 \rho^{(q)}(q, t; \boldsymbol{\varphi}(t)), \quad (354)$$

where the spatial density $\rho^{(q)}$ again might be sourced by the system itself or can be external.

In our applications in the following sections, we use scale factor a and redshift z as our time parameters, respectively. This induces a change in the conjugate momentum and introduces a Jacobi determinant into the Lagrangian due to the requirement of invariance of the action. Due to both of these effects, the Hamiltonian changes its form slightly. A simple calculation yields

$$\mathcal{H}(\boldsymbol{\varphi}(a), a) = \frac{\boldsymbol{\varphi}^{(p)}(a) \cdot \boldsymbol{\varphi}^{(p)}(a)}{2m_0 a^3 H(a)} + \sum_{j=1}^N \frac{m_0 V(\varphi_j^{(q)}(a), a; \boldsymbol{\varphi}(a))}{a H(a)} \quad \text{and} \quad (355)$$

$$\mathcal{H}(\boldsymbol{\varphi}(z), z) = -\frac{(1+z) \boldsymbol{\varphi}^{(p)}(z) \cdot \boldsymbol{\varphi}^{(p)}(z)}{2m_0 H(z)} - \sum_{j=1}^N \frac{m_0 V(\varphi_j^{(q)}(z), z; \boldsymbol{\varphi}(z))}{(1+z) H(z)}, \quad (356)$$

respectively. We emphasized that despite the use of the same symbol, the conjugate momenta $\boldsymbol{\varphi}^{(p)}$ are not the same in the two cases.

In both cases, we have a time dependent factor in the kinetic term. This was anticipated in equation (305) and the setup considered there is recovered by setting

$$m(a) = 2m_0 a^3 H(a) \quad \text{and} \quad m(z) = -\frac{m_0 H(z)}{(1+z)}, \quad (357)$$

respectively. These can be regarded as effective masses for the particles and absorb the effect of the spatial expansion. Using these definitions, the equations and constructions from section 3.3 are directly applicable.

4.1.2 Cosmic Neutrino Background

According to the Λ CDM-model, the universe had been in thermodynamic equilibrium during the first second of its existence. In part, this is due to the high density and very low mean free paths, but as long as matter is relativistic its energy density decreases as a^{-4} like radiation anyway. Only once the non-zero rest mass of the particles is comparable to their kinetic energy, interactions are needed to keep thermodynamic equilibrium. Electrons, protons and photons are tightly coupled by electromagnetic interaction.

In contrast, neutrinos and neutrons are only coupled to the radiation bath via the weak force. As long as the weak reaction rate Γ_w can keep up with the expansion rate H , the neutrinos and neutrons stay in thermodynamic equilibrium. However, once the condition

$$G_F^2 T^5 \propto \Gamma_w \lesssim H \propto G^{\frac{1}{2}} T^2 \quad (358)$$

is reached, where G_F and G are the Fermi and the gravitational constant, respectively, the neutrons and neutrinos freeze out. This happens at a temperature T corresponding to roughly 1 MeV.[48]

While the neutrons either decay or combine with protons to form (mostly) Helium, the neutrinos form the Cosmic Neutrino Background (CvB). Due to

their very small interaction cross-section, these neutrinos propagate through the universe almost entirely unaffected by major events in cosmic history like Big Bang Nucleosynthesis (BBN), the release of the CMB and reionization. Aside from potential gravitational wave measurements, the CνB is the earliest direct probe of the universe's history.

While in equilibrium, the neutrinos in the CνB have a relativistic Fermi-Dirac distribution. Because the temperature has the same dependence on redshift as the comoving momentum, this distribution is retained during cosmic evolution. Only once the neutrinos become sufficiently affected by gravitational interactions, this distribution may be altered. This happens once the mean velocity of cosmic neutrinos becomes comparable to the escape velocity of galaxies. Therefore, for any redshift prior to this, the CνB is spatially homogeneous and its momentum distribution is

$$P_{\text{FD}}(x_j^{(p)}) = \frac{1}{(2\pi\hbar)^3} \left(\exp\left(\frac{c\|x_j^{(p)}\|}{k_B T_0}\right) + 1 \right)^{-1}, \quad (359)$$

where T_0 is the temperature of the CνB today. The integral over the distribution yields the mean neutrino number density.[49]

The existence of the CνB has been confirmed indirectly via measurements of light element abundances in BBN.[48, 50] Moreover, the measurement of the number of effective relativistic degrees of freedom N_{eff} through CMB observations provides additional confirmation.[16] However, a direct detection has not been achieved and the current best observational constraint is an upper bound on the CνB number density 11 orders of magnitude higher than the predicted value.[51] Future experiments have been proposed, but it will be challenging to reduce the bound by the required amount.[52, 53]

While detection of neutrinos generally is challenging, the very low temperature of the CνB provides an additional difficulty. Indeed, the temperature of the CνB is even lower than the one of the CMB. This is because the neutrino freeze-out happens prior to the annihilation of electron-positron-pairs.[48] Hence, this process injects energy into the photon field, but not the CνB.

Specifically, the relative energy density between photons and neutrinos is approximately altered from

$$\Omega_\nu = 3 \cdot \frac{7}{8} \cdot \Omega_\gamma \quad \text{to} \quad \Omega_\nu = 3 \cdot \frac{7}{8} \cdot \left(\frac{4}{11}\right)^{\frac{4}{3}} \cdot \Omega_\gamma. \quad (360)$$

The factors in these expressions might seem somewhat arbitrary, but actually they can be understood quite easily. The number 3 corresponds to the three neutrino species.¹³ Secondly, neutrinos are fermions which leads to a factor of $\frac{7}{8}$ when comparing energy densities in thermal equilibrium in the relativistic limit. Finally, there is the factor of $\frac{4}{11}$ to the power $\frac{4}{3}$. It arises from a constant-entropy argument for the electron-positron annihilation which explains the exponent upon recalling that entropy scales as $\propto T^3$. Moreover, the factor of $\frac{11}{4} = 1 + \frac{7}{8} + \frac{7}{8}$ encodes the change from having photons, electrons and positrons to only photons.[48]

¹³ More precisely, the effective number of relativistic N_{eff} should be used here.

As a consequence, the expected temperature of the C ν B today is

$$T_0 = \left(\frac{4}{11}\right)^{\frac{1}{3}} T_{\text{CMB}} \approx 1.95 \text{ K}. \quad (361)$$

While this low energy makes the detection of individual neutrinos in the C ν B very difficult, it also allows for an interesting effect affecting its detection: neutrino clustering. It has been experimentally observed that neutrinos have a non-zero rest mass.[54, 55] Hence, the cosmic neutrinos making up the C ν B become non-relativistic at some point in cosmic history due to redshifting and can potentially be captured in gravitational potentials caused by galaxies.

Neutrino clustering leads to an increase of the local cosmic neutrino density relative to the cosmological average. The larger the neutrino masses, the earlier clustering starts and the higher is the local cosmic neutrino density in the Milky Way. For very large overdensities, direct detection of the C ν B could be facilitated, though its information content about the early universe might be more complicated to access.

Experimental and observational constraints rule out neutrino masses above 1 eV.[56, 57] Hence, the clustering of cosmic neutrinos starts at redshifts $z < 3$ as can be shown by comparing their average velocity to typical escape velocities of galaxies.[49] As a consequence, late time clustering of cosmic neutrinos increases the local C ν B density by less than an order of magnitude.[49, 58] Moreover, the Fermi-Dirac distribution given in equation (359) is valid at redshifts $z \geq 3$.

4.1.3 Cosmic Microwave Background

Around redshift $z \approx 1600$, free protons and electrons begin to combine into hydrogen. The free electron fraction $\chi_e = \frac{n_e}{n_H}$ defined via the number density of free electrons n_e relative to the one of hydrogen nuclei n_H drops sharply due to this process.[59] The scattering rate of photons is strongly dependent on the free electron fraction and hence their mean free path becomes larger as more electrons are captured into hydrogen atoms. Once the mean free path is comparable to the size of the horizon scale, the photons effectively stream freely—the universe becomes transparent.

This transition of course does not happen instantly, and in fact the photons we observe today as the CMB radiation originate from a range of redshifts. The often invoked surface of last scattering is not actually a surface, but rather a spherical shell. The redshift range from which CMB photons originate peaks at $z \approx 1090$.[16] Given that the radiation and the baryonic matter had been in thermal equilibrium prior to CMB release, the photons exhibit a thermal distribution.[46]

Prior to decoupling, electromagnetic interactions between photons and baryons supplied a pressure component counteracting gravitational collapse. However, not partaking in these interactions, initial over-densities of CDM already started to grow. As such, the photon-baryon-plasma found itself in

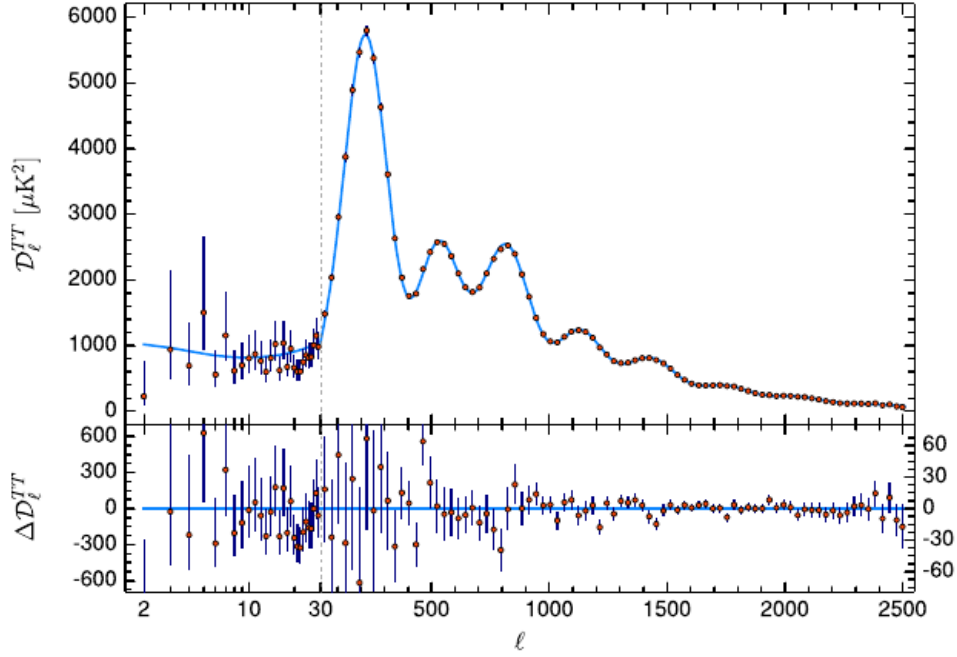


Figure 2: Temperature anisotropy power spectrum $\mathcal{D}_\ell^{\text{TT}} = \frac{1}{2\pi} \ell(\ell+1) \mathcal{C}_\ell^{\text{TT}}$ as measured by the Planck satellite, where $\mathcal{C}_\ell^{\text{TT}}(\ell)$ is the angular power spectrum. The blue line is the prediction from the best-fit Λ CDM-model. Figure 1 of [16].

a (slightly) inhomogeneous gravitational potential. Under these conditions, so-called BAO were sourced.[60]

These oscillations dominate the (slight) anisotropy of the CMB as shown in figure 2. Note that the temperature fluctuations are of the order of $1 : 10^5$. This corresponds to the scale of density fluctuations at the time of the release of the CMB. In fact, these fluctuations are so small that they are dominated by the Doppler shift of the CMB monopole which therefore has been subtracted from the data in figure 2.

The Doppler shift is due to the motion of Earth relative to the CMB rest frame. This frame corresponds to an observer comoving with the cosmic density field. It is for such observers that the universe described by a FLRW metric appears homogeneous and isotropic. In fact, their proper time defines a cosmological time coordinate we have been referring to throughout this section. For observers moving relative to them, the universe is not isotropic due to the Doppler effect.

As such, any observer traveling along some rocky planet around a G-type star in the outskirts of an ordinary spiral galaxy is expected to observe a Doppler shift of the CMB monopole in the direction of her velocity relative to the CMB rest frame. Coincidentally, our observations reveal a dipolar anisotropy in the CMB. This CMB dipole is most naturally explained as the Doppler shift of the CMB monopole.

Following this interpretation, our Solar System is moving with a velocity of $v = (369.82 \pm 0.11) \text{ km s}^{-1}$ relative to the CMB rest frame. It should be noted that the quoted uncertainty does not include the systematic error due to the possible presence of an intrinsic CMB dipole. Judging by the amplitude of

smaller-scale fluctuations, this intrinsic dipole would be expected to be of the order of about 1% of the observed dipole and point in an unknown direction relative to the kinetic (Doppler) dipole.[61]

Returning to figure 2, we recall that the Λ CDM-model supposes that there are small density inhomogeneities on top of the isotropic and homogeneous background. These adiabatic and Gaussian fluctuations are described by a near scale invariant spectrum, specified by the parameters A_s and n_s . The most prominent, but not exclusive, explanation for their origin are quantum fluctuations which were stretched to cosmological scales by a process like inflation.[62]

Regardless of their origin, these fluctuations gave rise to density inhomogeneities which in turn are responsible for temperature fluctuations observed in the CMB. Observations of the CMB confirm the absence of primordial non-Gaussianities.[63] Hence, the density fluctuations at redshift $z_i \approx 1090$ form a Gaussian random field which is solely described by its power spectrum P_δ .

The measurement of the angular power spectrum of temperature fluctuations of the CMB $C_\ell^{\text{T T}}(\ell)$ shown in figure 2 can be translated into the matter fluctuation power spectrum $P_\delta(k, z_i)$ at the redshift of CMB release. As shown in Appendix B of [1], this in turn yields the power spectrum of the velocity potential $P_\psi(k)$ at this redshift. Indeed, the comoving Poisson equation (354) implies the relationship

$$\kappa^2 k^4 P_\psi(k) = P_\delta(k, z_i) \quad (362)$$

for a certain constant κ defined in equation (B9) of [1].

As a final aspect in this subsection, we want to show in which way the temperature anisotropy spectrum constrains the parameters of the Λ CDM-model. As mentioned above, the temperature of the CMB T_{CMB} is measured through the frequency spectrum of the CMB monopole. All other parameters can be inferred through their effect on the temperature anisotropy power spectrum, as shown in table 1.

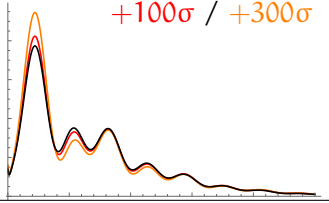
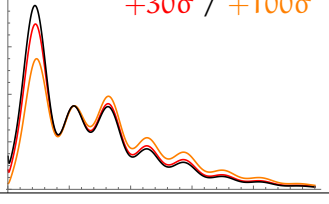
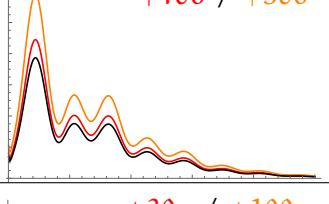
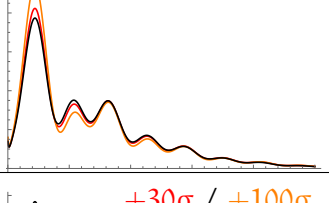
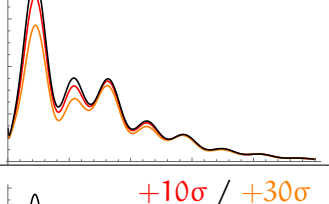
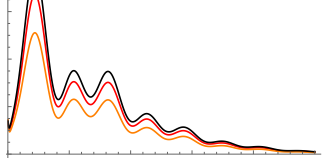
Parameter	Interpretation	Effect on $\mathcal{D}_\ell^{\text{TT}} (\ell \leq 2500)$
$100\theta_*$	Size of the sound horizon at recombination. Controls the position of the acoustic peaks, with an increase shifting their positions towards the left.	 $+100\sigma / +300\sigma$
n_s	Slope of the primordial fluctuations. Determines the tilt in the power spectrum with an increase lowering the first acoustic peak and boosting the high- ℓ tail.	 $+30\sigma / +100\sigma$
$\ln(10^{10}A_s)$	Amplitude of the primordial fluctuations. Directly proportional to the amplitude of the CMB anisotropy power spectrum.	 $+10\sigma / +30\sigma$
$h^2 \Omega_{\text{BM}}$	Baryonic matter density. Affects the odd-even modulation of the acoustic peaks, with an increase exaggerating the modulation.	 $+30\sigma / +100\sigma$
$h^2 \Omega_{\text{CM}}$	DM density. Its increase reduces the relative abundance of baryons and thus decreases the acoustic peaks.	 $+30\sigma / +100\sigma$
τ	Optical depth. Affects the amplitude of the CMB anisotropy power spectrum and thus is degenerate with A_s .	 $+10\sigma / +30\sigma$

Table 1: Overview of the effects of changing the Λ CDM-model parameters on the temperature anisotropy power spectrum. The black curve corresponds to the parameters given in the introductory section and the red and orange ones are obtained by increasing the respective parameter by multiples of their uncertainty. Plots created using CLASS.[64]

4.2 LARGE-SCALE STRUCTURE

In this section, we apply the formalism developed in the previous chapters to cosmic structure formation, i.e., the study of the formation of the large-scale structure in the universe. This has been the main application of KFT in the literature.[23, 32]

The main difficulty in this application are the initial conditions. We describe in detail how the sampling of particle positions and momenta from an initial density and velocity field yields initial conditions for the system which are correlated. This means that the probability distribution $P(\mathbf{x})$ cannot be factorized into probability distributions for the individual components. Moreover, the functional form of $P(\mathbf{x})$ is quite complicated.

To facilitate computations, we perform an expansion in the initial particle correlations in subsection 4.2.2. By means of a series expansion of a Gaussian exponential factor, we obtain expressions in which Fourier phase factors coming from the initial correlations can be combined with those coming from our Feynman rules. This allows an averaging of expressions of diagrams contributing to r -point density correlation functions.

The averaged diagrams can themselves be expressed via Feynman rules as we show in subsection 4.2.3. The newly constructed diagrams add correlation vertices and correlation edges to the diagrams contributing to the observable. It is shown that the mathematical expressions corresponding to these diagrams factorize into a scale factor and a wave-vector dependent part which can be constructed and evaluated independently. This reduces the computational complexity of the numerical evaluation of remaining integrals significantly.

Finally, we reproduce the main result of [1] that the linear growth of the cosmic density-fluctuation power spectrum is obtained from the contributions which are linear in the initial correlations. We also given an outlook to ongoing work in evaluating the contributions quadratic in the initial correlations.

This section is based on work presented in [1] as well as further investigations based on it in a joint effort with Shayan Hemmatyar. The method of expanding in the initial correlations was already applied in [23].

4.2.1 Correlated Initial Conditions

In order to describe the formation of structure in the universe with KFT, we consider the matter as a collection of interacting point-particles on an expanding spacetime. This is in analogy to the treatment in numerical N -body simulations, where these point-particles often have masses comparable to the ones of galaxies or even larger, gravitationally bound objects.[14] In our analytic treatment, we leave the particle rest mass m_0 arbitrary for the moment. It may correspond likewise to galaxy-scale objects, but can also take the value of ultra-light DM particles.

As described in subsection 4.1.3, through observations of the CMB we have a precise statistical characterization of the cosmic density field at a redshift of $z_i = 1090$. We take this as the initial time of our N -body system and thus

ought to set its initial conditions \mathbf{x} at this instance. We remark that numerical simulations usually use some form of hydrodynamic approximation to evolve the cosmic density field to redshifts of up to $z \approx 10$ (where the hydrodynamic approximation starts to break down on relevant scales) and set their initial conditions there.[65]

Unlike numerical simulations, we do not take a single sample of N point-particles from the cosmic density field and evolve it. Instead, we construct expectation values of observables based on a probability distribution of initial values. Conceptually, this corresponds to running an N -body simulation infinitely often for different samplings and averaging over them. Given that this is impossible in practice, one can instead do a smoothing as described in subsection 2.4.1 and study the statistics of the resulting density field. Modern N -body simulations use much more sophisticated methods of course.[14]

One main difficulty with the sampling of the cosmic density field is that we only know its statistics, but not its actual behavior. While conceptually this is fine, given that we are likewise only interested in the statistics of the present day cosmic density, it makes the description of the sampling somewhat more complicated. Effectively, we have taken a sample density $\rho^{(q)}$ from a probability distribution of initial cosmic density fields, as given through our knowledge of their statistical behavior.

For each such sample, we then take a sample of N point-particles and average over both sampling processes to obtain expectation values of observables. Written as an equation, the probability distribution of initial values \mathbf{x} is thus of the form

$$P(\mathbf{x}) = \int d\rho^{(q)} \left(\prod_{j=1}^N P(\mathbf{x}_j^{(q)} | \rho^{(q)}) P(\mathbf{x}_j^{(p)} | \rho^{(q)}) \right) P(\rho^{(q)}) . \quad (363)$$

Note that given the infinite dimensionality of $\rho^{(q)}$, the integral over it is to be treated with caution. Fortunately, we are able to replace it by a finite-dimensional integral below.

Two conditional probability distributions appear in equation (363). The first of them is simple, because sampling N point-particles from a density field can be done via the condition

$$P(\mathbf{x}_j^{(q)} | \rho^{(q)}) = \frac{1}{N} \rho^{(q)}(\mathbf{x}_j^{(q)}) \quad (364)$$

for each particle j . However, the conditional probability distribution of the momenta $P(\mathbf{x}_j^{(p)} | \rho^{(q)})$ requires additional discussion, because knowledge of the spatial density seems insufficient to assign momenta to the particles.

Once more we compare to the procedure of obtaining initial values in numerical simulations of cosmic structure formation. As mentioned above, there a hydrodynamic approximation is used to obtain the cosmic density field at some “initial” redshift. However, this hydrodynamic treatment provides not only the spatial density field, but also a velocity field. In fact, it is arguably the assumption of the existence of a well-defined velocity field which is the Achilles’ heel of the hydrodynamic approximation—shell crossing occurring in gravitational collapse violates this assumption.

Nonetheless, at sufficiently early times and large enough scales, the existence of a well-defined velocity field can be assumed. In order to be able to assign initial momenta to our sample of N point-particles, we make this assumption *at initial redshift z_i only*. Note that this is more conservative than the treatment for conventional N -body simulations which assume the existence of a velocity field until lower redshifts, where initial conditions are sampled.

As described in subsection 4.1.3, the density and velocity fields can be obtained from the velocity potential ψ . This allows us to rewrite equation (363) as

$$P(\mathbf{x}) = \int d\psi \left(\prod_{j=1}^N P(\mathbf{x}_j^{(q)} | \psi) P(\mathbf{x}_j^{(p)} | \psi) \right) P(\psi) \quad \text{with} \quad (365)$$

$$P(\mathbf{x}_j^{(q)} | \psi) = \frac{\bar{\rho}^{(q)}}{N} \left(1 - \kappa \nabla^2 \psi(\mathbf{x}_j^{(q)}) \right) \quad \text{and} \quad (366)$$

$$P(\mathbf{x}_j^{(p)} | \psi) = \delta_D \left(\mathbf{x}_j^{(p)} - m(a_i) \nabla \psi(\mathbf{x}_j^{(q)}) \right). \quad (367)$$

The effective mass $m(a)$ has been defined in subsection 4.1.1 and accounts for cosmic expansion. Here, it is evaluated at initial scale factor $a_i = (1 + z_i)^{-1}$. The constant κ is introduced in equation (362).

The conditional probabilities given in equations (366) and (367) depend on the velocity potential ψ only via the values of its gradient and Laplacian at the positions $\mathbf{x}^{(q)}$. Let us collect these in the vectors

$$\nabla^2 \psi := \left(\nabla^2 \psi(\mathbf{x}_1^{(q)}), \nabla^2 \psi(\mathbf{x}_2^{(q)}), \dots, \nabla^2 \psi(\mathbf{x}_N^{(q)}) \right) \quad \text{and} \quad (368)$$

$$\nabla \psi := \left(\nabla \psi(\mathbf{x}_1^{(q)}), \nabla \psi(\mathbf{x}_2^{(q)}), \dots, \nabla \psi(\mathbf{x}_N^{(q)}) \right). \quad (369)$$

This allows us to rewrite equation (365) as

$$P(\mathbf{x}) = \int d\nabla^2 \psi \int d\nabla \psi \left(\prod_{j=1}^N P(\mathbf{x}_j^{(q)} | \nabla^2 \psi) P(\mathbf{x}_j^{(p)} | \nabla \psi) \right) P(\nabla^2 \psi, \nabla \psi), \quad (370)$$

featuring the joint probability $P(\nabla^2 \psi, \nabla \psi)$.

As discussed in subsection 4.1.3, the velocity potential at redshift z_i is well-described as a Gaussian random field. As such, it is characterized solely by its power spectrum $P_\psi(k)$. Specifically, its values at points $\mathbf{x}^{(q)}$

$$\psi := \left(\psi(\mathbf{x}_1^{(q)}), \psi(\mathbf{x}_2^{(q)}), \dots, \psi(\mathbf{x}_N^{(q)}) \right) \quad (371)$$

form a multivariate Gaussian distribution given by

$$P(\boldsymbol{\psi}) = \frac{\exp \left(-\frac{1}{2} \boldsymbol{\psi}^T (\mathbf{C}\boldsymbol{\psi})^{-1} (\mathbf{x}^{(q)}) \boldsymbol{\psi} \right)}{\sqrt{(2\pi)^N \det(\mathbf{C}\boldsymbol{\psi}(\mathbf{x}^{(q)}))}} \quad \text{with} \quad (372)$$

$$C_{j\ell}^{\boldsymbol{\psi}}(\mathbf{x}^{(q)}) = \int \frac{dk''}{(2\pi)^3} P_\psi(k'') \exp \left(-ik'' \cdot (\mathbf{x}_j^{(q)} - \mathbf{x}_\ell^{(q)}) \right). \quad (373)$$

A simple calculation reveals that

$$\left\langle \boldsymbol{\psi}(\mathbf{x}_j^{(q)}) \boldsymbol{\psi}(\mathbf{x}_\ell^{(q)}) \right\rangle = \int d\boldsymbol{\psi} P(\boldsymbol{\psi}) \boldsymbol{\psi}(\mathbf{x}_j^{(q)}) \boldsymbol{\psi}(\mathbf{x}_\ell^{(q)}) = C_{j\ell}^{\boldsymbol{\psi}}(\mathbf{x}^{(q)}). \quad (374)$$

This expression can be used to obtain the two-point correlations of $\nabla^2\psi$ and $\nabla\psi$. As a result we obtain an expression for the joint probability distribution

$$P(\nabla\psi, \nabla^2\psi) = \frac{\exp\left(-\frac{1}{2} \begin{pmatrix} \nabla^2\psi \\ \nabla\psi \end{pmatrix}^T \mathbf{C}^{-1}(\mathbf{x}^{(q)}) \begin{pmatrix} \nabla^2\psi \\ \nabla\psi \end{pmatrix}\right)}{\sqrt{(2\pi)^{4N} \det(\mathbf{C}(\mathbf{x}^{(q)}))}} \quad \text{with} \quad (375)$$

$$\mathbf{C}_{j\ell}(\mathbf{x}^{(q)}) = \begin{pmatrix} \mathbf{C}_{j\ell}^{\delta\delta}(\mathbf{x}^{(q)}) & \mathbf{C}_{j\ell}^{\delta p}(\mathbf{x}^{(q)}) \\ -(\mathbf{C}_{j\ell}^{\delta p})^T(\mathbf{x}^{(q)}) & \mathbf{C}_{j\ell}^{pp}(\mathbf{x}^{(q)}) \end{pmatrix} \quad (376)$$

$$= \int \frac{d\mathbf{k}''}{(2\pi)^3} \begin{pmatrix} \|\mathbf{k}''\|^4 & -i\mathbf{k}''^T \|\mathbf{k}''\|^2 \\ i\mathbf{k}'' \|\mathbf{k}''\|^2 & \mathbf{k}''\mathbf{k}''^T \end{pmatrix} P_\psi(\mathbf{k}'') \exp\left(-i\mathbf{k}'' \cdot (\mathbf{x}_j^{(q)} - \mathbf{x}_\ell^{(q)})\right). \quad (377)$$

Inserting it and the conditional probability distributions given in equations (366) and (367) into equation (370) yields an expression which can be immediately simplified significantly. Indeed, the Dirac δ -function in equation (367) replaces $\nabla\psi$ by $\frac{1}{m(\mathbf{a}_i)}\mathbf{x}^{(p)}$ by canceling the associated integral. This results in

$$P(\mathbf{x}) = \int d\nabla^2\psi \frac{1}{(m(\mathbf{a}_i))^{3N}} \left(\prod_{j=1}^N \frac{\bar{\rho}^{(q)}}{N} \left(1 - \kappa \nabla^2\psi(\mathbf{x}_j^{(q)})\right) \right) \frac{\exp\left(-\frac{1}{2(m(\mathbf{a}_i))^2} \begin{pmatrix} m(\mathbf{a}_i) \nabla^2\psi \\ \mathbf{x}^{(p)} \end{pmatrix}^T \mathbf{C}^{-1}(\mathbf{x}^{(q)}) \begin{pmatrix} m(\mathbf{a}_i) \nabla^2\psi \\ \mathbf{x}^{(p)} \end{pmatrix}\right)}{\sqrt{(2\pi)^{4N} \det(\mathbf{C}(\mathbf{x}^{(q)}))}} \quad (378)$$

$$= \int d\Delta \left(\prod_{j=1}^N \frac{\bar{\rho}^{(q)}}{N} \left(1 - \frac{\kappa}{m(\mathbf{a}_i)} \Delta_j\right) \right) \frac{\exp\left(-\frac{1}{2(m(\mathbf{a}_i))^2} \begin{pmatrix} \Delta \\ \mathbf{x}^{(p)} \end{pmatrix}^T \mathbf{C}^{-1}(\mathbf{x}^{(q)}) \begin{pmatrix} \Delta \\ \mathbf{x}^{(p)} \end{pmatrix}\right)}{\sqrt{(2\pi)^{4N} (m(\mathbf{a}_i))^{8N} \det(\mathbf{C}(\mathbf{x}^{(q)}))}}, \quad (379)$$

where in the second equality we defined $\Delta := m(\mathbf{a}_i)\nabla^2\psi$ for compactness.

4.2.2 Series Expansion of Correlations

Averaging observables over the probability distribution given in equation (379) is a difficult task. The main problem is the non-trivial dependence of the correlation matrix \mathbf{C} on the initial particle positions $\mathbf{x}^{(q)}$. However, using the specialization of microscopic perturbation theory to N-body systems performed in section 3.3, it is actually possible to make some progress. Recall, that this comes with a restriction to systems which interact via a position-dependent pairwise interaction potential v and to the use of Fourier space density correlation functions as observables.

Under these conditions, we have shown that in any order n of the series expansions in the interactions, the diagrams contributing to the r -point density correlation function depend on the initial conditions \mathbf{x} only through a factor of the form $\exp(i\mathbf{f} \cdot \mathbf{x})$, as shown in equation (348). The scalar product $\mathbf{f} \cdot \mathbf{x}$ has contributions from only $r + n$ terms, corresponding to the indices associated to the density nodes in the diagrams.

In order to obtain the expectation values of r -point density correlation functions, we need to average the expressions encoded by the diagrams contributing to it over $P(\mathbf{x})$. The preceding discussion implies that the result can be inferred from averaging over the factor $\exp(i\mathbf{f} \cdot \mathbf{x})$. This yields the so-called characteristic function of the probability distribution P , given by

$$\Phi(\mathbf{f}) = \int d\mathbf{x} P(\mathbf{x}) \exp(i\mathbf{f} \cdot \mathbf{x}) \quad (380)$$

$$= \int d\mathbf{x} \int d\Delta \left(\prod_{j=1}^N \frac{\bar{\rho}^{(q)}}{N} \left(1 + \frac{\kappa}{m(a_i)} \frac{\partial}{\partial \xi_j} \right) \right) \exp(i(\mathbf{i}\xi) \cdot \Delta) \Big|_{\xi=0} \\ \frac{\exp\left(-\frac{1}{2(m(a_i))^2} \begin{pmatrix} \Delta \\ \mathbf{x}^{(p)} \end{pmatrix}^T \mathbf{C}^{-1}(\mathbf{x}^{(q)}) \begin{pmatrix} \Delta \\ \mathbf{x}^{(p)} \end{pmatrix}\right)}{\sqrt{(2\pi)^{4N} (m(a_i))^{8N} \det(\mathbf{C}(\mathbf{x}^{(q)}))}} \exp(i\mathbf{f} \cdot \mathbf{x}) \quad (381)$$

$$= \int d\mathbf{x}^{(q)} \exp(i\mathbf{f}^{(q)} \cdot \mathbf{x}^{(q)}) \left(\prod_{j=1}^N \frac{\bar{\rho}^{(q)}}{N} \left(1 + \frac{\kappa}{m(a_i)} \frac{\partial}{\partial \xi_j} \right) \right) \\ \exp\left(-\frac{(m(a_i))^2}{2} \begin{pmatrix} \mathbf{i}\xi \\ \mathbf{f}^{(p)} \end{pmatrix}^T \mathbf{C}(\mathbf{x}^{(q)}) \begin{pmatrix} \mathbf{i}\xi \\ \mathbf{f}^{(p)} \end{pmatrix}\right) \Big|_{\xi=0}. \quad (382)$$

The introduction of the auxiliary variable ξ allowed us to perform the $4N$ -dimensional Fourier transform of the Gaussian.

While the evaluation of the integrations over Δ and $\mathbf{x}^{(p)}$ are significant progress, the remaining expression remains very complicated. Even ignoring that the actual expressions coming from diagrams contain additional factors and integrals, the remaining integral over $\mathbf{x}^{(q)}$ is on its own a major challenge. While it is possible to make some further progress in simplifying it, a simpler approach is to perform a series expansion in the correlation matrix \mathbf{C} .

Specifically, we perform a series expansion of the Gaussian exponential. Our aim is to work consistently in powers of the power spectrum $P_\psi(k)$, which can be expressed in terms of the matter fluctuation power spectrum $P_\delta(k, a_i)$ at initial scale factor via equation (362). The main motivation for this is that the components of the correlation matrix \mathbf{C} depend on $\mathbf{x}^{(q)}$ via Fourier phase factors. Upon a series expansion, these can be combined with the factor $\exp(i\mathbf{f}^{(q)} \cdot \mathbf{x}^{(q)})$ and the integral over $\mathbf{x}^{(q)}$ yields Dirac δ -functions which subsequently remove some of the integrals over wave-numbers.

In preparation for the series expansion, let us consider the argument of the Gaussian exponential factor in more detail. It is

$$\begin{aligned} & \begin{pmatrix} i\xi \\ \mathbf{f}^{(p)} \end{pmatrix}^T \mathbf{C}(\mathbf{x}^{(q)}) \begin{pmatrix} i\xi \\ \mathbf{f}^{(p)} \end{pmatrix} \\ &= - \sum_{j,j'=1}^N \int \frac{d\mathbf{k}''}{(2\pi)^3} P_\Psi(\mathbf{k}'') \exp\left(-i\mathbf{k}'' \cdot (\mathbf{x}_j^{(q)} - \mathbf{x}_{j'}^{(q)})\right) \\ & \quad \left(\|\mathbf{k}''\|^2 \xi_j + \mathbf{k}'' \cdot \mathbf{f}_j^{(p)} \right) \left(\|\mathbf{k}''\|^2 \xi_{j'} + \mathbf{k}'' \cdot \mathbf{f}_{j'}^{(p)} \right). \end{aligned} \quad (383)$$

The factorization in the last line suggests treating the density-density-, density-momentum- and momentum-momentum-correlations encoded in the correlation matrix \mathbf{C} as emergent from a product of two components representing the density and the momentum. We use this in the definition of our correlated Feynman rules in the following subsection. By acting with the products of derivatives

$$\prod_{j=1}^N \frac{\bar{\rho}^{(q)}}{N} \left(1 + \frac{\kappa}{m(\mathbf{a}_i)} \frac{\partial}{\partial \xi_j} \right) \quad (384)$$

onto this term and setting $\xi = 0$ afterwards, we obtain

$$\begin{aligned} & - \left(\frac{\bar{\rho}^{(q)}}{N} \right)^N \sum_{j,j'=1}^N \int \frac{d\mathbf{k}''}{(2\pi)^3} P_\delta(\mathbf{k}'', \mathbf{a}_i) \exp\left(-i\mathbf{k}'' \cdot (\mathbf{x}_j^{(q)} - \mathbf{x}_{j'}^{(q)})\right) \\ & \quad \left(\frac{1 - \delta_{jj'}}{m(\mathbf{a}_i)} + \frac{1}{\kappa} \frac{\mathbf{k}'' \cdot \mathbf{f}_j^{(p)}}{\|\mathbf{k}''\|^2} \right) \left(\frac{1 - \delta_{jj'}}{m(\mathbf{a}_i)} + \frac{1}{\kappa} \frac{\mathbf{k}'' \cdot \mathbf{f}_{j'}^{(p)}}{\|\mathbf{k}''\|^2} \right), \end{aligned} \quad (385)$$

where Kronecker δ -symbols take into account that derivatives with respect to any index can only be taken once. We also replaced the power spectrum using equation (362).

Recall that $\mathbf{f}_j^{(p)} = 0$, if the index j does not appear in the expression for the diagram which we average over. However, the term associated to the density coming from the factor of ξ_j also vanishes in that case. Indeed, it comes with a lone factor of $\exp(-i\mathbf{k}'' \cdot \mathbf{x}_j^{(q)})$ which yields $\delta_D(\mathbf{k}'')$ upon integration over $\mathbf{x}_j^{(q)}$. Using that $P_\delta(0, \mathbf{a}_i) = 0$, the entire term vanishes. This shows that the sum over j and j' actually only runs over indices corresponding to density nodes in the diagram under consideration. Note that this remains true at higher orders in a series expansion of the exponential, where we obtain a product of sums of this form.

Let us return to the factor $\exp(i\mathbf{f}^{(q)} \cdot \mathbf{x}^{(q)})$ which was a major reason for performing a series expansion. In m^{th} order in a series expansion of the Gaussian exponential, it can be combined with the Fourier phase factors coming from the correlation matrix, yielding

$$\exp\left(i \sum_{j=1}^N \mathbf{f}_j^{(q)} \cdot \mathbf{x}_j^{(q)} - i \sum_{t=1}^m \mathbf{k}_t'' \cdot (\mathbf{x}_{j_t}^{(q)} - \mathbf{x}_{j'_t}^{(q)}) \right), \quad (386)$$

where we gave an index t to the particle indices j, j' and wave-vectors k'' to distinguish the different orders.

This is the only term retaining a dependence on $\mathbf{x}^{(q)}$ such that we can perform the integration over $\mathbf{x}^{(q)}$ and obtain

$$\prod_{j=1}^N (2\pi)^3 \delta_D \left(\mathbf{f}_j^{(q)} + \sum_{t=1}^m \mathbf{k}_t'' (\delta_{jj_t} - \delta_{jj_t}) \right). \quad (387)$$

Of course, only $r + n$ of these Dirac δ -functions—those with particle index j , corresponding to a density node of the diagram under consideration—are non-trivial. The remaining factors are $(2\pi)^3 \delta_D(0)$ and cancel $N - (r + n)$ of the N factors $\frac{\bar{\rho}^{(q)}}{N}$.¹⁴ But there are also $n + r$ sums over particle indices in the diagram, each of which yields a factor N , such that remaining prefactor is $(\bar{\rho}^{(q)})^{r+n}$.

In the following, we assume that all indices ℓ_\bullet corresponding to density nodes in diagrams are different. This effectively removes terms with equal indices from the sum in equation (341) which have any pairwise equal indices. These terms are shot-noise terms as discussed in subsection 2.4.5 in the context of density correlation functions.

The two limits discussed in that subsection are also applicable now. The remaining expressions do not have any dependence on the total particle number N , the volume V or the particle rest mass m_0 , though this becomes more transparent through the Feynman rules we define in the following subsection. As such, both these limits are trivial and leave the expressions completely unchanged. They do, however, justify the removal of the shot noise terms described above as these vanish in the limits.

4.2.3 Correlated Feynman Rules

In the previous subsection, we investigated the averaging of the contribution of a diagram to the density r -point correlation function over correlated initial conditions. Specifically, our initial conditions emerge from sampling the cosmic density field at the time of the release of the CMB. Performing a series expansion in the density-fluctuation power spectrum at the scale factor a_i , the resulting expression takes the form of a product of sums over contributions encoding correlations between particles.

Physically it is clear that only correlations between particles actually present in the diagram can contribute which manifests mathematically in having contributions only for particle indices corresponding to density nodes in the diagram. We can encode these contributions via the various ways of connecting a *correlation vertex* to these black circles. Given the different nature of the contributions from density- and momentum-correlations, it seems advisable to use two different kinds of edges to symbolize them.

However, creating Feynman rules for expectation values also requires changes to the elements of the diagrams which we already defined. Specifically, we have performed the integrations over the initial conditions in our manipulations

¹⁴ This cancellation corresponds to the normalization condition of $P(\mathbf{x}_j^{(q)})$.

in the previous subsection, by which the factor of $\exp(i\mathbf{k} \cdot \mathbf{x})$ —part of the expression of the diagram—got removed. Moreover, we want to make use of the Dirac δ -functions obtained in equation (387) to remove the integrations over wave-vectors.

In order to convert the Feynman rules presented in section 3.3.4 to expectation values, recall that our definitions for vertices and edges were

$$\bullet \boxed{s, a} = \exp\left(-i\mathbf{k}_s \cdot \bar{\varphi}_{\ell_s}^{(q)}(a; \mathbf{x})\right), \quad (388)$$

$$\circ \text{b} = v(k'_b, a'_b) \exp\left(-i\mathbf{k}'_b \cdot \bar{\varphi}_{\ell'_b}^{(q)}(a'_b; \mathbf{x})\right), \quad (389)$$

$$\text{b} \text{---} \boxed{s, a} = -m(a'_b) g(a, a'_b) k'_b \cdot k_s \exp\left(i\mathbf{k}'_b \cdot \bar{\varphi}_{\ell'_b}^{(q)}(a'_b; \mathbf{x})\right), \quad (390)$$

$$\text{b} \text{---} \text{c} = -m(a'_b) g(a'_c, a'_b) k'_b \cdot k'_c \exp\left(i\mathbf{k}'_b \cdot \bar{\varphi}_{\ell'_c}^{(q)}(a'_b; \mathbf{x})\right), \quad (391)$$

$$\text{b} \text{---} \text{c} = m(a'_b) g(a'_c, a'_b) k'_b \cdot k'_c \exp\left(i\mathbf{k}'_b \cdot \bar{\varphi}_{\ell'_c}^{(q)}(a'_b; \mathbf{x})\right), \quad (392)$$

where ℓ_\bullet is the particle index associated to the edge leaving vertex b . We have replaced the time variables by scale factors, in accordance with the discussion of subsection 4.1.1 and changed the labels of the interaction vertices to avoid possible confusion. The n^{th} order contribution to the r -point density correlation function was given by the sum of all diagrams formed from r density and n interaction vertices. The expression for each of these diagrams was given by the product of the above mathematical expressions, integrated over scale factors and wave-vectors and summed over particle indices as described in equation (341).

Evidently, the first step in translating these Feynman rules to expectation values is the removal of the exponential factors containing the free evolution map $\bar{\varphi}$. Secondly, the sums over particle indices are removed. Thirdly, the prefactor $(\bar{\rho}^{(q)})^{r+n}$ can be reproduced by assigning a copy of $\bar{\rho}^{(q)}$ to each density and interaction vertex. We postpone the fourth step of replacing wave-vectors using the Dirac δ -functions from equation (387) and the removal of the corresponding integrals over wave-vectors.

The fifth and most complicated step is the introduction of the correlation vertex and edges encoding the correlations. We define the correlation vertex as

$$\diamond \text{t} = \frac{1}{2} P_\delta(k''_t, a_i) \quad (393)$$

and include overall integrations over k''_t for all $k = 1, 2, \dots, m$ as well as a factor of $\frac{1}{m!}$ coming from the series expansion of the Gaussian exponential. We refer to the number m of correlation vertices as the *correlation order* of the expectation value of the diagram.

Each correlation vertex comes with two edges which connect its upper and lower corners with density nodes of the diagrams. We introduce two types of

edges and refer to them as *density edges* and *momentum edges*, respectively. The density edge is defined via

$$\begin{array}{c} \diamond t \\ \text{---} \end{array} \text{---} \square s, a := 1, \quad (394)$$

$$\begin{array}{c} \diamond t \\ \text{---} \end{array} \text{---} \bigcirc b := 1 \quad (395)$$

and the momentum edge encodes the expression

$$\begin{array}{c} \diamond t \\ \text{---} \end{array} \text{---} \square s, a := \frac{m(a_i)}{\kappa \|k_t''\|^2} k_t'' \cdot f_{\ell_a}^{(p)}, \quad (396)$$

$$\begin{array}{c} \diamond t \\ \text{---} \end{array} \text{---} \bigcirc b := \frac{m(a_i)}{\kappa \|k_t''\|^2} k_t'' \cdot f_{\ell_b}^{(p)}. \quad (397)$$

Like in the other Feynman rules, the transparent vertices mean that the vertex factor is not included here. The expressions for edges beginning at the top of the correlation vertex are the same, though they are associated to the two terms with opposite signs in equation (387) in a sense explained below.

A correlation vertex with two density edges encodes density-density-correlations $C_{\ell_b' \ell_c'}^{\delta\delta}$, where ℓ_b' and ℓ_c' are the particle indices corresponding to the density nodes it connects to. Similarly, density-momentum-correlations $C_{\ell_b' \ell_c'}^{\delta p}$ and $C_{\ell_b' \ell_c'}^{p\delta}$ have one density and one momentum edge and momentum-momentum-correlations $C_{\ell_b' \ell_c'}^{pp}$ have two momentum edges.

Due to the way density correlations appear through a product of derivatives with respect to ξ_j , no two density edges may end at the same vertex. In contrast, momentum correlations—even ones originating from the same correlation vertex—may end at the same vertex. This means, that any density node in the diagram is connected to by up to one density and arbitrarily many momentum edges. As before, edges coming from interaction vertices can also connect to these density nodes.

The two remaining difficulties are the factors $f_j^{(p)}$ in the momentum edges as well as the implementation of the Dirac δ -functions from equation (387). Let us again postpone the discussion of the latter and further study the momentum edges. Their definition is complicated by the dependence on all vertices connected to the density node it connects to. This can be remedied by subdividing these contributions.

Specifically, we change the Feynman rules stated above in favor of

$$\begin{array}{c} \diamond t \\ \text{---} \end{array} \text{---} \square s, a := \frac{m(a_i)}{\kappa \|k_t''\|^2} g(a, a_i) k_t'' \cdot k_s, \quad (398)$$

$$\begin{array}{c} \diamond t \\ \text{---} \end{array} \text{---} \bigcirc b := \frac{m(a_i)}{\kappa \|k_t''\|^2} g(a_b', a_i) k_t'' \cdot k_b', \quad (399)$$

$$\begin{array}{c} \diamond t \\ \text{---} \end{array} \text{---} \bigcirc b := \frac{m(a_i)}{\kappa \|k_t''\|^2} g(a_b', a_i) k_t'' \cdot k_b'. \quad (400)$$

All contributions coming from the third kind combine to yield the factor $f^{(p)}$ present previously. However, avoiding this factor is not even the main achieve-

ment of this change. Provided that the interaction potential factorizes into a product of the form



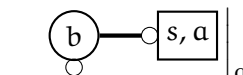

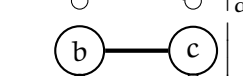
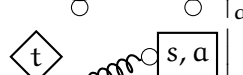


$$v(\mathbf{k}, \mathbf{a}) = v^{(\mathbf{k})}(\mathbf{k}) v^{(\mathbf{a})}(\mathbf{a}), \tag{401}$$

each diagram corresponds to a product of a term depending exclusively on scale factors and a term depending exclusively on wave-vectors.

The factorization of the contributions allows us to perform the integrations over scale factors and wave-vectors separately which reduces the computational complexity significantly. To facilitate the factorization, let us define separate Feynman rules for the two terms. For maximal clarity, we give the complete instructions for the construction of the contribution to the r -point density correlation function in n^{th} interaction and m^{th} correlation order.

Consider all diagrams which can be formed from r density vertices, n interaction vertices and m correlation vertices, such that each interaction vertex has exactly one outgoing edge which can connect to another interaction vertex or to a density node. Together with these edges, the density and interaction vertices form a forest, where each density vertex is a root for one of the trees. Interaction vertices are labeled from 1 to n increasingly towards the root of their trees. In case there are multiple possible labelings, each of them is considered a different diagram. Each correlation vertex has two correlation edges connected to its upper and lower corners. These can either be density or momentum edges. Each density edge connects to a density node, while each momentum edge connects either to a density node or an interacting vertex. No two density edges may be connected to the same density node.

Each individual diagram corresponds to a product of two mathematical expressions. The first of these is based on the product \prod_a of the following expressions associated to the vertices and edges appearing in the diagram:

	$= \bar{\rho}^{(q)},$	(402)
	$:= \bar{\rho}^{(q)} v^{(a)}(a'_b),$	(403)
	$:= -m(a'_b) g(a, a'_b),$	(404)
	$:= -m(a'_b) g(a'_c, a'_b),$	(405)
	$:= m(a'_b) g(a'_c, a'_b),$	(406)
	$:= -m(a_i) g(a, a_i),$	(407)
	$:= -m(a_i) g(a'_b, a_i),$	(408)
	$:= m(a_i) g(a'_b, a_i).$	(409)

As before, transparent vertices indicate that their contribution is not included. The subscript a next to the diagrams helps to clarify that these are only the

contributions of the objects to the first term. Any vertices or edges which are not on this list supply a factor of 1 and hence can be ignored for constructing the first term. The product Π_a is to be integrated over all scale factors associated to interaction vertices abiding time-ordering, i.e., the first expression is obtained as

$$\int_{a_i}^a da'_1 \int_{a'_1}^a da'_2 \dots \int_{a'_{n-1}}^a da'_n \Pi_a, \quad (410)$$

where a is the scale factor at which the density correlation function is to be evaluated.

The second expression takes care of all terms involving wave-vectors as well as the Dirac δ -functions. First, we form the product Π_k which is given by $\frac{1}{m!} (2\pi)^{3(r-m)}$ times the product of the expressions

$$\begin{array}{c} \text{◇} \text{t} \\ \text{---} \text{k} \end{array} \Big|_k := \frac{1}{2} P_\delta(k_t'', a_i), \quad (411)$$

$$\begin{array}{c} \text{○} \text{b} \text{---} \text{○} \text{s, a} \\ \text{---} \text{k} \end{array} \Big|_k := v^{(k)}(k'_b) k'_b \cdot k_s, \quad (412)$$

$$\begin{array}{c} \text{○} \text{b} \text{---} \text{○} \text{c} \\ \text{---} \text{k} \end{array} \Big|_k := v^{(k)}(k'_b) k'_b \cdot k_s, \quad (413)$$

$$\begin{array}{c} \text{○} \text{b} \text{---} \text{○} \text{c} \\ \text{---} \text{k} \end{array} \Big|_k := v^{(k)}(k'_b) k'_b \cdot k'_c, \quad (414)$$

$$\begin{array}{c} \text{◇} \text{t} \text{---} \text{○} \text{s, a} \\ \text{---} \text{k} \end{array} \Big|_k := \frac{-1}{\kappa \|k_t''\|^2} k_t'' \cdot k_s, \quad (415)$$

$$\begin{array}{c} \text{◇} \text{t} \text{---} \text{○} \text{b} \\ \text{---} \text{k} \end{array} \Big|_k := \frac{-1}{\kappa \|k_t''\|^2} k_t'' \cdot k'_b, \quad (416)$$

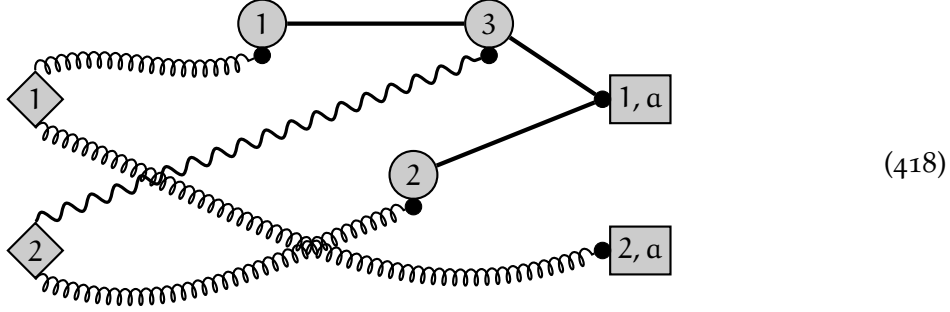
$$\begin{array}{c} \text{◇} \text{t} \text{---} \text{○} \text{b} \\ \text{---} \text{k} \end{array} \Big|_k := \frac{-1}{\kappa \|k_t''\|^2} k_t'' \cdot k'_b. \quad (417)$$

for each such vertex and edge in the diagram. Next, we form a linear system of equations corresponding to the density nodes. For this purpose, we assign to each edge a wave-vector and a density node as follows: An density or correlation edge corresponds to the wave vector of its correlation vertex, though it comes with a minus sign if the edge is connected to the bottom of the correlation vertex. Each edge coming from an interaction vertex corresponds to the wave-vector of that vertex. Any edge is associated to the density node it connects to. If it connects to an interaction vertex instead, it is assigned iteratively the same density node as the edge leaving that vertex. Provided these preparations, for each density node, the wave-vector associated to it, i.e., the wave-vector of the density or interaction vertex it touches, equals the sum over all wave-vectors corresponding to edges associated to it. Note that each of these equations corresponds to one of the Dirac δ -functions in equation (387). We solve the linear system of equations for all k'_b for $b = 1, \dots, n$ and replace them accordingly in Π_k . The remaining equations are multiplied to Π_k as Dirac δ -functions. Finally, we integrate the result over all k_t'' for $t = 1, \dots, m$, obtaining the second expression of the contribution of the diagram.

We emphasize that this procedure precisely reproduces the previous Feynman rules as well as the Dirac δ -functions in equation (387). As such, we obtain the

correct mathematical expression for the diagrams. Their sum then yields the desired contribution to the r -point density correlation function at n^{th} interaction and m^{th} correlation order.

Given the admitted complexity of the description, let us perform it explicitly for the diagram



contributing to the expectation value of the 2-point density correlation function at third interaction and second correlation order. The structure of the diagram already suggests that the initial correlations symbolized by the correlation vertices create a correlation between the density vertices.

Let us start with the scale factor part of the expression. The product of the relevant expressions yields

$$\begin{aligned} \Pi_\alpha = & (\bar{\rho}^{(q)})^5 v^{(a)}(a'_1) (m(a'_1) g(a'_3, a'_1)) v^{(a)}(a'_2) (-m(a'_2) g(a, a'_2)) \\ & v^{(a)}(a'_3) (-m(a'_3) g(a, a'_3)) (-m(a_i) g(a'_1, a_i)) \\ & (-m(a_i) g(a'_2, a_i)) (-m(a_i) g(a, a_i)) \end{aligned} \quad (419)$$

and needs to be integrated over the scale factors a'_1, a'_2, a'_3 under the time-ordering condition $a_i \leq a'_1 \leq a'_2 \leq a'_3 \leq a$. As hinted at in subsection 3.2.3, this integration can in practice be performed iteratively relying on the results from lower order diagrams.

The wave-vector part of the expression is actually much easier than the description above would suggest. We follow the prescription and obtain

$$\begin{aligned} \Pi_\kappa = & \frac{(2\pi)^3}{2!} \frac{1}{2} P_\delta(k''_1, a_i) \frac{1}{2} P_\delta(k''_2, a_i) \frac{(-1)}{\kappa \|k''_1\|^2} k''_1 \cdot k'_1 \frac{(-1)}{\kappa \|k''_1\|^2} k''_1 \cdot k_2 \\ & \frac{(-1)}{\kappa \|k''_2\|^2} k''_2 \cdot k'_2 v^{(k)}(k'_1) k'_1 \cdot k'_3 v^{(k)}(k'_2) k'_2 \cdot k_1 v^{(k)}(k'_3) k'_3 \cdot k_1. \end{aligned} \quad (420)$$

Next, we ought to assign wave-vectors and density nodes to all edges. The wave-vectors are simply the ones associated to the left end of each edge. The only edge not connected directly to a density node is the edge between interaction

vertices 1 and 3 which gets associated to the density node at the density vertex with label 1. The resulting system of equations is thus

$$\begin{cases} k'_1 = -k''_1 \\ k'_2 = k''_2 \\ k'_3 = -k''_2 \\ k_1 = k'_1 + k'_2 + k'_3 \\ k_2 = k''_1 \end{cases} \Rightarrow \begin{cases} k'_1 = -k''_1 \\ k'_2 = k''_2 \\ k'_3 = -k''_2 \\ k_1 = -k''_1 \\ k_2 = k''_1 \end{cases} \quad (421)$$

where in the right-hand system we used the top three equations to simplify the fourth. Performing the replacements in Π_k leads to many cancellations and we are left with

$$\Pi_k = -\frac{(2\pi)^3}{8\kappa^3} P_\delta(k''_1, a_i) P_\delta(k''_2, a_i) v^{(k)}(k''_1) (-k''_1) \cdot (-k''_2) v^{(k)}(k''_2) k''_2 \cdot k_1 v^{(k)}(k''_1) (-k''_2) \cdot k_1 \delta_D(k_1 + k''_1) \delta_D(k_2 - k''_1). \quad (422)$$

We used symmetry of the interaction potential $v^{(k)}(-k) = v^{(k)}(k)$ to absorb some signs. As a final step, we integrate this expression over k''_1 and k''_2 . Note that one of the integrals cancels and the result is proportional to a factor $\delta_D(k_1 + k_2)$. We have found a contribution to the density power spectrum!

We conclude this subsection with two remarks. Firstly, from the structure of the linear system of equations, it follows immediately that if the diagram has an interaction with a density node which is not connected to any edge, then the entire contribution vanishes. This is because the wave-vector associated to it appears in the product and is set to zero.¹⁵

Secondly, if exactly one edge is associated at a density node, cancellations can happen in Π_k . For momentum correlations, we have encountered this in the example thrice. The one of the wave-vectors of the scalar product is replaced by the other and thus cancels against the norm squared in the denominator. In case of a Newtonian interaction potential $v^{(k)}(k) \propto \|k\|^{-2}$, the same happens if a single interaction edge ends at a density node.

Based on the second remark, for a Newtonian interaction potential, the form of the expression depending on wave-vectors thus only depends on the topology of the diagram. For example, one can show that

$$\text{Diagram 1} \propto \text{Diagram 2} \quad (423)$$

¹⁵ The factor $v^{(k)}(0)$ does not spoil this conclusion, as argued in appendix A of [1].

up to constant factors. In case of $v^{(k)}(k) = \|k\|^{-2}$, the diagrams have the exact same wave-vector dependent structure.

The further development and algorithmic implementation of this formalism is subject of current study. Using the splitting of the contributions into scale factor and wave-vector dependent factors should make the computation of contributions to the density-fluctuation power spectrum in Newtonian gauge and for quadratically expanded initial correlations feasible for high interaction orders. Preliminary results suggest that interaction orders up to 20 and beyond are feasible. An optimized implementation might allow even for the study of cubic initial correlations at moderately high interaction orders.

4.2.4 Density-Fluctuation Power Spectrum

We have explained in the previous subsection in detail, how to obtain expectation values for r-point correlation functions an expansion in interactions and initial correlations in the KFT framework. We have seen in equation (196) that for $r = 2$, these are directly related to the density-fluctuation power spectrum. Specifically, it is

$$\begin{aligned} \langle G_{\bar{\rho}\bar{\rho}}^{(q)} \rangle (k_1, k_2, a) &= (2\pi)^6 \delta_D(k_1) \delta_D(k_2) (\bar{\rho}^{(q)})^2 \\ &+ (2\pi)^3 \delta_D(k_1 + k_2) P_{\bar{\delta}}^{(q)}(k_1, a), \end{aligned} \tag{424}$$

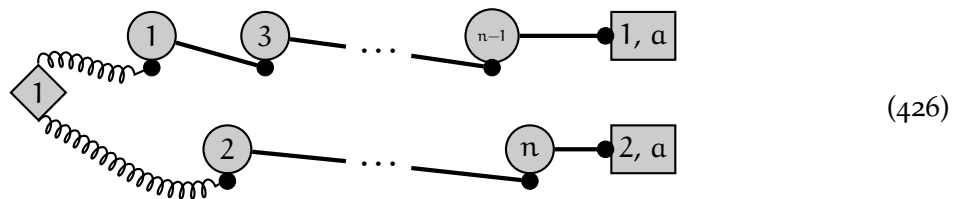
It is easy to see that the first term in that equation is given by the zeroth order diagram

$$\begin{aligned} \bullet \boxed{1, a} \\ \bullet \boxed{2, a} \end{aligned} = (2\pi)^6 \delta_D(k_1) \delta_D(k_2) (\bar{\rho}^{(q)})^2 \tag{425}$$

implying that all other contributions to $\langle G_{\bar{\rho}\bar{\rho}}^{(q)} \rangle$ directly contribute to the density-fluctuation power spectrum.

There are no other contributions at zeroth correlation order, since the existence of an interaction would make the expression vanish due to the absence of correlation edges which could connect to the associated density node. As such, this single diagram gives the full contribution in zeroth order in the expansion in initial contributions. Physically, it is clear that there cannot be any contributions to the density-fluctuation power spectrum from an uncorrelated diagram.

The contributions to the expectation value of the two-point density correlation function are from diagrams like



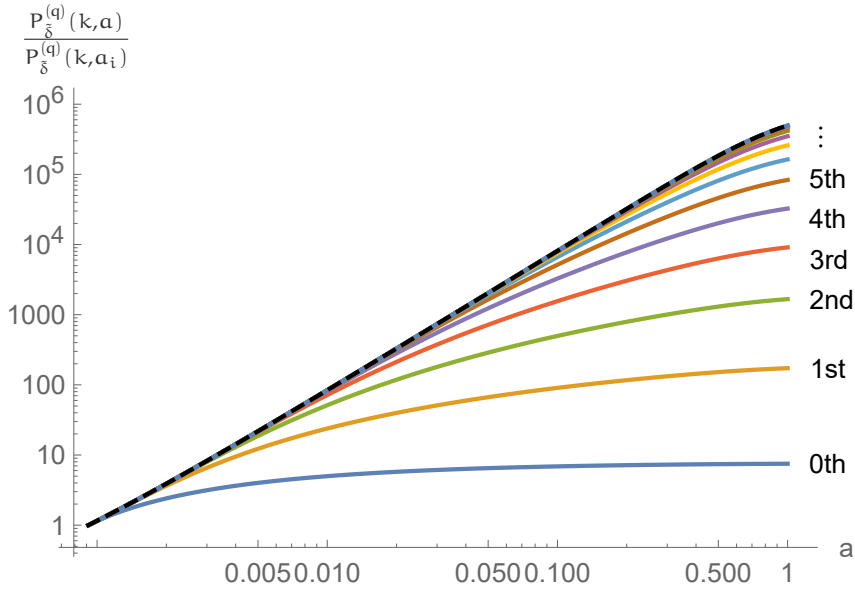
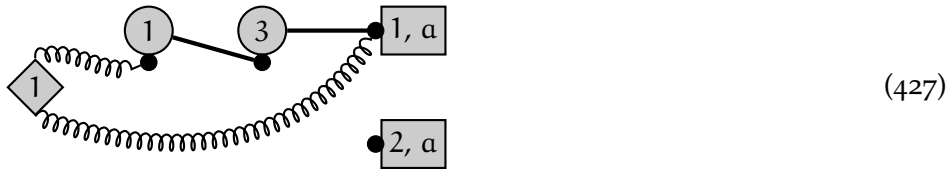


Figure 3: Contributions to the linear growth of the cosmic density-fluctuation power spectrum from diagrams with a single correlation vertex at various interaction orders n . The black dashed line is the expected behavior of the linear growth factor squared. Figure 3 of [1].

for all orderings of interaction vertices and all possible connections between the correlation vertex and the density nodes of the two left-most interaction vertices. This includes all combinations of density and momentum edges as well as connecting the top of the correlation vertex to the density node of interaction vertex in the lower tree and the bottom of it to the upper tree.

This form of the diagrams is forced due to the need of having at least one edge connected to each density node. Note that this condition also extends to density vertices, because a diagram like



would be proportional to a factor $\delta_D(k_2)$. Of course, it would not be impossible for $\langle G_{\rho\rho}^{(q)} \rangle$ to feature such terms, provided they cancel upon adding contributions from all diagrams. In either case, they do not contribute to the density-fluctuation power spectrum.¹⁶

In [1] and [35] it was shown that the diagrams of the from (426) combine to yield the linear growth of the cosmic density-fluctuation power spectrum. This is shown in figure 3. For a %-level agreement with the behavior of the linear growth factor squared, one needs to consider contributions up to 12th order in the interactions.

¹⁶ A more detailed analysis of the linear system of equations shows that contributions involving trees which are not connected to other trees via correlations always vanish. Trees consisting of a single density vertex are the sole exception to this.

As a consequence, the non-linear growth of the cosmic density-fluctuation power spectrum is fully encoded in contributions from diagrams at second and higher order in the expansion in initial correlations. Work is ongoing to obtain the contributions from quadratically expanded initial correlations in Newtonian gauge, extending the results of [35] which determined them up to eighth order in the interactions.

4.3 NEUTRINO CLUSTERING

Cosmic neutrinos released in the early universe have been traveling mostly unperturbed due to their very low mass. As highly relativistic particles, they behave similarly to radiation. Hence, the ν B thus has similar properties to the CMB. However, cosmic neutrinos have been continuously losing kinetic energy due to the expansion of spacetime. As such, they have relatively recently become slow enough to be affected by gravitational potentials.[49]

Specifically, while the ν B was to good approximation homogeneous around redshift $z = 3$, it has been becoming more and more correlated with the inhomogeneous distribution of matter. This clustering of neutrinos should result into an overdensity inside galactic halos relative to their mean density. In this section, we predict this overdensity with perturbative methods of KFT.

Compared to the application to the formation of the large scale structure of the universe presented in the previous section 4.2, we can neglect the pairwise interactions between the neutrinos here. This N-1-body approximation was introduced in [66] and is applied to our formalism in the first subsection below. Considering only the interaction of the system of N neutrinos with an external potential factorizes the system and allows to consider each neutrino individually.

In subsection 4.3.2, we obtain expressions for perturbative contributions of the expectation value for the neutrino number density. The calculations are based on the microscopic perturbation theory in the KFT formalism presented in this thesis. We obtain expressions for up to second order in the expansion in interactions.

Concluding this section, we summarize the results of [2] and discuss them. There, only the first order contribution to the local cosmic neutrino density on Earth is considered. While the results agree well with numerical simulations for realistic neutrino masses, the clustering is underestimated at higher values of the mass. We provide a brief outlook to ongoing work of including the second order contribution which should improve the agreement for a larger range of neutrino masses.

This section is based on [2] which is joint work with Isabel M. Oldengott and Emil Brinch Holm as well as ongoing work on its extension. The idea of the project, the relevant neutrino physics and the adaption to the Milky Way were contributed by Isabel. Emil implemented the numerical evaluation, created figure 4 and contributed in the adaptation to the Milky Way.

4.3.1 N-1-body Approximation

Neutrinos have a very small, but non-zero mass.[54–57] Regarding them as point-particles moving in a universe filled with inhomogeneously distributed matter, the pairwise gravitational interactions are strongly suppressed relative to their interaction with the gravitational potentials of dark matter halos. This allows for a so-called N-1-body approximation proposed in [66].

As derived in equation (356), the Hamiltonian of a system of N point-particles in an expanding spacetime interacting with an external potential $V(q, z)$ is

$$\mathcal{H} = \frac{1}{2m(z)} \mathbf{x}^{(p)} \cdot \mathbf{x}^{(p)} + \sum_{j=1}^N \frac{m(z)}{H(z)^2} V\left(x_j^{(q)}, z\right), \quad (428)$$

when choosing redshift z as a time parameter and working in comoving coordinates. Recall that the negative signs appear because redshift decreases during the evolution of the system. The effective mass is given by

$$m(z) = -\frac{m_\nu H(z)}{1+z}, \quad (429)$$

where m_ν is the neutrino mass¹⁷ and $H(z)$ the Hubble function.

Due to the absence of interactions between the particles, the Hamiltonian can be written as a sum

$$\mathcal{H} = \sum_{j=1}^N \mathcal{H}_j \quad \text{with} \quad (430)$$

$$\mathcal{H}_j = \frac{1}{2m(z)} x_j^{(p)} \cdot x_j^{(p)} + \frac{m(z)}{H(z)^2} V\left(x_j^{(q)}, z\right). \quad (431)$$

Analogously to our example of N independent harmonic oscillators in subsection 2.2.2, this yields N identical copies of the single-particle equation of motion

$$E_j[\varphi_j](z) = \frac{d}{dz} \varphi_j(z) + \left(\begin{array}{c} -m(z) \varphi_j^{(p)}(z) \\ \frac{m(z)}{H(z)^2} \nabla V\left(\varphi_j^{(q)}(z), z\right) \end{array} \right), \quad (432)$$

where ∇V is the gradient of the potential with respect to its first argument.

Let $\tilde{\varphi}_j(t; \mathbf{x})$ be the solution of these equations of motion for initial value \mathbf{x} . Evidently, the physical evolution of the j^{th} particle $\tilde{\varphi}_j$ is independent of all other particles $\ell \neq j$. Indeed, the initial values for its equations of motion are only the component x_j of \mathbf{x} . Given our setup, this was to be expected since we did not assume any interaction between the neutrinos.

In our application, we are interested in the overdensity of the $C_{\nu B}$ in a dark matter halo. Therefore, we consider the macroscopic spatial density of the system

$$\tilde{\rho}^{(q)}(q, z; \mathbf{x}) = \sum_{j=1}^N \tilde{\rho}_j^{(q)}(q, z; x_j) = \sum_{j=1}^N \delta_D\left(q - \tilde{\varphi}_j^{(q)}(z; x_j)\right). \quad (433)$$

Note that due to the independence of $\tilde{\varphi}_j$ from x_ℓ for $\ell \neq j$, the microscopic component densities $\tilde{\rho}_j^{(q)}$ in the sum only depend on x_j .

Provided an exact initial state \mathbf{x} of the $C_{\nu B}$ at initial redshift z_i , the macroscopic spatial density $\tilde{\rho}^{(q)}(q, z; \mathbf{x})$ is a sum of Dirac δ -functions. Each neutrino is a point-particle and has a precise position at redshift z . However, we of course

¹⁷ For simplicity, we focus on a single neutrino flavor with mass m_ν .

do not know the exact initial state \mathbf{x} and we are also not really interested in the exact positions of each individual neutrino at present time $z = 0$.

Instead, we would like to obtain the macroscopic spatial density when averaged over a reasonably sized volume which contains enough neutrinos to avoid statistical noise.¹⁸ Our knowledge of the initial state of the system is also quite limited. As discussed in subsection 4.1.2, choosing our initial redshift as $z_i = 3$ or earlier, the CvB is in good approximation spatially homogeneous and has a Fermi-Dirac momentum distribution.

The properties of the CvB at initial time can be regarded as a probability distribution for the initial state \mathbf{x} of the system of N neutrinos. Specifically, the initial state \mathbf{x} is obtained by taking a sample of N point particles subject to the probability distributions

$$P(x_j) = \frac{1}{N} P_{\text{FD}}(x_j^{(p)}) = \frac{1}{(2\pi\hbar)^3 N} \left(\exp \left(\frac{c \|x_j^{(p)}\|}{k_B T_0} \right) + 1 \right)^{-1} \quad (434)$$

for all j . The Fermi-Dirac distribution P_{FD} is taken from equation (359). Note that integration over P_{FD} yields the mean comoving cosmic neutrino density. Hence, the probability distribution for the entire system is given by

$$P(\mathbf{x}) = \prod_{j=1}^N P(x_j) = \left(\frac{1}{(2\pi\hbar)^3 N} \right)^N \prod_{j=1}^N \left(\exp \left(\frac{c \|x_j^{(p)}\|}{k_B T_0} \right) + 1 \right)^{-1}. \quad (435)$$

The expectation value of the macroscopic spatial density subject to this probability distribution of initial values is

$$\langle \tilde{\rho}^{(q)} \rangle(q, z) = \int d\mathbf{x} P(\mathbf{x}) \tilde{\rho}^{(q)}(q, z; \mathbf{x}). \quad (436)$$

As explained in subsection 2.4.3 it is equal to an average over the final positions of the N neutrinos. This can be regarded as a spatial average over an infinitesimally small volume and thus exceeds the desired average over a small, but finite volume mentioned above.

Having identified the expectation value in equation (436) as the observable of interest, let us further investigate it. It is

$$\langle \tilde{\rho}^{(q)} \rangle(q, z) = \int d\mathbf{x} P(\mathbf{x}) \sum_{j=1}^N \tilde{\rho}_j^{(q)}(q, z; x_j) \quad (437)$$

$$= \sum_{j=1}^N \int dx_j P(x_j) \tilde{\rho}_j^{(q)}(q, z; x_j). \quad (438)$$

In the second equality, we have performed the integrations over x_ℓ for all $\ell \neq j$. We can rewrite this equation as

$$\langle \tilde{\rho}^{(q)} \rangle(q, z) = \sum_{j=1}^N \langle \tilde{\rho}_j^{(q)} \rangle(q, z). \quad (439)$$

¹⁸ Experimentally, an idealized direct detection measurement would observe the total number of neutrinos traversing a detector in a certain time. Assuming local homogeneity in space and time, this corresponds to the mean spatial density averaged over a volume proportional to the neutrino velocity, the observation time and the detector volume.

The expectation value of the spatial density of a sample of N independent particles is the sum over the expectation values of each particle sampled individually. Note that this is only possible because the probability distribution and the equations of motion factorized. Moreover, since all neutrinos are subject to equivalent equations of motion and distributions of initial values, it is

$$\langle \tilde{\rho}^{(q)} \rangle(q, z) = N \langle \tilde{\rho}_i^{(q)} \rangle(q, z). \quad (440)$$

Equation (440) suggests to replace our system by a single neutrino. This is the $N-1$ -body approximation alluded to at the beginning of this subsection. Because we neglected interactions between the neutrinos, they evolve independently. Additionally, given that the probability distribution of initial values is given by a product of independent distributions for each neutrino, the entire system factorizes.

The $N-1$ -body approximation allows us to study the component system subject to the equation of motion and probability distribution of initial values,

$$E[\varphi](z) = \frac{d}{dz} \varphi(z) + \begin{pmatrix} -\frac{1}{m(z)} \varphi^{(p)}(z) \\ \frac{m(z)}{H(z)^2} \nabla V(\varphi^{(q)}(z), z) \end{pmatrix} \quad \text{and} \quad (441)$$

$$P(x) = \frac{1}{(2\pi \hbar)^3} \left(\exp \left(\frac{c \|x^{(p)}\|}{k_B T_0} \right) + 1 \right)^{-1}, \quad (442)$$

respectively, instead of the composite system of N neutrinos. Note that there is no factor $\frac{1}{N}$ in the probability distribution, because we only sample a single particle.

4.3.2 Density Expectation Value

We perform a split of the equations of motion (441) by working in Newtonian gauge. The free part of the equations of motion becomes

$$E[\varphi](z) = \frac{d}{dz} \varphi(z) - \begin{pmatrix} \frac{1}{m(z)} \varphi^{(p)}(z) \\ 0 \end{pmatrix} \quad (443)$$

and admits the Green's function

$$G(z, z') = \begin{pmatrix} \theta(z' - z) \mathbb{I}_3 & g(z, z') \theta(z' - z) \mathbb{I}_3 \\ 0 & \theta(z' - z) \mathbb{I}_3 \end{pmatrix} \quad \text{with} \quad (444)$$

$$g(z, z') = \int_z^{z'} dz'' \frac{1}{m(z'')}. \quad (445)$$

We note that the Heaviside θ -functions have negative argument compared to the one in equation (311) due to the decreasing time parameter z . In particular, it is $G(z, z') = 0$ for $z \geq z'$.

We are interested in the expectation value of the spatial density which in the N-1-body approximation takes the form

$$\langle \tilde{\rho}^{(q)} \rangle(q, z) = \int dx P(x) \tilde{\rho}^{(q)}(q, z; x) = \int dx P(x) \delta_D(q - \tilde{\varphi}^{(q)}(z; x)) \quad (446)$$

$$= \int dx P(x) \int \frac{dk}{(2\pi)^3} \exp(ik \cdot q) \exp(-ik \cdot \tilde{\varphi}^{(q)}(z; x)). \quad (447)$$

In the second line, we replaced the Dirac δ -function by its Fourier transform. We intent to approximate $\langle \tilde{\rho}^{(q)} \rangle$ by truncations of a series expansion in the interactions, i.e., apply the perturbative formalism presented in chapter 3. This requires functional derivatives of our observable which would become very involved when applied to a Dirac δ -function.

Therefore, let us regard the Fourier space spatial density

$$\tilde{\rho}^{(q)}(k, z; x) = \exp(-ik \cdot \tilde{\varphi}^{(q)}(z; x)) \quad (448)$$

as our observable. According to equation (252), we can expand $\tilde{\rho}^{(q)}$ into an infinite sum of perturbative contributions of the form

$$\tilde{\rho}_n^{(q)}(k, z; x) = i^n \int_{z_f}^{z_i} dz'_n \cdots \int_{z'_2}^{z'_1} dz'_1 \hat{\Gamma}_I(z'_1) \cdots \hat{\Gamma}_I(z'_n) \exp(-ik \cdot \tilde{\varphi}^{(q)}(z; x)) \quad (449)$$

for all non-negative integers n . Provided convergence of this sum, a truncation yields an approximation to $\tilde{\rho}^{(q)}$ which improves in accuracy for higher orders n . The value of z_f does not matter as long as it is not greater than the redshift at which we evaluate observables.

Likewise, an approximation for the expectation value of the density is obtained via the truncated sum

$$\langle \tilde{\rho}^{(q)} \rangle(q, z) \approx \int \frac{dk}{(2\pi)^3} \exp(ik \cdot q) \left(\langle \tilde{\rho}_0^{(q)} \rangle(k, z) + \dots + \langle \tilde{\rho}_n^{(q)} \rangle(k, z) \right). \quad (450)$$

The expectation values on the right-hand side of this equation are simply given by integrating the product of $P(x)$ with the expression in equation (449) over the initial values x .

In equation (449), the free neutrino trajectory appears. It is given via the action of the Green's function on the initial conditions, i.e.,

$$\tilde{\varphi}^{(q)}(z; x) = G(z, z_i) x = \begin{pmatrix} x^{(q)} + g(z, z_i) x^{(p)} \\ x^{(p)} \end{pmatrix}. \quad (451)$$

It corresponds to motion in a straight line, but the comoving distance traveled does not increase uniformly. This is due to both the choice of time parameter z and the expansion of the spacetime.

The operators $\hat{\Gamma}_I$ are up to reparametrization of the form given in equation (317). Using that the interaction part of the equations of motion is given by $E_1^{(q)} = 0$ and

$$E_1^{(p)}[\varphi](z) = \frac{m(z)}{H(z)^2} \nabla V(\varphi^{(q)}(z), z), \quad (452)$$

we have

$$i \hat{\Gamma}_I(z') = - \int_{z_f}^{z'} dz'' \frac{m(z') g(z'', z')}{H(z')^2} \nabla V(\bar{\varphi}^{(q)}(z'; \mathbf{x}), z') \cdot \frac{\delta}{\delta(\bar{\varphi}^{(q)})^T(z''; \mathbf{x})}. \quad (453)$$

Having collected all the necessary ingredients, let us compute the contributions to the expectation value of the spatial density up to second order. At zeroth order, we find

$$\tilde{\rho}_0^{(q)}(\mathbf{k}, z; \mathbf{x}) = \exp(-i\mathbf{k} \cdot \bar{\varphi}^{(q)}(z; \mathbf{x})). \quad (454)$$

In order to obtain the contribution to the expectation value of the spatial density, we need to average this quantity over the distribution $P(\mathbf{x})$ and perform an inverse Fourier transform. Performing the latter first we obtain

$$\langle \tilde{\rho}^{(q)} \rangle_0(\mathbf{q}, z) = \int d\mathbf{x} P(\mathbf{x}) \delta_D(\mathbf{q} - \bar{\varphi}^{(q)}(z; \mathbf{x})) \quad (455)$$

$$= \int d\mathbf{x}^{(p)} \frac{1}{(2\pi \hbar)^3} \left(\exp\left(\frac{c \|\mathbf{x}^{(p)}\|}{k_B T_0}\right) + 1 \right)^{-1}. \quad (456)$$

The remaining integral over the Fermi-Dirac distribution yields the mean comoving cosmic neutrino density.

The first order contribution is given by

$$\tilde{\rho}_1^{(q)}(\mathbf{k}, z; \mathbf{x}) = \int_{z_f}^{z_i} dz'_1 i \hat{\Gamma}_I(z'_1) \exp(-i\mathbf{k} \cdot \bar{\varphi}^{(q)}(z; \mathbf{x})) \quad (457)$$

$$= - \int_z^{z_i} dz'_1 \frac{m(z'_1) g(z, z'_1)}{H(z'_1)^2} \nabla V(\bar{\varphi}^{(q)}(z'_1; \mathbf{x}), z'_1) \cdot (-i\mathbf{k}) \exp(-i\mathbf{k} \cdot \mathbf{x}^{(q)} - i g(z, z_i) \mathbf{k} \cdot \mathbf{x}^{(p)}), \quad (458)$$

where the integral over z'_1 inside $\hat{\Gamma}_I$ is canceled by the Dirac δ -function originating from taking the functional derivative. The condition $z'' \leq z'_1$ encoded in its boundaries yields the condition $z \leq z'_1$ in the boundary of the integration over z'_1 in the second line.

In order to perform the inverse Fourier transform and the averaging over $P(\mathbf{x})$, consider the integration by parts

$$- \int d\mathbf{x}^{(q)} \nabla V(\bar{\varphi}^{(q)}(z'_1; \mathbf{x}), z'_1) \cdot (-i\mathbf{k}) \exp(-i\mathbf{k} \cdot \mathbf{x}^{(q)}) = - \int d\mathbf{x}^{(q)} \nabla V(\mathbf{x}^{(q)} + g(z, z_i) \mathbf{x}^{(p)}, z'_1) \cdot \frac{\partial}{\partial \mathbf{x}^{(q)}} \exp(-i\mathbf{k} \cdot \mathbf{x}^{(q)}) \quad (459)$$

$$= \int d\mathbf{x}^{(q)} \frac{\partial}{\partial \mathbf{x}^{(q)}} \cdot \nabla V(\mathbf{x}^{(q)} + g(z, z_i) \mathbf{x}^{(p)}, z'_1) \exp(-i\mathbf{k} \cdot \mathbf{x}^{(q)}) \quad (460)$$

$$= \int d\mathbf{x}^{(q)} \nabla^2 V(\bar{\varphi}^{(q)}(z'_1; \mathbf{x}), z'_1) \exp(-i\mathbf{k} \cdot \mathbf{x}^{(q)}). \quad (461)$$

The last equality introduces the Laplacian of V which can be justified through a simple chain rule. Via use of a Fourier transform and an integration by parts, we have effectively shifted the functional derivative in $\hat{\Gamma}_I$ from the observable to the potential.

Utilizing this procedure, the only term in $\langle \tilde{\rho}_1^{(q)} \rangle$ depending on the wave-vector k is the Fourier transform of the zeroth order spatial density. We have shown the formula

$$\langle \tilde{\rho}^{(q)} \rangle_1(q, z) = \int dx P(x) \int_z^{z_i} dz'_1 \frac{m(z'_1) g(z, z'_1)}{H(z'_1)^2} \nabla^2 V(\bar{\varphi}^{(q)}(z'_1; x), z'_1) \tilde{\rho}_0^{(q)}(q, z; x). \quad (462)$$

Note that its derivation relied on the fact that $P(x)$ is independent of $x^{(q)}$, though otherwise we could have used a product rule in the integration by parts and would have obtained a second term involving the partial derivative of $P(x)$ with respect to $x^{(q)}$.

Recall that the zeroth order contribution to the density,

$$\tilde{\rho}_0^{(q)}(q, z; x) = \delta_D(q - \bar{\varphi}(z; x)) = \delta_D(q - x^{(q)} - g(z, z_i) x^{(p)}), \quad (463)$$

is given in terms of a Dirac δ -function. This makes the integration over $x^{(q)}$ in equation (462) trivial and we obtain

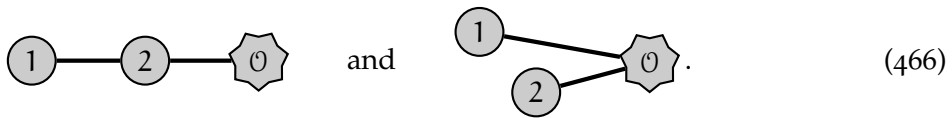
$$\langle \tilde{\rho}^{(q)} \rangle_1(q, z) = \int dx^{(p)} \frac{1}{(2\pi \hbar)^3} \left(\exp\left(\frac{c \|x^{(p)}\|}{k_B T_0}\right) + 1 \right)^{-1} \int_z^{z_i} dz'_1 \frac{m(z'_1) g(z, z'_1)}{H(z'_1)^2} \nabla^2 V(q - g(z, z'_1) x^{(p)}, z'_1). \quad (464)$$

We used that the argument of the potential is

$$q - g(z, z_i) x^{(p)} + g(z'_1, z_i) x^{(p)} = q - g(z, z'_1) x^{(p)} \quad (465)$$

after $x^{(q)}$ is replaced.

In a similar fashion, we can calculate the second order contribution. Recalling the construction of our Feynman rules, we expect two contributions corresponding to the diagrams



Let us consider the left-hand diagram first. It corresponds to the term obtained by acting with $\hat{\Gamma}_I(z'_1)$ on $\hat{\Gamma}_I(z'_2)$ in

$$\tilde{\rho}_2^{(q)}(k, z; x) = \int_{z_f}^{z_i} dz'_2 \int_{z'_2}^{z_i} dz'_1 i^2 \hat{\Gamma}_I(z'_1) \hat{\Gamma}_I(z'_2) \exp(-ik \cdot \bar{\varphi}^{(q)}(z; x)). \quad (467)$$

Evaluating the functional derivatives, we obtain the expression

$$\int_z^{z_i} dz'_2 \int_{z'_2}^{z_i} dz'_1 \frac{m(z'_1) g(z, z'_1)}{H(z'_1)^2} \frac{m(z'_2) g(z'_1, z'_2)}{H(z'_2)^2} \exp(-ik \cdot \bar{\varphi}(z; x)) (\nabla V(\bar{\varphi}^{(q)}(z'_1; x), z'_1) \cdot \nabla) \nabla V(\bar{\varphi}^{(q)}(z'_2; x), z'_2) \cdot (-ik). \quad (468)$$

Performing the exact same steps as for the first order contribution, we can replace the factor $(-ik)$ by a derivative with respect to $x^{(q)}$ which subsequently

can be shifted by means of an integration by parts. However, this time there are two potential terms resulting in a product rule. Evaluating it yields the contribution

$$\begin{aligned}
& - \int dx P(x) \int_z^{z_i} dz'_2 \int_{z'_2}^{z_i} dz'_1 \frac{m(z'_1) g(z, z'_1)}{H(z'_1)^2} \frac{m(z'_2) g(z'_1, z'_2)}{H(z'_2)^2} \tilde{\rho}_0^{(q)}(q, z; x) \\
& \quad \left(\text{tr} \left((\nabla^T \nabla) V \left(\tilde{\varphi}^{(q)}(z'_1; x), z'_1 \right) (\nabla^T \nabla) V \left(\tilde{\varphi}^{(q)}(z'_2; x), z'_2 \right) \right) \right. \\
& \quad \left. + \nabla V \left(\tilde{\varphi}^{(q)}(z'_1; x), z'_1 \right) \cdot \nabla \nabla^2 V \left(\tilde{\varphi}^{(q)}(z'_2; x), z'_2 \right) \right) \quad (469)
\end{aligned}$$

to the expectation value $\langle \tilde{\rho}_2^{(q)} \rangle$, in analogy to equation (462). The terms $(\nabla^T \nabla) V$ in the trace in the second line are the Hessian matrices of the potential with respect to its first argument. In the third line, a third derivative of the potential appears, specifically the gradient of the Laplacian. Yet again, the inverse Fourier transform resulted in the zeroth order contribution to the spatial density. It cancels the integration over $x^{(q)}$ and replaces the arguments of the potential terms, in the same way as for the first order contribution.

The right-hand diagram in equation (466) corresponds to acting with both $\hat{\Gamma}_1(z'_1)$ and $\hat{\Gamma}_1(z'_2)$ on $\tilde{\rho}_0^{(q)}$ in equation (467). This results in the expression

$$\begin{aligned}
& \int_z^{z_i} dz'_2 \int_{z'_2}^{z_i} dz'_1 \frac{m(z'_1) g(z, z'_1)}{H(z'_1)^2} \frac{m(z'_2) g(z, z'_2)}{H(z'_2)^2} \exp(-ik \cdot \tilde{\varphi}(z; x)) \\
& \quad \nabla V \left(\tilde{\varphi}^{(q)}(z'_1; x), z'_1 \right) \cdot (-ik) \nabla V \left(\tilde{\varphi}^{(q)}(z'_2; x), z'_2 \right) \cdot (-ik) \quad (470)
\end{aligned}$$

featuring two factors $(-ik)$. This does not change our strategy, but requires two integrations by parts and consequently yields four terms. Performing the calculation results in the contribution

$$\begin{aligned}
& \int dx P(x) \int_z^{z_i} dz'_2 \int_{z'_2}^{z_i} dz'_1 \frac{m(z'_1) g(z, z'_1)}{H(z'_1)^2} \frac{m(z'_2) g(z, z'_2)}{H(z'_2)^2} \tilde{\rho}_0^{(q)}(q, z; x) \\
& \quad \left(\text{tr} \left((\nabla^T \nabla) V \left(\tilde{\varphi}^{(q)}(z'_1; x), z'_1 \right) (\nabla^T \nabla) V \left(\tilde{\varphi}^{(q)}(z'_2; x), z'_2 \right) \right) \right. \\
& \quad + \nabla V \left(\tilde{\varphi}^{(q)}(z'_1; x), z'_1 \right) \cdot \nabla \nabla^2 V \left(\tilde{\varphi}^{(q)}(z'_2; x), z'_2 \right) \\
& \quad + \nabla \nabla^2 V \left(\tilde{\varphi}^{(q)}(z'_1; x), z'_1 \right) \cdot \nabla V \left(\tilde{\varphi}^{(q)}(z'_2; x), z'_2 \right) \\
& \quad \left. + \nabla^2 V \left(\tilde{\varphi}^{(q)}(z'_1; x), z'_1 \right) \nabla^2 V \left(\tilde{\varphi}^{(q)}(z'_2; x), z'_2 \right) \right), \quad (471)
\end{aligned}$$

where again the integral over $x^{(q)}$ can be performed immediately. Evidently, the first two terms are identical with the ones of the other diagram except for the arguments of the functions g and thus can be combined.

Using the identity $g(z, z'_2) - g(z'_1, z'_2) = g(z, z'_1)$ and replacing the arguments of the potentials appropriately, the second order contribution to the expectation value of the spatial density is

$$\begin{aligned}
& \langle \tilde{\rho}^{(q)} \rangle_2(q, z) \\
&= \int dx^{(p)} P_{\text{FD}}(x^{(p)}) \int_z^{z_i} dz'_2 \int_{z'_2}^{z_i} dz'_1 \frac{m(z'_1) g(z, z'_1)}{H(z'_1)^2} \frac{m(z'_2)}{H(z'_2)^2} \\
& \quad \left(g(z, z'_1) \text{tr} \left((\nabla^T \nabla) V(q - g(z, z'_1) x^{(p)}, z'_1) (\nabla^T \nabla) V(q - g(z, z'_2) x^{(p)}, z'_2) \right) \right. \\
& \quad + g(z, z'_1) \nabla V(q - g(z, z'_1) x^{(p)}, z'_1) \cdot \nabla \nabla^2 V(q - g(z, z'_2) x^{(p)}, z'_2) \\
& \quad + g(z, z'_2) \nabla \nabla^2 V(q - g(z, z'_1) x^{(p)}, z'_1) \cdot \nabla V(q - g(z, z'_2) x^{(p)}, z'_2) \\
& \quad \left. + g(z, z'_2) \nabla^2 V(q - g(z, z'_1) x^{(p)}, z'_1) \nabla^2 V(q - g(z, z'_2) x^{(p)}, z'_2) \right). \quad (472)
\end{aligned}$$

4.3.3 Local Neutrino Density

In the subsection above we found expressions for the perturbative contributions to the expectation value of the spatial density up to second order using microscopic perturbation theory in the KFT framework. In order for them to yield the local neutrino density, we need to specify the potential V to be the local gravitational potential. But prior to this, we have to define more explicitly our usage of the term “local”.

The main motivation for studying the local cosmic neutrino density is to assess the feasibility of a direct detection of the $C\nu B$. While its mean density can be inferred from the Fermi-Dirac distribution in equation (359), clustering due to gravitational interaction might significantly alter the density of cosmic neutrinos on Earth. This question has been investigated by earlier studies using numerical simulations.[49, 58, 66] In order to test our (semi-)analytical approach¹⁹ based on KFT, we follow the exact treatment in [58] as a first step.

Specifically, we consider a spherically symmetric NFW potential[67] truncated at the virial radius $R_{\text{vir}}(z)$, induced by a DM density of the form

$$\rho_{\text{DM}}^{(q)}(q, z) = \begin{cases} \frac{\rho_0(z) R_s(z)^3}{\|q\| (\|q\| + R_s(z))^2}, & \|q\| < R_{\text{vir}}(z), \\ 0, & \|q\| > R_{\text{vir}}(z). \end{cases} \quad (473)$$

Here, $\rho_0(z)$ is the central density and $R_s(z)$ is the scale radius. The time evolution of the quantities $\rho_0(z)$, $R_s(z)$ and $R_{\text{vir}}(z)$ is taken directly from [58] to enable a direct comparison to the numerical results obtained there. Likewise, we take from there the distance of Earth from the galactic center (8.2 kpc) and use their choice of parameters $\Omega_{m,0} = 0.3111$, $\Omega_\Lambda = 0.6889$ and $H_0 = 67.77 \text{ km s}^{-1} \text{ Mpc}^{-1}$ for the Λ CDM-model.

¹⁹ The prescription of microscopic perturbation theory and thus the obtained expressions in the previous subsection are fully analytic. However, the efficient numerical evaluation of the resulting integrals still poses a significant challenge, especially at higher orders.

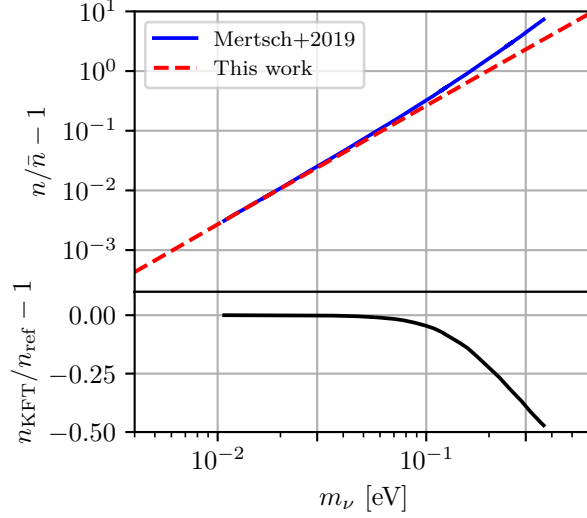


Figure 4: First order result from the KFT-based approach (dotted red) compared to the result of numerical simulations (blue). The labels n are spatial number densities which we denote by $\rho^{(q)}$ in this thesis. This is figure 1 of [2], “Mertsch+2019” is referring to [58].

The gravitational potential can be obtained from the DM density distribution $\rho_{\text{DM}}^{(q)}$ via the comoving Poisson equation

$$\nabla^2 V(q, z) = \frac{4\pi G}{(1+z)^2} \rho_{\text{DM}}^{(q)}(q, z) \quad (474)$$

which we introduced in equation (354). However, in many of the terms obtained in the previous subsection, the DM density can be directly inserted due to the dependence on the Laplacian of the potential.

In fact, let us consider this replacement explicitly for the first order contribution to the expectation value derived in equation (464). Upon inserting the Poisson equation, it is

$$\langle \tilde{\rho}^{(q)} \rangle_1(q, z) = \int dx^{(p)} \frac{G}{2\pi^2 \hbar^3} \left(\exp\left(\frac{c \|x^{(p)}\|}{k_B T_0}\right) + 1 \right)^{-1} \int_z^{z_i} dz'_1 \frac{m(z'_1) g(z, z'_1)}{H(z'_1)^2 (1+z'_1)^2} \rho_{\text{DM}}^{(q)}(q - g(z, z'_1) x^{(p)}, z'_1). \quad (475)$$

This shows that the neutrino overdensity is in first order sourced by the DM mass density integrated along free trajectories ending at the position q .

This first order contribution was computed in [2]. The result is shown in figure 4. For low neutrino rest masses m_ν there is excellent agreement, but the overdensity is underestimated for higher neutrino masses. While neutrino masses above $m_\nu \approx 0.1$ eV are disfavored observationally[57], the discrepancy in figure 4 for this mass range is still worth investigating. After all, this application is also intended as a test of microscopic perturbation theory in KFT in a realistic setting.

The obvious explanation for this discrepancy is the first order approximation in the interaction. This is supported by the fact that our results underestimate

the neutrino clustering only for high neutrino masses. For such masses, neutrinos become non-relativistic earlier and their paths are modeled worse by free motion.

Work is ongoing to implement the second order contribution given in equation (472) to test this hypothesis. In parallel, we are working on a comparison to other (semi-)analytical methods. However, even at this stage it is evident that microscopic perturbation theory in KFT is a viable approach to this problem, especially for realistic neutrino masses.

CONCLUSION

In this thesis we have performed a construction of Kinetic Field Theory (KFT) and its microscopic perturbation theory. We have done so in a very general setting, allowing the framework to be applied to any classical physical systems described by a Hamiltonian, even allowing for the configuration space to be a manifold. Based on this, we introduced a new formalism of encoding perturbative contributions with diagrams and applied it to two problems in cosmology, namely the formation of the large-scale structure in the universe and local clustering of cosmic neutrinos.

While KFT has been introduced as an approach to study cosmic structure formation [23] and has been mostly applied in this field [32], the framework is very general. Indeed, as we showed, the generating functional Z can be defined for any classical physical system described by a Hamiltonian \mathcal{H} . In such cases, it can be brought into the form

$$Z[\mathbf{J}; \mathbf{x}] = C^{-1} \int_{\mathbf{x}} \mathcal{D}\boldsymbol{\varphi} \int \mathcal{D}\boldsymbol{\chi} \exp\left(i \int_{t_i}^{t_f} dt' (\boldsymbol{\chi}(t') \cdot \mathbf{E}[\boldsymbol{\varphi]}(t') + \mathbf{J}(t') \cdot \boldsymbol{\varphi}(t'))\right), \quad (476)$$

where $C = \det(\partial_t)$ and $\mathbf{E}[\boldsymbol{\varphi}]$ are Hamilton's equations as given in equation (16). Moreover, \mathbf{x} is the state of the system at initial time t_i .

By means of functional derivatives with respect to the source field \mathbf{J} we can extract observables from the generating functional. We described the details in subsection 2.2.1. This corresponds to the first of the three key ideas of KFT we followed in our construction. They are:

1. *Determine analytic expressions for observables without explicitly solving the system.*
2. *Split evolution from interactions while keeping the description exact.*
3. *Determine observables given a stochastic initial state.*

Unless considering a very simple system, the observables obtained from the generating functional in the form given above are not particularly useful. The problem is that they require the evaluation of the path integral over the auxiliary field $\boldsymbol{\chi}$ which leads to a Dirac δ -functional of the form $\delta_{\mathbf{D}}(\mathbf{E}[\boldsymbol{\varphi}])$. The evaluation of the path integral over $\boldsymbol{\varphi}$ then corresponds to solving the equations of motion.

This is where the second key idea of KFT allowed us to make further progress. In section 2.3 we showed that splitting the equations of motion into a free and an interaction part leads to an expression of the generating functional in the form

$$Z[\mathbf{J}; \mathbf{x}] = \exp\left(i \int_{t_i}^{t_f} dt' \frac{\delta}{i \delta \mathbf{K}(t')} \cdot \mathbf{E}_{\mathbf{I}} \left[\frac{\delta}{i \delta \mathbf{J}^{\mathbf{T}}} \right] (t')\right) \exp\left(i \int_{t_i}^{t_f} dt' \int_{t_i}^{t'} dt'' \mathbf{J}^{\mathbf{T}}(t') \mathbf{G}(t', t'') (\delta_{\mathbf{D}}(t'' - t_i) \mathbf{x} - \mathbf{K}(t''))\right) \Bigg|_{\mathbf{K}=0} \quad (477)$$

featuring the Green's function \mathbf{G} of the free part \mathbf{E}_0 , and the interaction part $\mathbf{E}_{\mathbf{I}}$ of the equations of motion.

In the KFT literature, this equation is often taken as the most general form of the generating functional.[23, 32] The exponential in the second line is referred to as the free generating functional and the argument of the exponential in the first line is the interaction operator. In subsection 2.3.4 we showed that this expression can be further simplified and the auxiliary source field \mathbf{K} can be removed yielding

$$Z[\mathbf{J}; \mathbf{x}] = \mathcal{T} \exp \left(i \int_{t_i}^{t_f} dt' \hat{\mathcal{L}}_I(t') \right) Z_0[\mathbf{J}; \mathbf{x}] \quad \text{with} \quad (478)$$

$$\hat{\mathcal{L}}_I(t') = - \int_{t'}^{t_f} dt'' \mathbf{J}^T(t'') \mathbf{G}(t'', t') \mathbf{E}_I \left[\frac{\delta}{i \delta \mathbf{J}^T} \right] (t') \quad \text{and} \quad (479)$$

$$Z_0[\mathbf{J}; \mathbf{x}] = \exp \left(i \int_{t_i}^{t_f} dt' \mathbf{J}^T(t') \mathbf{G}(t', t_i) \mathbf{x} \right), \quad (480)$$

where $\mathcal{T} \exp$ is the time-ordered exponential. The functional Z_0 in the last line is our simplified version of the free generating functional.

The expression for the generating functional above relied on a splitting of the equations of motion into a free and an interaction part. However, the conditions on this splitting are relatively liberal, we only demand the existence of a Green's function \mathbf{G} for the free equation of motion $\mathbf{E}_I[\varphi] = 0$. If the splitting does not correspond to a split $\mathcal{H} = \mathcal{H}_0 + \mathcal{H}_I$ of the Hamiltonian, there is an additional technical condition on certain functional determinants.

As a result, there is substantial freedom in the choice of splitting. Note that for any of these choices the generating functional Z remains unchanged, but the free generating functional Z_0 and the operator $\hat{\mathcal{L}}_I$ may change significantly. In subsection 2.3.2 we regard this as a gauge freedom. We highlighted natural gauge choices and provided a naive prescription for gauge transformations.

Further formalizing and investigating this splitting freedom might well turn out very useful. It is a central result of [35] that the perturbative treatment of interactions in cosmic structure formation is converging much more quickly in Zel'dovich gauge than in Newtonian gauge. This demonstrates that the choice of gauge can have a significant impact on microscopic perturbation theory in KFT. Gauge choice should likewise impact the accuracy of the mean field approximation to interactions presented in [34].

Returning to the three key ideas of KFT, let us recall the averaging of observables over probability distributions of initial states. We provided a detailed discussion of its motivation and practical benefits in subsection 2.4.3. As we have seen in our applications in chapter 4, this approach to obtaining smoothed observables from a discrete system is particularly suited for initial conditions obtained via a sampling process.

We remark that the averaging over observables can be replaced by an averaging of the generating functional over the probability distribution of initial values. This approach is taken in most of the KFT literature.[32] In this convention, the exact same expressions we use in this thesis to obtain observables, then immediately yield expectation values. However, it can make the description somewhat less transparent.

In chapter 3 we have introduced a new formalism for microscopic perturbation theory in KFT. It is based on the series expansion

$$Z[\mathbf{J}; \mathbf{x}] = \sum_{n=0}^{\infty} i^n \int_{t_i}^{t_f} dt'_n \cdots \int_{t_i}^{t'_2} dt'_1 \hat{L}_I(t'_n) \cdots \hat{L}_I(t'_1) Z_0[\mathbf{J}; \mathbf{x}] \quad (481)$$

of the generating functional. Truncating the infinite sum at order n yields approximations to the generating functional and the observables derived from it.

We have seen in a simple example that for the harmonic oscillator this series does converge and the n^{th} order approximation to the phase space trajectory $\tilde{\varphi}(t; \mathbf{x})$ corresponds to its Taylor approximation of order $(2n + 1)$ in the position and of order $2n$ in the momentum. The difference in orders is related to the choice of Newtonian gauge and is, e.g., absent in stationary gauge.²⁰

However, a detailed study of the convergence properties of the expansion in interactions in the general case would be desirable. This was beyond the scope of this thesis and thus is left for future research. Note that the availability of an estimate of the truncation error would be a very useful tool for optimizing the choice of splitting gauge.

Our formalism of microscopic perturbation theory in section 3.1 expresses the contributions at any order in terms of commutators of the operator \hat{L}_I . This treatment quickly becomes tedious due to the combinatorial complexity, but allowed us to find a way to reformulate the series expansion as

$$Z[\mathbf{J}; \mathbf{x}] = \sum_{n=0}^{\infty} i^n \int_{t_i}^{t_f} dt'_n \cdots \int_{t_i}^{t'_2} dt'_1 \hat{\Gamma}_I(t'_1) \cdots \hat{\Gamma}_I(t'_n) Z_0[\mathbf{J}; \mathbf{x}] \quad \text{with} \quad (482)$$

$$\hat{\Gamma}_I(t') = - \int_{t'}^{t_f} dt'' \mathbf{E}_I^\dagger[\tilde{\varphi}(\bullet; \mathbf{x})](t') \mathbf{G}^T(t'', t') \frac{\delta}{i \delta \tilde{\varphi}^T(t''; \mathbf{x})}. \quad (483)$$

Compared to the series expansion in terms of the operator \hat{L}_I , this removes reference to the source field \mathbf{J} in the operators. Moreover, the functional derivatives appear no longer inside the interaction part of the equations of motion, but as a simple multiplicative factor. In subsection 3.1.2 we show that based on the series expansion in $\hat{\Gamma}_I$ the n^{th} order contribution to an observable \mathcal{O} can be written as

$$\tilde{\mathcal{O}}_n(\chi, t; \mathbf{x}) = i^n \int_{t_i}^{t_f} dt'_n \cdots \int_{t_i}^{t'_2} dt'_1 \hat{\Gamma}_I(t'_1) \cdots \hat{\Gamma}_I(t'_n) \mathcal{O}(\chi; \tilde{\varphi}(t; \mathbf{x})) \quad (484)$$

without any reference to the (free) generating functional remaining.

This equation is arguably the central result of this thesis. It provides an approximation scheme for observables of classical physical systems under very general conditions. We have showed in subsection 3.2.2 that for the phase space or spatial trajectory of the system, the first order approximation implied by the equation above coincides with the Born approximation.

²⁰ One can show easily that the analogous calculation in stationary gauge yields Taylor polynomials of n^{th} order when truncating the expansion in the interactions at order n in both position and momentum.

However, for other observables or higher orders there are differences to the (iterative) Born approximation. Our discussion shows that microscopic perturbation theory in KFT corresponds to a substantial reordering of the iterative Born series. Some terms of the n^{th} Born iteration appear at arbitrarily high orders in the KFT approximation. Conversely, all terms in the n^{th} order in the KFT formalism appear at most at the n^{th} iteration of the Born approximation.

It would be interesting to compare the perturbative contributions to observables in the microscopic perturbation theory presented here to other approximation schemes, too. In particular, a comparison to approximation schemes of the Boltzmann or Vlasov equations might be worthwhile. Their formulation is on phase space, too, and finding a correspondence would be just as interesting as investigating inherent differences.

In order to determine the perturbative contributions to observables in our formulation of microscopic perturbation theory in the KFT framework, we presented a diagrammatic treatment in subsection 3.2.1. This is a generalization of the Feynman rules we presented in [1]. The diagrammatic treatment also allows for an iterative determination of contributions to observables as we outlined in subsection 3.2.3. A precise formulation of this is subject to current study.

In subsection 3.3 we specialized our perturbative treatment to interacting N-body systems. This recovers the results of [1], though we made some minor adjustments to make the Feynman rules more compatible with the diagrammatic treatment independently proposed in [35]. The specialization to N-body system was in preparation to the two applications we presented in chapter 4.

In section 4.2 we summarized the application of our perturbative treatment to the cosmic structure formation presented in [1]. It relies on an expansion in the initial correlations between particles. In [1] it was shown that the contributions of first order in this expansion reproduces the linear growth of the cosmic matter fluctuation power spectrum when going to sufficiently high order in the expansion in the interactions.

In [35] it was shown that the convergence observed in figure 3 can be formalized. Indeed, a full resummation of the terms can be performed yielding exactly the linear growth as the interaction order goes to infinity. Moreover, this work studied the contributions of quadratic order in the initial correlations.

In Newtonian gauge the work [35] obtained results for quadratic correlations for up to eighth order in the interactions. Considering that for linear correlations contributions from interaction orders up to 12 are relevant, this is insufficient. Indeed, the obtained correction to the linearly evolved power spectrum in [35] is minimal. However, by working in Zel'dovich gauge, it is shown that already at very low interaction orders a convergence can be obtained.

As discussed in [35], the inclusion of the large-scale gravitational interaction into the free motion of particles speeds up the convergence of the perturbative series significantly. This is in accordance with our comments on the choice of splitting gauge. The convergence is against the 1-loop correction of standard perturbation theory. This is a behavior which is observed in Resummed Kinetic Field Theory (RKFT), too.[41]

This is a somewhat surprising result, as the conceptual issues related to shell crossing in standard perturbation theory should not be present in KFT. However, if the correspondence holds at higher correlation orders, too, the perturbative treatment of KFT would exhibit similar divergence problems of higher order contributions. In [35], this is blamed on the expansion in the correlations. While this is an obvious culprit, it should be mentioned that in the presence of divergences the choice of splitting gauge might have a non-trivial effect on perturbative results.

In the work leading up to this thesis, we independently investigated the contributions to the cosmic matter fluctuation power spectrum coming from quadratic and higher orders in the initial correlations. In order to facilitate these calculations, we defined new Feynman rules for expectation values of r -point density correlation functions. These might allow to obtain contributions in higher interaction orders in Newtonian gauge.

The diagrams for expectation values of density correlation functions of an N -body system subject to correlated initial conditions are an extension of the Feynman rules constructed in section 3.3.4. They introduce correlation vertices and edges corresponding to initial density and momentum correlations between particles. Due to their compatibility with the diagrams for the observables themselves, the averaging can naturally be performed over individual diagrams.

We have shown that it is possible to factorize the contributions of each diagram into a term depending on time and a term involving wave-vectors. This allows to perform the integrations over these terms separately significantly reducing the computational complexity. Moreover, the term involving wave-vectors is only dependent on the diagram topology which reduces the number of possible integrals significantly further facilitating the numerical evaluation of the expressions.

As a second application, we present the work of [2] on the local clustering of cosmic neutrinos in section 4.3. Again, aside from summarizing the methods and results of this work, we go beyond it and give an outlook to ongoing work for contributions beyond first order in KFT perturbation theory. The main result of this section is a reproduction of results from numerical approaches to this problem for realistic neutrino masses.

The application to neutrino clustering shows that microscopic perturbation theory in KFT is viable even in case it would be confirmed that the application to cosmic structure formation is plagued by the same problems as conventional analytic approaches. In fact, even for cosmic structure formation, the expansion in the interactions may not be to blame. A non-perturbative treatment of the initial particle correlations may remove the suspected coincidence with the results of standard perturbation theory.

In any case, in the form presented in this thesis, KFT and its microscopic perturbation theory yield approximations to observables and their expectation values in classical physical systems. Applications for such approximation schemes are manifold. As such, KFT is a powerful framework for studying classical physical systems with stochastic initial conditions.

LIST OF PUBLICATIONS

PEER-REVIEWED

- [1] Lavinia Heisenberg, Shayan Hemmatyar, and Stefan Zentarra. “Kinetic field theory: Higher-order perturbation theory.” In: *Phys. Rev. D* 106.6 (2022), p. 063513. DOI: [10.1103/PhysRevD.106.063513](https://doi.org/10.1103/PhysRevD.106.063513). arXiv: [2207.10504](https://arxiv.org/abs/2207.10504) [hep-th].
- [2] Emil Brinch Holm, Isabel M. Oldengott, and Stefan Zentarra. “Local clustering of relic neutrinos with kinetic field theory.” In: *Phys. Lett. B* 844 (2023), p. 138073. DOI: [10.1016/j.physletb.2023.138073](https://doi.org/10.1016/j.physletb.2023.138073). arXiv: [2305.13379](https://arxiv.org/abs/2305.13379) [hep-ph].
- [3] Andrea Giusti, Stefan Zentarra, Lavinia Heisenberg, and Valerio Faraoni. “First-order thermodynamics of Horndeski gravity.” In: *Phys. Rev. D* 105.12 (2022), p. 124011. DOI: [10.1103/PhysRevD.105.124011](https://doi.org/10.1103/PhysRevD.105.124011). arXiv: [2108.10706](https://arxiv.org/abs/2108.10706) [gr-qc].
- [4] Fabio D’Ambrosio, Lavinia Heisenberg, and Stefan Zentarra. “Hamiltonian Analysis of $f(Q)$ Gravity and the Failure of the Dirac–Bergmann Algorithm for Teleparallel Theories of Gravity.” In: *Fortschritte der Physik* (2023). DOI: [10.1002/prop.202300185](https://doi.org/10.1002/prop.202300185). arXiv: [2308.02250](https://arxiv.org/abs/2308.02250) [gr-qc].

ARXIV

- [5] Fabio D’Ambrosio, Mudit Garg, Lavinia Heisenberg, and Stefan Zentarra. “ADM formulation and Hamiltonian analysis of Coincident General Relativity.” In: (July 2020). arXiv: [2007.03261](https://arxiv.org/abs/2007.03261) [gr-qc].
- [6] Fabio D’Ambrosio et al. “Gravitational Waves in Full, Non-Linear General Relativity.” In: (Jan. 2022). arXiv: [2201.11634](https://arxiv.org/abs/2201.11634) [gr-qc].

UNPUBLISHED

- [7] Stefan Zentarra. “Jacobi Fields and their Applications in Kinetic Field Theory.” MA thesis. Heidelberg University, 2010.

BIBLIOGRAPHY

- [11] Steven Weinberg. “The cosmological constant problem.” In: *Reviews of modern physics* 61.1 (1989), p. 1.
- [12] Lavinia Heisenberg. “A systematic approach to generalisations of General Relativity and their cosmological implications.” In: *Phys. Rept.* 796 (2019), pp. 1–113. DOI: [10.1016/j.physrep.2018.11.006](https://doi.org/10.1016/j.physrep.2018.11.006). arXiv: [1807.01725 \[gr-qc\]](https://arxiv.org/abs/1807.01725).
- [13] Taishi Katsuragawa and Shinya Matsuzaki. “Dark matter in modified gravity?” In: *Phys. Rev. D* 95 (4 Feb. 2017), p. 044040. DOI: [10.1103/PhysRevD.95.044040](https://doi.org/10.1103/PhysRevD.95.044040). URL: <https://link.aps.org/doi/10.1103/PhysRevD.95.044040>.
- [14] Michael Boylan-Kolchin, Volker Springel, Simon DM White, Adrian Jenkins, and Gerard Lemson. “Resolving cosmic structure formation with the Millennium-II Simulation.” In: *Monthly Notices of the Royal Astronomical Society* 398.3 (2009), pp. 1150–1164.
- [15] Katherine Garrett and Gintaras Duda. “Dark matter: A primer.” In: *Advances in Astronomy* 2011 (2011), pp. 1–22.
- [16] Planck Collaboration. “Planck 2018 results - VI. Cosmological parameters.” In: *A&A* 641 (2020), A6. DOI: [10.1051/0004-6361/201833910](https://doi.org/10.1051/0004-6361/201833910). URL: <https://doi.org/10.1051/0004-6361/201833910>.
- [17] Brian D. Fields, Keith A. Olive, Tsung-Han Yeh, and Charles Young. “Big-Bang Nucleosynthesis after Planck.” In: *Journal of Cosmology and Astroparticle Physics* 2020.03 (Mar. 2020), p. 010. DOI: [10.1088/1475-7516/2020/03/010](https://doi.org/10.1088/1475-7516/2020/03/010). URL: <https://dx.doi.org/10.1088/1475-7516/2020/03/010>.
- [18] Mark Vogelsberger, Federico Marinacci, Paul Torrey, and Ewald Puchwein. “Cosmological simulations of galaxy formation.” In: *Nature Reviews Physics* 2.1 (2020), pp. 42–66.
- [19] Francis Bernardeau, S Colombi, E Gaztanaga, and R Scoccimarro. “Large-scale structure of the Universe and cosmological perturbation theory.” In: *Physics reports* 367.1-3 (2002), pp. 1–248.
- [20] Richard B Larson. “Insights from simulations of star formation.” In: *Reports on Progress in Physics* 70.3 (2007), p. 337.
- [21] Christian Fidler et al. “Relativistic interpretation of Newtonian simulations for cosmic structure formation.” In: 2016.09 (Sept. 2016), p. 031. DOI: [10.1088/1475-7516/2016/09/031](https://doi.org/10.1088/1475-7516/2016/09/031). URL: <https://dx.doi.org/10.1088/1475-7516/2016/09/031>.
- [22] Florin Diacu. “The solution of the N-body problem.” In: *Mathematical Intelligencer* 18.3 (1996), pp. 66–70.

- [23] Matthias Bartelmann et al. "A microscopic, non-equilibrium, statistical field theory for cosmic structure formation." In: *New Journal of Physics* 18.4 (Apr. 2016), p. 043020. DOI: [10.1088/1367-2630/18/4/043020](https://doi.org/10.1088/1367-2630/18/4/043020). URL: <https://dx.doi.org/10.1088/1367-2630/18/4/043020>.
- [24] Felix Fabis. "A Statistical Field Theory for Classical Particles - Foundations and Applications in Cosmological Structure Formation." PhD thesis. Heidelberg University, 2015. DOI: [10.11588/heidok.00018676](https://doi.org/10.11588/heidok.00018676).
- [25] E Gozzi. "Hidden BRS invariance in classical mechanics." In: *Physics Letters B* 201.4 (1988), pp. 525–528.
- [26] E Gozzi, M Reuter, and W D Thacker. "Hidden BRS invariance in classical mechanics. II." In: *Physical Review D* 40.10 (1989), p. 3363.
- [27] E Gozzi and M Reuter. "Algebraic characterization of ergodicity." In: *Physics Letters B* 233.3-4 (1989), pp. 383–392.
- [28] E Gozzi and M Regini. "Addenda and corrections to work done on the path-integral approach to classical mechanics." In: *Physical Review D* 62.6 (2000), p. 067702.
- [29] E Deotto, E Gozzi, and D Mauro. "Hilbert space structure in classical mechanics. I." In: *Journal of Mathematical Physics* 44.12 (2003), pp. 5902–5936.
- [30] G F Mazenko. "Fundamental theory of statistical particle dynamics." In: *Physical Review E* 81.6 (2010), p. 061102.
- [31] S P Das and G F Mazenko. "Field theoretic formulation of kinetic theory: basic development." In: *Journal of Statistical Physics* 149.4 (2012), pp. 643–675.
- [32] Matthias Bartelmann et al. "Cosmic structure formation with kinetic field theory." In: *Annalen der Physik* 531.11 (2019), p. 1800446.
- [33] Sara Konrad and Matthias Bartelmann. "Kinetic field theory for cosmic structure formation." In: *Riv. Nuovo Cim.* 45.11 (2022), pp. 737–799. DOI: [10.1007/s40766-022-00037-y](https://doi.org/10.1007/s40766-022-00037-y). arXiv: [2202.11077](https://arxiv.org/abs/2202.11077) [astro-ph.CO].
- [34] Matthias Bartelmann et al. "Kinetic field theory: Non-linear cosmic power spectra in the mean-field approximation." In: *SciPost Phys.* 10 (6 2021), p. 153.
- [35] Christophe Pixius. "On the Perturbative Treatment of Interactions in Kinetic Field Theory - Applications to Cosmic Structure Formation." PhD thesis. Heidelberg University, 2023. DOI: [10.11588/heidok.00033589](https://doi.org/10.11588/heidok.00033589).
- [36] Brian C Hall. *Quantum theory for mathematicians*. Springer, 2013.
- [37] Vladimir Igorevich Arnold, Valery V Kozlov, Anatoly I Neishtadt, and I Iacob. *Mathematical aspects of classical and celestial mechanics*. Vol. 3. Springer, 2006.
- [38] Ana Cannas Da Silva. *Lectures on symplectic geometry*. Vol. 3575. Springer, 2001.

- [39] R. Penrose. “Gravitational collapse: The role of general relativity.” In: *Riv. Nuovo Cim.* 1 (1969), pp. 252–276. DOI: [10.1023/A:1016578408204](https://doi.org/10.1023/A:1016578408204).
- [40] Hayato Motohashi and Teruaki Suyama. “Third order equations of motion and the Ostrogradsky instability.” In: *Phys. Rev. D* 91 (8 Apr. 2015), p. 085009. DOI: [10.1103/PhysRevD.91.085009](https://doi.org/10.1103/PhysRevD.91.085009). URL: <https://link.aps.org/doi/10.1103/PhysRevD.91.085009>.
- [41] Robert Lilow. “Structure Formation in Dark and Baryonic Matter within Resummed Kinetic Field Theory.” PhD thesis. Heidelberg University, 2018. DOI: [10.11588/heidok.00024828](https://doi.org/10.11588/heidok.00024828).
- [42] Robert Lilow, Felix Fabis, Elena Kozlikin, Celia Viermann, and Matthias Bartelmann. “Resummed Kinetic Field Theory: general formalism and linear structure growth from Newtonian particle dynamics.” In: *Journal of Cosmology and Astroparticle Physics* 2019.04 (Apr. 2019), p. 001. DOI: [10.1088/1475-7516/2019/04/001](https://doi.org/10.1088/1475-7516/2019/04/001). URL: <https://dx.doi.org/10.1088/1475-7516/2019/04/001>.
- [43] J. Zinn-Justin. “Renormalization and stochastic quantization.” In: *Nuclear Physics B* 275.1 (1986), pp. 135–159. ISSN: 0550-3213. DOI: [https://doi.org/10.1016/0550-3213\(86\)90592-4](https://doi.org/10.1016/0550-3213(86)90592-4). URL: <https://www.sciencedirect.com/science/article/pii/0550321386905924>.
- [44] Matthias Bartelmann. “Trajectories of point particles in cosmology and the Zel’dovich approximation.” In: *Physical Review D* 91.8 (2015), p. 083524.
- [45] Douglas Scott. “The standard model of cosmology: A skeptic’s guide.” In: *Proc. Int. Sch. Phys. Fermi* 200 (2020), pp. 133–153.
- [46] DJ Fixsen. “The temperature of the cosmic microwave background.” In: *The Astrophysical Journal* 707.2 (2009), p. 916.
- [47] FABRIZIO Nicastro et al. “Observations of the missing baryons in the warm-hot intergalactic medium.” In: *Nature* 558.7710 (2018), pp. 406–409.
- [48] Cyril Pitrou, Alain Coc, Jean-Philippe Uzan, and Elisabeth Vangioni. “Precision big bang nucleosynthesis with improved Helium-4 predictions.” In: *Phys. Rept.* 754 (2018), pp. 1–66. DOI: [10.1016/j.physrep.2018.04.005](https://doi.org/10.1016/j.physrep.2018.04.005). arXiv: [1801.08023](https://arxiv.org/abs/1801.08023) [astro-ph.CO].
- [49] Shweta Singh and Chung-Pei Ma. “Neutrino clustering in cold dark matter halos: Implications for ultrahigh energy cosmic rays.” In: *Phys. Rev. D* 67 (2 Jan. 2003), p. 023506. DOI: [10.1103/PhysRevD.67.023506](https://doi.org/10.1103/PhysRevD.67.023506). URL: <https://link.aps.org/doi/10.1103/PhysRevD.67.023506>.
- [50] Miguel Escudero, Alejandro Ibarra, and Victor Maura. “Primordial lepton asymmetries in the precision cosmology era: Current status and future sensitivities from BBN and the CMB.” In: *Phys. Rev. D* 107.3 (2023), p. 035024. DOI: [10.1103/PhysRevD.107.035024](https://doi.org/10.1103/PhysRevD.107.035024). arXiv: [2208.03201](https://arxiv.org/abs/2208.03201) [hep-ph].

- [51] KATRIN Collaboration. “New Constraint on the Local Relic Neutrino Background Overdensity with the First KATRIN Data Runs.” In: *Phys. Rev. Lett.* 129.1 (2022), p. 011806. DOI: [10.1103/PhysRevLett.129.011806](https://doi.org/10.1103/PhysRevLett.129.011806). arXiv: [2202.04587](https://arxiv.org/abs/2202.04587) [nucl-ex].
- [52] E Baracchini et al. “PTOLEMY: A proposal for thermal relic detection of massive neutrinos and directional detection of MeV dark matter.” In: *arXiv preprint arXiv:1808.01892* (2018).
- [53] Vedran Brdar, P. S. Bhupal Dev, Ryan Plestid, and Amarjit Soni. “A new probe of relic neutrino clustering using cosmogenic neutrinos.” In: *Phys. Lett. B* 833 (2022), p. 137358. DOI: [10.1016/j.physletb.2022.137358](https://doi.org/10.1016/j.physletb.2022.137358). arXiv: [2207.02860](https://arxiv.org/abs/2207.02860) [hep-ph].
- [54] Super-Kamiokande Collaboration. “Evidence for Oscillation of Atmospheric Neutrinos.” In: *Phys. Rev. Lett.* 81 (8 Aug. 1998), pp. 1562–1567. DOI: [10.1103/PhysRevLett.81.1562](https://doi.org/10.1103/PhysRevLett.81.1562). URL: <https://link.aps.org/doi/10.1103/PhysRevLett.81.1562>.
- [55] SNO Collaboration. “Measurement of the Rate of $\nu_e + d \rightarrow p + p + e^-$ Interactions Produced by ^8B Solar Neutrinos at the Sudbury Neutrino Observatory.” In: *Phys. Rev. Lett.* 87 (7 July 2001), p. 071301. DOI: [10.1103/PhysRevLett.87.071301](https://doi.org/10.1103/PhysRevLett.87.071301). URL: <https://link.aps.org/doi/10.1103/PhysRevLett.87.071301>.
- [56] KATRIN Collaboration. “Improved Upper Limit on the Neutrino Mass from a Direct Kinematic Method by KATRIN.” In: *Phys. Rev. Lett.* 123 (22 Nov. 2019), p. 221802. DOI: [10.1103/PhysRevLett.123.221802](https://doi.org/10.1103/PhysRevLett.123.221802). URL: <https://link.aps.org/doi/10.1103/PhysRevLett.123.221802>.
- [57] Isabelle Tanseri, Steffen Hagstotz, Sunny Vagnozzi, Elena Giusarma, and Katherine Freese. “Updated neutrino mass constraints from galaxy clustering and CMB lensing-galaxy cross-correlation measurements.” In: *Journal of High Energy Astrophysics* 36 (2022), pp. 1–26. ISSN: 2214-4048. DOI: <https://doi.org/10.1016/j.jheap.2022.07.002>. URL: <https://www.sciencedirect.com/science/article/pii/S2214404822000374>.
- [58] P. Mertsch et al. “Neutrino clustering in the Milky Way and beyond.” In: *JCAP* 01 (2020), p. 015. DOI: [10.1088/1475-7516/2020/01/015](https://doi.org/10.1088/1475-7516/2020/01/015). arXiv: [1910.13388](https://arxiv.org/abs/1910.13388) [astro-ph.CO].
- [59] Wan Yan Wong, Adam Moss, and Douglas Scott. “How well do we understand cosmological recombination?” In: *Monthly Notices of the Royal Astronomical Society* 386.2 (Apr. 2008), pp. 1023–1028. ISSN: 0035-8711. DOI: [10.1111/j.1365-2966.2008.13092.x](https://doi.org/10.1111/j.1365-2966.2008.13092.x). eprint: <https://academic.oup.com/mnras/article-pdf/386/2/1023/3629046/mnras0386-1023.pdf>. URL: <https://doi.org/10.1111/j.1365-2966.2008.13092.x>.
- [60] D.J. Eisenstein. “Dark energy and cosmic sound.” In: *New Astronomy Reviews* 49.7 (2005). Wide-Field Imaging from Space, pp. 360–365. ISSN: 1387-6473. DOI: <https://doi.org/10.1016/j.newar.2005.08.005>. URL: <https://www.sciencedirect.com/science/article/pii/S1387647305000850>.

- [61] Planck Collaboration. “Planck 2018 results-III. High Frequency Instrument data processing and frequency maps.” In: *Astronomy & Astrophysics* 641 (2020), A3.
- [62] Planck Collaboration. “Planck 2013 results. XXII. Constraints on inflation.” In: *Astronomy & Astrophysics* 571 (2014), A22.
- [63] Planck Collaboration. “Planck 2018 results-IX. Constraints on primordial non-Gaussianity.” In: *Astronomy & Astrophysics* 641 (2020), A9.
- [64] Diego Blas, Julien Lesgourgues, and Thomas Tram. “The Cosmic Linear Anisotropy Solving System (CLASS). Part II: Approximation schemes.” In: *Journal of Cosmology and Astroparticle Physics* 2011.07 (July 2011), pp. 034–034.
- [65] Adrian Jenkins. “Second-order Lagrangian perturbation theory initial conditions for resimulations.” In: *Monthly Notices of the Royal Astronomical Society* 403.4 (2010), pp. 1859–1872.
- [66] Andreas Ringwald and Yvonne Y. Y. Wong. “Gravitational clustering of relic neutrinos and implications for their detection.” In: *JCAP* 12 (2004), p. 005. DOI: [10.1088/1475-7516/2004/12/005](https://doi.org/10.1088/1475-7516/2004/12/005). arXiv: [hep-ph/0408241](https://arxiv.org/abs/hep-ph/0408241).
- [67] Julio F. Navarro, Carlos S. Frenk, and Simon D. M. White. “The Structure of cold dark matter halos.” In: *Astrophys. J.* 462 (1996), pp. 563–575. DOI: [10.1086/177173](https://doi.org/10.1086/177173). arXiv: [astro-ph/9508025](https://arxiv.org/abs/astro-ph/9508025).

ACKNOWLEDGMENTS

A number of persons have directly impacted the content of this thesis:

- Shayan Hemmatyar has significantly contributed to the development of the presented approach to microscopic perturbation theory in KFT, particularly through hundreds of pages of handwritten calculations which helped to detect and confirm patterns in the expressions.
- The application of KFT to neutrino clustering was conceived of by Isabel M. Oldengott and jointly worked on with her and Emil Brinch Holm.
- Minor corrections mostly of linguistic and orthographic nature were suggested by
 - Tim Adler,
 - Athanasia-Konstantina Angelopoulou,
 - Cornelius Bauer,
 - Bruno Faigle-Cedzich,
 - Thomas Kirchner,
 - Ricardo Waibel.
- Individual contributions and references for each section are listed in the final introductory paragraph of the respective section in *italic text*.

I want to thank Lavinia Heisenberg for the opportunity of conducting a PhD thesis in her group. I am particularly grateful for the exceptional care and flexibility offered during the past four years. Many thanks also to the Heisenberg group for making the time of my doctorate a chapter of my life I will fondly look back at.

I want to thank all collaborators on projects during my PhD, in particular Shayan Hemmatyar, Isabel M. Oldengott and Emil Brinch Holm, Fabio D'Ambrosio, Andrea Guisti, Federica Tarsitano and Alexandre Refregier. Moreover, I want to sincerely thank Matthias Bartelmann for advice and encouragement as well as fruitful discussions over many years.

My thanks also goes to the members of my examination committee to whom I also wish to apologize for handing in my thesis just prior to the winter holidays.

I am grateful to my friends and family for their positive impact on my life.

Thank You!

DECLARATION

Concerning the present doctoral thesis with my signature I confirm:

- that I am its sole author and I have compiled it in my own words,
- that I have not submitted it to any other university,
- that I have not committed any of the forms of plagiarism described in the “Citation etiquette”,
- that I have documented all methods, data and processes truthfully,
- that I have not manipulated any data,
- that I have mentioned all persons who were significant facilitators of the work.

Zürich, 14th of February 2024



Stefan Zentarra